UNIVERSITY OF ALBERTA

Determination of the Concentration of Silver (I) Species in the Presence of its Chloro- and Hydroxo- Complexes by the Ion-exchange Column Equilibration-AAS Technique

BY

Yusuf Idris Haji Muombwa ©

A thesis submitted to the Faculty of Graduate Studies and Research in partial fulfillment of the requirements for the degree of **Master of Science**

DEPARTMENT OF CHEMISTRY

EDMONTON, ALBERTA

SPRING, 1997

UNIVERSITY OF ALBERTA

LIBRARY RELEASE FORM

NAME OF AUTHOR: Yusuf I. H. Muombwa

TITTLE OF THESIS: Determination of the concentration of silver (I) species in the presence of its chloro- and hydroxo- complexes by the ion-exchange column equilibration-AAS technique

DEGREE: Master of Science

YEAR THIS DEGREE GRANTED: 1997

AUTHOR'S SIGNATURE: 
Yusuf I. H. Muombwa

PERMANENT ADDRESS: P.O. BOX 1377
ZANZIBAR
TANZANIA

DATE: January 8, 1997

UNIVERSITY OF ALBERTA

Faculty of Graduate Studies and Research

The undersigned certify that they have read, and recommended to the Faculty of Graduate Studies and Research for acceptance, a thesis entitled **Determination of the Concentration of Silver (I) Species in the Presence of its Chloro- and Hydroxo-Complexes by the Ion-exchange Column Equilibration-AAS Technique.** Submitted by **Yusuf I. H. Muombwa** in partial fulfillment of the requirements for the degree of **Master of Science.**

F. F. Cantwell
Dr. F. F. Cantwell, Supervisor

B. Kratochvil
Dr. B. Kratochvil

M. J. Dudas
Dr. M. J. Dudas

Date: January 8, 1997

Dedicated to my father, Mr. Idris H. Muombwa and my mother, Tatu H. Mbarouk,

for their endless love and support.

Abstract

A non-perturbing, flow-through column equilibration method, with element-selective detection by atomic absorption spectrophotometry, is described for the measurement of concentration of the free silver (I) species (i.e. [Ag^+]) in the presence of its chloro- and hydroxo-complexes. Columns of Dowex 50W-X8 cation exchange resin are used. The theoretical basis of the method is described. At equilibrium, the technique requires that only a small fraction of the resin exchange sites may be occupied by silver ions. This is accomplished by making the concentration of electrolyte in the samples and standards equal and high.

Loading, breakthrough and elution curves and sorption isotherms were measured as part of the method development. The method has been applied successfully to the determination of free silver in solutions containing the ligands Cl^- and OH^-. The values of [Ag^+] measured by the column equilibration technique are in satisfactory agreement with the values measured by using a silver ion-selective electrode method (ISE) and with values calculated using total metal and total ligand concentrations, solubility products and conditional stability constants of the metal-ligand complexes.

The ion-exchange column equilibration-AAS technique is selective for Ag^+ in the presence of the soluble species $AgCl_2^-$, $AgCl_3^{2-}$, $AgCl_4^{3-}$, $Ag(OH)_2^-$ and $Ag(OH)_3^{2-}$ and also

in the presence of colloidal particles of AgCl(s) and Ag_2O(s) at pAg and pH above their points of zero charge. The soluble neutral complexes species AgCl and AgOH are sorbed by the exchanger but a correction can be made for their interference in the determination of free silver ion.

Acknowledgments

I would like to express my sincere gratitude to my Supervisor, Professor F.F. Cantwell for his support, encouragement, and invaluable scholarly guidance during the course of this work. Without his supervision and suggestions the objective of this work could not have been accomplished. Also, I would like to express my gratitude to Dr. B. Kratochvil and Dr. M. J. Dudas, the members of the thesis committee, for their valuable comments and suggestions. I am grateful to all other members of Professor Cantwell's research group for their friendship, support and sharing of experiences. Also, I am grateful to all the staff, supporting staff and fellow students of the Department of Chemistry for their assistance in many different ways.

The financial assistance from the Canadian Commonwealth Scholarship and Fellowship Plan, from the Department of Chemistry, University of Alberta and from a research contract provided by Sherrit-Westaim Inc. is gratefully acknowledged.

I wish to acknowledge the assistance and support extended to me and my family by our various friends in Edmonton and Calgary. In particular, I would like to thank Mr. and Mrs. Ramachandran, Mr. and Mrs. Raji, Mr. and Mrs. Abdul-hamid Y. Mzee, Miss Rosemary R. Mr. Derege, L. Mr. Hassan Chomhoh and his family and Mr. Hemed Khalfan and his family. Their kindness, friendship, and good sense of humor made our stay in Canada very comfortable, enjoyable and rewarding. May ALLAH bless you and your families.

A special debt of gratitude is owed to Dr. M. G. Bilal and Mr. Hassan H. Mussa for their support, encouragement and bringing me this far, May ALLAH bless you.

I would like also to extend my deepest gratitude and appreciation to my wife, Jamila and my son Idris, for their support, as well as the times they spent alone.

Also, I would like to extend my warmest thanks to all my friends in the MSA at the University of Alberta and to all other friends who helped me in many different ways throughout the course of my studies at University of Alberta.

Finally, I give sincere gratitude to ALLAH (swt), for bringing me this far. To ALLAH be all the glory.

TABLE OF CONTENTS

CHAPTER **PAGE**

ONE INTRODUCTION

1.1 Role of speciation....1

1.2 Importance of free metal ion determination....2

1.3 Speciation techniques....5

1.3.1 Ion-selective electrode potentiometry....6

1.3.2 Ion-exchange column equilibration technique....7

1.4 Research objectives....10

TWO THEORETICAL CONSIDERATIONS

2.1 Silver species distribution....11

2.1.1 Introduction....11

2.1.2 Equations for calculation of silver species distribution....11

2.1.2.a In the absence of solid AgCl(s) and Ag_2O(s) and with chloride not in large excess....14

2.1.2.b In the presence of solid AgCl(s) and the absence of solid Ag_2O(s) 18

2.1.3 Properties of silver chloride colloid....21

2.1.3.1 Solubility of silver chloride....21

2.1.3.2 Light absorption and Tyndall effect....22

2.1.3.3 Adsorption of ions....23

2.2 Theoretical background of free silver ion speciation measurement by the ion-exchange column equilibration method....24

2.2.1 Introduction....24

2.2.2 Ion-exchange equilibria under trace conditions.....25
2.2.2.1 Sorption isotherm.....26
2.2.3 Ion-exchange equilibria under non-trace resin loading conditions.....28
2.2.4 Sorption of species other than free metal.....29
2.2.5 Elution in the presence of complexing ligand.....32

THREE EXPERIMENTAL

3.1 Apparatus.....35
3.1.1 Column construction.....35
3.1.1.1 Construction of 1.4 g resin - large column.....35
3.1.1.2 Construction of 15 mg resin - small column.....37
3.1.2 Flow systems.....38
3.1.2.1 Large column flow system.....38
3.1.2.2 Small column flow systems.....40
3.1.2.2.a Single pass flow for small column.....40
3.1.2.2.b Recycle flow for small column.....42
3.1.3 pH and Ion-selective electrode systems.....42
3.2 Reagents and chemicals.....44
3.3 Resin.....45
3.4 Procedures.....46
3.4.1 Column operation.....46
3.4.2 ISE potentiometric measurement of free silver ion, [Ag^+] concentration.....47
3.4.3 AAS - measurement of silver concentration.....49
3.4.4 Cleaning of equipment and flow systems.....50

FOUR CHARACTERIZATION OF THE ION-EXCHANGE COLUMN EQUILIBRATION-AAS TECHNIQUE FOR FREE SILVER ION DETERMINATION

4.1 Introduction.....52

4.2 Experimental.....52

4.2.1 Apparatus.....52

4.3 Breakthrough studies.....53

4.3.1 Introduction.....53

4.3.2 Procedure.....53

4.3.3 Results and discussion.....53

4.4 Pre-conditioning study.....57

4.5 Elution studies.....61

4.5.1 Introduction.....61

4.5.2 Procedure.....63

4.5.3 Results and discussion.....64

4.5.3.1 Effect of NH_3/NH_4^+ buffer on elution efficiency.....64

4.5.3.2 Effect of eluent flow rate on elution efficiency.....64

4.5.3.3 Effect of eluent concentration on elution efficiency.....69

4.5.3.4 Elution study with a 15 mg resin column.....71

4.6 Equilibration (loading) studies.....74

4.6.1 Introduction.....74

4.6.2 Procedure.....74

4.6.3 Results and discussion.....75

4.6.3.1 Effect of flow rate on equilibration time.....75

4.6.3.2 Effect of ionic strength on equilibration time.....78

4.6.3.3 Effect of silver concentration on equilibration time.....82

4.7 Sorption isotherm.....85
4.7.1 Introduction.....85
4.7.2 Procedure.....85
4.7.3 Results and discussion.....86

FIVE DETERMINATION OF FREE SILVER ION CONCENTRATION, [Ag^+], IN SYNTHETIC SOLUTIONS

5.1 Introduction.....91
5.2 Experimental.....91
5.2.1 Apparatus.....91
5.2.2 Sample solution preparation.....92
5.2.2.1 Sample solution preparation for chloride ligand.....92
5.2.2.2 Sample solution preparation for hydroxide ligand.....92
5.2.3 Procedure for free metal determination.....93
5.3 Results and discussion.....94
5.3.1 Determination of free silver ion concentration, [Ag^+], in the presence of chloride ligand.....94
5.3.1.1 Loading study in the presence of chloride ligand and AgCl(s).....95
5.3.1.2 Determination of free silver ion concentration under trace conditions.....99
5.3.1.3 Determination of free silver ion concentration under non-trace conditions.....109
5.3.1.4 Effect of ionic strength and aging of AgCl(s) on Ag^+ concentration.....115

5.3.2 Determination of free silver ion concentration, [Ag^+], in the presence of hydroxide ligand.....122

5.3.2.1 Equilibrium sorption of Ag^+ in the presence of hydroxide ligand and $Ag_2O(s)$.....124

5.3.2.2 Determination of free silver ion concentration at different pH.....127

5.4 Summary and conclusion.....138

BIBLIOGRAPHY.....140

APPENDIX

A Computer programs.....145

B Tables for Chapter four.....166

C Tables for Chapter five.....186

D Derivation of an expression for the fraction of free silver in the presence of EDTA as the only complexing ligand.....192

LIST OF TABLES

Table		Page
2.1	List of the stability and solubility product constants for Ag^+ with Cl^-, OH^-, EDTA (Y^{4-}), NO_3^- and NH_3 and, for Na^+ with EDTA (Y^{4-}), at specific ionic strength, (I) and temperature	13
5.1	Results obtained by varying the amount of total chloride, C_{Cl}, in solutions containing a fixed concentration ($1x10^{-5}$ M) of total silver, 0.3 M total ionic strength and pH 7 buffer	101
5.2	Results obtained by varying the amount of total chloride, C_{Cl}, in solutions containing a fixed concentration ($1x10^{-4}$ M) of total silver, 0.3 M total ionic strength and pH 7 buffer	102
5.3	Comparison of the experimental (fitted) and the litrature values of conditional stability and solubility product constants	103
5.4	Composition of sample solutions and other parameters used in the determination of $[Ag^+]$ at different ionic strengths	116
5.5	Results obtained for the determination of $[Ag^+]$ in the presence of varying amounts of $NaNO_3$ (ionic strength) in solutions of fixed total silver ($1x10^{-4}$ M) and total chloride ($3x10^{-5}$ M) concentrations	117
5.6	Values of $[Ag^+]$ for the filtered saturated solutions of $Ag_2O(s)$	129
5.7	Composition of sample solutions used for the determination of free silver ion concentration in solutions of different pH	132
A.1	The spreadsheet used to estimate the value of the concentration of free chloride, $[Cl^-]$, using computer program A.1	148
A.2	The spreadsheet used to estimate the value of the concentration of free chloride, $[Cl^-]$, using computer program A.2	151

A.3a The spreadsheet used to estimate the value of Ksp and $\beta_{1,Cl}$ (Stage 1)..... 155

A.3b The spreadsheet used to estimate the value of $\beta_{2,Cl}$, $\beta_{3,Cl}$, and $\beta_{4,Cl}$ (at constant Ksp and $\beta_{1,Cl}$) (Stage 2)..... 156

A.3c The spreadsheet used to estimate the value of Ksp, $\beta_{1,Cl}$, $\beta_{2,Cl}$, $\beta_{3,Cl}$, and $\beta_{4,Cl}$ (Stage 3)..... 157

A.3d The average values of Ksp, $\beta_{1,Cl}$, $\beta_{2,Cl}$, $\beta_{3,Cl}$, and $\beta_{4,Cl}$ (Stage 4)..... 158

A.4 The spreadsheet used to calculate the species distribution of Ag-Cl system using computer program A.4..... 161

A.5 The spreadsheet used to estimate the value of the distribution coefficient, λ_{AgCl} of AgCl(aq) between the resin phase and the solution phase using computer program A.5..... 164

A.6 The spreadsheet used to estimate the value of the distribution coefficient, λ_{AgOH} of AgOH(aq) between the resin phase and the solution phase using computer program A.5..... 165

B.1 Ag^+ breakthrough data on Dowex 50W-X8 resin for 1.85 μmol l^{-1} and 46.35 μmol l^{-1} Ag^+ in 0.2 M $NaNO_3$ and pH 7 buffer..... 167

B.2 Ag^+ breakthrough data on Dowex 50W-X8 resin for 1.85μmol l^{-1} and 46.35 μmol l^{-1} Ag^+ in 0.3 M $NaNO_3$ and pH 7 buffer..... 168

B.3 Ag^+ breakthrough data on Dowex 50W-X8 resin for $1x10^{-4}$ M Ag^+ in 0.3 M $NaNO_3$ and pH 7 buffer..... 169

B.4 Pre-conditioning data for 10.0 μmol l^{-1} Ag^+ in 0.3 M $NaNO_3$ and pH 7 buffer..... 170

B.5 Elution data for Ag^+ on Dowex 50W-X8 resin for 92.7 μmol l^{-1} Ag^+ in 0.3 M $NaNO_3$ and pH 7 buffer. Different concentrations of ammonium buffer were added in the eluent (0.05 M EDTA at pH 10)..... 171

B.6 Elution data for Ag^+ on Dowex 50W-X8 resin for 92.7 μmol l^{-1} Ag^+ in 0.3 M $NaNO_3$ and pH 7 buffer. The eluent 0.04 M EDTA at pH 10 was passed at a flow rate of 1 ml $min.^{-1}$..... 172

B.7 Elution data for Ag^+ on Dowex 50W-X8 resin for 92.7 μmol l^{-1} Ag^+ in 0.3 M $NaNO_3$ and pH 7 buffer. The eluent 0.04 M EDTA at pH 10 was passed at a flow rate of 2 ml $min.^{-1}$..... 173

B.8 Elution data for Ag^+ on Dowex 50W-X8 resin for 92.7 μmol l^{-1} Ag^+ in 0.3 M $NaNO_3$ and pH 7 buffer. The eluent 0.04 M EDTA at pH 10 was passed at a flow rate of 10 ml $min.^{-1}$..... 174

B.9 Elution data for Ag^+ on Dowex 50W-X8 resin for 0.005, 0.01 and 0.1 μmol l^{-1} Ag^+ in 0.3 M $NaNO_3$ and pH 7 buffer..... 175

B.10 Elution data for Ag^+ on Dowex 50W-X8 resin for 92.7 μmol l^{-1} Ag^+ in 0.3 M $NaNO_3$ and pH 7 buffer. Different concentrations of eluent (EDTA) at pH 10 were used for elution..... 176

B.11 Elution data for Ag^+ on Dowex 50W-X8 resin for 1.0, 10 and 100 μmol l^{-1} Ag^+ in 0.3 M $NaNO_3$ and pH 7 buffer..... 177

B.12 Ag^+ loading curve data on Dowex 50W-X8 resin for 9.27 μmol l^{-1} Ag^+ in 0.3 M $NaNO_3$ and pH 7 buffer. The solution was loaded onto a 1.4 g column for different lengths of time and different flow rates..... 178

B.13 Ag^+ loading curve data on Dowex 50W-X8 resin. The solution composition and experimental conditions are the same as in Table B.12..... 179

B.14 Ag^+ loading curve data on Dowex 50W-X8 resin for 1.0 μmol l^{-1} Ag^+ in solutions of different ionic strength (X M $NaNO_3$) and pH 7 buffer..... 180

B.15 Data showing the values of distribution coefficient of Ag^+ between the resin phase and solution phase at different ionic strengths..... 181

B.16 Ag^+ loading curve data on Dowex 50W-X8 resin for 0.1μmol l^{-1}, 1.0 μmol l^{-1} and 10.0 μmol l^{-1} Ag^+ in 0.3 M $NaNO_3$ and pH 7 buffer..... 182

B.17 Ag^+ loading curve data on Dowex 50W-X8 resin for 1.0 μmol l^{-1}, 10.0 μmol l^{-1} and 100 μmol l^{-1} Ag^+ in 0.3 M $NaNO_3$ and pH 7 buffer..... 183

B.18 Ag^+ sorption isotherm data on Dowex 50W-X8 resin. The solutions contain different concentrations of Ag^+ in 0.3 M $NaNO_3$ and pH 7 buffer were loaded onto a 1.4 g column for 40 minutes at a flow rate 7 ml $min.^{-1}$..... 184

B.19 Ag^+ sorption isotherm data on Dowex 50W-X8 resin. The solutions contain different concentrations of Ag^+ in 0.3 M $NaNO_3$ and pH 7 buffer were loaded onto a 15 mg column for 5 minutes at a flow rate 7 ml $min.^{-1}$..... 185

C.1 Ag^+ loading curve data on Dowex 50W-X8 resin for $1x10^{-4}$ M total silver and $3x10^{-5}$ M total chloride in 0.3 M $NaNO_3$ and pH 7 buffer (1.4 g resin column)..... 187

C.2 Ag^+ loading curve data on Dowex 50W-X8 resin for $1x10^{-4}$ M total silver and $3x10^{-5}$ M total chloride in 0.3 M $NaNO_3$ and pH 7 buffer (15 mg resin column)..... 188

C.3 Results obtained for the determination of free silver ion concentration in the presence of varying amounts of total silver and total chloride concentrations (0.3 M total ionic strength and pH 7 buffer)..... 189

C.4 Ag^+ equilibrium sorption data for solutions contain different concentration of total silver, C_{Ag} in 0.3 M $NaNO_3$ at pH 10..... 190

C.5 Results obtained for the determination of free silver ion concentration in solutions of different pH and 0.3 M total ionic strength..... 191

LIST OF FIGURES

Figure **Page**

1.1 Concept of column equilibration technique.....8

3.1 Cross-section diagram of the columns used for the column equilibration studies.....36

3.2 Schematic diagram of the large column flow system.....39

3.3 Schematic diagram of the single pass flow system.....41

3.4 Schematic diagram of the recycle flow system.....43

3.5 Linear region of the ISE calibration curve for silver standard solutions.....48

3.6 Linear region of the AAS calibration curve for silver standard solutions.....51

4.1 Breakthrough curves for 1.85 μmol l^{-1} and 46.35 μmol l^{-1} Ag^+ solutions in 0.2 M $NaNO_3$ and pH 7 buffer.....55

4.2 Breakthrough curves for 1.85 μmol l^{-1} and 46.35 μmol l^{-1} Ag^+ solutions in 0.3 M $NaNO_3$ and pH 7 buffer.....56

4.3 Breakthrough curves for 1.85 μmol l^{-1} Ag^+ solution in 0.2 M and 0.3 M $NaNO_3$ and pH 7 buffer.....58

4.4 Breakthrough curves for 46.35 μmol l^{-1} Ag^+ solution in 0.2 M and 0.3 M $NaNO_3$ and pH 7 buffer.....59

4.5 Comparison of breakthrough curves obtained by using 1.4 g and 15 mg resin columns.....60

4.6 Resin pre-conditioning curve. The resin was pre-conditioned for different lengths of time with a solution containing 0.3 M $NaNO_3$ and pH 7 buffer.....62

4.7 Elution profiles showing the effect of NH_3/NH_4^+ buffer on elution of Ag^+ from Dowex 50W-X8 strong acid cation exchanger.....65

4.8 Elution profiles showing the effect of eluent flow rate on elution of Ag^+ from Dowex 50W-X8 strong acid cation exchanger (Volume).....67

4.9 Elution profiles showing the effect of eluent flow rate on elution of Ag^+ from Dowex 50W-X8 strong acid cation exchanger (Time).....68

4.10 Elution profiles for different low concentrations of Ag^+ in 0.3 M $NaNO_3$ and pH 7 buffer (1.4 g resin column).....70

4.11 Elution profiles showing the effect of eluent concentration on elution of Ag^+ from Dowex 50W-X8 strong acid cation exchanger.....72

4.12 Elution profiles for different concentrations of Ag^+ in 0.3 M $NaNO_3$ and pH 7 buffer. (15 mg resin column).....73

4.13 Loading curves showing the dependence of loading time on sample flow rate for 9.27 μmol l^{-1} Ag^+ solution in 0.3 M $NaNO_3$ and pH 7 buffer.....76

4.14 Loading curves showing the dependence of sample volume on sample flow rate for 9.27 μmol l^{-1} Ag^+ solution in 0.3 M $NaNO_3$ and pH 7 buffer.....77

4.15 Loading curves showing the effect of ionic strength on equilibration time.....79

4.16 Distribution coefficient (λ_{Ag^+}) of Ag^+ between the resin phase and the solution phase as a function of ionic strength.....81

4.17 Loading curves showing the effect of Ag^+ concentration on equilibration time (1.4 g resin column).....83

4.18 Loading curves showing the effect of Ag^+ concentration on equilibration time (15 mg resin column).....84

4.19 Sorption isotherm of Ag^+ on Dowex 50W-X8 resin. Solutions of differing concentrations of Ag^+ in 0.3 M $NaNO_3$ and pH 7 buffer were loaded onto a 1.4 g resin column for 40 minutes at a flow rate of 7 ml $min.^{-1}$.....88

4.20 Sorption isotherm of Ag^+ on Dowex 50W-X8 resin. Solutions of differing concentrations of Ag^+ in 0.3 M $NaNO_3$ and pH 7 buffer were loaded onto a 15 mg resin column for 5 minutes at a flow rate of 7 ml $min.^{-1}$.....89

4.21 Linear region of the sorption isotherm in Figure 4.19, on the 1.4 g resin column.....90

5.1 Equilibration curves for filtered (0.45 μm) saturated solutions of silver chloride (1.4 g resin column).....96

5.2 Equilibration curves for filtered (0.45 μm) saturated solutions of silver chloride (15 mg resin column).....97

5.3 Variation of $[Ag^+]$ with total chloride concentration, C_{Cl}, in pH 7 buffered solutions containing fixed concentration ($1x10^{-5}$ M) of total silver and 0.3 M total ionic strength (before correcting for sorption of AgCl) 104

5.4 Variation of $[Ag^+]$, with total chloride concentration, C_{Cl}, in pH 7 buffered solutions containing fixed concentration ($1x10^{-4}$ M) of total silver and 0.3 M total ionic strength (before correcting for sorption of AgCl) 105

5.5 Silver species distribution as a function of log C_{Cl}. 106

5.6 Variation of $[Ag^+]$ with total chloride concentration in pH 7 buffered solutions containing fixed concentration ($1x10^{-5}$ M) of total silver and 0.3 M total ionic strength (after correcting for sorption of AgCl).....110

5.7 Variation of $[Ag^+]$ with total chloride concentration in pH 7 buffered solutions containing fixed concentration ($1x10^{-4}$ M) of total silver and 0.3 M total ionic strength (after correcting for sorption of AgCl).....111

5.8 Ion-exchange calibration curve (sorption isotherm) for Ag^+ in 0.3 M total ionic strength and pH 7 buffered standard solutions.....113

5.9 Comparison of the values of $[Ag^+]$ measured by the column equilibration method by the ion-selective electrode method and the predicted values.....114

5.10 A pictorial model of AgCl(s) particle with $Ag^+ (H_2O)_x$ adsorbed on it, drawn to scale to show their relative dimensions.....123
5.11 Equilibrium sorption of Ag^+ on Dowex 50W-X8 resin in the presence of hydroxide ligand and $Ag_2O(s)$.....125
5.12 Lower concentration part (the first region) of Figure 5.11.....126
5.13 Ion-exchange calibration curve (sorption isotherm) for Ag^+ in 0.3 M total ionic strength and pH 7 buffered standard solutions.....128
5.14 Silver species distribution as a function of pH.....130
5.15 Ion-exchange calibration curve (sorption isotherm) for Ag^+ in 0.3 M total ionic strength and pH 7 buffered standard solutions.....133
5.16 Variation of $[Ag^+]$ with pH in solutions of 0.3 M total ionic strength (before correction for sorption of AgOH).....135
5.17 Values of $[Ag^+]$ shown in Figure 5.16 after correction for sorption of AgOH....137

List of symbols and abbreviatios

Symbol	Description
AAS	Atomic absorption spectrophotometry
AES	Atomic emission spectrophotometry
C_{Ag}	Total concentration of silver (analytical concentration)
$C_{Ag,sol}$	Total concentration of silver in solution
C_{Cl}	Total concentration of chloride
C_{IEX}	Total exchange capacity of the resin (meq/g)
C_{L}	Total concentration of ligand L
C_{M}	Total concentration of metal M
$C_{M,sol}$	Total concentration of metal M in solution
$C_{R,+,TOTAL}$	Total concentration of cations in the resin phase
C_{RM}	Total concentration of metal M in the resin phase
$C_{sol,+,TOTAL}$	Total concentration of cations in the solution phase
D_{Ag}	Distribution ratio of Ag^{+} between the resin phase and the solution phase (L/g)
G_{R}	Weight of dry resin (g)
[i]	Equilibrium concentration of species i
I	Ionic strength
ICP-AES	Inductive coupled plasma atomic emission spectrophotometry
ISE	Ion-selective electrode
k'_{Ag}	Capacity factor
K_{IE}^{C}	Concentration ion-exchange equilibrium constant
K_{IE}^{TH}	Thermodynamic ion-exchange equilibrium constant

Ksp	Solubility product constant
Kn	Equilibrium constant for a given reaction
$K_n^{'}$	Conditional equilibrium constant for a given reaction
l	Liter
L	Ligand
M	Metal
M^{+}	Hydrated metal ion
$[ML]_R$	Concentration of species ML in the resin phase
pX	Negative logarithm of the concentration of the species X
PZC	Point of zero charge
R	Resin site
RM	Metal M in the resin phase
V	Volume (ml)
Y^{4-}	EDTA (fully deprotonated)
$Y^{'}$	Total concentration of EDTA that is not complex by metal, M
Zi	Charge of the ionic species I
a_i	Activity of ionic species i
f_i	Fraction of species i in solution
$n_{AgCl(s)}$	Number of moles of silver chloride solid
α_i	Fraction of metal-complex species i
α_{M+}	Fraction of free metal ion M^{+}
α_{ML}	Fraction of free metal M when L is the only ligand present
β	Stability constant

β'	Conditional stability constant
β^{TH}	Thermodynmic stability constant
$\beta_{n,L}^{I,n}$	Conditional concentration stability constant of the species i at ionic strength I
$\beta_{n,L}^{TH}$	Thermodynamic stability constant of the species i
γ_i	Activity coefficient of the ionic species i
λ_i	Distribution coefficient of species i between the resin phase and the solution phase

CHAPTER ONE

INTRODUCTION

1.1 Role of speciation

Ideally, speciation is defined as the determination of the individual species of an element or compound which together make up its total concentration in a system [1]. For example, speciation of a system involving a single metal ion and a complexing ligand should reveal the following; total concentration of the metal (i.e. sum of all forms), total concentration of the ligand, free metal ion and free ligand concentration and the concentrations of the various species of the metal-ligand complexes. It is difficult to obtain all the above information with one analytical technique because metals in aquatic systems may be present in a variety of forms, which may include particulate matter and dissolved forms such as simple inorganic species, organic complexes and the metal adsorbed on a variety of colloidal particles.

The importance of the speciation of metals is evident in situations where only one (or several) species of a metal play a role. In such a situation the determination of one (or more) individual species is more important than determining only the total analytical concentration. Hence speciation has also been defined as the determination of one or more specific species of an element or compound present in a system [1].

Release of metals from various metal handling activities (e.g. mining, metal processing, dumping of industrial waste, etc.) could lead to negative effects in the environment, if these metals are present as toxic species. Therefore, knowledge about speciation of metals is of critical importance and is needed in, among other areas: industrial applications (metallurgy, electroplating and food processing), environmental studies and medicine and toxicology [2].

Two major conceptual approaches have been widely used in speciation studies, namely calculations and experimental methods. By using sophisticated ionic-equilibria computer programs and experimental values for pH, total concentrations of every metal and every ligand and equilibrium constants, trace metal species distributions can be calculated. This approach is adequate for synthetic solutions and for major ions (Ca^{2+} and Mg^{2+}) in natural waters, but cannot be used for the speciation of trace heavy metals in natural waters because neither the nature, nor the concentration, of all the complexing agents present are known. Experimental methods for speciation measurements include techniques like electroanalysis, ion-exchange, size exclusion and solvent extraction. There are significant problems with experimental speciation techniques, including: perturbation of equilibria in the sample, insufficient sensitivity for use in natural waters, lack of selectivity and other interference.

1.2 Importance of free metal ion determination

Research during the last few decades show that the knowledge of the total metal concentration alone is inadequate to allow conclusions regarding the system [1,3-6]. Metal species exhibit different physical and chemical properties and different toxicity. For example, if the free metal ion species, M^+, of the metal, M, is the only species taken up by an organism, then measurement of the total concentration of the metal does not provide adequate information about its influence on aquatic life. This is because the species M^+ represents only a fraction of the total concentration of the metal. Two systems may both contain 100 $\mu g\ l^{-1}$ of total dissolved metal. If a system has most of the metal bound in different forms there may be little or no effect on algae and fish, but if the system has free metal ion, M^+, as the main species, significant effects on aquatic life could be observed.

In fact, several studies have demonstrated that the toxicity of trace metals is directly dependent on the concentration of the free metal ion rather than on the total metal

concentration. For example, Sunda and Guillard [7] found that, in highly chelating sea water media, the growth rate and copper content of algal cells are related to the cupric ion, Cu^{2+}, activity and not to the total copper concentration. Allen et al. [4] found that the toxicity of zinc to algae is directly dependent on the concentration of free metal ion (Zn^{2+}) rather than on the total metal concentration. Several authors [8-19] have suggested that free silver ion, Ag^{+}, is more toxic to aquatic organisms than compounds of silver. Hence it is of critical importance to determine the concentration of the free metal ion in a given system in order to be able to predict metal impacts in the aquatic environment.

Silver occurs naturally in several oxidation states. The most common states are the elemental silver (Ag^{o}) and the monovalent silver ion, Ag(I). Compounds with higher oxidation states of silver (Ag(II) and Ag(III)) are also known [19]. In natural waters silver occurs mainly in the +1 oxidation state. The nature of the species depend on which ligands are present. For example, in hot springs and waters which are highly charged with H_2S, sulfide and polysulfide complexes are the major species [20]. In waters containing high concentrations of chloride, e.g. sea water, complexes of the form AgCl, $AgCl_2^{-}$, $AgCl_3^{-2}$ and $AgCl_4^{-3}$ occur [21]. In photographic waste water silver thiosulphate complexes are the dominate species [20]. Silver may also exist in natural waters in colloidal form such as AgCl(s), Ag_2S(s), Ag_2Se(s) etc. as an integral part of, or adsorbed onto, various humic complexes [22].

Silver is one of the metals with very high oligodynamic activity, being second only to copper in many circumstances. The term oligodynamic activity refers to solutions with germicidal properties in which the concentration of the metal ion is many orders of magnitude below that which would be lethal to mammals [23].

Silver has no known function in the human body and is considered to be a contaminant when found in human tissues. According to Klein [24] 10% of the ingested silver is absorbed, but only 4% is then retained in the tissues. Sollmann [25] observed that ingestion of silver nitrate by humans in doses of 0.01 g - 1.0 g produce no symptoms, but

that of 2 - 30 g cause death within a few hours to a few days. Argyria which is characterized by a slate-gray coloring of the skin and hair is caused by deposition of silver in the tissues [20]. This is the most common effect of chronic exposure to silver. It can occur as an occupational disease or as a result of medicinal applications of silver. The primary sites of silver deposition in the human body are the liver, skin, pancreas, adrenals, kidney, brain, blood vessel walls, spleen and testes [20].

Toxicity of silver to aquatic life has been studied extensively [8-19]. The ionic silver, Ag^+, is more toxic to aquatic organisms than compounds of silver. For example, stable silver thiosulphate complex, a component of the photographic industry effluent, and insoluble Ag_2S were shown to have no effect on activated sludge at levels of 100 000 μg/L, but much smaller concentrations of freely dissociated $AgNO_3$ (10 000 μg/L) and of AgCl (10 000 μg/L) cause an 84% and a 43% inhibition of oxygen uptake, respectively [13]. For silver to be toxic in low doses, the ionic form of the metal must come into direct contact with metabolically active sites, such as the cell membranes of microorganisms. The action of silver ions at low concentration is believed to involve reversible bonding with sulfhydryl groups (-SH) of enzymes or other active compounds at the cell surface [14].

Comparison of toxicity of metal ions to aquatic life forms made by Hutchinson [15] and Albright et. al. [16] reveals that silver ion is the most toxic of the metals tested. According to Hutchinson, the general order of metal toxicity for Chlorella is Ag > Cd > Hg > Se > Ni > Co > Pb, and for Scenedesmus is Ag > Cd > Ni > Se > Cu > Ba > Pb. Albright et. al. attributed the lethal action of the metal salts tested to be due to the metallic cations and the order of bacterial sensitivity is $Ag^+ >> Cu^{2+}$, $Ni^{2+} > Ba^{2+}$, Cr^{3+}, $Hg^{2+} > Zn^{2+}$, Pb^{2+}, Na^+, Cd^{2+}.

There are several factors that influence the distribution of a particular metal among its several forms [26]. These include nature and concentration of the ligands present, stability of the various metal-ligand complexes, concentrations of competing cations, temperature.

pH, ionic strength and the degree to which chemical equilibrium is attained (reaction kinetics).

The species of interest may be either kinetically labile (have the ability to interconvert rapidly with one another) or kinetically inert (remain intact). Speciation of kinetically inert species can be accomplished relatively easily by using standard separation techniques such as filtration [27], solvent extraction [28], chromatography [29] and ion-exchange [30]. Speciation of kinetically labile metal species is a much more delicate matter because care must be taken to ensure that the original equilibria of the system are not perturbed [31]. Sample pre-treatment or interaction of the analytical probe with the sample can perturb the equilibrium of a system. If the existing equilibrium is perturbed then what is measured is not the concentration of the species that normally exist in equilibrium, but the concentration of the species that exist in equilibrium after the changes imposed by the method on the system. Therefore an ideal speciation technique requires no sample pre-treatment and does not perturb the equilibria of the system during measurement.

1.3 Speciation technique

Currently available techniques suitable for speciation of kinetically labile species include: anodic stripping voltammetry (ASV) [32,33], indicator-dye spectrophotometry [34], fluorimetry [35], ion-selective electrode potentiometry (ISE) [36], ion-exchange column equilibration coupled with elemental analysis [37,38,39]. Below, the ion-selective electrode method and the ion-exchange column equilibration method will be discussed.

1.3.1 Ion-selective electrode potentiometry

Ion-selective electrodes are electrochemical sensors that respond selectively to the

activity of a given type of ion in solution in the presence of other ions, without disturbing significantly the equilibria of the system. Ion-selective electrode potentiometry is therefore a suitable technique for free metal ion determination in kinetically labile systems. The particular ion to which an ion-selective electrode responds depends upon the chemical make up of its sensing membrane. Analytical methods using ion-selective electrodes are used extensively due to the versatility, speed and economy of the technique [40].

Metal ion-selective electrodes commercially available include those for Cd^{2+}, Ca^{2+}, Cu^{2+}, Pb^{2+}, Ca^{2+}/Mg^{2+} (water hardness), Li^{+}, K^{+}, Na^{+} and Ag^{+} [41]. The number of metal ions measurable by this method however is limited mainly by the lack of selectivity of the electrodes.

In this work a silver (I) ion-selective electrode was used to measure the concentration of the free silver ion in aqueous samples. A typical silver (I) ion-selective electrode includes a silver sulfide sensing element bonded into an epoxy body. When a sensing element is in contact with a solution containing silver ions an electrode potential develops across the sensing element. This potential, which depends on the activity of free silver ion in solution, is measured against a constant reference potential of a reference electrode with a meter. If the background ionic strength is high and constant relative to the sensed ion concentration the activity coefficient is constant and activity is directly proportional to the concentration. The electrode exhibits good response in one minute or less for concentrations above 10^{-5} M Ag^{+}. Below this value response time varies from 2 to 5 minutes [42].

All ion-selective electrodes have at least some unintended response to additional ions and if there are present at high enough levels, they will interfere. Mercury (Hg^{2+}) is the major interfering ion for measurement of free silver ion [42,43].

1.3.2 Ion-exchange column equilibration technique

The ion-exchange column equilibration technique is an attractive technique for trace metal speciation because measurements can be achieved with no or little manipulation of the sample. Like ion-selective electrode potentiometry, the ion-exchange column equilibration technique is non-perturbing. The technique has been previously used to measure the concentration of the free nickel ion, $[Ni^{2+}]$, in sewage [31], the free copper ion, $[Cu^{2+}]$, in natural waters [37], the free calcium ion, $[Ca^{2+}]$, and the free magnesium ion, $[Mg^{2+}]$, in aqueous solutions [38]. The column equilibration technique is comprised of three main procedural steps namely; loading step, elution step and analysis (quantitation) step.

Pumping of sample solution through a cation exchange resin column is called the loading step. The sample solution is passed through the column until all of the resin in the column has come to equilibrium with the sample solution, i.e. no further removal of species of interest from the solution occurs. If loading of sample solution is repeated at various lengths of time, a loading (equilibration) curve which is a plot of moles sorbed against time (volume) can be constructed. Typical loading curves are shown in Chapter 4, section 4.6.3. Alternatively, if sample solution is pumped continuously into the column and the effluent at the exit of the column is monitored continuously, a plot similar to Figure 1.1 will be obtained. This is a breakthrough curve, which is a plot of the ratio of the effluent concentration, Ce, to the influent concentration, Ci, against time (volume). The time for the ratio of Ce/Ci to reach unity (plateau in the figure) is called the complete breakthrough time.

The process of removing sorbed metal ions from the resin phase is called the elution step. The sorbed metal ions are removed from the resin by the ion-exchange process. However, elution can be enhanced by secondary processes such as inclusion of a strong ligand in the eluent.

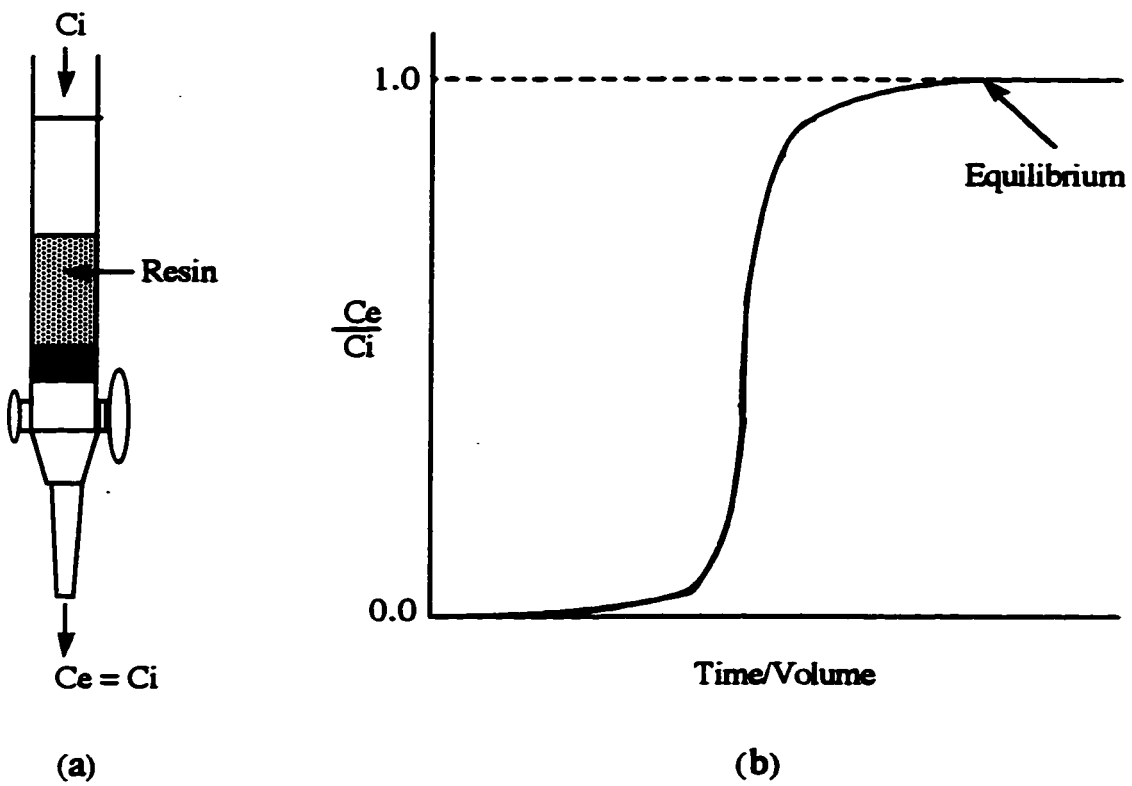

Figure 1.1 **Concept of column equilibration technique. (a) Resin is at equilibrium with sample stream. (b) A breakthrough curve.**

The analysis step involves quantitation of the metal in the eluate from the column. Element specific techniques like atomic absorption spectrophotometry (AAS) or inductively coupled plasma-atomic emission spectroscopy (ICP-AES) may be used to quantify the concentration of eluted metal.

The column equilibration-atomic absorption spectrophotometry method has several desirable characteristics. The original equilibria in the sample solution are not perturbed. This makes the method especially suitable for studies of kinetically labile systems. The amount of resin in the bed can be adjusted to increase the sensitivity of the method and metal concentrations as low as 10^{-8} to 10^{-9} mol l^{-1} can be measured. By using a strong acid type cation exchange resin, the method can be used to measure free metal ion concentration over a wide range of pH. Unlike ion-selective electrode potentiometry, the ion-exchange method is not limited to a small number of elements. It can be applied to many different metals and, when an element-specific detection technique such as AAS is used to analyze the column eluate, the presence of other metals does not cause an interference.

The major disadvantages of the method are the following: The length of time required for the analysis is long (especially with large amounts of resin) compared with ion-selective electrode potentiometry. The method requires maintenance of trace ion-exchange conditions, which can be achieved by addition of an inert electrolyte to the sample. However, addition of large quantities of electrolyte may cause shifting of the original equilibria of the system by changing the activity coefficients of the species. The method is intrinsically less specific than the ion-selective electrode. That is, if a metal-ligand complex sorbs onto the resin the signal obtained from the AAS or ICP-AES would be due to a combination of the free metal ion and the metal-ligand complex. This thesis will focus on the development of an ion-exchange column equilibration-atomic absorption method for speciation of free silver ion in the presence of its chloro- and hydroxo-complexes.

1.4 Research objectives

Silver metal and silver compounds are widely used chemicals in many applications. These include: weather modification (as AgI), photographic industry (as silver halides) and manufacturing industry (e.g. plated ware, jewelry, coin, electrical and electronic products, medical supplies etc.). As a result of natural processes like weathering and volcanic activities, and of various industrial and human activities, silver enters the environment through different pathways. Bertine and Goldberg [44] estimated the amount of silver entering the world's oceans as a result of weathering to be 11 000 tones per year.

As mentioned above, very small amounts of silver ion appear to be of great toxicity to aquatic life as compared to other toxic ions such as Hg^{2+}, Cu^{2+} and Cd^{2+}. Most of the previous studies from this laboratory dealt with the determination of free metal ions of the type M^{2+} e.g. Ca^{2+} , Mg^{2+} , Cu^{2+} and Ni^{2+} using the column equilibration technique. Because of the above mentioned reasons, Ag^{+} was chosen for a detailed investigation of the ion-exchange method of determining an M^{+} species in the presence of its kinetically labile complexes.

Therefore the objective of the present study is to determine the concentration of free silver ion present in equilibrium with kinetically labile ligand-bonded silver species without perturbing the existing equilibria, by using the ion-exchange column equilibration technique with atomic absorption spectroscopy as detector to measure the quantity of silver that is eluted from the resin phase.

CHAPTER TWO

THEORETICAL CONSIDERATIONS

2.1 Silver species distribution

2.1.1 Introduction

In the study of specificity of the ion-exchange column equilibration technique for the metal ion, M^+, in the presence of ligand, L, it is necessary to calculate the species distribution so as to be able to compare the predicted and the experimental values of the concentration of the free metal ion, $[M^+]$. In this section the algebra of complex formation and general equations for predicting the fractions of free metal and metal-ligand species for the silver-chloride system will be outlined.

2.1.2 Equations for calculation of silver species distribution

The solubility and equilibrium properties of the silver-chloride system have been studied extensively [45-52]. Chloride, Cl^-, forms four complexes with silver (I) [46,47,49-54]. Free ligand concentration can be calculated by considering the equilibria involved. The formation expressions for these four complexes are given below:

$$Ag^+ + Cl^- \rightleftharpoons AgCl$$

$$\beta_{1,Cl} = \frac{[AgCl]}{[Ag^+][Cl^-]} \quad \text{and} \quad [AgCl] = \beta_{1,Cl}[Ag^+][Cl^-] \qquad \text{..... 2.1.1}$$

$$Ag^+ + 2Cl^- \rightleftharpoons AgCl_2^-$$

$$\beta_{2,Cl} = \frac{[AgCl_2^-]}{[Ag^+][Cl^-]^2} \quad \text{and} \quad [AgCl_2^-] = \beta_{2,Cl}[Ag^+][Cl^-]^2 \quad \text{..... 2.1.2}$$

$$Ag^+ + 3Cl^- \rightleftharpoons AgCl_3^{2-}$$

$$\beta_{3,Cl} = \frac{[AgCl_3^{2-}]}{[Ag^+][Cl^-]^3} \quad \text{and} \quad [AgCl_3^{2-}] = \beta_{3,Cl}[Ag^+][Cl^-]^3 \quad \text{..... 2.1.3}$$

$$Ag^+ + 4Cl^- \rightleftharpoons AgCl_4^{3-}$$

$$\beta_{4,Cl} = \frac{[AgCl_4^{3-}]}{[Ag^+][Cl^-]^4} \quad \text{and} \quad [AgCl_4^{3-}] = \beta_{4,Cl}[Ag^+][Cl^-]^4 \quad \text{..... 2.1.4}$$

Their respective stability constants as given in [53,54] are shown in Table 2.1.

Depending on the pH of the solution the metal ions may also interact with hydroxide ion, OH^-. The hydroxide ion forms three complexes with silver (I) [55]. The formation expressions for these three complexes are given below:

$$Ag^+ + OH^- \rightleftharpoons AgOH$$

$$\beta_{1,OH} = \frac{[AgOH]}{[Ag^+][OH^-]} \quad \text{and} \quad [AgOH] = \beta_{1,OH}[Ag^+][OH^-] \quad \text{..... 2.1.5}$$

$$Ag^+ + 2OH^- \rightleftharpoons Ag(OH)_2^-$$

$$\beta_{2,OH} = \frac{[Ag(OH)_2^-]}{[Ag^+][OH^-]^2} \quad \text{and} \quad [Ag(OH)_2^-] = \beta_{2,OH}[Ag^+][OH^-]^2 \quad \text{..... 2.1.6}$$

$$Ag^+ + 3OH^- \rightleftharpoons Ag(OH)_3^{2-}$$

Table 2.1 List of the stability and solubility product constants for silver with chloride, hydroxide, EDTA (Y^{4-}), nitrate and ammonia, and for Na^+ with EDTA (Y^{4-}), at specific ionic strength (I) and temperature. Charges on the species are not shown for convenience.

Equilibrium	logβ (I, temp. °C)
[AgCl] / [Ag] [Cl]	2.9 (0.2, 25)
$[AgCl_2]$ / [Ag] $[Cl]^2$	4.7 (0.2, 25)
$[AgCl_3]$ / [Ag] $[Cl]^3$	5.0 (0.2, 25)
$[AgCl_4]$ / [Ag] $[Cl]^4$	5.9 (0.2, 25)
[Ag] [Cl]	-9.74 (0.0, 25)
[AgOH] / [Ag] [OH]	2.3 (0.0, 25)
$[Ag(OH)_2]$ / [Ag] $[OH]^2$	3.6 (0.0, 25)
$[Ag(OH)_3]$ / [Ag] $[OH]^3$	4.8 (0.0, 25)
[Ag] [OH]	-7.37 (0.0, 25)
$[AgY^{3-}]$ / [Ag] $[Y^{4-}]$	7.22 (0.1, 25)
$[AgHY^{2-}]$ / $[AgY^{3-}]$ $[H^+]$	6.01 (0.1, 25)
$[AgNO_3]$/[Ag] $[NO_3]$	- 0.2 (0.0, 25)
$[AgNH_3]$/ [Ag] $[NH_3]$	3.31 (0.0,25)
$[Ag(NH_3)_2]$/ [Ag] $[NH_3]^2$	7.22 (0.1,25)
$[NaY^{3-}]$/$[Na^+][Y^{4-}]$	1.84 (0.1,25)

$$\beta_{3,OH} = \frac{[Ag(OH)_3^{2-}]}{[Ag^+][OH^-]^3} \text{ and } [Ag(OH)_3^{2-}] = \beta_{3,OH}[Ag^+][OH^-]^3 \quad \text{..... 2.1.7}$$

Their respective stability constants as given in [54] are shown in Table 2.1.

2.1.2.a In the absence of solid AgCl(s) and Ag_2O(s) and with chloride not in large excess

The fraction of metal present in the free form, α_M depends on the free ligand concentration, [L]. When the total concentration of the ligand, C_L, is much greater than that of the metal, C_M, i.e. $C_L >> C_M$ and the ligand is not involved in reaction other than complex formation; then $C_L \approx [L]$. That is concentration of complexed ligand can be neglected and the total ligand concentration can be used for calculations of α's instead of the free ligand concentration. However if the metal and the ligand are present in comparable amounts i.e. $C_L \leq 10C_M$ then the concentration of complexed ligand cannot be neglected and the use of free ligand concentration in calculating α's is inevitable [56].

The total concentration of the metal in solution, $C_{Ag,sol}$, both complexed and uncomplexed is given by:

$$C_{Ag,sol} = [Ag^+] + [AgCl] + [AgCl_2^-] + [AgCl_3^{2-}] + [AgCl_4^{3-}] + [AgOH] + [Ag(OH)_2^-] + [Ag(OH)_3^{2-}] \quad \text{..... 2.1.8}$$

Substituting for each species concentration in terms of its formation constant, free metal and ligand concentrations we obtain:

$$C_{Ag,sol} = [Ag^+]\{1 + \beta_{1,Cl}[Cl^-] + \beta_{2,Cl}[Cl^-]^2 + \beta_{3,Cl}[Cl^-]^3 + \beta_{4,Cl}[Cl^-]^4 + \beta_{1,OH}[OH^-] + \beta_{2,OH}[OH^-]^2 + \beta_{3,OH}[OH^-]^3\} \quad \text{..... 2.1.9}$$

The term $1 + \beta_{1,OH}[OH^-] + \beta_{2,OH}[OH^-]^2 + \beta_{3,OH}[OH^-]^3$ is the reciprocal of the fraction of free silver in solution, $\alpha_{Ag+,OH}$ if hydroxide ion is the only complexing ligand present. Thus we can write:

$$\alpha_{Ag+,OH} = \frac{1}{1 + \beta_{1,OH}[OH^-] + \beta_{2,OH}[OH^-]^2 + \beta_{3,OH}[OH^-]^3} \quad \text{..... 2.1.10}$$

For a solution of known pH and therefore known $[OH^-]$, $\alpha_{Ag+,OH}$ can be easily evaluated. The fraction of other silver-hydroxo species expressed in terms of $\alpha_{Ag+,OH}$ are given by:

$$\alpha_{AgOH} = \beta_{1,OH}[OH^-]\ \alpha_{Ag+,OH} \quad \text{..... 2.1.11.a}$$

$$\alpha_{Ag(OH)2} = \beta_{2,OH}[OH^-]^2\ \alpha_{Ag+,OH} \quad \text{..... 2.1.11.b}$$

$$\alpha_{Ag(OH)3} = \beta_{3,OH}[OH^-]^3\ \alpha_{Ag+,OH} \quad \text{..... 2.1.11.c}$$

Equation 2.1.9 can be re-written as follows:

$$C_{Ag,sol} = [Ag^+]\left\{\beta_{1,Cl}[Cl^-] + \beta_{2,Cl}[Cl^-]^2 + \beta_{3,Cl}[Cl^-]^3 + \beta_{4,Cl}[Cl^-]^4 + 1/\alpha_{Ag+,OH}\right\}$$

.....2.1.12

Similarly, we can write the total concentration of the ligand, C_{Cl} in terms of formation constants, free silver and chloride concentrations as:

$$C_{Cl} = [Cl^-] + [Ag^+]\left\{\beta_{1,Cl}[Cl^-] + 2\beta_{2,Cl}[Cl^-]^2 + 3\beta_{3,Cl}[Cl^-]^3 + 4\beta_{4,Cl}[Cl^-]^4\right\}$$

.....2.1.13

The concentration of complexed chloride is given by:

$$C_{Cl} - [Cl^-] = [Ag^+]\left\{\beta_{1,Cl}[Cl^-] + 2\beta_{2,Cl}[Cl^-]^2 + 3\beta_{3,Cl}[Cl^-]^3 + 4\beta_{4,Cl}[Cl^-]^4\right\}$$

..... 2.1.14

Dividing equation 2.1.14 by equation 2.1.12 we obtain:

$$\frac{C_{Cl} - [Cl^-]}{C_{Ag,sol}} = \frac{\beta_{1,Cl}[Cl^-] + 2\beta_{2,Cl}[Cl^-]^2 + 3\beta_{3,Cl}[Cl^-]^3 + 4\beta_{4,Cl}[Cl^-]^4}{\beta_{1,Cl}[Cl^-] + \beta_{2,Cl}[Cl^-]^2 + \beta_{3,Cl}[Cl^-]^3 + \beta_{4,Cl}[Cl^-]^4 + 1/\alpha_{Ag+,OH}} \quad \text{..... 2.1.15}$$

Rearranging equation 2.1.15 and collecting terms with similar power we obtain:

$$\beta_{4,Cl}[Cl^-]^5 + (4C_{Ag,sol}\beta_{4,Cl} - C_{Cl}\beta_{4,Cl} + \beta_{3,Cl})[Cl^-]^4 +$$

$$(3C_{Ag,sol}\beta_{3,Cl} - C_{Cl}\beta_{3,Cl} + \beta_{2,Cl})[Cl^-]^3 + (2C_{Ag,sol}\beta_{2,Cl} - C_{Cl}\beta_{2,Cl} + \beta_{1,Cl})[Cl^-]^2$$

$$+ (C_{Ag,sol}\beta_{1,Cl} - C_{Cl}\beta_{1,Cl} + 1/\alpha_{Ag+,OH})[Cl^-] - \frac{C_{Cl}}{\alpha_{Ag+,OH}} = 0 \quad \text{..... 2.1.16}$$

By defining the following:

$$A^* = \beta_{4,Cl} \quad \text{..... 2.1.17.a}$$

$$B^* = 4C_{Ag,sol}\beta_{4,Cl} - C_{Cl}\beta_{4,Cl} + \beta_{3,Cl} \quad \text{..... 2.1.17.b}$$

$$C^* = 3C_{Ag,sol}\beta_{3,Cl} - C_{Cl}\beta_{3,Cl} + \beta_{2,Cl} \quad \text{..... 2.1.17.c}$$

$$D^* = 2C_{Ag,sol}\beta_{2,Cl} - C_{Cl}\beta_{2,Cl} + \beta_{1,Cl} \quad \text{..... 2.1.17.d}$$

$$E^* = C_{Ag,sol}\beta_{1,Cl} - C_{Cl}\beta_{1,Cl} + 1/\alpha_{Ag+,OH} \quad \text{and} \quad \text{..... 2.1.17.e}$$

$$F^* = \frac{C_{Cl}}{\alpha_{Ag+,OH}} \quad \text{..... 2.1.17.f}$$

and substituting these coefficients into equation 2.1.16 we obtain:

$$A^*[Cl^-]^5 + B^*[Cl^-]^4 + C^*[Cl^-]^3 + D^*[Cl^-]^2 + E^*[Cl^-] - F^* = 0 \quad \text{..... 2.1.18}$$

Computer software, Excel 5.0 was used to write computer program A.1, Appendix A, which uses an iteration procedure to find a value of $[Cl^-]$ which satisfies equation 2.1.18.

Next, the fraction of free silver, α_{Ag+} can be calculated by rearranging equation 2.1.12 as follows:

$$\alpha_{Ag+} = \frac{[Ag^+]}{C_{Ag,sol}}$$

$$= \frac{1}{1 + \beta_{1,Cl}[Cl^-] + \beta_{2,Cl}[Cl^-]^2 + \beta_{3,Cl}[Cl^-]^3 + \beta_{4,Cl}[Cl^-]^4 + \cdots \cdots \beta_{1,OH}[OH^-] + \beta_{2,OH}[OH^-]^2 + \beta_{3,OH}[OH^-]^3} \quad \text{..... 2.1.19}$$

The fractions of other silver-ligand species expressed in terms of α_{Ag+} are given by:

$$\alpha_{AgCl} = \beta_{1,Cl}[Cl^-]\,\alpha_{Ag+} \quad \text{..... 2.1.20.a}$$

$$\alpha_{AgCl2} = \beta_{2,Cl}[Cl^-]^2\,\alpha_{Ag+} \quad \text{..... 2.1.20.b}$$

$$\alpha_{AgCl3} = \beta_{3,Cl}[Cl^-]^3\,\alpha_{Ag+} \quad \text{..... 2.1.20.c}$$

$$\alpha_{AgCl4} = \beta_{4,Cl}[Cl^-]^4\,\alpha_{Ag+} \quad \text{..... 2.1.20.d}$$

$$\alpha_{AgOH} = \beta_{1,OH}[OH]\,\alpha_{Ag+} \quad \text{..... 2.1.20.e}$$

$$\alpha_{Ag(OH)2} = \beta_{2,OH}[OH]^2\,\alpha_{Ag+} \quad \text{..... 2.1.20.f}$$

$$\alpha_{Ag(OH)3} = \beta_{3,OH}[OH]^3\,\alpha_{Ag+} \quad \text{..... 2.1.20.g}$$

All these calculations can be done easily using computer programs given in Appendix A.

2.1.2.b In the presence of solid AgCl(s) and in the absence of solid Ag_2O(s)

In the presence of solid AgCl(s) the following equilibria in addition to those given in section 2.1.2 must be considered.

$$AgCl(s) \rightleftharpoons AgCl(aq) \rightleftharpoons [Ag^+] + [Cl^-]$$

$$Ksp = [Ag^+][Cl^-] \quad \text{and} \quad [Ag^+] = \frac{Ksp}{[Cl^-]} \qquad \text{..... 2.1.21}$$

Where Ksp is the solubility product constant of solid AgCl(s).

Again, the total concentration of silver, C_{Ag}, complexed, uncomplexed and in solid form is given by 2.1.9, with one additional term.

$$C_{Ag} = [Ag^+]\{1+\beta_{1,Cl}[Cl^-]+\beta_{2,Cl}[Cl^-]^2+\beta_{3,Cl}[Cl^-]^3+\beta_{4,Cl}[Cl^-]^4+$$

$$\beta_{1,OH}[OH^-]+\beta_{2,OH}[OH^-]^2+\beta_{3,OH}[OH^-]^3\}+\frac{n_{AgCl(s)}}{V} \qquad \text{..... 2.1.22}$$

Where: $n_{AgCl(s)}$ is the moles of solid AgCl(s) present expressed in equivalent concentration units of moles per volume.

Note: V is the volume of solution; for large volumes of solution, the volume occupied by the solid AgCl(s) is negligibly small.

Similarly, the total concentration of ligand, C_{Cl}, is given by equation 2.1.13, with one additional term.

$$C_{Cl} = [Cl^-] + [Ag^+]\{\beta_{1,Cl}[Cl^-]+2\beta_{2,Cl}[Cl^-]^2+3\beta_{3,Cl}[Cl^-]^3+$$

$$4\beta_{4,Cl}[Cl^-]^4\}+\frac{n_{AgCl(s)}}{V} \qquad \text{.....2.1.23}$$

Subtracting equation 2.1.22 from 2.1.23 we obtain:

$$C_{Cl} - C_{Ag} = [Cl^-] + \beta_{2,Cl}[Ag^+][Cl^-]^2 + 2\beta_{3,Cl}[Ag^+][Cl^-]^3 + 3\beta_{4,Cl}[Ag^+][Cl^-]^4 - [Ag^+] - \beta_{1,OH}[Ag^+][OH^-] - \beta_{2,OH}[Ag^+][OH^-]^2 - \beta_{3,OH}[Ag^+][OH^-]^3$$

..... 2.1.24

Substituting equation 2.1.21 we can write:

$$C_{Cl} - C_{Ag} = [Cl^-] + \beta_{2,Cl}\,Ksp[Cl^-] + 2\beta_{3,Cl}\,Ksp[Cl^-]^2 + 3\beta_{4,Cl}\,Ksp[Cl^-]^3 - \frac{Ksp}{[Cl^-]}\{1 + \beta_{1,OH}[OH^-] + \beta_{2,OH}[OH^-]^2 + \beta_{3,OH}[OH^-]^3\}$$

..... 2.1.25

Since, $1 + \beta_{1,OH}[OH^-] + \beta_{2,OH}[OH^-]^2 + \beta_{3,OH}[OH^-]^3 = \frac{1}{\alpha_{Ag+,OH}}$

then,

$$C_{Cl} - C_{Ag} = (1 + \beta_{2,Cl}\,Ksp)[Cl^-] + 2\beta_{3,Cl}\,Ksp\,[Cl^-]^2 + 3\beta_{4,Cl}\,Ksp\,[Cl^-]^3 - \frac{Ksp}{\alpha_{Ag+,OH}[Cl^-]}$$

..... 2.1.26

Multiplying both sides of the equation 2.1.26 by $[Cl^-]$, we obtain:

$$(C_{Cl} - C_{Ag})\,[Cl^-] = (1 + \beta_{2,Cl}\,Ksp)[Cl^-]^2 + 2\beta_{3,Cl}\,Ksp\,[Cl^-]^3 + 3\beta_{4,Cl}\,Ksp\,[Cl^-]^4 - \frac{Ksp}{\alpha_{Ag+,OH}}$$

..... 2.1.27

By defining the following:

$A' = 3\beta_{4,Cl}Ksp$ 2.1.28.a

$B' = 2\beta_{3,Cl}Ksp$ 2.1.28.b

$C' = (1 + \beta_{2,Cl}Ksp)$ 2.1.28.c

$$D' = (C_{Cl} - C_{Ag}) \quad \text{and} \qquad \text{..... 2.1.28.d}$$

$$E' = \frac{Ksp}{\alpha_{Ag+,OH}} \qquad \text{..... 2.1.28.e}$$

and substituting these coefficients into equation 2.1.27 we obtain:

$$A' [Cl^-]^4 + B' [Cl^-]^3 + C' [Cl^-]^2 - D' [Cl^-] - E' = 0 \qquad \text{..... 2.1.29}$$

Computer software, Excel 5.0 was used to write computer program A.2, Appendix A, which uses an iteration procedure to find a value of $[Cl^-]$ which satisfies equation 2.1.29.

Table 2.1 above shows the literature values of the stability and solubility product constants which are normally reported at specific ionic strengths. Most of the experiments in this work were performed at an ionic strength of 0.3 M. The constants which are shown in Table 2.1 were corrected to the required ionic strength using appropriate equations. For example, for the formation of the metal-complex AgCl, the thermodynamic stability constant β^{TH} for this species can be written as follows:

$$\beta_{1,Cl}^{TH} = \beta_{1,Cl}^{I,1} \left(\frac{\gamma_{AgCl}}{\gamma_{Ag+}\ \gamma_{Cl-}}\right)_{I,1} = \beta_{1,Cl}^{I,2} \left(\frac{\gamma_{AgCl}}{\gamma_{Ag+}\ \gamma_{Cl-}}\right)_{I,2} \qquad \text{..... 2.1.30}$$

Where: γ_i is the activity coefficient of the species i.

$\beta_{1,Cl}^{TH}$ is the thermodynamic stability constant of the species AgCl.

$\beta_{1,Cl}^{I,1}$ is the conditional stability constant of the species AgCl at one ionic strength and $\beta_{1,Cl}^{I,2}$ at the other ionic strength.

Hence;

$$\beta_{1,Cl}^{I,2} = \beta_{1,Cl}^{I,1} \left(\frac{\gamma_{AgCl}}{\gamma_{Ag+}\ \gamma_{Cl-}}\right)_{I,1} \cdot \left(\frac{\gamma_{Ag+}\ \gamma_{Cl-}}{\gamma_{AgCl}}\right)_{I,2} \qquad \text{..... 2.1.31}$$

The activity coefficient γ_i for a given ionic strength can be calculated using Davies equation [57] in the form:

$$-\log \gamma_i = AZ^2 \left\{ \frac{(I)^{1/2}}{1 + (I)^{1/2}} - 0.3 \times I \right\} \quad \text{..... 2.1.32}$$

where: A is a constant equal to 0.51 for aqueous solutions at 25 °C.

Z is the charge of the ion

I is the ionic strength and

γ_i is the activity coefficient of the ionic species i.

The activity coefficient of uncharged species can be considered to be unity [52].

2.1.3 Properties of silver chloride colloids

The equations developed above take into account the presence of silver chloride precipitate but not specifically as a colloidal precipitate. Silver chloride colloids not only alter the species distribution but also the particles might be trapped or sorb onto the exchanger and be quantified as free silver, [58]. Below, some properties of silver chloride colloid will be outlined.

2.1.3.1 Solubility of silver chloride

The solubility of silver chloride in water is 0.00193 g l^{-1} at 25 °C and the solubility product, Ksp, is 1.8×10^{-10} at 25 °C [59]. Silver chloride is an example of a colloidal precipitate. When the precipitate is first formed by precipitation in dilute solutions it consist of extremely minute primary particles. When the primary particles are left in contact with the supernatant liquid they form loose aggregates by sharing a mutual sheath of solvent [60]. Thus the primary particles are subject to increase in size i.e. particle growth. The

process of Ostwald ripening, which involves the transfer of solute from small to large particles by way of the solution is considered secondary for silver chloride precipitate [60].

Brownian motion which is caused by the bombardment of the particles with the liquid medium in which the particles are suspended may cause the particles to collide and coalesce. In order for two colloidal particles of silver chloride to coalesce, they must collide with enough kinetic energy to overcome the electrostatic repulsion caused by the similar charge on the particle. The kinetic energy of the particles increase with increase in temperature.

Presence of an electrolyte e.g. $NaNO_3$ not having an ion in common with a silver chloride precipitate tends to increase its solubility to a slight extent due to change in activity coefficient. This is called the salt effect. As the concentration of an electrolyte is increased, the volume of the ionic atmosphere is reduced. Consequently the particles can come much closer to each other before their electrostatic repulsion becomes significant. This leads tc coagulation of the colloidal suspension and if it is allowed to stand for some time the precipitate may settle in heavy curdy masses leaving a clear supernatant liquid. Therefore, an electrolyte in this case plays a role of maintaining particle coherence. However, if the electrolyte is diluted, the volume of the ionic atmosphere increases and the charged solid particles repel each other and the curdy masses break up. This breaking up is called peptization. Silver chloride is a classical example of a precipitate that peptizes when washed with water. Peptization can be prevented by washing the precipitate with dilute nitric acid.

2.1.3.2 Light absorption and Tyndall effect

Silver chloride particles have no marked absorption in the visible region. Its light sensitivity is confined to the ultra-violet and deep violet regions (350-400 nm) [61]. When a beam of light is directed at the colloidal dispersion, some of the light will be absorbed,

some will be scattered, (Tyndall effect) and the remainder will be transmitted undisturbed through the sample. The absorbed beam of light may cause photodecomposition of silver chloride to silver, (Ag^{o}) and chlorine, (Cl_2). The silver coats the colloidal AgCl(s) imparting a purplish blue color to it. The decomposition proceeds quite rapidly in strong light (direct sunlight). It is therefore evident that solution handling must be carried out in subdued light and under no circumstances in direct sunlight.

2.1.3.3 Adsorption of ions

Surface charge is among the factors that determine the stability of colloidal particles. It is acquired by the presence of extra cations or anions on the particle's surface. The nature and concentration of the ions on a precipitate depend on the surrounding solution and can be changed if the solution is changed. For example, silver chloride suspended in the presence of excess chloride ions in solution, acquires a negative charge owing to the presence of extra chloride ions on the particle's surface. The negatively charged surface attracts cations and repels anions from the ionic atmosphere surrounding the particle. The negatively charged particle and the positively charged ionic atmosphere together are called the electrical double layer.

If silver nitrate is slowly added to the colloidal suspension, more silver chloride will precipitate. As addition is continued, a time will be reached when the concentration of silver ion in solution will be in excess. Under these conditions the silver chloride suspension will acquire a net positive charge owing to the presence of extra silver ions on the particles surface. In the same way a positively charged colloid can be made negatively charged by addition of chloride. If the addition of the reagent is controlled, a point will be reached when equivalent quantities of chloride and silver ions will be present at the particle's surface, and the net charge at the surface will be zero. This state is called the point of zero charge (PZC). It is characterized by the composition of the solution (pX) in

equilibrium with the particles, where pX is the negative logarithm (base 10) of the equilibrium concentration of potential determining ion (Ag^+ or Cl^-) when the net charge at the surface of the particle is zero [64]. For silver chloride pAg is 4.6 [62-64]. Since the energies of adsorption depend on the nature of the adsorbed ion, the PZC does not, in general, correspond to a solution containing equal amounts of chloride and silver ions (isostoichiometric solutions) but to a solution richer in the less adsorbable ionic species, and is not related to the solubility product. Electrokinetic behavior of colloidal silver chloride is beyond the scope of this work and, therefore, it is not discussed.

2.2 Theoretical background of free silver ion speciation measurement by the ion-exchange column equilibration method

2.2.1 Introduction

Ion-exchange is used for metal speciation measurements in two ways. In the batch method, a known volume of sample solution in a flask is equilibrated with a known weight of resin. This method was commonly used in the past [65-70]. The main drawback of the batch method is that it introduces perturbation. The effect of which can be eliminated by multiple equilibration [31].

In the column equilibration method, which was proposed in 1982 by Cantwell, Nielsen and Hrudey [31], a sample solution is passed through an ion-exchange resin column until equilibrium between the resin and sample solution is established. The method is non-perturbing, hence it is suitable for metal speciation measurements in kinetically labile systems. It has been used for metal speciation measurements with better and more reproducible results than the batch method [31,37,38,71-72]. This is the method used in this work.

2.2.2 Ion-exchange equilibria under trace conditions

Consider a solution containing the metal ion of interest, M^+, and a relative high concentration of an inert electrolyte (e.g. $NaNO_3$). If this solution is passed through and equilibrated with a known weight of strong acid type cation exchange resin, the following equilibrium will occur:

$$M^+ + RNa \rightleftharpoons RM + Na^+$$

where R represents ion-exchange sites in the resin phase.

The thermodynamic ion-exchange equilibrium constant, K_{IE}^{TH} for the metal ion distributed between the solution and the resin phases is given by:

$$K_{IE}^{TH} = \frac{a_{RM} \cdot a_{Na}}{a_M \cdot a_{RNa}} = \frac{[RM]\,[Na^+]}{[M^+]\,[RNa]} \cdot \frac{\gamma_{RM} \cdot \gamma_{Na}}{\gamma_M \cdot \gamma_{RNa}} \qquad \text{..... 2.2.1}$$

where [i] is the equilibrium concentration, a_i is the activity and γ_i is the activity coefficient of the species i. Charges on ions are omitted for convenience.

The concentration ion-exchange equilibrium constant, K_{IE}^{C} is given by:

$$K_{IE}^{C} = \frac{[RM]\,[Na^+]}{[M^+]\,[RNa]} \qquad \text{..... 2.2.2}$$

By rearranging equation 2.2.1, we can write

$$K_{IE}^{C} = K_{IE}^{TH} \frac{\gamma_M \cdot \gamma_{RNa}}{\gamma_{RM} \cdot \gamma_{Na}} \qquad \text{..... 2.2.3}$$

If the solution is "swamped" with inert electrolyte (i.e. $[Na^+] >> [M^+]$), such that the fraction of resin in the RM form is less than 1% of the resin total exchange capacity, C_{IEX}, then both the ionic strength and the activity coefficients are constant and the concentration ion-exchange equilibrium constant become a true constant for this particular solution. Also

[Na^+] and [RNa] in equation 2.2.2 become essentially constant and equation 2.2.2 reduces to:

$$\lambda_{M+} = \frac{[RM]}{[M^+]} = K_{IE}^{C} \frac{[RNa]}{[Na^+]} = \text{CONSTANT} \quad \text{..... 2.2.4}$$

where λ_{M+} is the distribution coefficient of the free metal ion, M^+, between the resin phase and the solution phase. The conditions stated above are called "trace ion-exchange conditions" [73].

Rearranging equation 2.2.4 we obtain:

$$[M^+] = \frac{[RM]}{\lambda_{M+}} \quad \text{..... 2.2.5}$$

This equation is used to calculate free metal ion concentration in all cases where trace ion-exchange conditions are satisfied.

Under these conditions the concentration of free metal, [M^+], in solution is directly proportional to the concentration of metal sorbed in the resin phase, [RM]. By matching the matrix of standard and sample solutions, a calibration curve (sorption isotherm) can be constructed, from which the concentration of free metal, [M^+], in the sample can be determined.

2.2.2.1 Sorption isotherm

At equilibrium in the column equilibration method, there is no further change in the concentration of metal sorbed in the resin phase and in the bulk solution. This equilibrium state is usually represented by a sorption isotherm, which is a plot of concentration of metal in the resin phase, [RM], against concentration of free metal ion, [M^+], in the standard solution. The ion-exchange sorption isotherm for a monovalent cation swamped by an inert electrolyte can be predicted by considering the following equation:

$$M^+ + RNa \rightleftharpoons RM + Na^+$$

$$K_{IE}^C = \frac{[RM]\,[Na^+]}{[M^+]\,[RNa]} \qquad \text{..... 2.2.6}$$

We can write the charge balance in the exchanger phase as follows:

$$C_{R,+,TOTAL} = RNa + RM \qquad \text{..... 2.2.7}$$

and in the solution phase as:

$$C_{sol,+,TOTAL} = Na^+ + M^+ \qquad \text{..... 2.2.8}$$

Where $C_{R,+,TOTAL}$ and $C_{sol,+,TOTAL}$ are total concentration of cations in the exchanger phase and in the solution phase, respectively.

Substituting equations 2.2.7 and 2.2.8 into equation 2.2.6 we obtain:

$$[RM] = [M^+]K_{IE}^C \frac{(C_{R,+,TOTAL} - [RM])}{(C_{sol,+,TOTAL} - [M^+])} \qquad \text{..... 2.2.9}$$

The terms in the brackets are not constant, they depend on composition in the resin phase and in the bulk solution. Hence a plot of [RM] against $[M^+]$ (sorption isotherm) is not linear. However, under trace ion-exchange conditions;

$$C_{R,+,TOTAL} >> RM \quad \text{and} \quad C_{sol,+,TOTAL} >> M^+$$

Thus, $C_{R,+,TOTAL} \approx RNa$ and $C_{sol,+,TOTAL} \approx Na^+$

Hence, the terms in the brackets are constant and equation 2.2.9 above reduces to:

$$[RM] = CONSTANT\ [M^+] \qquad \text{..... 2.2.10}$$

$$\text{Where CONSTANT} = K_{IE}^C \frac{C_{R,+,TOTAL}}{C_{sol,+,TOTAL}} = K_{IE}^C \frac{[RNa]}{[Na^+]}$$

Equation 2.2.10 above describes a linear isotherm, i.e. the concentration range of metal ion, M^+, in solution that gives a linear response. The CONSTANT (slope) is the

distribution coefficient, λ_{M+} of the metal ion, M^+, between the solution phase and the resin phase (see equation 2.2.4).

2.2.3 Ion-exchange equilibria under non-trace resin loading conditions

As discussed in section 2.2.2, the necessary conditions for maintenance of trace ion-exchange conditions are a relatively high concentration of electrolyte and less than about one percent fractional loading. When either of these conditions is not satisfied the proportionality between [RM] and $[M^+]$ will not hold.

For a high concentration of metal ion in solution, a very high concentration of electrolyte is required to maintain the trace ion-exchange conditions, but addition of such a high concentration of electrolyte can cause significant changes in solution activity coefficients which in turn can cause changes in the concentration of the free metal ion in the sample. If the concentration of the electrolyte is still much higher than that of metal ion, M^+, i.e. $[Na^+] >> [M^+]$, the ionic strength of the system is constant and K_{IE}^C can still be assumed to be constant. As the concentration of metal ion in solution is increased, the fraction of resin in the RM form also increases. If the increase is such that [RM] is more than 1% of the resin total exchange capacity, C_{IEX}, then trace resin loading conditions are not satisfied and equation 2.2.4 for this system can be written as follows:

$$\lambda_{M+} = \frac{[RM]}{[M^+]} = \text{CONSTANT} \cdot [RNa] \qquad \text{..... 2.2.11}$$

$$\text{where CONSTANT} = \frac{K_{IE}^C}{[Na^+]} \qquad \text{instead of} \qquad K_{IE}^C \frac{[RNa]}{[Na^+]}$$

For a given weight of resin, the total ion exchange capacity (C_{IEX}) is constant.

$$C_{IEX} = RNa + RM = CONSTANT \quad \text{..... 2.2.12}$$

As the concentration of the metal ion, M^+, in solution is increased, [RM] also increases but due to capacity constrains (equation 2.2.12) [RNa] decreases. According to equation 2.2.11 as [RNa] decreases, λ_{M^+} also decreases so that the calibration curve in this case is not linear. However with suitable computer software, an equation for the best-fit can be obtained for the calibration curve almost as easily as for a linear plot provided that the curvature is not severe.

In the cases of both trace and non-trace ion-exchange conditions, it is assumed that only the free metal ion, M^+, is sorbed onto the resin. However other cationic and perhaps neutral species may also be sorbed, depending on their distribution coefficients and fraction in solution relative to the metal ion, M^+. Whenever this assumption was in doubt, it was tested. In some cases significant deviations from this assumption were observed.

2.2.4 Sorption of species other than free metal

Equations derived in section 2.2.2 and 2.2.3 are based on the assumption that only metal ion, M^+, is sorbed. Species that are negatively charged are likely to be excluded from the resin phase, but metal-ligand species which are positively charged can undergo cation exchange and those that are neutral may also sorb onto a cation exchange resin [73]. Sorption of species other than the free metal ion will lead to erroneous results in free metal ion, M^+, determination. It is useful to be able to predict the extent of sorption of other species in the measurement of free metal ion concentration. In this section an equation will be derived which takes into account sorption of neutral species like ML, where L is a ligand.

Consider the system discussed in section 2.2.2, under trace conditions, with all conditions remaining the same, except the neutral metal-ligand species, ML also sorbs onto

the resin together with the metal ion, M^+. When ML also sorbs, the following equilibrium in addition to cation exchange of M^+ must be considered.

$$ML + RNa \rightleftharpoons RNa.ML$$

The distribution coefficient, λ_{ML}, of the species ML between the resin phase and the solution phase is given by:

$$\lambda_{ML} = \frac{[ML]_R}{[ML]} \qquad \text{..... 2.2.13}$$

Where $[ML]_R$ is the concentration of the species ML in the resin phase.

At low sorbed concentration, $[ML]_R$, in the linear region of its sorption isotherm, λ_{ML} will be constant.

Let C_{RM} be the equilibrium concentration of metal sorbed in all forms, i.e.

$$C_{RM} = [RM] + [ML]_R \qquad \text{..... 2.2.14}$$

The equilibrium concentration of metal, M, in the resin phase, [RM], can be obtained by rearranging equation 2.2.4 as follows.

$$[RM] = \lambda_{M^+}[M^+] = \lambda_M \alpha_M C_{M.sol} \qquad \text{.....2.2.15}$$

Where α_M is the fraction of all metal, M, in solution that is present as $[M^+]$, and $C_{M.sol}$ is the total concentration of the metal in solution. For example, α_{Ag^+} in the presence of Cl^- and OH^- ligands is given by equation 2.1.19 in section 2.1, above.

Similarly, from equation 2.2.13.

$$[ML]_R = \lambda_{ML}[ML] = \lambda_{ML} \alpha_{ML} C_{M.sol} \qquad \text{..... 2.2.16}$$

Where α_{ML} is the fraction of metal in solution that is present as [ML]. For example, α_{AgCl} for the soluble neutral complex AgCl, is given by equation 2.1.20.a in section 2.1, above. Substituting for [RM] and $[ML]_R$ in equation 2.2.14 we get.

$$C_{R.M} = (\lambda_{M+}\alpha_{M+} + \lambda_{ML}\alpha_{ML})\, C_{M.sol} \quad \ldots\ldots 2.2.17$$

Equation 2.2.17 above shows that the extent of sorption of metal ion, M^+ and metal-ligand complex ML depends on the λ's and α's of the species involved. Comparison of equation 2.2.5 and 2.2.17 shows that sorption of ML together with metal ion, M^+ results in addition of the term $\lambda_{ML}\alpha_{ML}C_{M.sol}$.

The values of α_{M+}, α_{ML} and $C_{M.sol}$ in equation 2.2.17 can be calculated for any ligand concentration, as shown in section 2.1. The value of λ_{M+} for the metal ion, M^+, can be obtained experimentally using standard solutions of M^+ containing no ligand. It is the slope of the linear part of the sorption isotherm of the metal ion, M^+.

The distribution coefficient, λ_{ML} for the metal-ligand complex ML can be estimated by curve fitting. This can be accomplished by comparing theoretically calculated and experimental values of C_{RM} i.e. total concentration of metal in the resin phase. Thus, if the experimental results do not fit equation 2.2.5 which assumes that only M^+ is sorbed by the resin, equation 2.2.17 can be used to evaluate the experimental data. If a good fit is obtained with equation 2.2.17, then the source of deviation can be attributed to the sorption of neutral complex ML and the value of λ_{ML} will have been obtained.

2.2.5 Elution in the presence of complexing ligand

In this work EDTA which forms negatively charged complexes with silver was used as an eluent. Consider a cation exchanger which has been equilibrated with a solution containing Ag^+ in contact with EDTA at a fixed pH. The following equilibria will be established:

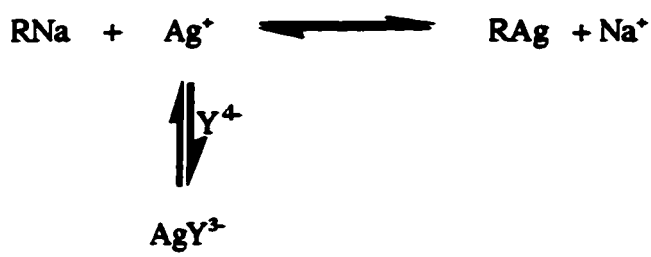

The presence of complexing ligand Y^{4-} will cause the ion-exchange equilibrium to be shifted to the left and the stable anionic AgY^{3-} complex which is formed will no longer be held by the exchanger. In a solution in which sodium ion concentration from EDTA salt is not high, the elution is caused more by complex formation than by the cation exchange process.

In section 2.2.2 we defined the distribution coefficient for the metal (Ag^+) between the resin phase and the solution phase as follows:

$$\lambda_{Ag^+} = \frac{[RAg]}{[Ag^+]} \qquad \text{..... 2.2.18}$$

In the presence of complexing ligand (eluent), the concentration of free silver ion, $[Ag^+]$, in solution is given by:

$$[Ag^+] = \alpha_{Ag^+} C_{Ag,sol} \qquad \text{..... 2.2.19}$$

Where α_{Ag^+} is the fraction of free silver in solution and is given by:

$$\frac{1}{\alpha_{Ag+}} = \frac{1}{\alpha_{Ag+,OH}} + \frac{1}{\alpha_{Ag+,EDTA}} - 1 \qquad \text{..... 2.2.20}$$

Where $\alpha_{Ag+,OH}$ is the fraction of free silver in solution if hydroxide ion is the only complexing ligand present. It is given by equation 2.1.10 in section 2.1.2.a, above. The fraction of free silver in solution, $\alpha_{Ag+,EDTA}$, if EDTA is the only ligand present is given by equation 2.2.21 below.

$$\alpha_{Ag+,EDTA} = \frac{1}{1 + \beta'_{Ag,EDTA}[Y']} \qquad \text{..... 2.2.21}$$

Where $[Y^{'}]$ is the total concentration of EDTA in solution that has not reacted with Ag^{+}. Derivation of equation 2.2.21 is given in Appendix D. Substituting equation 2.2.21 into equation 2.2.20 above we obtain:

$$\alpha_{Ag+} = \frac{\alpha_{Ag+,OH}}{1 + \beta'_{Ag,EDTA}[Y']\,\alpha_{Ag+,OH}} \qquad \text{..... 2.2.22}$$

It is desirable to have a very small value for α_{Ag+}, so that an eluent with very large conditional stability constant with the analyte is an asset.

Combining equation 2.2.18 and 2.2.22 above, we can write an equation for the distribution ratio, D_{Ag} as follows:

$$D_{Ag} = \frac{[RAg]}{C_{Ag,sol}} = \lambda_{Ag+}\,\alpha_{Ag+} \qquad \text{..... 2.2.23}$$

Capacity factor k'_{Ag} is given by:

$$k'_{Ag} = \lambda_{Ag+}\,\alpha_{Ag+}\,\frac{G_R}{V} \qquad \text{..... 2.2.24}$$

Where G_R and V are weight of resin in grams and volume of eluent in liters.

The formation of a stable negatively charged complex (large $\beta'_{Ag,EDTA}$) reduces the fraction of silver ions in solution, but the total concentration of silver in solution is increased. This in turn decreases the distribution ratio, D_{Ag} and therefore the capacity factor, k'_{Ag}. When α_{Ag+} is very small, the fraction of silver in solution, $f_{Ag,sol}$, given by equation 2.2.25 will be approximately equal to unity.

$$f_{Ag,sol} = \frac{1}{1 + k'_{Ag}} = \frac{1}{1 + \lambda_{Ag+}\,\alpha_{Ag+}\,\frac{G_R}{V}} \qquad \text{..... 2.2.25}$$

then, desorption of silver from the resin phase will be quantitative.

CHAPTER THREE

EXPERIMENTAL

3.1 Apparatus

The apparatus, resin conditioning and column construction, reagents and chemicals, procedures and the method for cleaning the equipment which are described in this chapter are common to all subsequent chapters. Specific details will be mentioned in each chapter.

3.1.1 Column construction

Two types of column were used in this work, a small 15 mg column and a large 1.4 g column. The columns were constructed using the procedure outlined below. Schematic diagrams of the columns are shown in Figure 3.1.

3.1.1.1 Construction of 1.4 g resin large column

A polyethylene burette (tube) 8.5 cm long by 0.8 cm id (Cat. No. M0621510 Mandel Scientific Co.) with a Teflon stopcock was used to make the column (Figure 3.1, left). Porous polyethylene frits (Cat. No. H13638 Bel-Art) 1.0 mm thickness, 8.0 mm diameter and about 35 μm nominal pore size, were placed at the top and bottom of the resin bed. A Teflon plug is threaded internally to accept a threaded polypropylene end fitting with flared Teflon inlet tube.

One polyethylene frit was carefully pressed into the tube and placed on top of the stopcock. About 1.4 g of de-fined analytical grade 50-100 mesh (300-150 μm diameter)

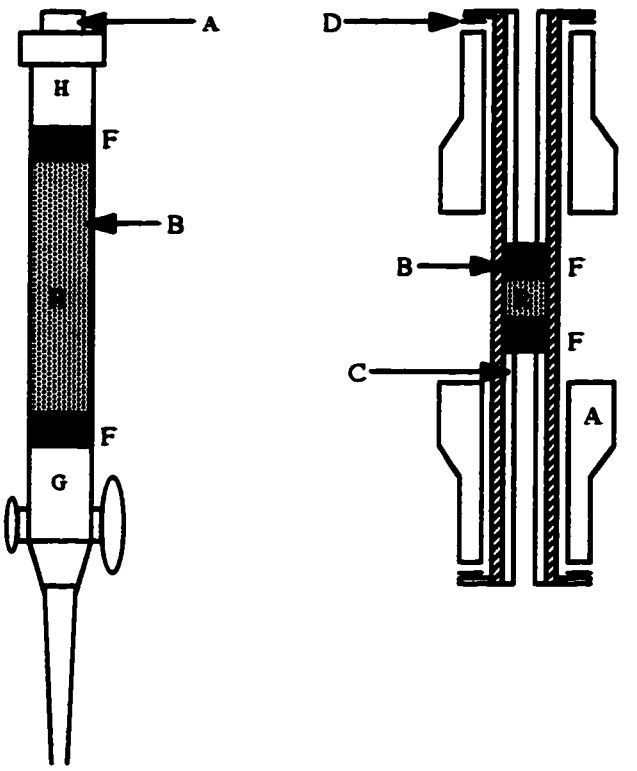

A Threaded polypropylene end fitting (Cheminert)

B Column tube (polyethylene on left; Teflon on right)

C Teflon retaining tube

D Stainless steel washer

R Resin particles

F Polyethylene frits

G Teflon stopcock

H Teflon plug

Figure 3.1 Cross-section diagram of the columns used for column equilibration studies. Left 1.4 g (large) and right 15 mg (small) resin columns.

Dowex 50W-X8, Na^+-form cation exchange resin in several milliliters of water was slurry packed into the tube. The resin bed is about 5.5 cm long. The second polyethylene frit was carefully pressed into the tube such that the resin bed was held loosely between the two frits to avoid excessive compression when the resin swells and to facilitate liquid flow. A total of three resin columns were packed in this way. The schematic diagram of the column is shown in Figure 3.1 (left).

3.1.1.2 Construction of 15 mg resin small column

The design of the 15 mg micro-column, shown in Figure 3.1, right, is similar to the one described in reference [39]. A Teflon tube 5 cm long by 0.15 cm id (Mandel Scientific Co.) was used to make the column. The tube is considerably longer than the resin bed in order to accommodate two cheminert end fittings.

The Teflon tube was flared at one end. A polyethylene frit (1.0 mm thickness, 1.5 mm diameter and about 35 μm nominal pore size) was carefully pressed into the Teflon tube and placed at about 1.5 cm from the flared end of the Teflon tube. The column was weighed. Small amounts of dry, de-fined, analytical grade cation exchange resin (Dowex 50W-X8, 100-200 mesh (150-75 μm diameter) - Na^+-form) were added into the column through the non-flared end using a Pasteur pipette. The column was weighed after each addition until the difference in weight was about 15 mg. The second polyethylene frit was carefully pressed into the column. The stainless steel washers and Cheminert end fitting connectors were fitted in place. Finally the other end of the tube was flared. Two small pieces of Teflon retaining tubes (0.15 cm od by 0.8 mm id), flared on one end, were inserted into the column at each end to hold the frits in place. The resin bed was held loosely between the two frits.

3.1.2 Flow systems

3.1.2.1 Large column flow system

The instrument setup used with the 1.4 g resin column is shown schematically in Figure 3.2. The Plexiglass water bath (constructed in the Machine shop, Department of Chemistry, University of Alberta) has dimensions of 50 x 40 x 25 (L x W x H) centimeters. A constant temperature circulating bath (Haake, type NBE No. 70 129) was used to set the temperature of the water bath via copper coils. The variable speed peristaltic pump (Gilson, Miniplus 2, Model No. E-82, 8 channels Villiers-le-Bel, France) was fitted with 8 pump tubes (Fisher purple-white, clear standard PVC pump tube 0.110" id). These tubes are connected to the rest of the system by Teflon tubing (Alltech, 1/16" od by 0.8 mm id). Three of the 8 tubes pumped the sample solution to each of three large columns and three other tubes pumped eluent to the three columns; one tube pumped water and the last tube was used to pump pre-conditioning solution.

All reagents are pumped through the column via the three-port Teflon slider valves, V_1 through V_4 (CAV3031, Laboratory Data Control). When any of the line(s) is not in use, the pump tube(s) is released from the pump. The selection between pre-conditioning solution (PRE.COND.) or water (WATER) is made using valve V_4. In one position, pre-conditioning solution flows through the column to waste. In the other position, water flows through the column to waste. Valve V_4 is connected to one column at a time by a threaded fitting in the connector H. The selection between sample solution (SAMPLE) or eluent (ELUENT) is made using valves V_1, V_2 and V_3. In one position (solid lines in Figure 3.2) sample solution flows through the column to waste for the required period of time. In the other position (dashed lines in Figure 3.2) the eluent flows through the columns. The eluate from each column is collected for analysis at the exit of the column.

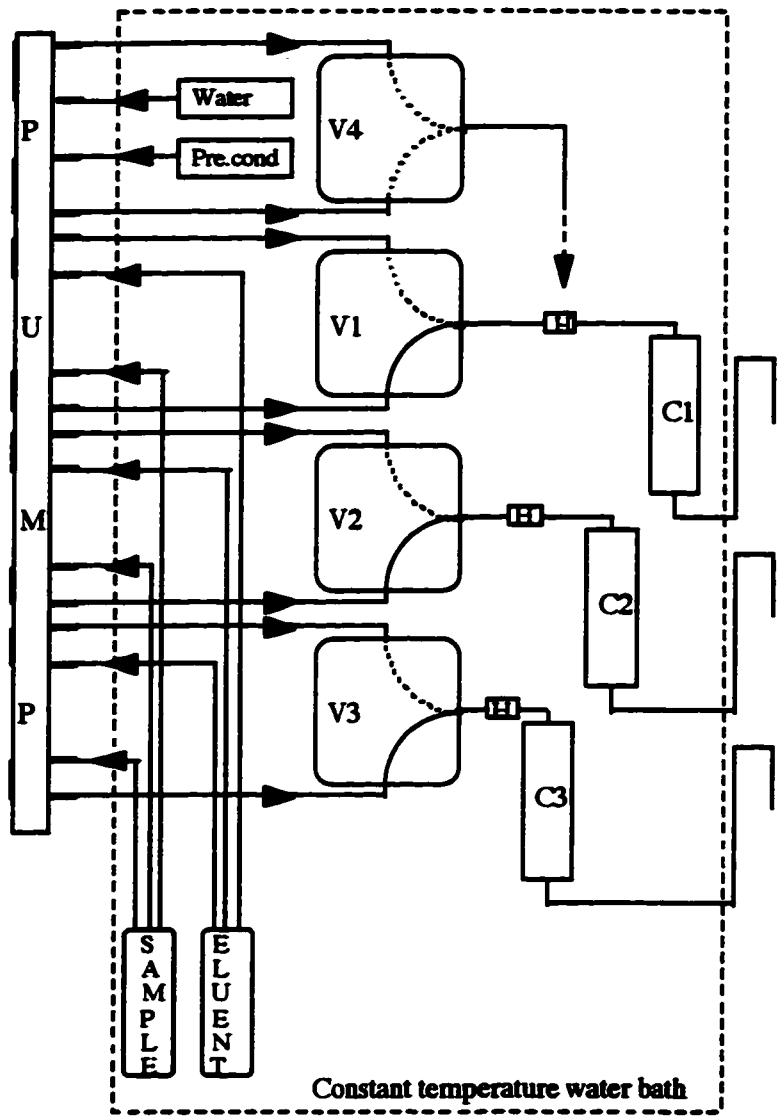

Figure 3.2 Schematic diagram of the large column flow system with 1.4 g resin columns. C_1 through C_3 are resin columns and V_1 through V_4 are 3-way slider valves. Pump is a peristaltic pump.

3.1.2.2 Small column flow systems

The instrument setup shown in Figure 3.2 was used in the first part of this work while the remainder of the work was done using the small column setups, these are shown in Figures 3.3 and 3.4. In addition to the column design, the main difference between the large and small column flow systems is the type of valve used. A six-port rotary valve was used instead of the slider valves. The small column flow systems are simpler and are easier to operate.

3.1.2.2.a Single pass flow for small column

In Figures 3.3 and 3.4 the variable speed peristaltic pump (Model No. D-83, 4 channels) was similar to the one described for the large column flow system except that in this case the pump has only 4 pump channels instead of 8 channels. The type of tubing used and connections were similar to those described for the large column flow system.

All reagents are pumped through the column via the six-port rotary valve, V (Cheminert R 603 1V6). The following sequences of steps is employed: (1) The pre-conditioning solution, PRE.COND is selected by switching valve V to position 5 and is pumped through the column to waste; (2) sample solution is passed through the column to waste for the required period of time by selecting SAMPLE valve V at position 1; (3) AIR is selected by switching valve V to position 2, this expels liquid from the interstitial spaces; (4) the column is washed by selecting WATER, valve V at position 3 and; (5) ELUENT is selected by switching valve V to position 4. The eluate from the column is collected for analysis at the exit of the column.

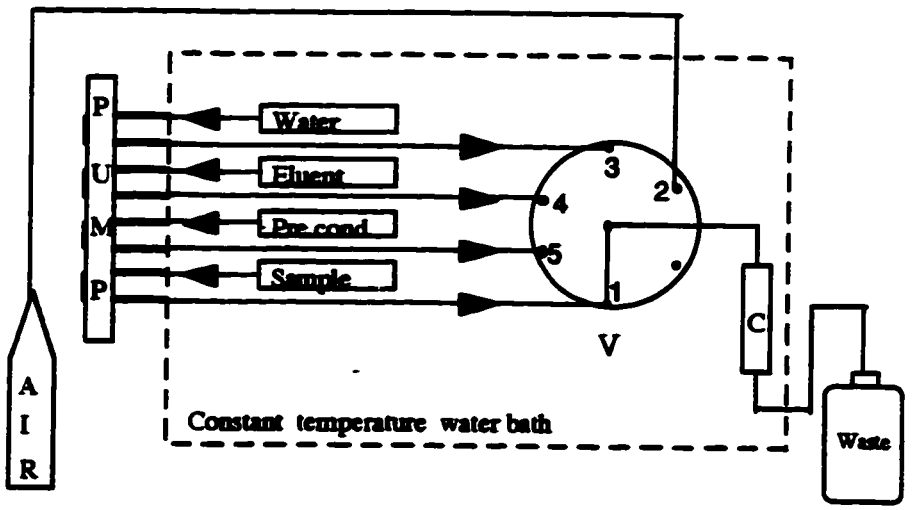

Figure 3.3 Schematic diagram of the single pass flow system with 15 mg resin colum. (V) six-port rotary valve. (C) 15 mg resin column. The figure shows the valve position during equilibration step. Pump is a peristaltic pump.

3.1.2.2.b Recycle flow for small column

The main difference between the single pass flow system shown in Figure 3.3 and the recycle flow system shown in Figure 3.4 is that in Figure 3.4 the sample solution, which comes from the sample cell, is recycled back to the cell. The cell is a polyethylene beaker with a Teflon lid. Through holes in the lid could be placed a silver (I) ion-selective electrode (A), a double junction reference electrode (B), a thermometer (T), a specially made glass capillary rod (1.0 mm bore size and 8.0 cm long) which can hold a 2 cm diameter 0.45 μm Nylon 66 membrane filter (D) and a Teflon sample return tube (E). The cell is placed in a 25.0 ± 0.1 °C jacketed water bath whose temperature is set by the constant temperature circulating bath. In this setup, free silver concentration can be measured simultaneously using both column equilibration and ion-selective electrode methods. The purpose of the threaded connector H in Figure 3.4 is to connect the column equilibration apparatus to the cell before each loading step and to disconnect it after each loading step. All valve positions are the same as described in the case of single pass flow system.

3.1.3 pH and Ion selective electrode systems

All potentiometric measurements of free silver ion concentration at 25.0 ± 0.1 °C were made with a Fisher Model 25 Accumet® pH/ion Meter with a silver ion-selective electrode (Orion, No. 9416BN), a double junction Ag/AgCl reference electrode (Orion, No. 90-02-00) with saturated silver chloride inner chamber filling solution (Orion cat. No. 90-00-02) and 10% KNO_3 outer chamber filling solution (Orion cat. No. 90-00-03), and a temperature probe (Fisher, cat. No. 13-620-16).

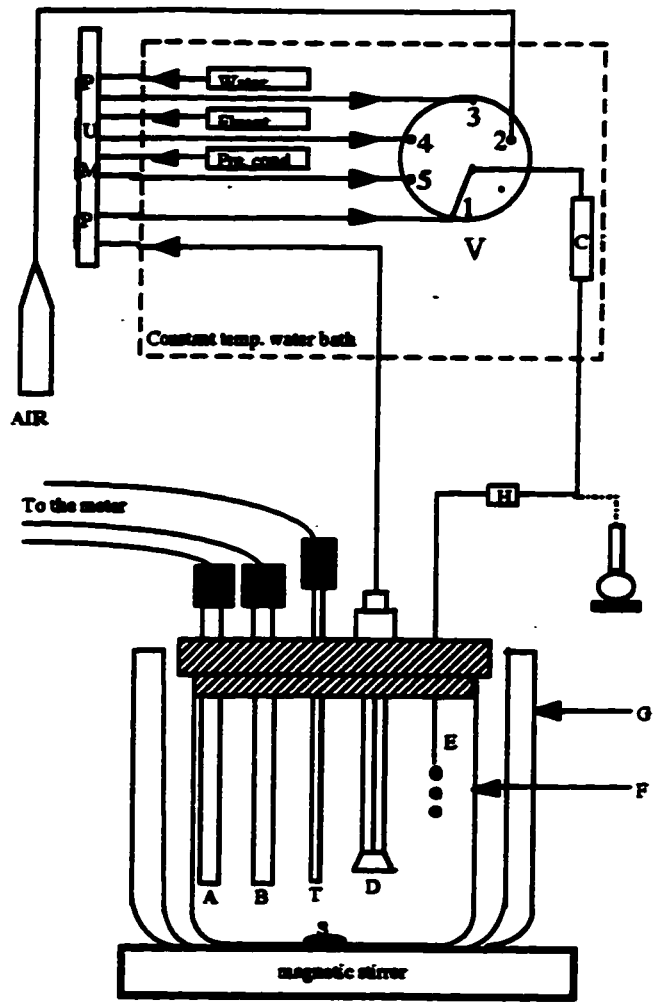

A	Indicator electrode (Ag^+)
B	Reference electrode
T	Temperature probe
D	On-line filter (0.45 μm)
E	Sample return tube
F	Cell
G	Jacket water bath
S	Stirring bar

Figure 3.4 Schematic diagram of the recycle flow system. Pumping and valve system is as in Figure 3.3.

All pH measurements were made with a Fisher Accumet® Model 350 expanded scale research pH Meter with a glass (Fisher, cat. No. 13-639-3) and calomel reference electrode (Fisher, cat. No. 13-620-51).

3.2 Reagents and chemicals

All chemicals used were of analytical-reagent grade, unless specified otherwise. A Nanopure™ system (Barnstead, model No. D 4751) was used throughout to purify water used for solution preparation and cleaning of equipment. All solutions were filtered with a 0.45 μm (Alltech No. 2024) nylon 66 membrane filter.

All silver standard and synthetic solutions were prepared using silver nitrate, (BDH). A 0.01 M stock solution was prepared by dissolving 0.42468 g of $AgNO_3$ salt in water to a volume of 250 ml. The stock solution was stored in a 250 ml polyethylene bottle, wrapped with aluminium foil.

Chloride was used as a ligand. Sodium chloride (BDH) stock solution (1.5 M NaCl) was prepared by dissolving 43.83 g of salt in water to a volume of 500 ml.

Sodium nitrate (BDH) was used as ionic strength adjuster. A stock solution of 3 M $NaNO_3$ was prepared by dissolving 254.97 g of salt in water to a volume of 1 L.

Sodium hydroxide (BDH) was used for pH adjustment and resin conditioning. Also hydroxide was used as a ligand. A stock solution of 3 M NaOH (CO_2 free) was prepared by dissolving 60.00 g of the base in water to a volume of 500 ml. The stock solution was stored in a 500 ml polyethylene bottle.

{N-[2-hydroxyethyl]piperazine-N'-[2-ethanesulfonic acid]}, HEPES (Sigma) was used as a buffering agent. A 0.01 M HEPES stock solution was prepared by dissolving 0.59575 g of the HEPES in about 200 ml of water, followed by addition of NaOH to bring the pH to about 7 before diluting to 250 ml.

Disodium salt of ethylenediaminetetraaceticacid, EDTA (BDH) was used as an eluent. A solution of 0.05 M EDTA was prepared by dissolving 9.306 g of salt in about 300 ml of water, followed by addition of NaOH to bring the pH to about 10 before diluting to 500 ml.

Nitric acid (BDH), 3 M HNO_3, was used for cleaning labware and the flow system. Hydrochloric acid, HCl (Anachemia) 0.2 M, 0.5 M, 1 M and 2 M and 99.8% methanol (Fisher) were used for resin conditioning.

3.3 Resin

The two resins used were both analytical grade Dowex 50W-X8 (J.T. Baker chemicals Co.)

strong acid type cation exchange resin in the H^+-form. One was 50-100 mesh, lot No. 30509 and the other was 100-200 mesh, lot No. 31404 with total exchange capacities of 5.0 meq g^{-1} and 5.1 meq g^{-1} (dry basis) respectively. The former was used in the large column and the latter in the small column.

The same procedure was used to condition both resins. About 10 g of resin was placed in a beaker of water. Fines were removed by repeated decanting of the suspension of resin in water until no more suspension was visible. The resin was then transferred to a glass column (2.3 cm id. and 30 cm long), which had a plug of glass wool as bed support above the stopcock.

In the column the resin was washed with water, then with small portions of 0.2 M, 0.5 M, 1 M and 2 M HCl until the effluent was colorless; followed by water wash. The resin was then converted to Na^+-form by washing with small portions of 0.2 M, 0.5 M, 1 M, and 2 M NaOH; followed by water wash. The resin was then washed with methanol to dissolve organic substances present as impurities. Finally , it was washed with water and air dried at room temperature. Both resins were stored in plastic bottles.

3.4 Procedures

3.4.1 Column operation

This section outlines the general procedure used to perform experiments using the column equilibration technique. Despite the differences between the flow systems, the procedure is common for all flow systems used in this work. The steps can be accomplished by manipulating appropriate valve positions in a given flow system.

Before starting an experiment, the system was first allowed to reach a constant temperature (25.0 ± 0.5 °C). This was accomplished by adjusting the temperature of the constant temperature circulating bath. The entire system was rinsed with water, then rinsed with 3 M HNO_3 except the column which was rinsed with the eluent (EDTA). The entire system was again rinsed with water. Finally, each line was flushed with appropriate reagent.

The desired reagent flow rate was set by using the peristaltic pump. The column was pre-conditioned by passing a pre-conditioning solution through the column to waste. This is called the pre-conditioning step. Sample solution containing silver was then passed through the column to waste for the period of time required to reach equilibrium. This is called the equilibration (loading) step. The time required to reach equilibrium (complete breakthrough) during the loading step was determined by studying equilibration (loading) curves. This is described in chapter 4. After the equilibration step, air was passed through the column for 1 minute to remove interstitial sample solution (the air line is not shown in Figure 3.2). The column was then washed with water. This is called wash step, during which the remaining interstitial sample solution is flushed to waste. The eluent was then passed through the column in order to desorb the sorbed silver (elution step). The eluate was collected at the exit of the column in a clean volumetric flask whose volume

corresponds to the volume of eluent required for complete elution. Finally, another water wash step was performed before starting another cycle.

The content of the volumetric flask was analyzed (analysis step) using atomic absorption spectrophotometry (AAS) as described below. In some cases appropriate dilution was made such that the signal obtained fell within the linear range of the AAS response. The concentration of silver in the resin phase (eluted silver) was quantitated by aspirating silver standard solutions. The composition of the standard solutions is the same as that of the eluent except that the concentration of silver in each standard solution is known.

3.4.2 ISE potentiometric measurement of free silver ion concentration, $[Ag^+]$

For the measurement of free silver ion concentration using ISE potentiometry, measurement and electrode cleaning procedures from reference [74] were adapted. The pH/ion meter was first calibrated using appropriate standard solutions selected from the series of silver standards used to calibrate the ion-exchange column equilibration system. The calibration procedure used was as follows:

About 100 ml of the most dilute standard solution was placed in a polyethylene beaker. The beaker was suspended in a jacketed water bath at 25.0 ± 0.1 °C. The electrodes and the temperature probe were then immersed in the solution. The solution was stirred using a magnetic stirrer. Measurements were made when the meter reading stabilized. After a measurement the electrodes and temperature probe were cleaned by rinsing with a stream of water from a wash bottle, blotted dry with a tissue and immersed in another standard solution of higher concentration than the previous one. A typical calibration curve is shown in Figure 3.5. The calibration curve, which is described by the equation

$$Y = 445.6 + 59.0\,X \qquad \text{..... 3.1}$$

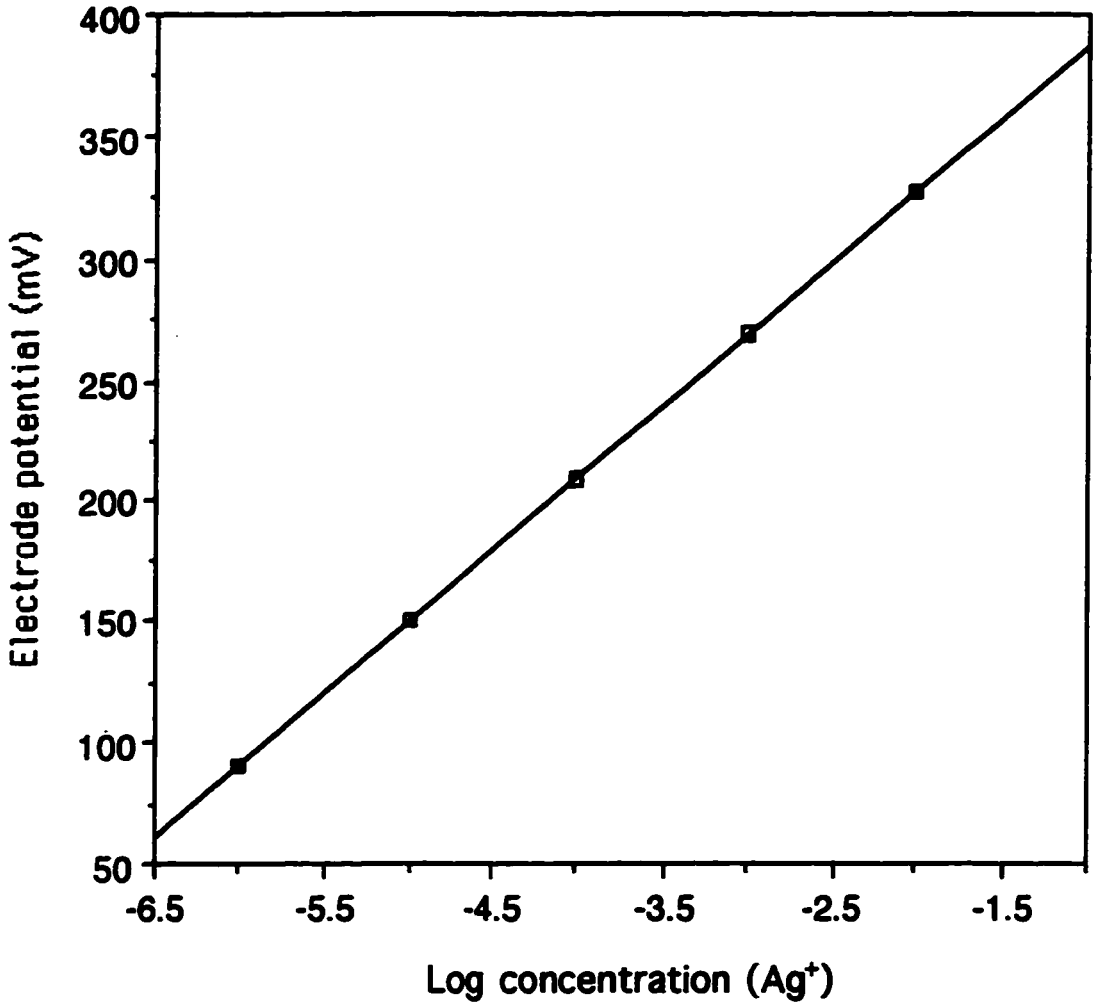

Figure 3.5 Linear region of the ISE calibration curve for silver standard solutions in 0.3 M $NaNO_3$, buffered at pH 7.

with correlation coefficient of unity (R^2 = 1.00), is linear down to 1 x 10^{-6} M Ag^+, (where Y = electrode potential in mv and X = log [Ag^+]). After calibrating the meter, the electrodes were in turn immersed in solutions of same total ionic strength as the standards but unknown silver ion concentration. Silver ion concentration in moles per liter was read directly from the meter. When not in use for a short time, the electrodes were stored in double deionized water.

3.4.3 AAS - measurement of silver concentration

All samples (eluate) were analyzed using atomic absorption spectrophotometry (AAS). A Varian Spectra AA-10 atomic absorption spectrometer was used under the following conditions:

wavelength	328.1 nm
lamp current	4 mA
spectral slit width	0.5 nm
aspiration rate	5 ml $min.^{-1}$
mode	Absorbance
signal	peak height
integration time	3 sec
acetylene pressure	1.5 psig
air pressure	3.5 psig
flame	oxidizing (lean blue)
recorder type	computer acquisition of data

The calibration procedure used for the measurement of silver using AAS was as follows:

Silver standard solutions of identical composition with sample solutions whose concentrations were to be determined were prepared and stored in 250 ml plastic bottles.

These standard solutions were used to calibrate the AAS before aspirating samples of unknown silver concentration. A typical AAS calibration curve is shown in Figure 3.6. The calibration curve which is described by equation

$$Y = 2.45 \times 10^{-3} + 1.06 \times 10^{-2} X \quad \text{..... 3.2}$$

with correlation coefficient (R^2) of 0.999, is linear in the concentration range 0.37 - 37.1 μmol l^{-1} Ag^+, (where Y = absorbance and X = concentration of silver in μmol l^{-1}).

3.4.4 Cleaning of equipment and flow systems

All labware used for solution handling was first cleaned with detergent (labware which was in contact with AgCl(s) was first soaked in 6 M ammonia), then thoroughly rinsed with distilled water. This was followed by soaking overnight in 3 M HNO_3, rinsing thoroughly before use with nano pure water and drying in a dust free atmosphere.

The flow systems were cleaned by pumping 3 M HNO_3 through all lines, and then washing with nano pure water. The procedure was repeated whenever necessary.

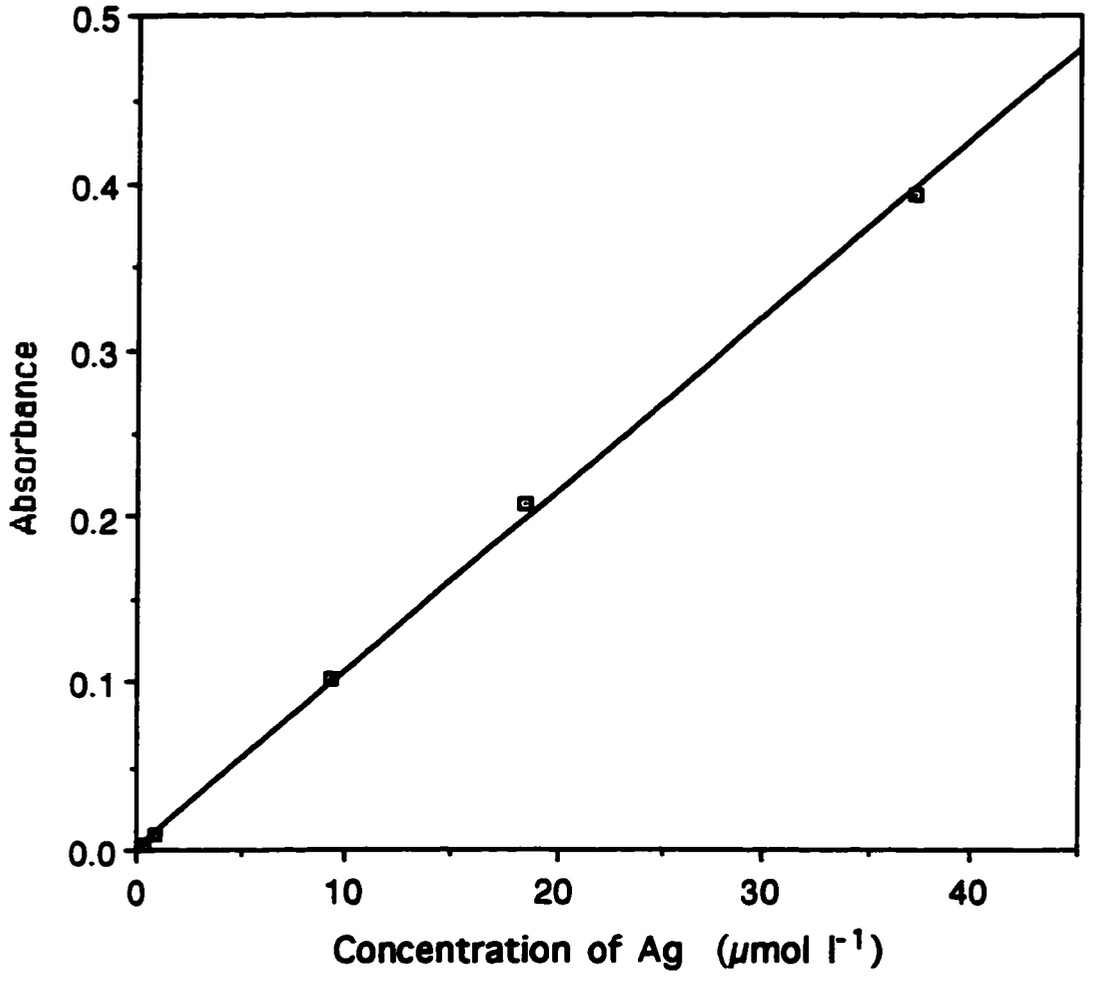

Figure 3.6 Linear region of the AAS calibration curve for silver standard solutions in 0.05 M EDTA, buffered at pH 10.

CHAPTER FOUR

CHARACTERIZATION OF THE ION-EXCHANGE COLUMN EQUILIBRATION-AAS TECHNIQUE FOR FREE SILVER ION DETERMINATION

4.1 Introduction

Before doing any studies with the column equilibration technique, various experimental parameters need to be characterized and optimized. This can be accomplished by conducting breakthrough, elution, equilibration time (loading) and sorption isotherm studies aimed at understanding the performance of the system under certain pre-selected conditions. By manipulating the conditions, optimum operating conditions, suitable for the determination of the metal ion of interest, can be obtained.

4.2 Experimental

The apparatus and general operating procedures are described in Chapter 3 above. Only details specific to the present studies are mentioned here.

4.2.1 Apparatus

One of the columns in the large column flow system, Figure 3.2, was used for all experiments which are described in this chapter. The small column, single pass flow system, Figure 3.3, was also used. The variable speed peristaltic pump was adjusted to provide the required flow rates.

4.3 Breakthrough studies

4.3.1 Introduction

The purpose of doing a breakthrough study is to determine the flow time or volume of sample solution required for complete breakthrough i.e. when the concentration of sample solution coming out of the column (effluent) is equal to the concentration of sample solution entering the column (influent).

4.3.2 Procedure

The column was washed and pre-conditioned as described in section 3.4.1, above. Sample solution containing a given concentration of silver was passed through the column at a flow rate of 7 ml $min.^{-1}$. The effluent was continuously monitored as the system approached equilibrium. This was accomplished by collecting fractions of the effluent at the column exit in volumetric flasks (5 ml for 15 mg column and 10 ml for 1.4 g column) over some period of time. The concentration of silver both in the collected effluent and in the initial sample solution (influent) were determined by AAS. Some of the samples were diluted prior to being aspirated into the AAS. A breakthrough curve, which is a plot of the ratio of concentration of silver in the effluent (Ce) and influent (Ci), (i.e. Ce/Ci) against time was constructed.

4.3.3 Results and discussion

Figure 4.1 shows the breakthrough curves obtained on the large column flow system, Figure 3.2, for two different concentrations of silver (1.85 μmol l^{-1} and 46.35 μmol l^{-1} Ag^{+}) in a solution of 0.2 M total ionic strength (0.2 M $NaNO_3$). The data are given in Table B.1

(Appendix B). Figure 4.1 shows that initially, before 60 minutes, Ce/Ci < 1. This is because the resin in the column is sorbing silver ions from the sample solution. As more sample solution is passed through the column, the ratio Ce/Ci approaches 1 (about 60 minutes). Finally, the influent and effluent concentrations become approximately equal and Ce/Ci is close to 1; i.e. complete breakthrough has been achieved and no more silver ions are removed from the sample solution as it passes through the resin bed. This is seen as a plateau in Figure 4.1. Under these conditions (flow rate 7 ml $min.^{-1}$ and ionic strength of 0.2 M) the times required to reach complete breakthrough are about 60 and 90 minutes for Ag^+ concentration of 46.35 and 1.85 μmol l^{-1}, respectively. The difference in breakthrough time is due to the difference in the distribution coefficient, λ_{Ag+}. This is evident from the displacement of the two curves which is observed in Figure 4.1. Ideally the two curves should be identical if λ_{Ag+} is the same; i.e. the concentrations under consideration are within the linear region of the sorption isotherm. The rate of migration of a species depends on the distribution coefficient of the species between the resin phase and the solution phase. The retardation is stronger when the fraction in the resin phase is large i.e. large λ_{Ag+}. Hence at concentrations where λ_{Ag+} is relatively small, breakthrough is achieved at relatively shorter times.

In order to reduce the time required for the system to reach complete breakthrough, a similar study was done at a higher ionic strength of 0.3 M. The results obtained are shown in Figure 4.2 and the data are given in Table B.2. Comparing Figure 4.1 (0.2 M $NaNO_3$) and Figure 4.2 (0.3 M $NaNO_3$) we see that the time for complete breakthrough has been reduced. This is because an increase in the concentration of the principal counter-ions, $[Na^+]$, is accompanied by decrease in the distribution coefficient, λ_{Ag+} of Ag^+ between the resin phase and the solution phase (see equation 2.2.4, Chapter 2). Therefore, less Ag^+ is

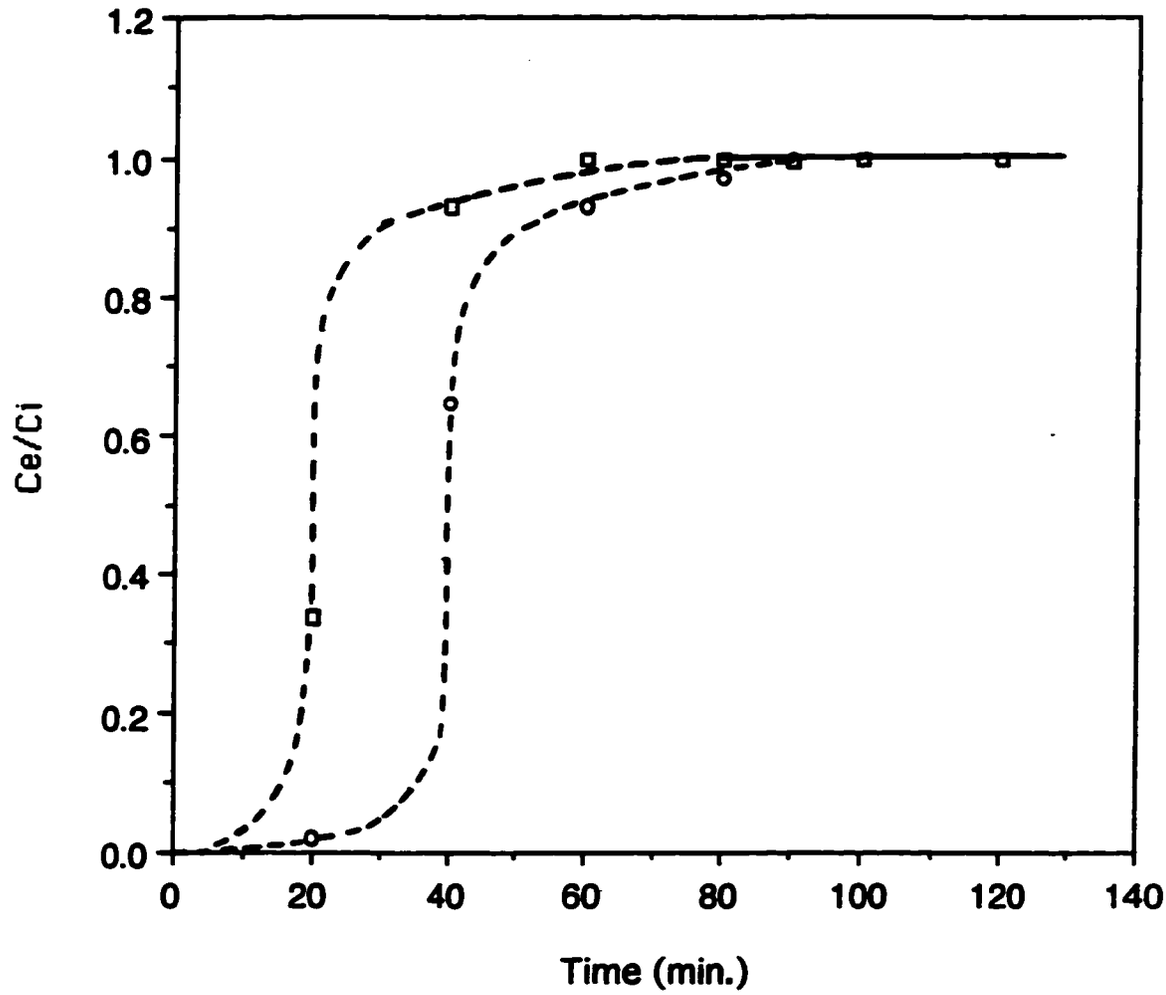

Figure 4.1 Breakthrough curves for 1.85 μmol l^{-1} and 46.35 μmol l^{-1} Ag^{+} solutions in 0.2 M $NaNO_3$ and pH 7 buffer. The solutions were loaded onto a 1.4 g resin column at a flow rate of 7 ml $min.^{-1}$. (○) 1.85 μmol l^{-1} and; (□) 46.35 μmol l^{-1} The dashed lines are estimated based on theoretical expectation of breakthrough curve shape. The data are shown in Table B.1

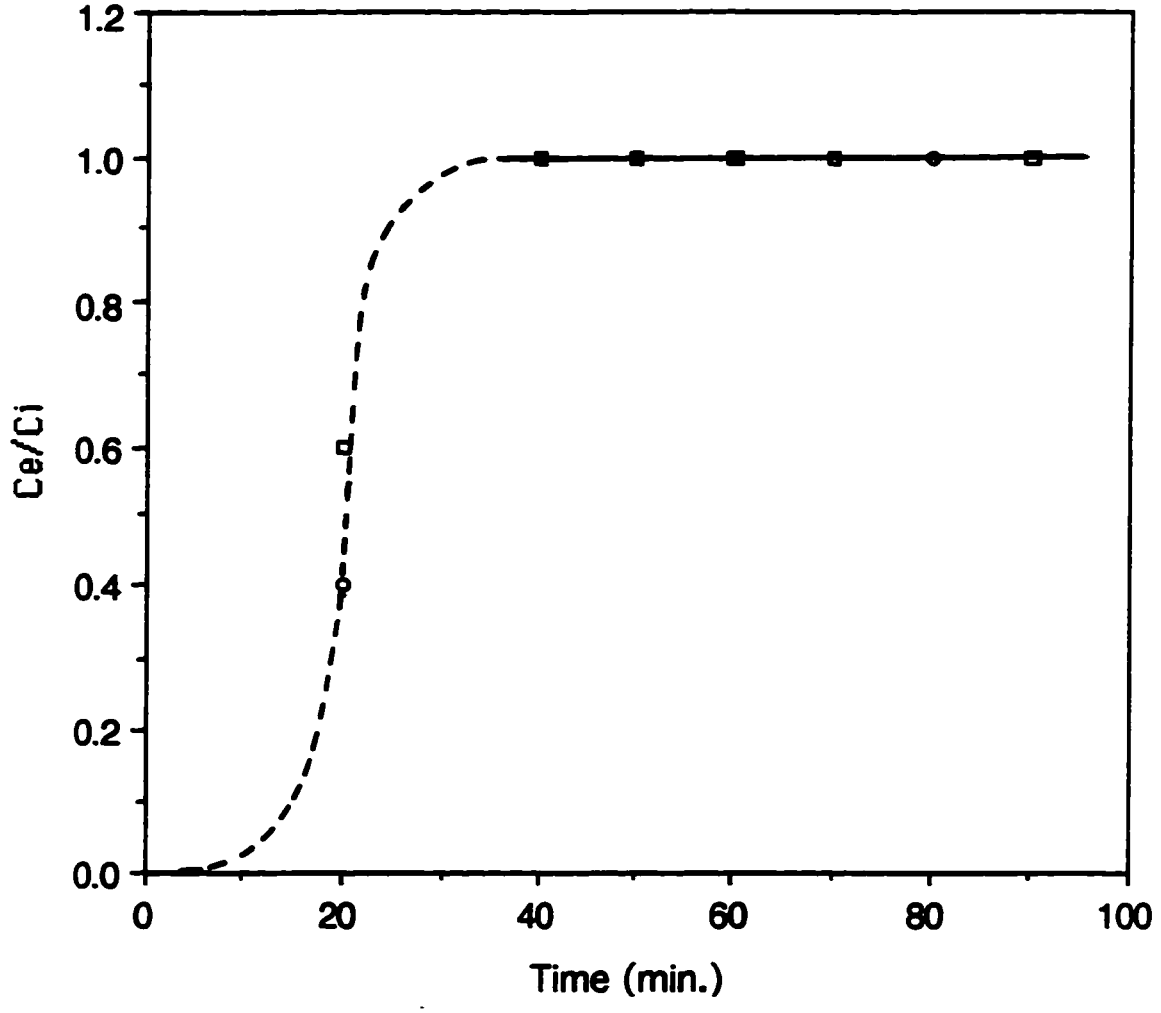

Figure 4.2 Breakthrough curves for 1.85 μmol l^{-1} and 46.35 μmol l^{-1} Ag^{+} solutions in 0.3 M $NaNO_3$ and pH 7 buffer. The solutions were loaded onto a 1.4 g resin column at a flow rate of 7 ml $min.^{-1}$. (○) 1.85 μmol l^{-1} and; (□) 46.35μmol l^{-1}. The dashed lines are estimated based on theoretical expectation of breakthrough curve shape. The data are shown in Table B.2.

sorbed onto the resin. Since λ_{Ag+} is relatively small, retardation is weak and thus, the time to reach complete breakthrough is reduced, provided that the system is not rate limited (see section 4.5.1, below).

The effect of [Na^+] on the breakthrough time can be clearly seen in Figures 4.3 and 4.4 in which data from Figures 4.1 and 4.2 are re-plotted. Figure 4.3 was obtained by plotting data from column two of Table B.1 and B.2 against time and Figure 4.4 by plotting data from column three of Tables B.1 and B.2 against time.

A breakthrough study was also done using a single pass flow system with a 15 mg micro-column, Figure 3.3. Sample solution containing 100 μmol l^{-1} of silver in 0.3 M $NaNO_3$ buffered at pH 7 was passed through the column at a flow rate of 7 ml $min.^{-1}$. The data are given in Table B.3. In Figure 4.5 these results are compared with those obtained using a 1.4 g resin column. Under these conditions i.e. 0.3 $NaNO_3$ M and flow rate 7 ml $min.^{-1}$, the time required to reach complete breakthrough was found to be about 2 minutes, which is much shorter than the approximately 40 minutes required on the 1.4 g resin column. This is because with the micro-column, the solution on its way through the resin bed gets into contact with relatively less layers of the exchanger particles than is the case of the 1.4 g resin column. Hence complete breakthrough is achieved much faster.

4.4 Pre-conditioning study

The purpose of pre-conditioning the resin column is to ensure that the solution in the column has similar composition (ionic strength and pH) as the sample solution to be loaded. In principle, pre-conditioning is not necessary in the column equilibration method, since the sample solution conditions the column itself if the sample is allowed to pass long enough and eventually equilibrium is achieved with the sample solution composition.

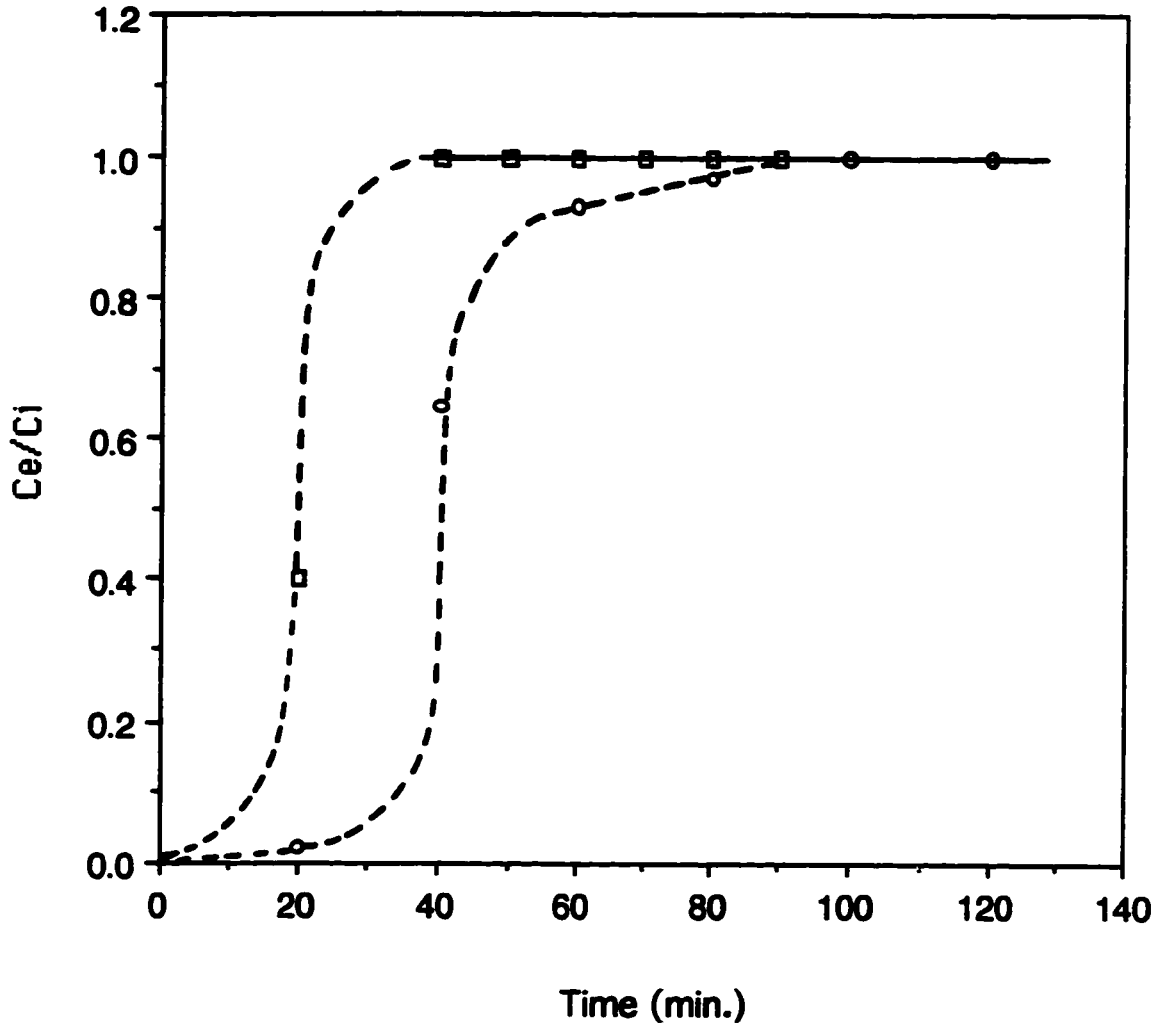

Figure 4.3 Breakthrough curves for 1.85 μmol l^{-1} Ag^{+} solution in 0.2 M and 0.3 M $NaNO_3$ and pH 7 buffer. The solutions were loaded onto a 1.4 g resin column at a flow rate of 7 ml $min.^{-1}$. (O) represent 0.2 M $NaNO_3$ and; (□) 0.3 M $NaNO_3$. The dashed lines are estimated based on theoretical expectation of breakthrough curve shape. The data are shown in Table B.1 and B.2.

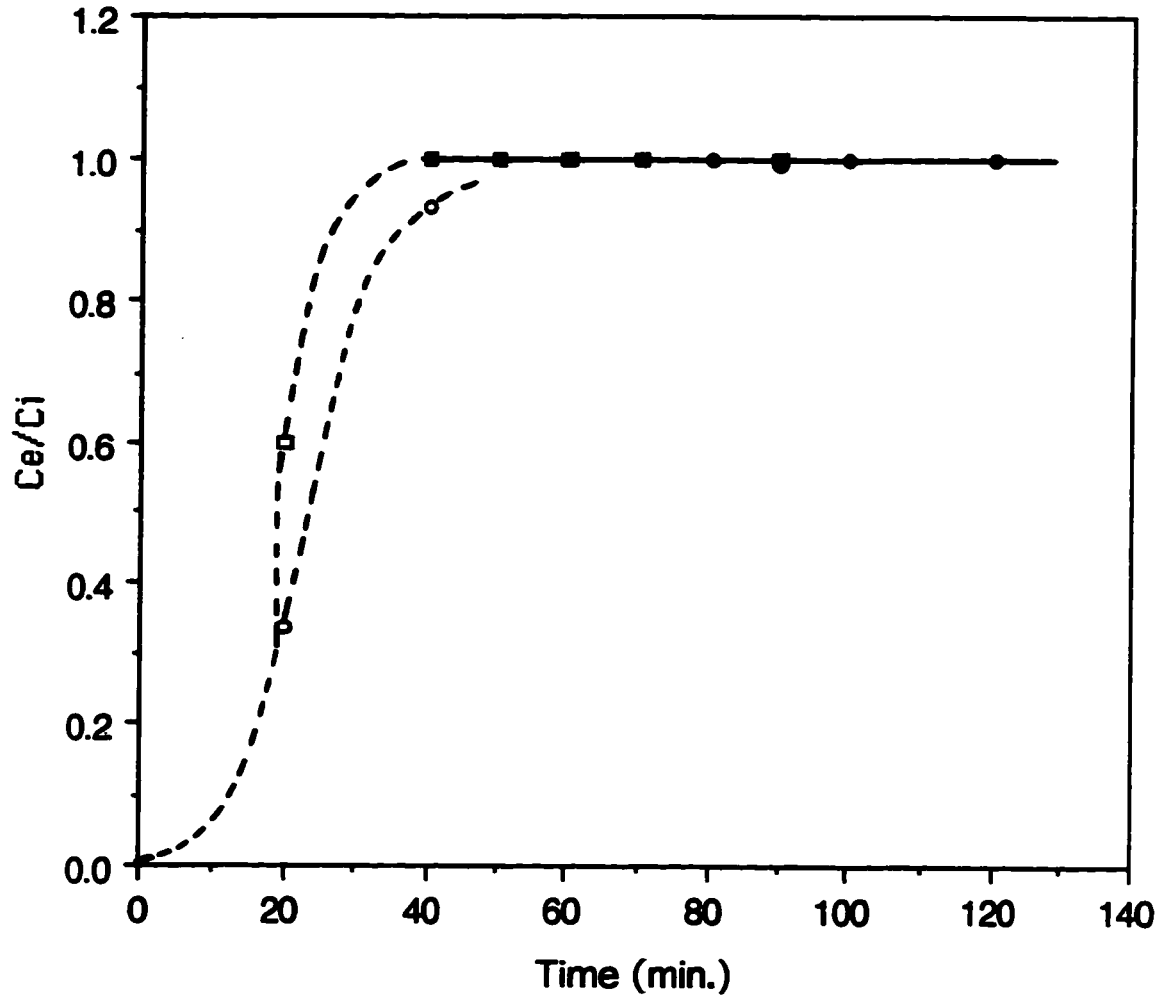

Figure 4.4 Breakthrough curves for 46.35 μmol l^{-1} Ag^{+} solution in 0.2 M and 0.3 M $NaNO_3$ and pH 7 buffer. The solutions were loaded onto a 1.4 g resin column at a flow rate of 7 ml $min.^{-1}$. (○) represent 0.2 M $NaNO_3$ and; (□) 0.3 M $NaNO_3$. The dashed lines are estimated based on theoretical expectation of breakthrough curve shape. The data are shown in Table B.1 and B.2.

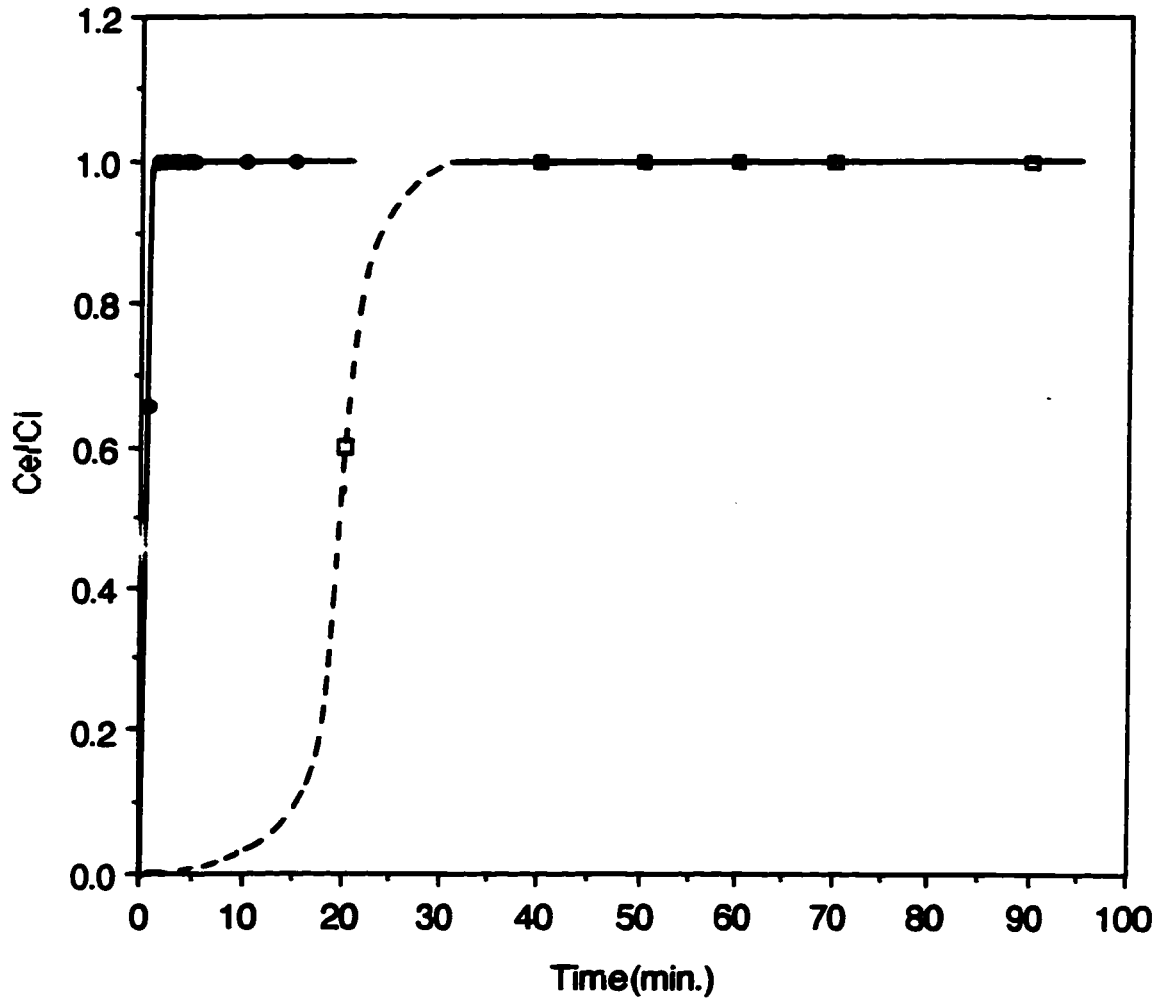

Figure 4.5 Comparison of breakthrough curves obtained by using 1.4 g (open squares) and 15 mg (closed circles) resin columns. The solutions 46.35 μmol l^{-1} and 100.0 μmol l^{-1} Ag^{+}, both in 0.3 M $NaNO_3$ and pH 7 buffer, were loaded onto 1.4 g and 15 mg columns, respectively. Both solutions were passed at a flow rate of 7 ml $min.^{-1}$. The dashed lines are estimated based on theoretical expectation of breakthrough curve shape. The data are shown in Tables B.2 and B.3.

The large column flow system, Figure 3.2, was used. The composition of pre-conditioning solution was the same as that of sample solution except no silver was added in the pre-conditioning solution. The resin was pre-conditioned for different lengths of time. After each pre-conditioning, the sample solution containing 10.0 μmol l^{-1} Ag^{+} in 0.3 M $NaNO_3$ buffered at pH 7 was passed for 40 minutes at a flow rate of 7 ml $min.^{-1}$. Sorbed silver was eluted with 0.04 M EDTA (pH 10) at flow rate of 2 ml $min.^{-1}$. Figure 4.6 shows a plot of μmols of silver eluted against pre-conditioning time.

From these results it is evident that, under these experimental conditions (especially loading time), pre-conditioning has no significant effect on the sorption of silver onto the resin. This is consistent with the principles of the method. Nevertheless, it was conservatively decided to pre-condition the columns throughout because during breakthrough and equilibration studies, shorter times were used to pass the sample solution through the column. The large column was pre-conditioned for 3 minutes and the small column for 1 minute.

4.5 Elution studies

4.5.1 Introduction

Elution studies are aimed at examining optimum operating conditions for desorbing all sorbed metal in order to determine it by AAS. Type of eluent, eluent concentration and eluent flow rate are among the parameters that affect elution efficiency.

EDTA (Y^{4-}) was chosen as an eluent because it forms stable negatively charged complexes with silver ion. During preliminary studies ammonia/ammonium buffer was added in the eluent. Neutral species like ammonia also form stable complexes with silver ion as follows:

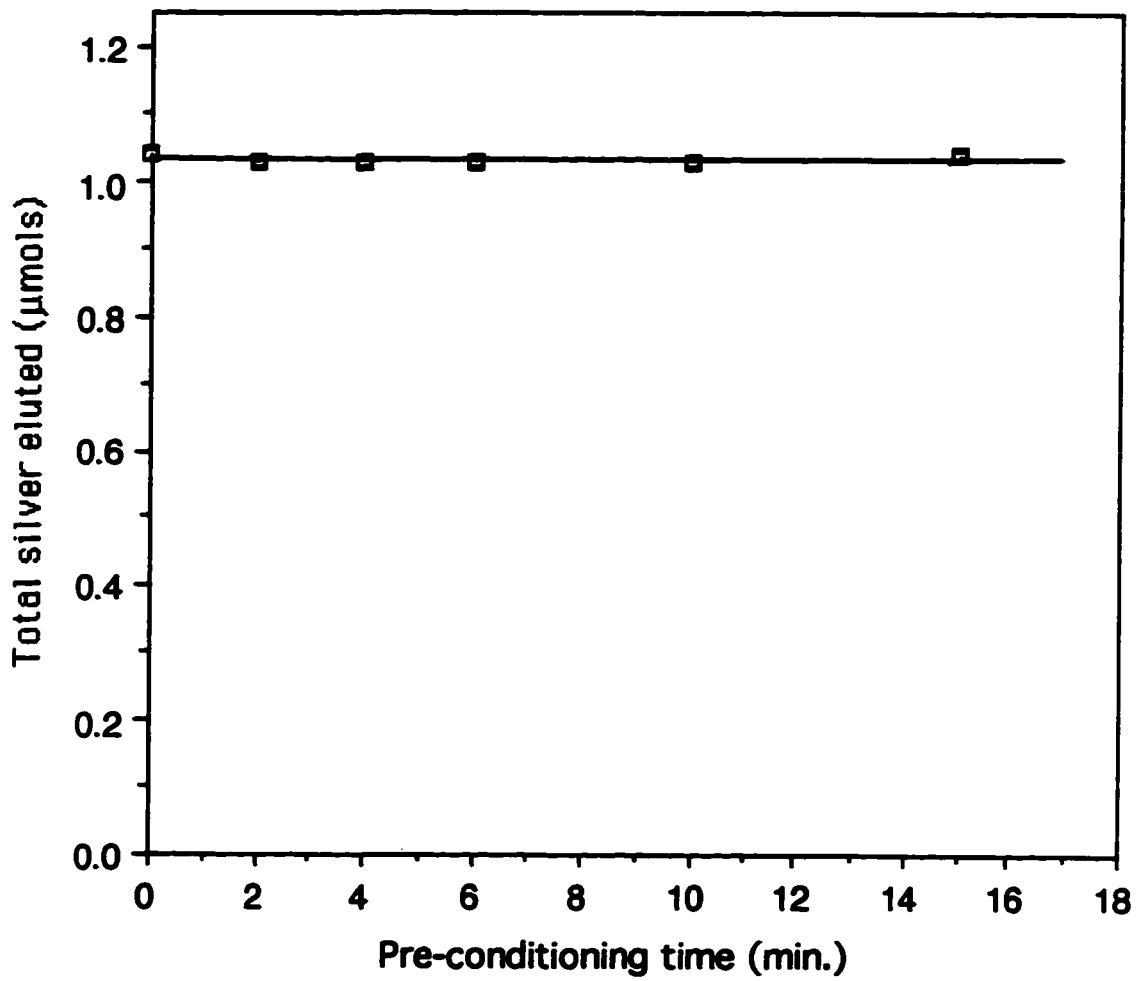

Figure 4.6 Resin pre-conditioning curve. The resin was pre-conditioned for different lengths of time with a solution containing 0.3 M $NaNO_3$ and pH 7 buffer. The solution containing 10.0 µmol l^{-1} Ag^+ in 0.3 M $NaNO_3$ and pH 7 buffer was loaded onto a 1.4 g resin column for 40 minutes. Both solutions were passed at a flow rate of 7 ml $min.^{-1}$. The eluent was 0.04 M EDTA at pH 10. The data are shown in Table B.4.

$$Ag^{+} + NH_3 \rightleftharpoons AgNH_3^{+}$$

$$Ag^{+} + 2NH_3 \rightleftharpoons Ag(NH_3)_2^{+}$$

but the complexes formed are positively charged. The presence of such silver containing species in the eluent is expected to reduce the elution efficiency due to sorption of the positively charged species during elution. This increases the distribution ratio of Ag^{+} between the resin phase and the eluent phase.

Elution of sorbed metal from the resin could be either reagent limited or desorption rate limited or a combination of both. If elution is reagent limited, then for a given time of flowing the eluent, the amount of silver eluted will strongly depend on the amount of reagent that has been passed through the column rather than on the flow rate at which the reagent is passed. When the amount of metal eluted is plotted against volume of eluent passed through the column, the elution curves at different flow rates will be identical. If time instead of volume is plotted on the horizontal axis, the curves will be displaced from one another along the time axis. Alternatively, when elution is desorption rate limited, plots of elution curves as moles eluted against time will be identical, but plots of elution curves as moles eluted against volume will be displaced from one another along the volume axis.

4.5.2 Procedure

The column was washed and pre-conditioned as described in section 3.4.1. Sample solution containing 92.7 μmol l^{-1} as Ag^{+} in 0.3 M $NaNO_3$ buffered at pH 7 was passed through the column at a flow rate of 7 ml $min.^{-1}$ for a sufficiently long time to reach equilibrium. (40 minutes for 1.4 g and 5 minutes for 15 mg resin column). Interstitial sample solution was removed by passing air, the column was washed with water and sorbed silver was eluted with 0.04 M EDTA at pH 10 (unless specified otherwise). The

eluate was continuously collected at the exit of the column in equal volume fractions as specified below.

4.5.3 Results and discussion

4.5.3.1 Effect of NH_3/NH_4^+ buffer on elution efficiency

The effect of $NH_3]/[NH_4^+$ buffer on elution efficiency was investigated by adding varying amounts of the buffer to the eluent (0.05 M EDTA at pH 10). The buffer ratio, $[NH_3]/[NH_4^+]$ was 5.6 in all cases. The large column flow system, Figure 3.2 was used. The eluent containing $NH_3]/[NH_4^+$ buffer was passed at a flow rate of 2 ml $min.^{-1}$. The eluate was continuously collected at the column exit in 10 ml fractions over a certain period of time, some 10 ml fractions were diluted before being aspirated to the AAS.

Figure 4.7 shows the results obtained and the data are given in Table B.5. Figure 4.7 shows that when no ammonia/ammonium buffer is present in the eluent, quantitative elution is achieved after a passage of 50 ml of eluent. However when the concentration of ammonia/ammonium buffer in the eluent is increased to 0.02 M and 0.05 M, quantitative elution is achieved after a passage of 70 ml and 110 ml of eluent respectively, i.e. as the concentration of ammonium buffer is increased elution efficiency decreases. Based on the results of this study, in all subsequent experiments no ammonia/ammonium buffer was added in the eluent. Instead the pH of the eluent was raised to pH 10 and the buffering effect of EDTA was utilized.

4.5.3.2 Effect of eluent flow rate on elution efficiency

The large column flow system, Figure 3.2, was used. The eluent, 0.04 M EDTA at pH 10, was used to elute sorbed silver at flow rates of 1, 2 and 10 ml $min.^{-1}$. The eluate was

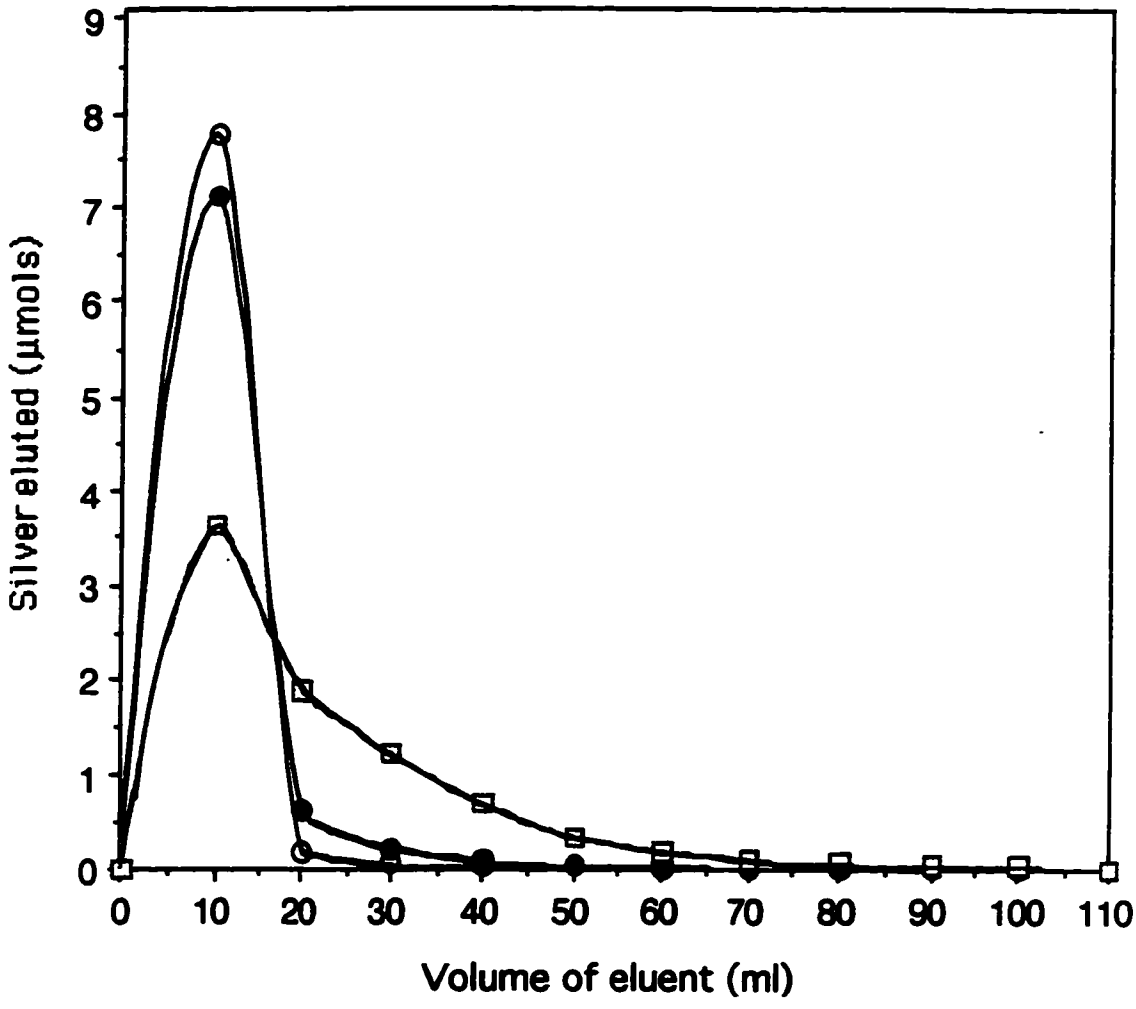

Figure 4.7 Elution profiles showing the effect of NH_3/NH_4^+ buffer on elution of Ag^+ from Dowex 50W-X8 strong acid cation exchanger. The solution containing 92.7 µmol l^{-1} Ag^+ in 0.3 M $NaNO_3$ and pH 7 buffer was loaded onto a 1.4 g resin column for 40 minutes at a flow rate of 7 ml $min.^{-1}$. The eluent was 0.05 M EDTA at pH 10, containing different amounts of $NH3/NH4^+$ buffer. (□) 0.05 M NH_3/NH_4^+; (●) 0.02 M NH_3/NH_4^+ and; (○) no NH_3/NH_4^+ added. The data are given in Table B.5.

collected in 10 ml fractions as described previously. The results obtained are shown in Figures 4.8 and 4.9 and the data are given in Tables B.6 through B.8.

The first column in each table is the time which the eluent is passed through the resin bed, it is calculated by dividing the total volume of eluent collected in ml by the flow rate in ml $min.^{-1}$. Figures 4.8 and 4.9 show plots of μmols of silver eluted against volume and time, respectively. When the curve is estimated by drawing a smooth line point-to-point the areas under the curves in Figure 4.8 should be approximately equal to one another. While the area under the curves in Figure 4.9 should be approximately proportional to the reciprocals of their respective flow rates (of course, the scarcity of points between 0 and 20 ml and between 0 and 20 minutes cause a large uncertainty in the shapes of the curves in these regions). The fact that the curves in Figure 4.8 are mostly, but not perfectly, superimposed (identical) and that those in Figure 4.9 are mostly, but not completely, displaced from one another suggests that elution is mostly, but not purely, reagent limited. Hence we can conclude that elution of silver from Dowex 50W-X8 50-100 mesh strongly depends on the supply of reagent (eluent) and to some extent depends on the rate of desorption (diffusion) of silver from the resin phase to the solution phase.

Specifically, the small desorption rate contribution is evident from the fact that increasing the eluent flow rate to 10 ml $min.^{-1}$ results in high dispersion (Figure 4.8). This is a result of desorption rate dependency because as the eluent flow rate is increased, the eluent has less time in contact with the resin. Hence relatively less silver has desorbed by that time. If elution in shorter time is desired, the eluent has to be passed at a faster flow rate (Figure 4.9), but, if elution in a smaller volume is desired then the eluent has to be passed at a slower flow rate, (Figure 4.8). For the best compromise of time and volume, in all subsequent studies it was decided to pass the eluent at a flow rate of 2 ml $min.^{-1}$

After equilibrating the resin with a 92.7 μmol l^{-1} Ag^{+} solution, elution with 0.04 M EDTA at pH 10 and a flow rate of 2 ml $min.^{-1}$ was quantitative after passage of about 50 ml

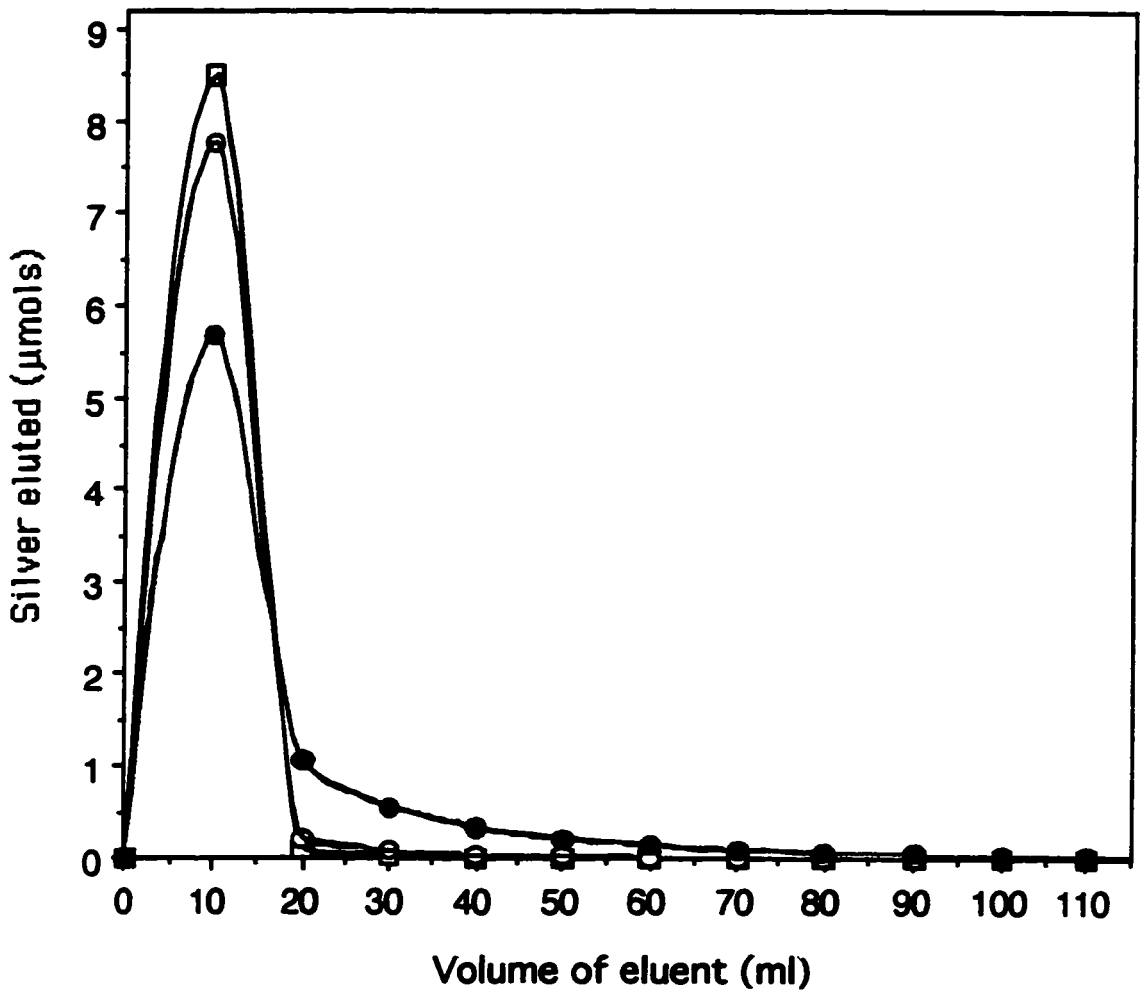

Figure 4.8 Elution profiles showing the effect of eluent flow rate on elution of Ag^+ from Dowex 50W-X8 strong acid cation exchanger. The solution containing 92.7 µmol l^{-1} Ag^+ in 0.3 M $NaNO_3$ and pH 7 buffer was loaded onto a 1.4 g resin column for 40 minutes at a flow rate of 7 ml $min.^{-1}$. The eluent was 0.04 M EDTA at pH 10. (●) eluent flow rate 10 ml $min.^{-1}$; (○) eluent flow rate 2 ml $min.^{-1}$ and; (□) eluent flow rate1 ml $min.^{-1}$. The data are given in Tables B.6 through B.8.

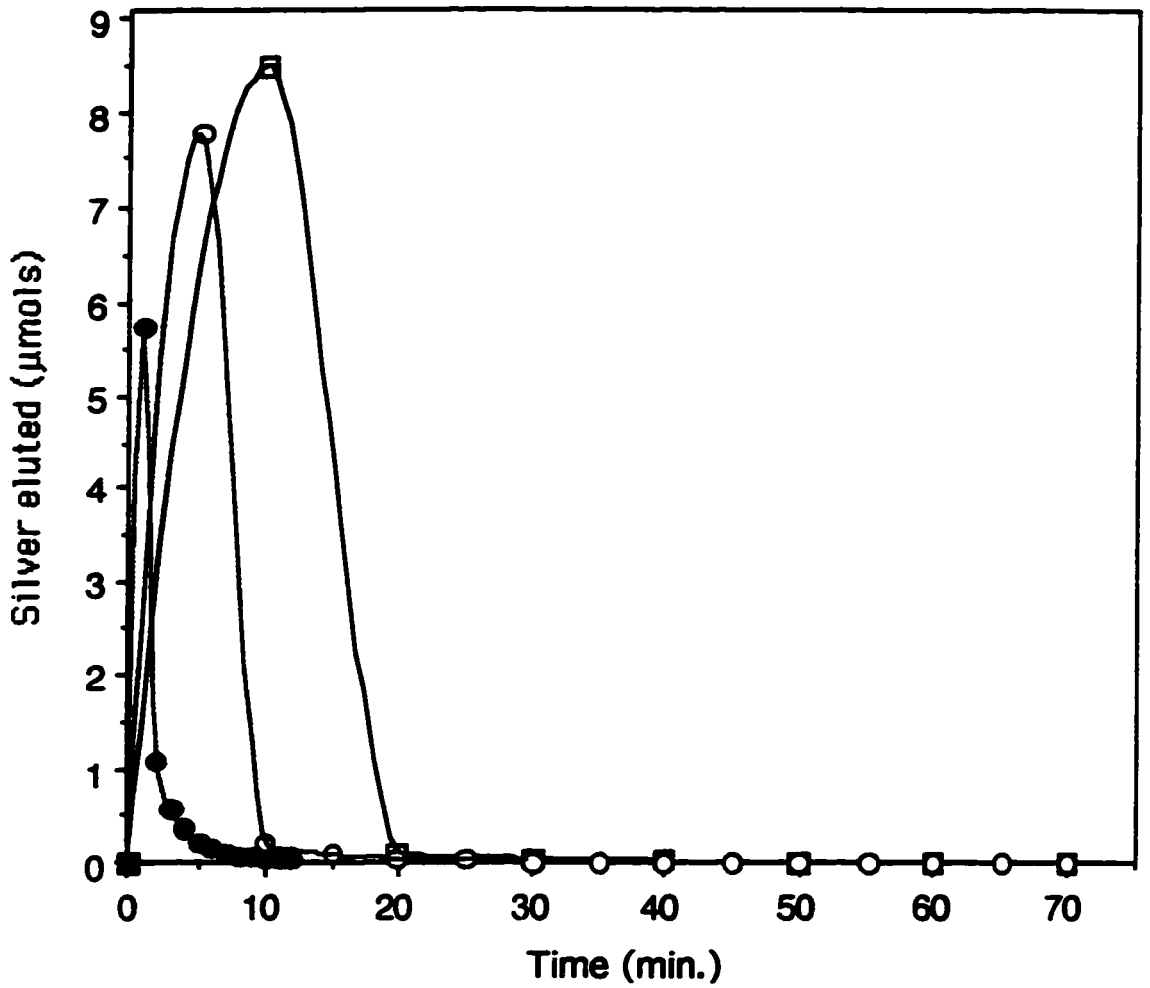

Figure 4.9 Elution profiles showing the effect of eluent flow rate on elution of Ag^+ from Dowex 50W-X8 strong acid cation exchanger. The solution containing 92.7 µmol l^{-1} Ag^+ in 0.3 M $NaNO_3$ and pH 7 buffer was loaded onto a 1.4 g resin column for 40 minutes at a flow rate of 7 ml $min.^{-1}$. The eluent was 0.04 M EDTA at pH 10. (●) eluent flow rate of 10 ml $min.^{-1}$; (O) eluent flow rate of 2 ml $min.^{-1}$ and; (□) eluent flow rate of 1 ml $min.^{-1}$. The data are given in Tables B.6 through B.8.

of the eluent (Figure 4.8). According to equation 2.2.5, Chapter 2, when less concentrated solutions of Ag^+ are loaded onto the resin column relatively less silver will be sorbed as RAg. An experiment was conducted to examine if volumes less than 50 ml could be used to elute all sorbed silver. Solutions containing $1x10^{-7}$ M, $1x10^{-8}$ M and, $5x10^{-9}$ M Ag^+ were passed in turn through the column at a flow rate of 7 ml $min.^{-1}$. In this case the eluent (0.04 M EDTA at pH 10) was continuously collected in 5 ml fractions. The results obtained are shown in Figure 4.10 and the data are given in Table B.9.

From Figure 4.10 it is evident that volumes of eluent less than 50 ml could be used to quantitatively elute all sorbed silver from dilute solutions of Ag^+ loaded onto the column. This observation is consistent with the fact that, since elution strongly depends on the supply of eluent, with a much smaller amount of silver sorbed, less eluent is needed for complete elution.

4.5.3.3 Effect of eluent concentration on elution efficiency

In the previous section, it has been demonstrated that elution efficiency depends more on the rate of supply of reagent (amount of eluent) than on the mass transfer rate of reagent. Therefore, an increase in the concentration of the eluent is expected to increase the elution efficiency at a given flow rate.

An experiment was conducted to investigate this effect. The large column flow system, Figure 3.2 was used. The eluent concentrations investigated were 0.02 M, 0.04 M and 0.08 M EDTA, all at pH 10. The eluent was passed at a flow rate of 2 ml $min.^{-1}$. The eluate was collected in 10 ml fractions as previously described.

The results obtained are shown in Figure 4.11 and the data are given in Table B.10. Figure 4.11 reveals that concentration of eluent has some effect on elution efficiency. As the eluent concentration is increased from 0.02 M to 0.04 M EDTA, the volume of eluent required for quantitative elution of silver from the resin decreases from 90 ml to 50 ml.

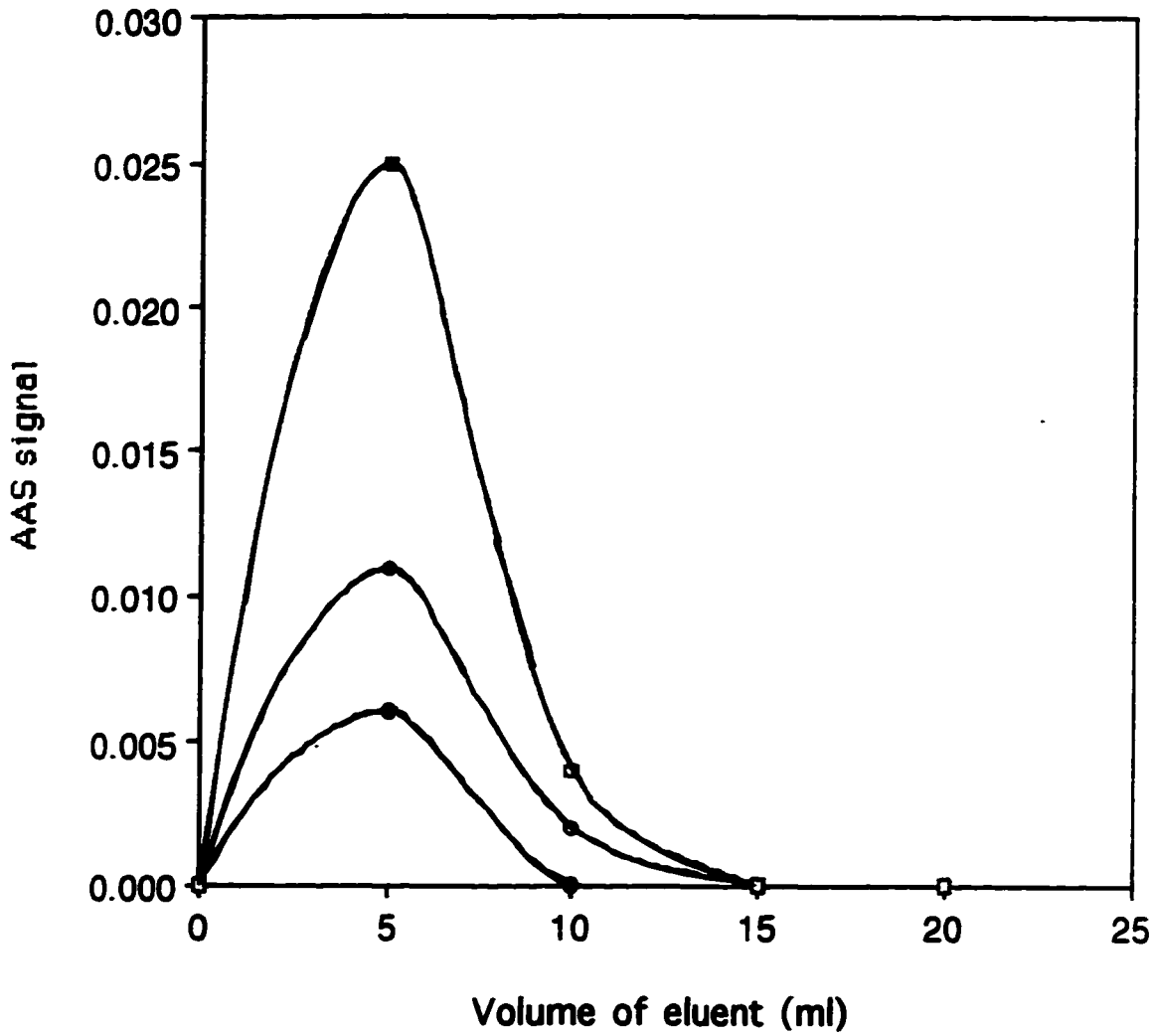

Figure 4.10 Elution profiles for different low concentrations of Ag^+ in 0.3 M $NaNO_3$ and pH 7 buffer. The solutions were loaded onto a 1.4 g resin column for 40 minutes at a flow rate of 7 ml $min.^{-1}$. The eluent was 0.05 M EDTA at pH 10. Each fraction represents 5 ml of eluent. (●) C_{Ag+} = $5x10^{-9}$ M; (○) C_{Ag+} = $1x10^{-8}$ M and; (□) C_{Ag+} = $1x10^{-7}$ M. The data are given in Table B.9.

The dispersion, which is evident as tailing, is higher for 0.02 M EDTA due to limited reagent. However, over 0.04 M EDTA no significant decrease in the eluent volume is observed i.e. a concentration limit has been reached where an increase in concentration of eluent is not accompanied by decrease in volume of eluent needed for quantitative elution. Thus under these conditions elution efficiency is no longer reagent limited but is, rather, desorption rate limited. In subsequent studies, elution with 0.05 M EDTA at a flow rate of 2 ml $min.^{-1}$ was used.

4.5.3.4 Elution study with a 15 mg resin column

An elution study was also done with a micro-column (15 mg resin column), Figure 3.3, to determine the volume of eluent needed for quantitative elution of sorbed silver. Solutions of $1x10^{-6}$ M, $1x10^{-5}$ M and $1x10^{-4}$ M Ag^+ were equilibrated, in turns, with the 15 mg resin column using the procedure described previously. An eluent 0.05M EDTA at pH 10 was passed at a flow rate of 2 ml $min.^{-1}$. Eluted silver was continuously collected in 5 ml fractions as described previously. The results obtained are shown in Figures 4.12 and the data are given in Table B.11.

For a $1x10^{-4}$ M Ag^+ solution, quantitative elution was achieved after the second 5 ml fraction. This fraction contains only about 0.5% of the total silver eluted. However, for both $1x10^{-5}$ M and $1x10^{-6}$ M Ag^+ solutions, quantitative elution was achieved after the first 5 ml fraction. The amount of Ag^+ present in the second 5 ml fraction could not be detected. For all subsequent experiments with the micro-column 5 ml of eluent was used for Ag^+ concentration of $1x10^{-5}$ M and less, 10 ml was used for Ag^+ concentration of $1x10^{-5}$ M to $1x10^{-4}$ M. For Ag^+ concentrations greater than $1x10^{-4}$ M larger volumes of eluent were used and extra 5 ml fractions were collected to check if elution was quantitative.

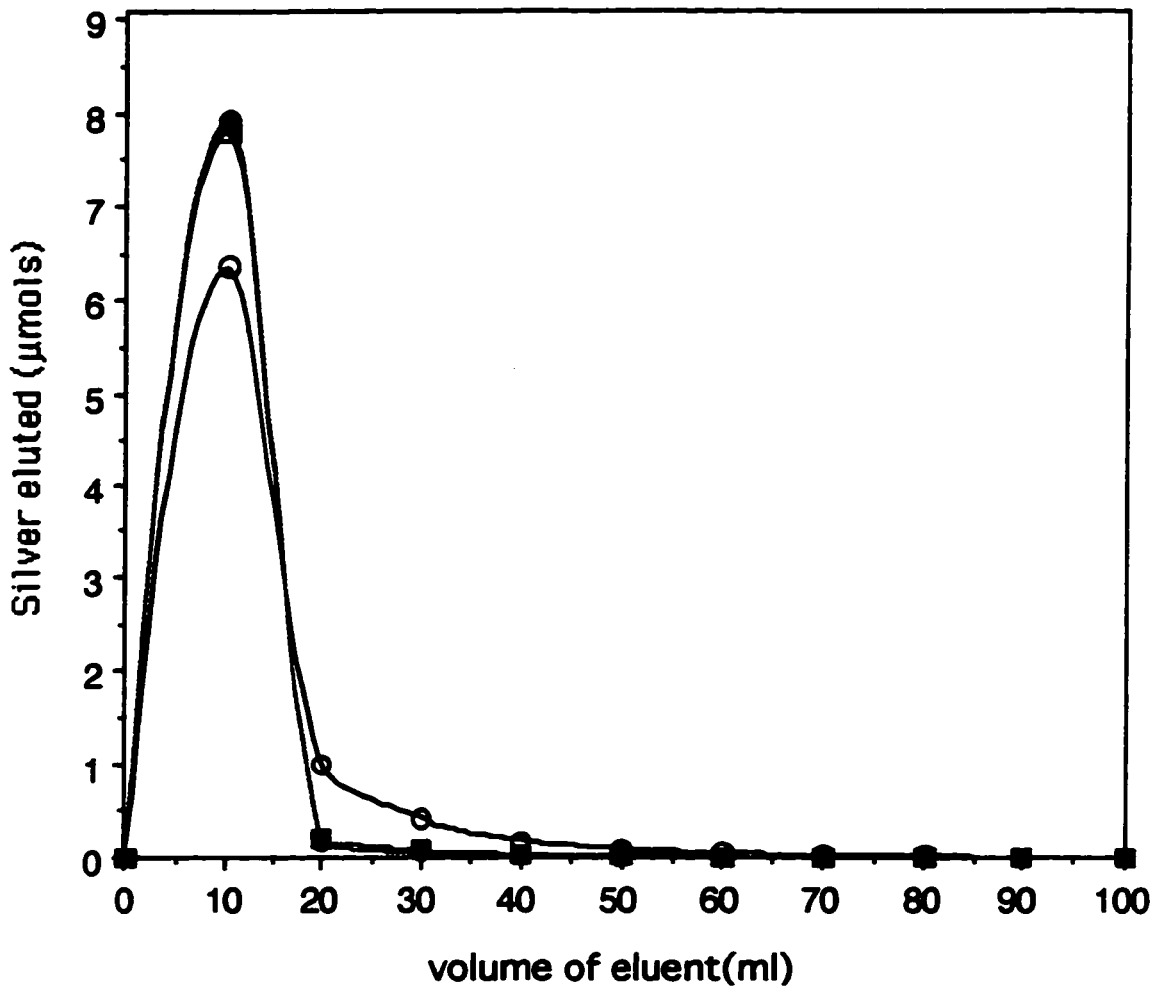

Figure 4.11 Elution profiles showing the effect of eluent concentration on elution of Ag^+ from Dowex 50W-X8 strong acid cation exchanger. The solutions containing 92.7 µmol l^{-1} Ag^+ in 0.3 M $NaNO_3$ and pH 7 buffer were loaded onto a 1.4 g resin column for 40 minutes at a flow rate of 7 ml $min.^{-1}$. Different concentration of eluent (EDTA) at pH 10 were used for elution. The eluent was passed at a flow rate of 2 ml $min.^{-1}$. (●) 0.08 M EDTA; (□) 0.04 M EDTA and; (○) 0.02 M EDTA. The data are given in Table B.10.

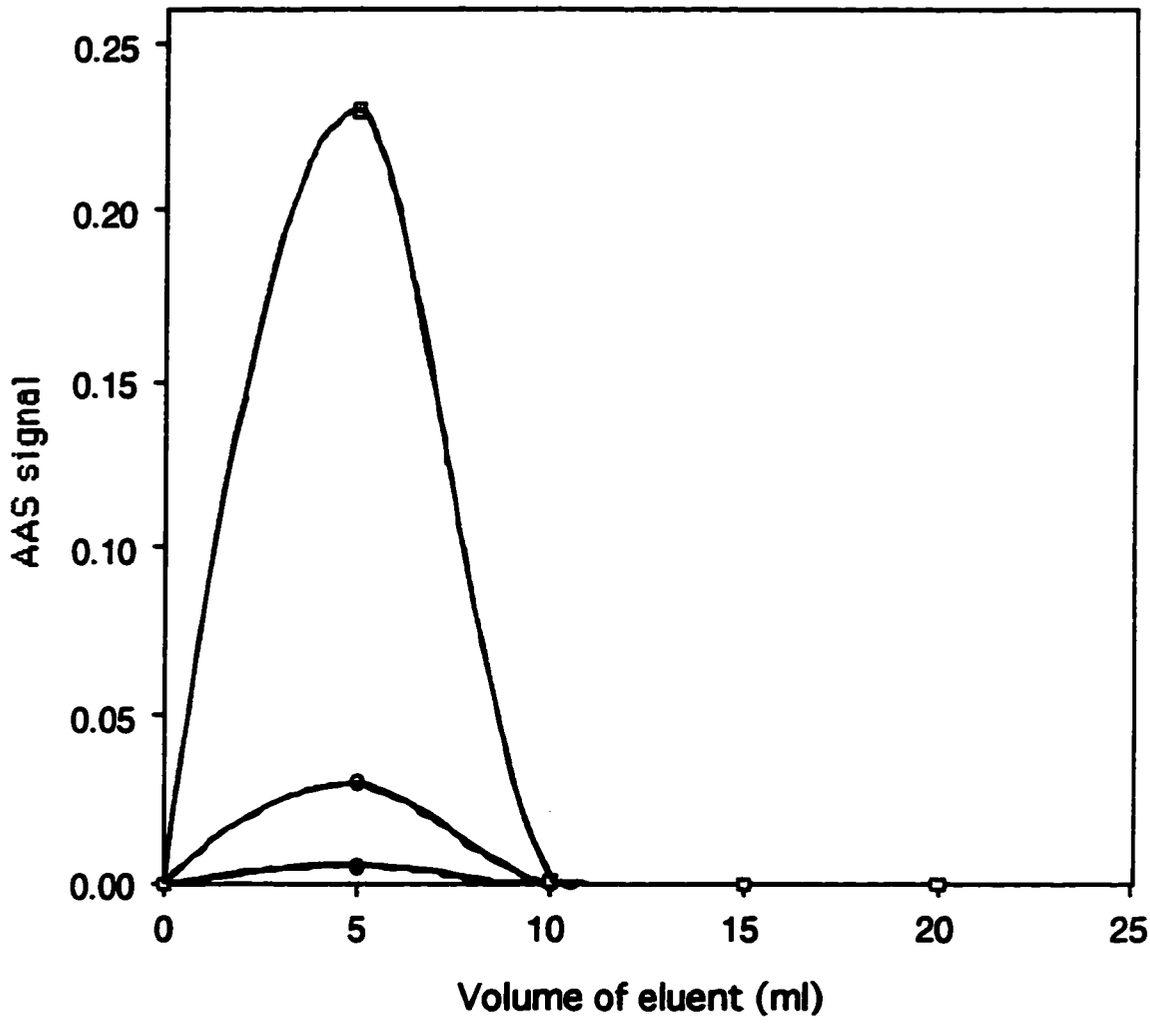

Figure 4.12 Elution profiles for different concentrations of Ag^+ in 0.3 M $NaNO_3$ and pH 7 buffer. The solutions were loaded onto a 15 mg resin column for 5 minutes at a flow rate of 7 ml $min.^{-1}$. The eluent was 0.05 M EDTA at pH 10. Each fraction represents 5 ml of eluent. (●) $C_{Ag+} = 1x10^{-6}$ M; (○) $C_{Ag+} = 1x10^{-5}$ M and; (□) $C_{Ag+} = 1x10^{-4}$ M. The data are given in Table B.11.

4.6 Equilibration (loading) studies

4.6.1 Introduction

Among the requirements of the column equilibration technique is attainment of complete equilibrium between the resin phase and the sample solution. Complete equilibrium could be different from breakthrough because, experimentally, complete breakthrough can appear to be achieved before equilibrium is reached. This is so in cases where loading of analyte is rate limited. Therefore it is necessary to determine accurately how long the sample solution has to be passed through the resin column until complete equilibrium is attained, i.e. no further sorption of analyte is occurring. This can be accomplished by performing an equilibration (loading) study in which the amount of analyte sorbed by the resin is measured as a function of loading time or volume.

4.6.2 Procedure

A series of equilibration experiments were conducted using both large column flow system, Figure 3.2, and small column flow system, Figure 3.3. The column was washed and pre-conditioned as described in section 3.4.1. Sample solution containing 9.27 μmol l^{-1} Ag^{+} in 0.3 M $NaNO_3$ buffered at pH 7.0 was passed through the column at a flow rate of 7 ml $min.^{-1}$ for a given length of time (the loading time), after which the sorbed analyte was eluted and the concentration of silver in the eluate was determined by AAS. This procedure was repeated with various loading times (normally from shorter to longer times) in order to construct the equilibration curve, which is a plot of moles of metal sorbed versus time or volume.

4.6.3 Results and discussion

4.6.3.1 Effect of flow rate on equilibration time

Figures 4.13 and 4.14 show the equilibration curves obtained by passing sample solution through a 1.4 g resin column, at flow rates of 2, 7 and 10 ml $min.^{-1}$. The data are given in Tables B.12 and B.13.

Figure 4.13 reveals that at a flow rate of 2 ml $min.^{-1}$ equilibration of silver on Dowex 50W-X8 depends more on the volume of silver ion containing solution supplied than on the contact time with the resin, that is, it is supply limited rather than sorption rate limited. At this flow rate it takes about 100 minutes for the resin to equilibrate. At a faster flow rate, the system takes a shorter time to reach equilibrium than at slow flow rates where less Ag^{+} is supplied in a given time. At flow rates of 7 and 10 ml $min.^{-1}$ it takes only about 30 minutes to equilibrate 1.4 g of resin in the column. When the flow rate is increased from 7 ml $min.^{-1}$ to 10 ml $min.^{-1}$, no further decrease in equilibration time is observed. This implies that at a flow rate of 7 ml $min.^{-1}$ or more, the loading is limited by slow diffusion of silver ions onto the resin beads. This is because at faster flow rates enough sample is supplied but the sample has less time to diffuse to and into the resin beads. Thus, the plateau is approached more slowly in the case of faster flow rates (7 and 10 ml $min.^{-1}$) than at a slow flow rate of 2 ml $min.^{-1}$ (Figure 4.14). At any of these flow rates a passage of about 280 ml of sample is needed for the resin to reach complete equilibrium with the sample solution (Figure 4.14). In subsequent experiments, a flow rate of 7 ml $min.^{-1}$ and equilibration time of 40 minutes (280 ml) was used to equilibrate the sample solution with the 1.4 g resin column. This amount of sample is the same as the amount of sample required for complete breakthrough, Figure 4.2 (40 min. x 7 ml $min.^{-1}$ = 280 ml).

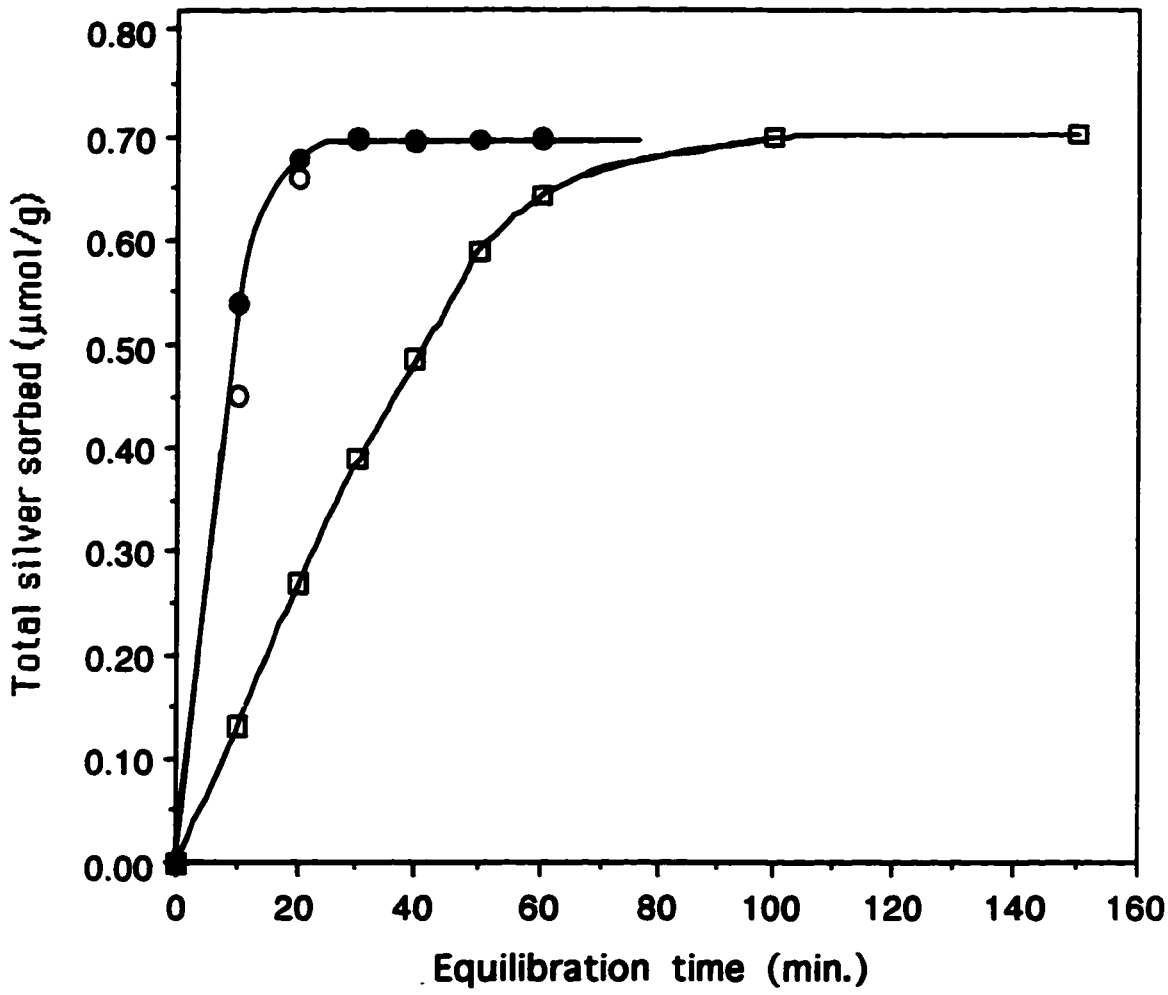

Figure 4.13 Loading curves showing the dependence of loading time on sample flow rate for 9.27 µmol l^{-1} Ag^{+} solution in 0.3 M $NaNO_3$ and pH 7 buffer. The solution was loaded onto a 1.4 g resin column at different flow rates. The eluent was 0.05 M EDTA at pH 10. (□) sample flow rate 2 ml $min.^{-1}$; (○) sample flow rate 7 ml $min.^{-1}$ and; (●) sample flow rate 10 ml $min.^{-1}$. The data are given in Table B.12.

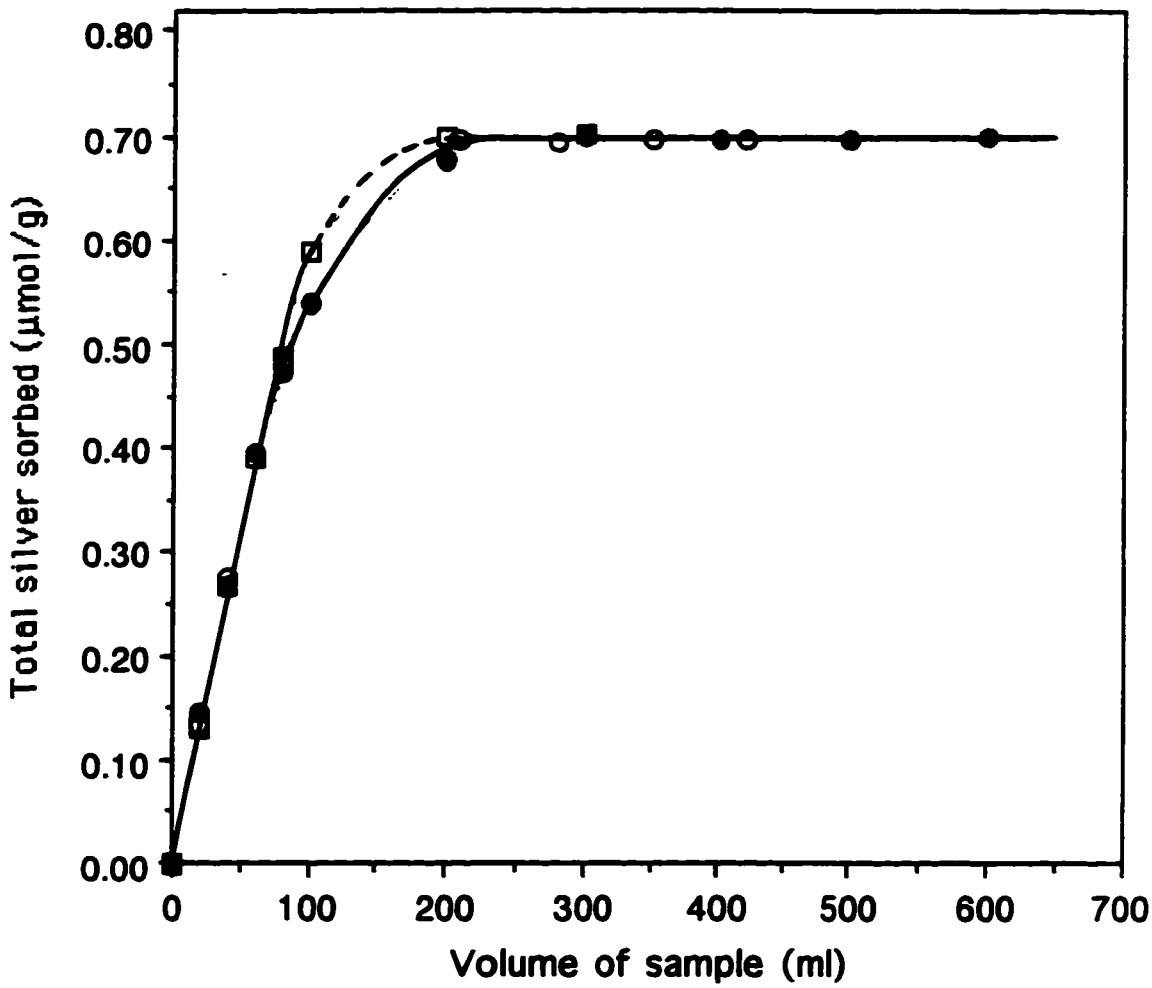

Figure 4.14 Loading curves showing the dependence of sample volume on sample flow rate for 9.27 µmol l^{-1} Ag^{+} solution in 0.3 M $NaNO_3$ and pH 7 buffer. The solution was loaded onto a 1.4 g resin column at different flow rates. The eluent was 0.05 M EDTA at pH 10. (□) sample flow rate 2 ml $min.^{-1}$; (○) sample flow rate 7 ml $min.^{-1}$ and; (●) sample flow rate 10 ml $min.^{-1}$. The data are given in Table B.13.

4.6.3.2 Effect of ionic strength on equilibration time

In section 4.3.3 it was demonstrated that a change in the concentration of the principal counter-ions (i.e. Na^+) of the solution phase alters the distribution coefficient, λ_{Ag+}, for the Ag^+ ion. When a 1:1 swamping electrolyte such as $NaNO_3$ is used then $[Na^+]$ is essentially equal to the ionic strength of the solution. The second effect of ionic strength (I) results from the decrease in activity coefficient with ionic strength, as described in section 2.2.2. This second effect of ionic strength is generally much smaller than the effect of change in principal counter-ion concentration,$[Na^+]$, and will mostly be ignored in the discussion below.

An equilibration study of pH 7 buffered solutions with different total ionic strengths but the same concentration of Ag^+ ($1x10^{-6}$ M) was conducted to examine the effect of ionic strength on equilibration time. The solutions were passed through the 15 mg resin column (Figure 3.3) at a constant flow rate of 7 ml $min.^{-1}$. The results obtained are shown in Figure 4.15a through 4.15e and the data are given in Table B.14.

From Figures 4.15a through 4.15e, it is evident that as the ionic strength of the sample solution is increased the amount of silver sorbed onto the resin at equilibrium decreases. This is due to decrease in the distribution coefficient, λ_{Ag+} between the resin phase and the solution phase. The quantitative relationship between the distribution coefficient, λ_{Ag+} and ionic strength (Na^+) can be obtained by rearranging equation 2.2.4, Chapter 2 as shown below:

$$\lambda_{Ag+} = \frac{[RAg]}{[Ag^+]} = K_{IE}^{C} \frac{[RNa]}{[Na^+]} \qquad \text{..... 4.1}$$

But, under trace ion exchange conditions;

$$K_{IE}^{C}[RNa] = \text{Constant} \qquad \text{..... 4.2}$$

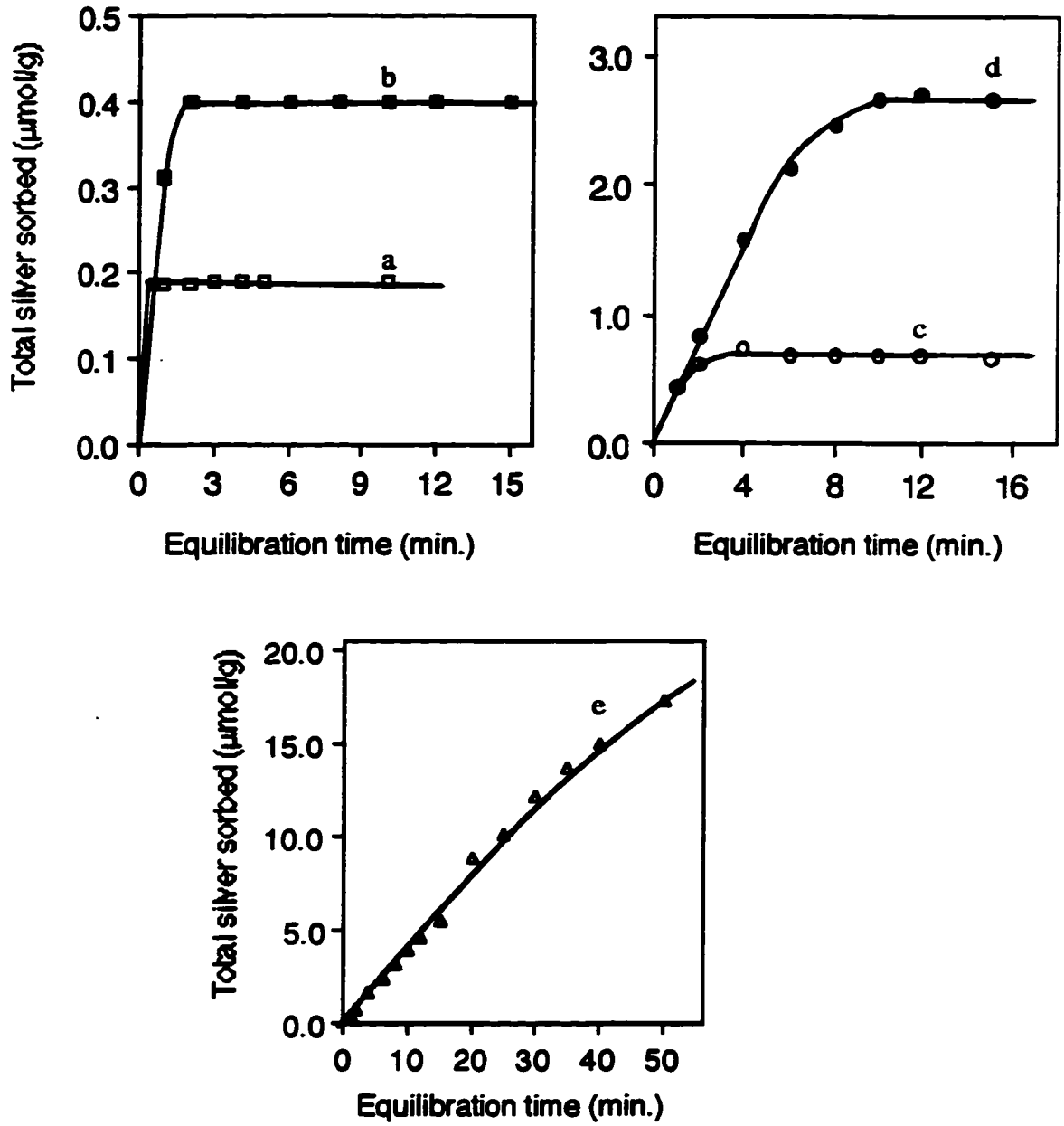

Figure 4.15 Loading curves showing the effect of ionic strength on equilibration time. Solutions of differing total ionic strength (X Na^+) contain $1x10^{-6}$ M Ag^+ and pH 7 buffer, were loaded onto a 15 mg resin column at a flow rate of 7 ml $min.^{-1}$. The eluent was 0.05 M EDTA at pH 10. Total ionic strength; (a) □ I = 0.3 M; (b) ■ I = 0.15 M, (c) o I = 0.01 M; (d) ● I = 0.05 M and; (e) ▵ I = 0.001 M. The data are given in Table B.14.

Therefore, we can write equation 4.1 as follows:

$$\lambda_{Ag+} = \text{Constant} \frac{1}{[Na^+]} \quad \text{..... 4.3}$$

Therefore, from the above equation, λ_{Ag+} is inversely proportional to the ionic strength.

The values of λ_{Ag+} at different ionic strengths (Na^+) were calculated by dividing the values of the equilibrium concentration of the total silver sorbed, [RAg], Figure 4.15a - d by the concentration of Ag^+ in solution (1.0 μmol l^{-1}). The values of λ_{Ag+} obtained for each ionic strength are shown in Table B.15. The decrease in distribution coefficient, λ_{Ag+} with increase in ionic strength is shown in Figure 4.16. The solid line is the fitted line which gives the best-fit to the relationship between λ_{Ag+} and $1/[Na^+]$ as given by equation 4.3 above. The strong dependence of λ_{Ag+} on the ionic strength reveals the importance of accurately matching the ionic strength between the sample and the standard solutions during free metal ion determination by the column equilibration method.

The time required to achieve complete equilibrium increases as the ionic strength of the sample solution is decreased. For the case of 0.3 M, 0.15 M, 0.05 M and 0.01 M total ionic strengths (Figure 4.15), curves (a) through (d), complete equilibrium is achieved in less than 2 minutes, 2, 4 and 12 minutes of loading, respectively. This is because as the ionic strength is decreased, the amount of Ag^+ sorbed by the exchanger increases. Since, the analyte is supplied at a fixed rate (i.e. fixed concentration of Ag^+ and fixed flow rate), then, relatively longer equilibration times will be required to equilibrate the exchanger when larger amount of Ag^+ is sorbed (large λ_{Ag+}). This means that as the ionic strength is decreased loading becomes supply-limited. In the case of 0.001 M total ionic strength equilibrium was not reached even after 50 minutes of loading (Figure 4.15, curve (e)). At such a low ionic strength the distribution coefficient, λ_{Ag+} is much greater than at higher

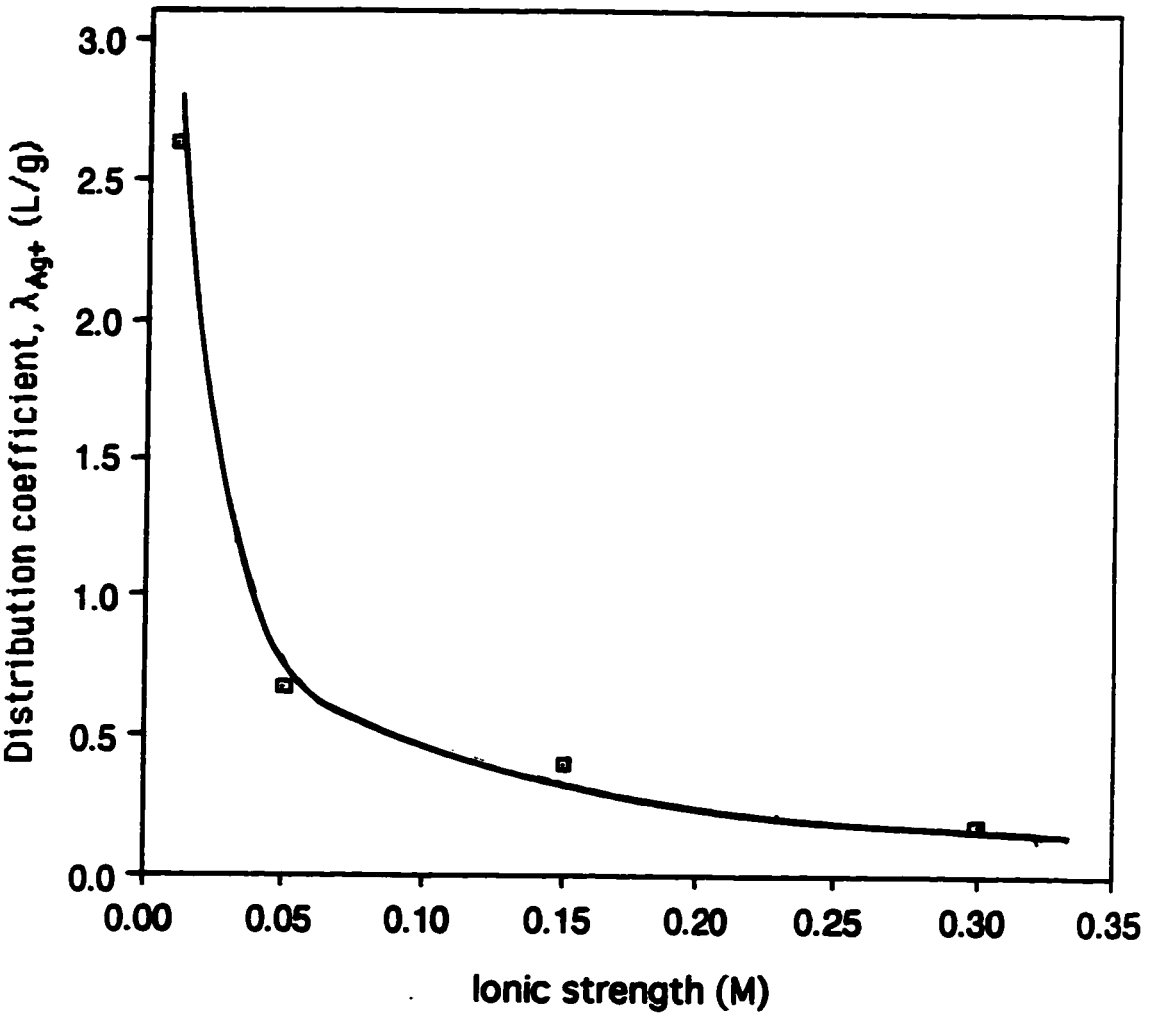

Figure 4.16 Distribution coefficient (λ_{Ag+}) of free silver ion between the resin phase and the solution phase as a function of ionic strength. The equilibrium values of silver sorbed per gram of resin for each ionic strength (Table B.14) were used to calculate the corresponding value of the distribution coefficient. The values of λ_{Ag+} obtained for each ionic strength are shown in Table B.15. The solid line is the best-fit to the relationship between λ_{Ag+} and $1/[Na^+]$ as per equation 4.3.

ionic strengths so the resin can sorb relatively large amounts of Ag^+. Therefore, a longer equilibration time is required for complete equilibrium to be reached. In all subsequent experiments when solutions of different ionic strength were loaded onto the resin column, appropriate equilibration times were used to ensure that the exchanger is in equilibrium with the sample solution.

4.6.3.3 Effect of silver concentration on equilibration time

Concentration of the analyte in the sample solution may also be a factor that can influence the ion-exchange kinetics and, hence, the equilibration time. For example, for dilute solutions the rate of exchange may be controlled by film diffusion while for concentrated solutions the rate may be controlled by bead diffusion, where all other experimental conditions are kept unchanged [75].

In sorption isotherm studies and free metal ion determination using the column equilibration technique, solutions of varying metal concentration are equilibrated with the resin under a given set of experimental conditions. Hence, it is necessary to examine whether the same equilibration time can be used to equilibrate solutions of different metal concentrations with the resin.

An equilibration study of solutions having the same total ionic strength but varying concentrations of Ag^+ was conducted to examine the effect of silver ion concentration on equilibration time. Both large column (Figure 3.2) and single pass small column (Figure 3.3) flow systems were used. The results obtained are shown in Figure 4.17 for the large column and Figure 4.18 for the single pass small column flow systems. The data are given in Tables B.16 and B.17 respectively. Both Figures 4.17 and 4.18 reveal that for all concentrations studied, the equilibrium is reached after 40 and 2 minutes of loading for the large and small columns, respectively. This is consistent with the results obtained in sections 4.6.3.1 and 4.6.3.2, above.

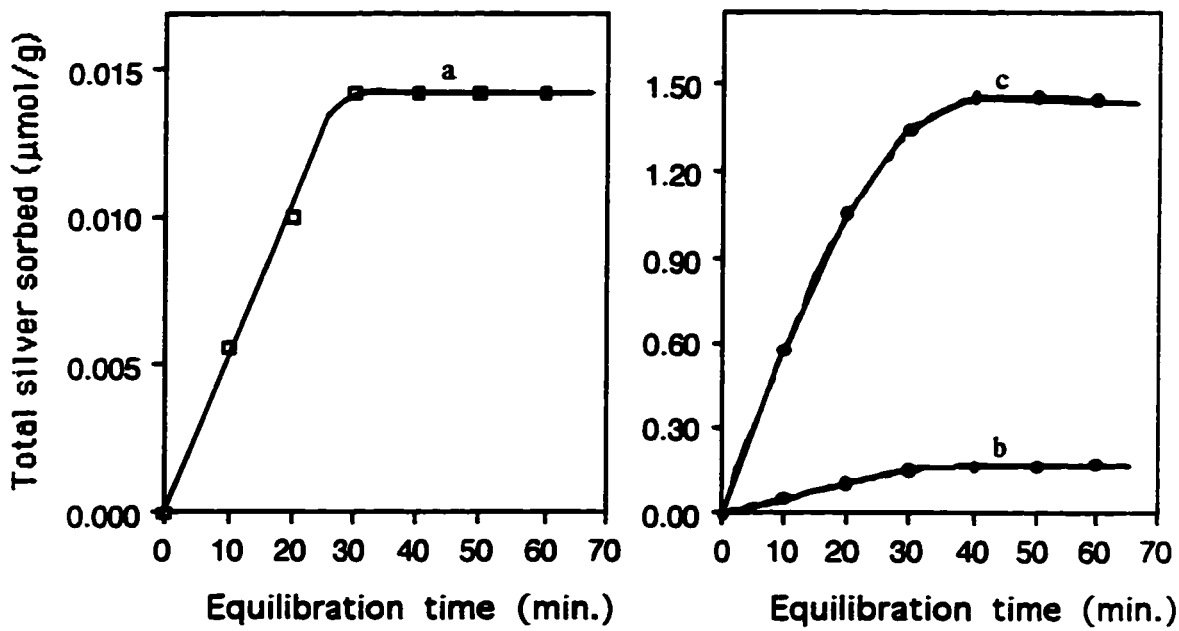

Figure 4.17 Loading curves showing the effect of Ag^+ concentration on equilibration time. The solutions containing differing amount of Ag^+ (X M Ag^+) in 0.3 M $NaNO_3$ and pH 7 buffer were loaded onto a 1.4 g resin column at a flow rate of 7 ml $min.^{-1}$. The eluent was 0.05 M EDTA at pH 10. Total silver concentration, C_{Ag^+}, (a) □ 0.1µmol l^{-1} Ag^+; (b) o 1.0 µmol l^{-1} Ag^+ and ; (c) ● 10 µmol l^{-1} Ag^+. The data are given in Table B.16.

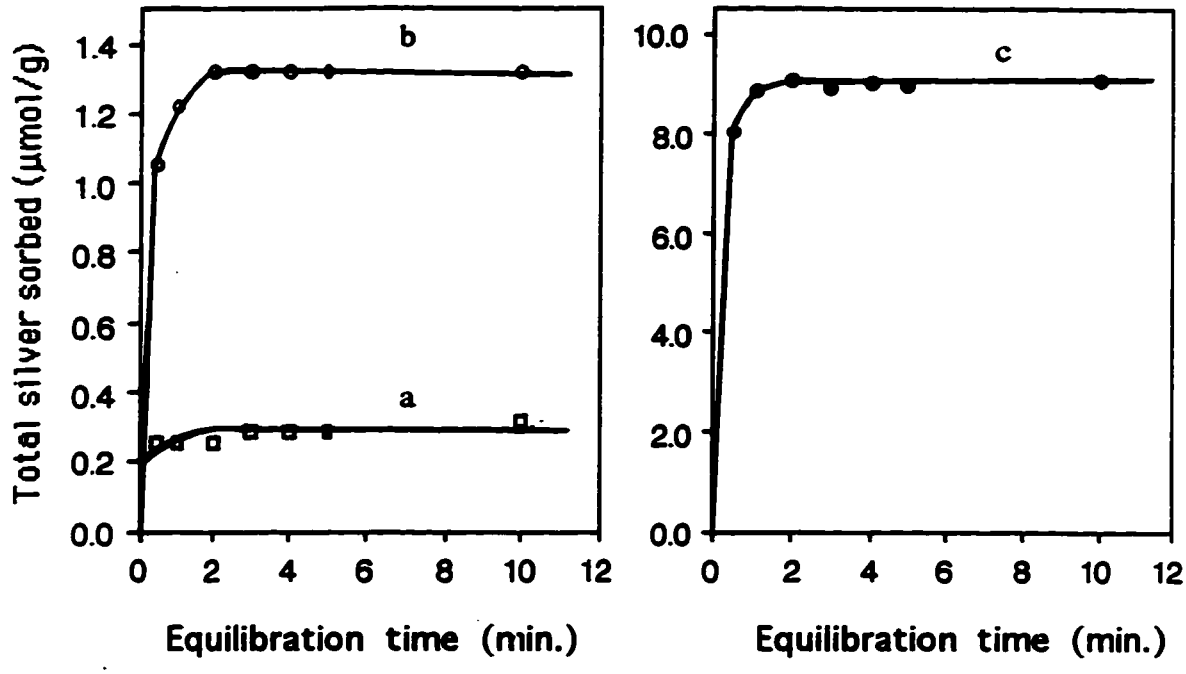

Figure 4.18 Loading curves showing the effect of Ag^+ concentration on equilibration time. The solutions containing differing amount of Ag^+ (X M Ag^+) in 0.3 M $NaNO_3$ and pH 7 buffer were loaded onto a 15 mg resin column at a flow rate of 7 ml $min.^{-1}$. The eluent was 0.05 M EDTA at pH 10. Total silver concentration, C_{Ag+}, (a) □ 1.0 µmol $^{-1}$; (b) o 10.0 µmol l^{-1} and; (c) ● 100 µmol l^{-1}. The data are given in Table B.17.

In light of these results we can conclude that under these conditions, there is no significant difference in equilibration time for different concentrations of silver in solution. Therefore a fixed equilibration time can be used for each column over a wide range of Ag^{+} concentrations.

4.7 Sorption isotherm

4.7.1 Introduction

At equilibrium in the column equilibration method, there is no change in the concentration of metal sorbed in the resin phase, which is now at equilibrium with the influent, unperturbed sample solution. A sorption isotherm is a plot of concentration of metal ion sorbed by the exchanger at equilibrium, [RM], against the concentration of the metal ion in solution, $[M^{+}]$.

4.7.2 Procedure

The column was washed and pre-conditioned as described in section 3.4.1. The resin was equilibrated, in turn, with pH 7 buffered sample solutions of varying concentration of silver but the same total ionic strength of 0.3 M, at a flow rate of 7 ml $min.^{-1}$. An equilibration time of 40 minutes was used for the large resin column, Figure 3.2 and 5 minutes for the small column, Figure 3.3. After passing each sample solution through the column, interstitial sample solution was removed by passing air, the column was washed with water and finally sorbed silver was eluted. The eluate was collected in volumetric flasks and determined by AAS. Some of these eluted samples were diluted prior to being aspirated into the AAS.

4.7.3 Results and discussion

The sorption isotherms obtained in 0.3 M $NaNO_3$ for large and small resin columns are shown in Figures 4.19 and 4.20 and the data are given in Tables B.18 and B.19, respectively. Both isotherms are slightly curved. A non-linear isotherm was expected for the case of the 15 mg column because higher concentrations of Ag^+ were used with the small column. However, the 1.4 g resin column was operated under trace conditions for the whole range of silver concentration and silver sorbed occupies less than 1% of the total sites (Table B.18). The values of the percentage of resin sites occupied by Ag^+ are shown in column 3 of both Tables B.18 and B.19 for the large and small columns, respectively. These values were calculated for each data point using the equation

$$\% \text{ of resin sites occupied by } Ag^+ = \frac{X\ (\mu mol\ g^{-1})}{C_{IEX}\ (\mu mol\ g^{-1})} \times 100 \qquad \ldots\ldots 4.4$$

where X is the amount of silver sorbed and C_{IEX} is the total exchange capacity of the resin. The value of C_{IEX} (for the small column) is 5.1 meq g^{-1} (5100 μmol g^{-1}) of dry resin (see section 3.3).

The slight downward curvature observed in these isotherms could be due to the presence of weak acid (e.g. carboxylic acid) groups in addition to strong acid sulfonic groups. This is likely because of the strong oxidizing conditions used in sulfonation of styrene-divinyl benzene copolymer spheres using sulfuric acid. Sulfuric acid is known to act as an oxidizing agent at high temperatures and high concentrations [76]. Oxidation in the synthesis of sulfonic acid cation exchange resin can produce carboxylic acid groups accounting for up to 5% of the total exchange capacity [77]. The presence of carboxylic acid groups, even in small amounts, will produce deviations because the exchanger will have ionic sites of different energy and hence different sorption behavior.

The isotherms are linear up to about 10.0 μmol l^{-1}. For the large column the linear region of the isotherm is shown in Figure 4.21. In this linear region the isotherm is described by the equation

$$[RAg] = 1.60 \times 10^{-3} + 0.144\ [Ag^{+}] \quad \text{Correlation coefficient} = 0.999 \quad \ldots\ldots \quad 4.5$$

The slope (0.144 lg^{-1}) is the distribution coefficient, λ_{Ag+} of Ag^{+} between the resin phase and the solution phase. The isotherms were used as calibration curves for free metal ion determination.

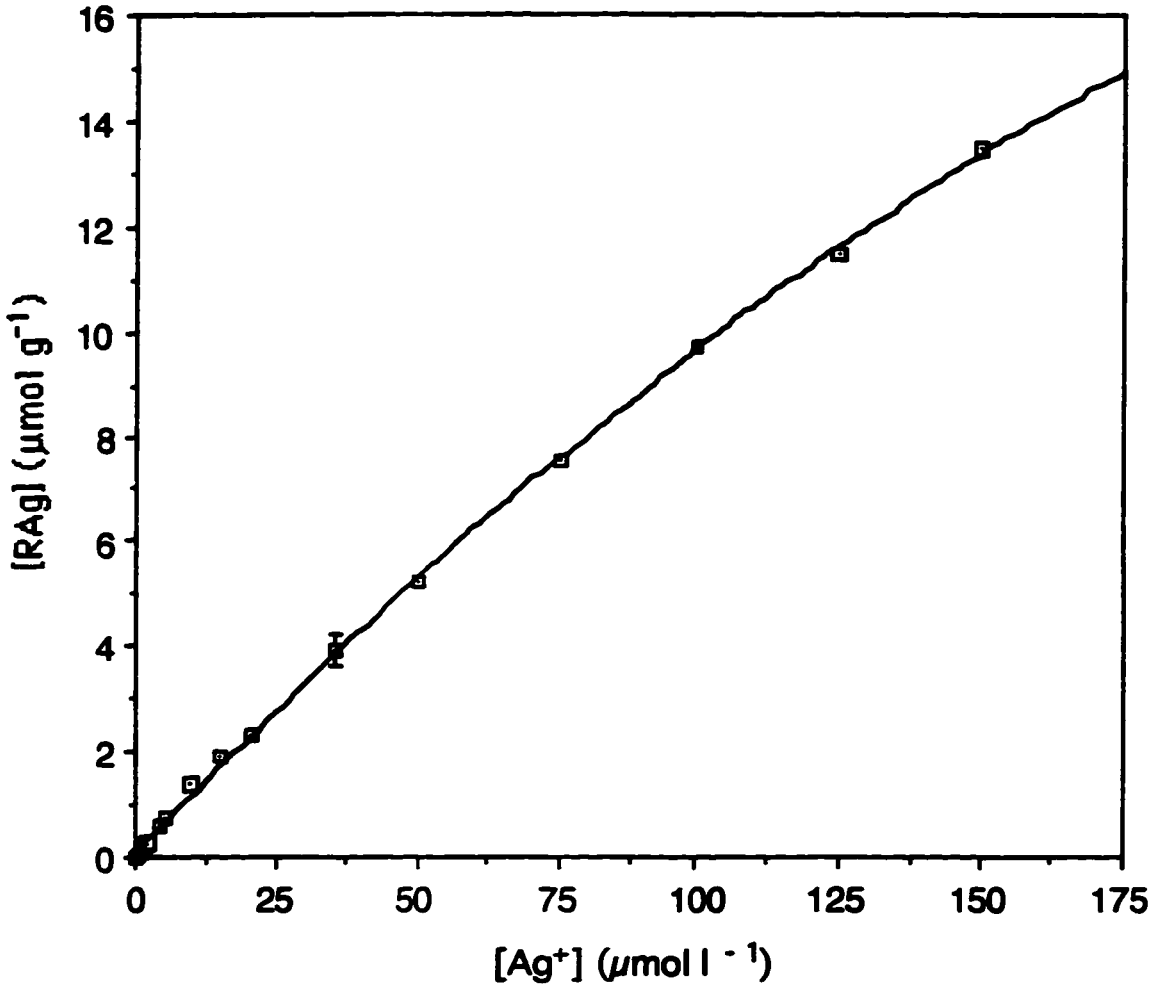

Figure 4.19 Sorption isotherm of Ag^+ on Dowex 50W-X8 resin. Solutions of differing concentrations of Ag^+ in 0.3 M $NaNO_3$ and pH 7 buffer were loaded onto a 1.4 g resin column for 40 minutes at a flow rate of 7 ml $min.^{-1}$. The eluent was 0.05 M EDTA at pH 10. The data are given in Table B.18.

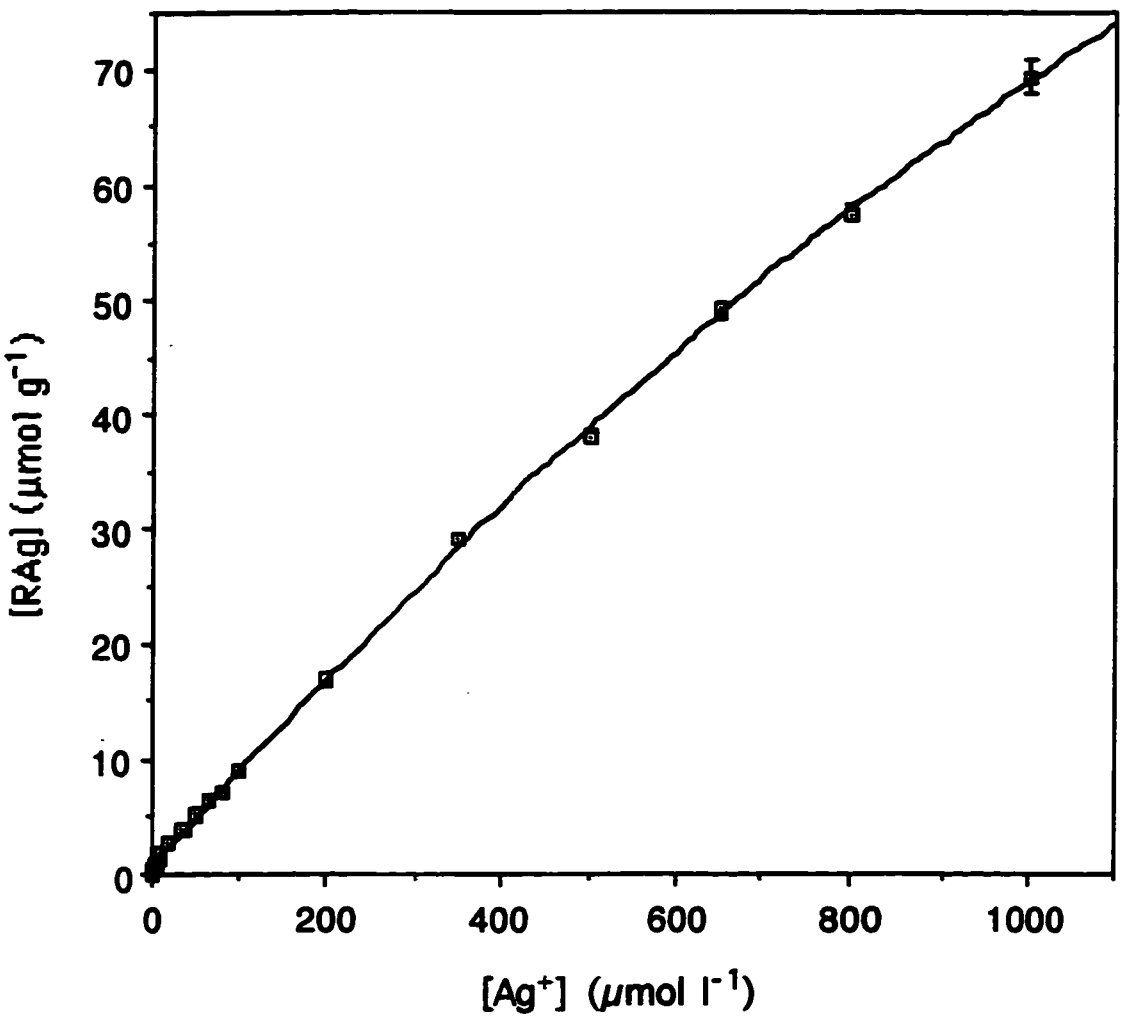

Figure 4.20 Sorption isotherm of Ag^+ on Dowex 50W-X8 resin. Solutions of differing concentrations of Ag^+ in 0.3 M $NaNO_3$ and pH 7 buffer were loaded onto a 15 mg resin column for 5 minutes at a flow rate of 7 ml $min.^{-1}$. The eluent was 0.05 M EDTA at pH 10. The data are given in Table B.19.

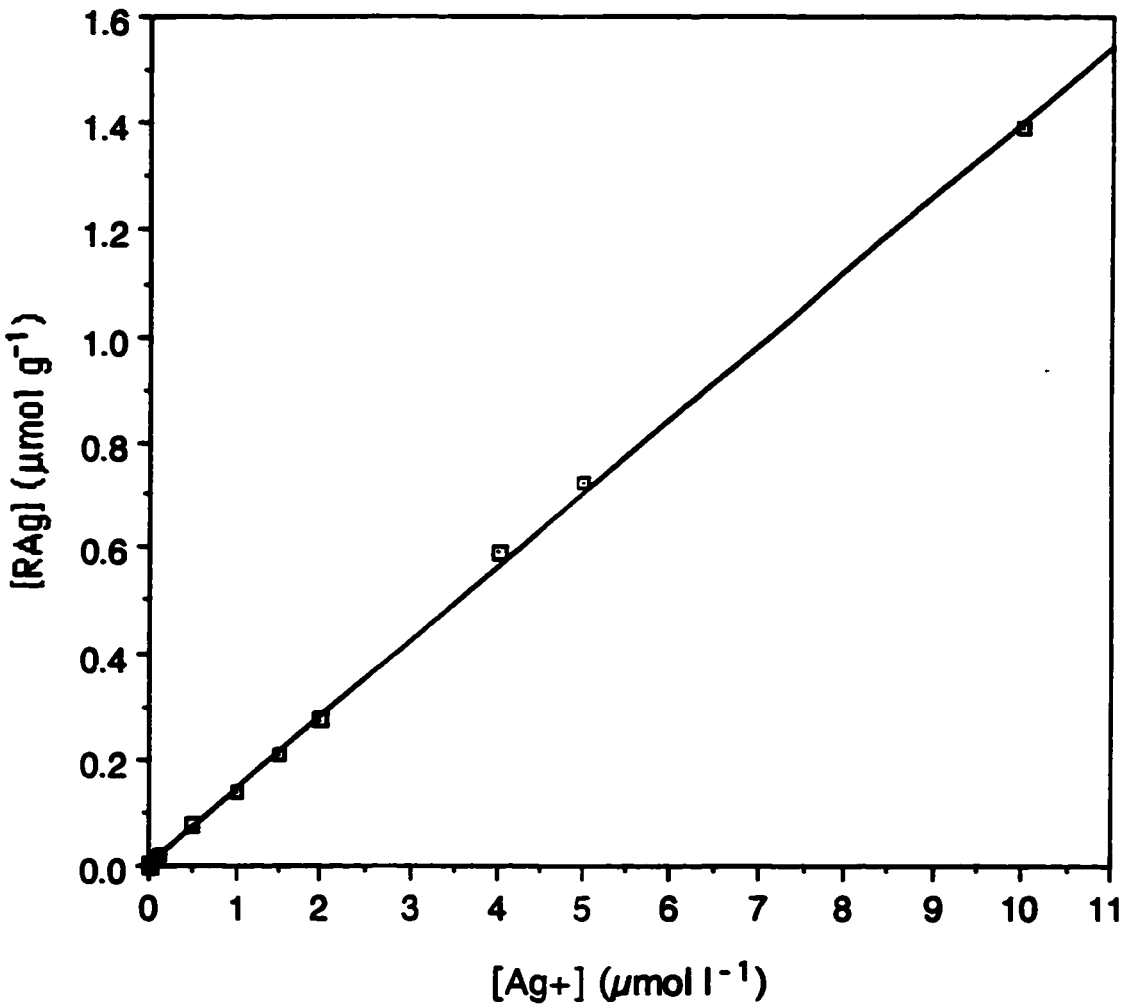

Figure 4.21 Linear region of the sorption isotherm in Figure 4.19, on the 1.4 g resin column.

CHAPTER FIVE

DETERMINATION OF FREE SILVER ION CONCENTRATION, [Ag^+], IN SYNTHETIC SOLUTIONS

5.1 Introduction

The underlying idea of these studies is to determine the concentration of free silver ion in the presence of the complexing ligands chloride and hydroxide. Solutions with differing concentrations of free silver ion were prepared by combining various initial amounts of Cl^-, OH^- and Ag^+ (as $AgNO_3$).

5.2 Experimental

The apparatus, and general operating procedures are described in Chapter 3, above. Only details specific to the present studies are mentioned here.

5.2.1 Apparatus

All three flow systems described in section 3.1.2 were used. The Fisher Accumet® Model 320 pH meter was used for all pH measurements. Also, the Fisher Accumet® Model 25 pH/ion meter with silver ion-selective electrode was used for all potentiometric measurements of free silver ion concentrations. Both meters are described in section 3.1.3. The atomic absorption spectrophotometer was also used as described in section 3.4.3.

5.2.2 Sample solution preparation

5.2.2.1 Sample solution preparation for chloride ligand

In general, a sample solution was prepared by dispensing the required amount of 3 M sodium nitrate stock solution, 100 ml of $1x10^{-2}$ M HEPES buffer, and the required amount of ligand (NaCl) into a 1 liter volumetric flask containing about 700 ml of water. The pH of the solution was adjusted to pH 7 by adding small amount of dilute NaOH. While stirring the solution, the required amount of dilute silver nitrate was added slowly to the volumetric flask. In all sample solutions prepared using this procedure, the amount of Na^+ in each solution was in excess as compared to that of Ag^+. The pH of the solution was measured again and adjusted whenever necessary using small amount of either dilute HNO_3 or NaOH. The solution was diluted to volume. Finally the solution was transferred into a 1 L plastic bottle and placed in a water bath at 25.0 ± 0.5 °C for the required period of time (normally 15 hrs) under dim light conditions.

The same procedure was used to prepare the pre-conditioning and the silver standard solutions, except that no silver was added to the pre-conditioning solutions and no ligand was added to the standard solutions. The range of silver concentration in the standards was made in such a way that it bracketed the concentrations of silver in the sample solutions. These standards were used for the calibration of both the ion-selective electrode and the column equilibration systems. The eluent, 0.05 M EDTA at pH 10, was also prepared as described in section 3.2.

5.2.2.2 Sample solution preparation for hydroxide ligand

A sample solution was prepared by dispensing the required amount of 3 M sodium nitrate stock solution into a 500 ml volumetric flask containing about 250 ml of water. The

total ionic strength of the solution was adjusted to 0.3 M using $NaNO_3$. The pH of the solution was adjusted to the desired value by using 0.5 M NaOH. While stirring the solution, the required amount of 0.01 M $AgNO_3$ was added slowly to the volumetric flask. The solution was diluted to volume. Finally the solution was transferred to a 500 ml plastic bottle and placed in a water bath at 25.0 ± 0.5 °C under dim light conditions for about 15 hours to equilibrate. After 15 hours, the pH of the sample solution was measured again. The pre-conditioning solution containing 0.3 M $NaNO_3$ at pH 12.5 and silver standard solutions were also prepared as described in section 5.2.2.1. The standards were used for the calibration of both the column equilibration and the ion-selective electrode measurement systems. The eluent, 0.05 M EDTA at pH 10, was also prepared as described in section 3.2.

5.2.3 Procedure for free metal determination

The procedure for the measurement of free silver ion concentration, [Ag^+] using the ion-selective electrode has been previously described in section 3.4.2. This section outlines a general procedure used for the measurement of free silver ion concentration using the column equilibration technique. Cleaning of the column equilibration flow system, column pre-conditioning, loading of sample solution, removal of interstitial sample solution with air and washing with water have been described previously in section 3.4.1. In all experiments the eluent, 0.05 M EDTA at pH 10 was used to elute sorbed silver. The eluent was passed at a flow rate of 2 ml $min.^{-1}$ in all cases. For the large column (Figure 3.2) and small column single pass flow (Figure 3.3) systems a sample solution flow rate of 7 ml $min.^{-1}$ was used throughout. However, for the small column recycle flow system (Figure 3.4), a sample solution flow rate of 6 ml $min.^{-1}$ was the maximum obtainable and was used throughout. The sample and the standard solutions were placed in turn in the cell, (Figure 3.4). After use with each solution the cell was rinsed well with the next

solution. With this setup, the concentration of free silver ion was measured simultaneously using both the column equilibration and the ion-selective electrode methods.

For each experiment the column equilibration system was first calibrated using silver standard solutions. The standard solutions were equilibrated, in turns, with the resin column. Silver in the eluate from the eluted column was quantified by using AAS (e.g. calibration curve Figure 3.6) to obtain the concentration of sorbed silver, [RAg], in $\mu molg^{-1}$ of resin. Similarly, sample solutions containing ligand were also equilibrated with the resin column and the concentration of sorbed silver was obtained upon elution.

The concentration of sorbed silver, [RAg], in $\mu mol\ g^{-1}$ obtained after loading the standard solutions was plotted against the known concentration of free silver in the standard solution, $[Ag^+]$, to give the ion-exchange calibration curve (e.g. sorption isotherm, Figure 4.21). The concentration of sorbed silver, [RAg], obtained after loading and eluting the sample solutions,was used to quantitate the concentration of free silver ion, $[Ag^+]$, in the sample solutions by interpolating the value of free silver from the ion-exchange calibration curve, just described above.

5.3 Results and Discussion

5.3.1 Determination of free silver ion concentration, $[Ag^+]$, in the presence of chloride ligand

The underlying idea for these studies is to determine the concentration of free silver ion in the presence of silver-chloro species. Therefore, the complexing ligand chloride will be used. By adding different amounts of the chloride ligand, sample solutions having various concentrations of free silver ion can be obtained.

5.3.1.1 Loading study in the presence of chloride ligand and AgCl(s)

The presence of chloride ligand in solutions containing high concentration of silver results in the formation of a silver chloride precipitate. As mentioned in Chapter 2, section 2.1.3, silver chloride precipitate is an example of a colloidal precipitate. The presence of colloidal silver chloride in the sample solution is not desirable. If these particles are filtered out or sorbed by the ion-exchange column, they will be eluted and quantified as though they were free silver, thus, giving erroneous results for free metal concentration. Loading experiments were conducted to examine the equilibration (loading) curves of filtered saturated solutions of silver chloride.

Sample solutions of total silver concentration $1x10^{-4}$ M and total chloride concentration of $3x10^{-5}$ M were prepared as described in section 5.2.2.1 above. The solutions were buffered at pH 7 and the total ionic strength of each solution was adjusted to 0.3 M. The solutions were placed in a water bath at 25.0 ± 0.5 °C for different lengths of time before being filtered through a 0.45 μm membrane filter. The sample solutions which were filtered after aging for 15 hours were less cloudy compared to those which were filtered just after preparation or after aging for an hour. Also small chunks of AgCl(s) were observed only in solutions which were left to age for of 15 hours. The filtrate from each sample solution was loaded on one of the three resin columns (Figure 3.2) for different lengths of time and at a constant flow rate of 7 ml $min.^{-1}$. The results obtained are shown in Figure 5.1 and the data are given in Table C.1 (Appendix C).

From the loading curves it is evident that each curve reaches a plateau after about 30 minutes of loading. The same experiment was done using the small column flow system (Figure 3.3). The loading curves obtained are shown in Figure 5.2, and the data are given in Table C.2. The curves shown in Figure 5.2 are similar in shape with those obtained

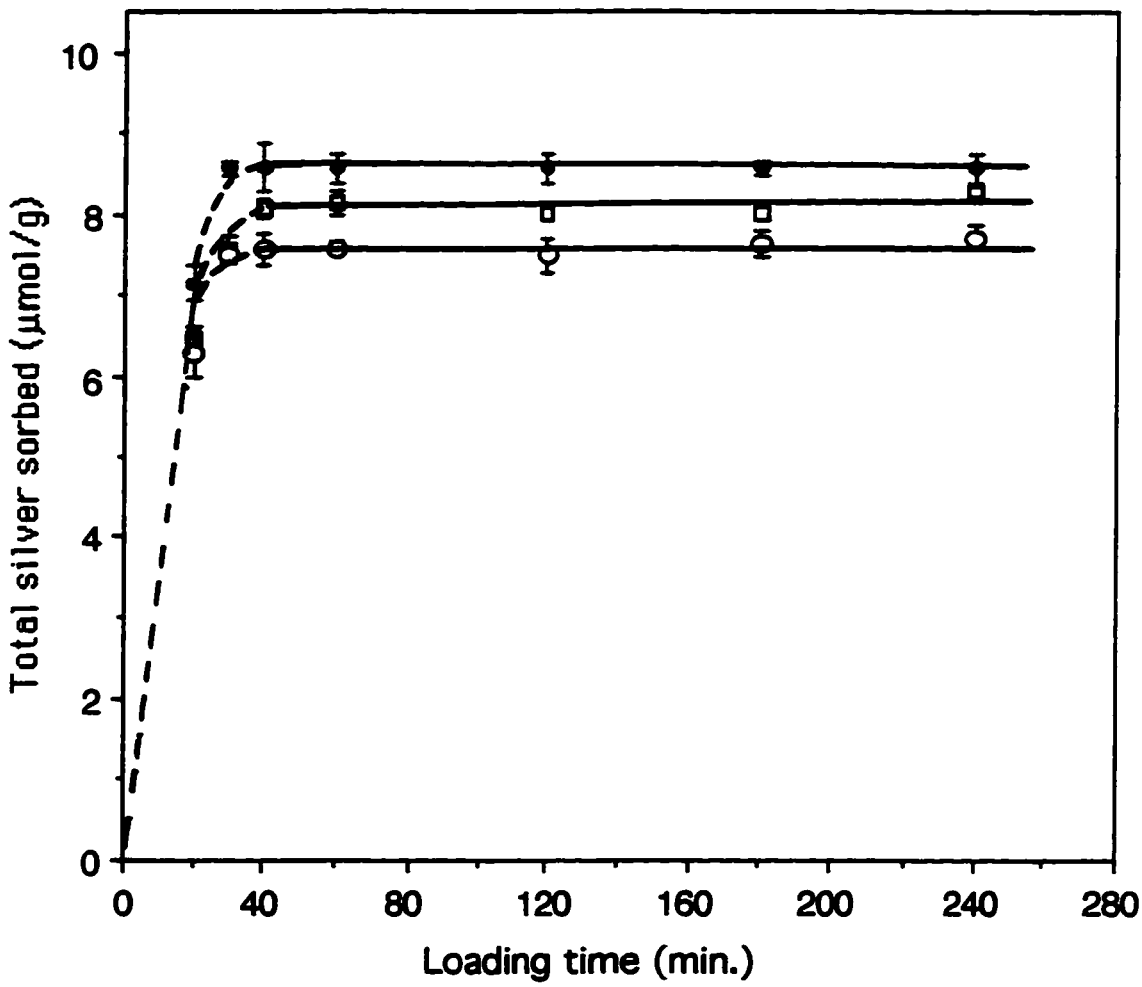

Figure 5.1 Loading curves for filtered (0.45 µm) saturated solutions of silver chloride. The solutions contain $1x10^{-4}$ M total silver and $3x10^{-5}$ M total chloride in pH 7 buffer and 0.3 M ionic strength. The solutions were loaded onto a 1.4 g resin column at a flow rate of 7 ml $min.^{-1}$. The eluent was 0.05 M EDTA at pH 10. Filtration of solution commenced immediately after mixing(□); after aging for an hour (○) and; after aging for 15 hours (●). The data are given in Table C.1.

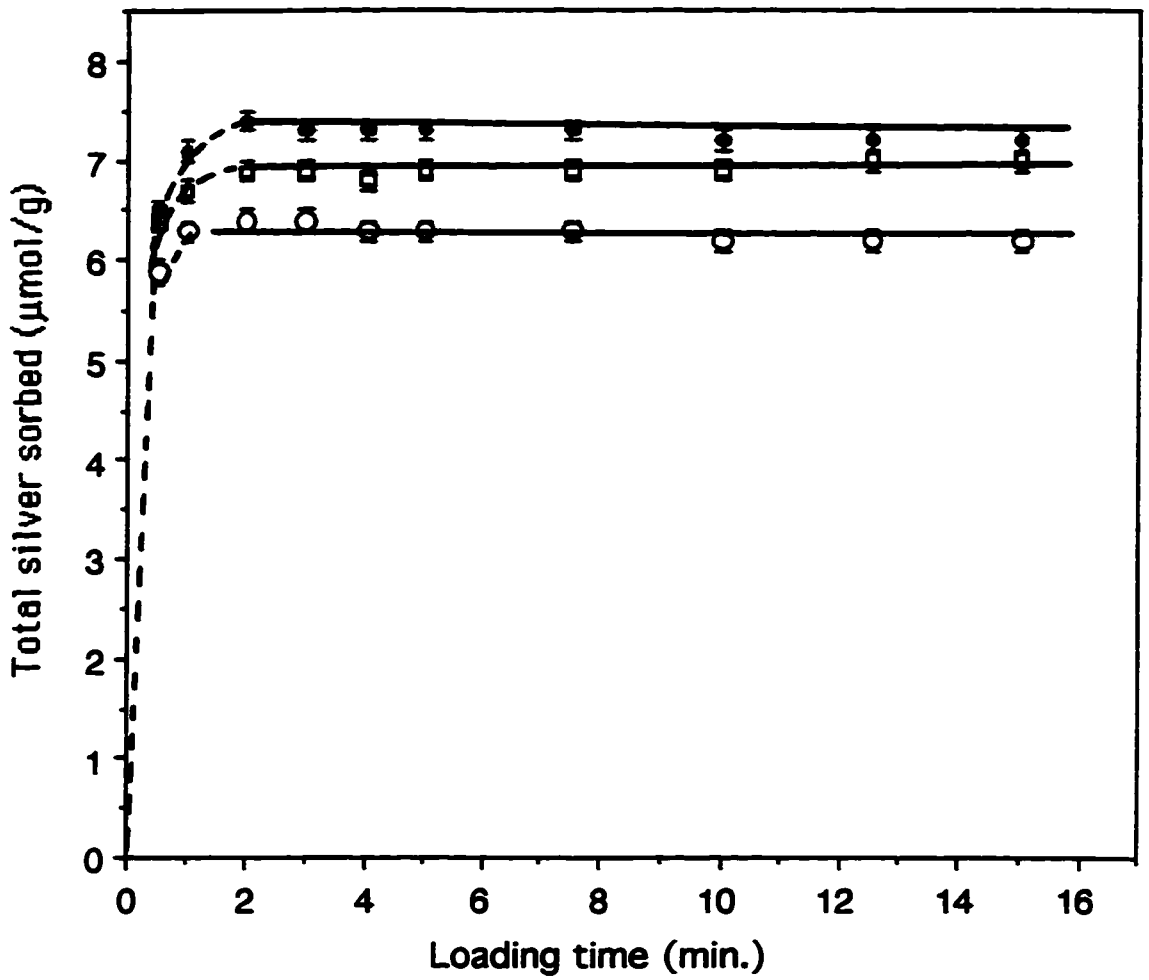

Figure 5.2 Loading curves for filtered (0.45 µm) saturated solutions of silver chloride. The solutions contain $1x10^{-4}$ M total silver and $3x10^{-5}$ M total chloride in pH 7 buffer and 0.3 M ionic strength. The solutions were loaded onto a 15 mg resin column at a flow rate of 7 ml $min.^{-1}$. The eluent was 0.05 M EDTA at pH 10. Filtration of solution commenced immediately after mixing(□); after aging for an hour (○) and; after aging for 15 hours (●). The data are given in Table C.2.

using the large column (Figure 5.1), except that the curves reach a plateau after 2 minutes of loading. The equilibration (loading) times observed in these experiments are consistent with those obtained in previous loading studies under similar conditions i.e. ionic strength and flow rate, section 4.6.3, above. The fact that all curves reach a plateau within 30 minutes for the large resin column and 2 minutes for the small resin column suggests that there is no filtration of colloidal particles out of the solution by the cation exchange resin column. The theoretical predicted concentration of free silver ion, Ag^+ in these solutions is about 75.2 $\mu mol\ l^{-1}$ (pAg = 4.1) and the point of zero charge (PZC) of silver chloride colloid is about pAg 4.6 [62-64], so the particles are likely to be positively charged. If there were filtration of colloidal silver chloride by the resin, there would be a continuous rise of the loading curve(s) with time as more and more particles are filtered out or sorbed by the exchanger [37]. Finally the curve(s) would level off at times much longer than 30 minutes for the large column and 2 minutes for the small column.

Both Figures 5.1 and 5.2 show that the curves reach different plateau values. This means that the concentration of free silver ion, $[Ag^+]$ in these solutions is different. Calculation of the concentration of free silver ion in the filtered solutions requires the use of calibrating standards. The standards were run in the small column experiment only. The procedure described in section 5.2.3 was used. For comparison purpose the silver ion-selective electrode was also used. The values of free silver ion concentration obtained by both the ion-selective electrode and the column equilibration methods are shown in Table 5.5c (see pg 118). From Table 5.5c it can be seen that, indeed there is a difference in concentration of free silver ion in these solutions. It will be shown in section 5.3.1.4 below that the different plateau loading values seen after different aging times in both Figures 5.1 and 5.2 arise from the kinetics of precipitation and colloid coagulation.

From the similarities in shape of the three curves in each of the Figures 5.1 and 5.2 we can conclude that the presence of colloidal silver chloride does not affect the equilibrium loading time and that aging time affects the level of free silver ion in the solution (see

section 5.3.1.4). In light of these results an aging time of 15 hours was used, because after this length of time the level of Ag^+ in the solution has stabilized (equilibrated) and more reproducible results can be obtained.

5.3.1.2 Determination of free silver ion concentration under trace conditions

An experiment was carried out to measure the concentration of free silver ion down to nanomolar (nM) levels. The large column flow system (Figure 3.2) was used. The sample, standard, and the pre-conditioning solutions were prepared as described in section 5.2.2.1. The sample solutions, which all had the same total silver concentration were adjusted to various free silver ion concentrations by adding different amounts of chloride ligand ($1x10^{-6}$ M - 0.3 M). All sample solutions were buffered at pH 7 and the total ionic strength of each sample solution was adjusted to 0.3 M by adding an appropriate amount of sodium nitrate. The sample solutions, which were saturated with AgCl(s), were filtered by using the Nylon 66 0.45 μm membrane filter. Both filtrate and precipitate were analyzed using AAS. Silver chloride precipitate was dissolved from the membrane filter using 0.05 M EDTA at pH 10. The procedure used to determine the concentration of free silver ion was as described in section 5.2.3. An equilibration time of 40 minutes was used for both standard and sample solutions. The results obtained are given in Tables 5.1 and 5.2. The data are plotted in Figures 5.3 and 5.4.

The amount of total chloride in each solution is shown in column 1 of each table. The value of free chloride, Cl^-, in each solution is shown in column 2. These values were calculated using Computer program A.1 or A.2, (see Appendix A) depending on whether AgCl(s) was present or absent. The values of the total concentration of silver in the filtrate, $C_{Ag,sol}$ are shown in column 3. The concentration of solid silver chloride, $n_{AgCl(s)}$ /V is shown in column 4 and; the mass balance obtained by adding the values in column 3 and 4

are shown in column 5. An average recovery of 98 ± 3% has been achieved. Ideally the mass balance should be 10.0 μmol l^{-1} in Table 5.1 and 100.0 μmol l^{-1} in Table 5.2. Columns 6 and 8 show the values of free silver ion concentration obtained by the column equilibration method and the ion-selective electrode method (ISE).

Column 9 shows the expected values of free silver ion concentration, calculated for each solution using computer program A.4. The values of Ksp, $\beta_{1,Cl}$, $\beta_{2,Cl}$, $\beta_{3,Cl}$, and $\beta_{4,Cl}$ in computer program A.4 are shown in column 4 of the Table 5.3. These were calculated by an iterative procedure using the data for free chloride, [Cl^-], from column 2 of Table 5.1, as described in Appendix A.3. The uncertainty in the predicted values of [Ag^+] in all cases were calculated by using the Stolzberg approach [78]. The first three values of free silver ion concentration in Table 5.2, column 6 were obtained by interpolating the values of free silver using a non-linear fit to the ion-exchange calibration curve (e.g. Figure 4.19) as they are outside of the linear region of the sorption isotherm. Other values were obtained by interpolating the values of free silver using a linear fit (as predicted by equation 2.2.5) to the ion-exchange calibration curve (e.g. Figure 4.21). The values of free silver plotted as log free silver against log total chloride concentration are shown in Figures 5.3 and 5.4 for total silver concentration of $1x10^{-5}$ M and $1x10^{-4}$ M, respectively.

Figures 5.3 and 5.4 show that the measured free silver ion concentration decreases with increasing concentration of the chloride ligand, as expected. Also good agreement is observed among the values of free silver ion concentration obtained by the column equilibration method, the ion-selective electrode method and the theoretical equilibrium calculations (the bottom solid line in Figures 5.3 and 5.4.) up to a total chloride concentration of $7.5x10^{-4}$ M (log C_{Cl} = -3.1). At total chloride concentration above $7.5x10^{-4}$ M, the extent of the decrease in the values of free Ag^+ with increasing concentration of chloride ligand, as measured by the column equilibration method, is much less than that measured by the ion-selective electrode method or predicted by theoretical

Table 5.1 Results obtained by varying the amount of total chloride, C_{Cl}, in solutions containing a fixed concentration of total silver, C_{Ag}, $1x10^{-5}$ M, 0.3 M total ionic strength and pH 7 buffered. The solutions were equilibrated with the 1.4 g resin column for 40 minutes at a flow rate of 7 ml $min.^{-1}$. The eluent was 0.05 M EDTA. Silver chloride precipitate was dissolved from the membrane filter using the same eluent. The values of free silver concentration are plotted in Figure 5.3 and 5.6.

Total chloride, C_{Cl}, M	Free chloride, $[Cl^-]$, M	$C_{Ag,sol}$ $\mu mol\ l^{-1}$	$n_{AgCl(s)}/V$ $\mu mol\ l^{-1}$	C_{Ag} [mass balance] $\mu mol\ l^{-1}$	Values of $[Ag^+]$ obtained by the ion-exchange method, $\mu mol\ l^{-1}$		Values of $[Ag^+]$ obtained by the ISE method, $\mu mol\ l^{-1}$	Predicted values of $[Ag^+]$, $\mu mol\ l^{-1}$
					Before correction	After correction		
$3.0x10^{-6}$	$2.98x10^{-6}$	9.9 ± 0.1	-	9.9 ± 0.1	10.2 ± 0.1	10.2 ± 0.10	9.87 ± 0.18	9.98 ± 0.13
$3.0x10^{-5}$	$2.98x10^{-5}$	9.9 ± 0.1	-	9.9 ± 0.1	9.93 ± 0.39	9.93 ± 0.39	9.83 ± 0.18	9.80 ± 0.13
$7.5x10^{-5}$	$7.05x10^{-5}$	5.8 ± 0.1	3.56 ± 0.34	9.4 ± 0.4	6.13 ± 0.18	6.13 ± 0.18	6.30 ± 0.12	5.51 ± 0.13
$3.0x10^{-4}$	$2.91x10^{-4}$	1.6 ± 0.1	8.99 ± 0.32	10.6 ± 0.4	1.62 ± 0.13	1.62 ± 0.13	1.60 ± 0.03	1.33 ± 0.08
$7.5x10^{-4}$	$7.41x10^{-4}$	0.8 ± 0.1	9.57 ± 0.20	10.4 ± 0.3	0.66 ± 0.06	0.53 ± 0.05	0.536 ± 0.013	0.53 ± 0.02
$3.0x10^{-3}$	$2.99x10^{-3}$	0.4 ± 0.1	9.41 ± 0.21	9.8 ± 0.3	0.20 ± 0.01	0.12 ± 0.01	-	0.13 ± 0.01
$7.5x10^{-3}$	$7.49x10^{-3}$	0.3 ± 0.1	9.24 ± 0.09	9.5 ± 0.2	0.14 ± 0.01	0.057 ± 0.004	–	0.052 ± 0.002
$3.0x10^{-2}$	$3x10^{-2}$	0.7 ± 0.1	8.88 ± 0.24	9.6 ± 0.3	0.043 ± 0.008	0.0083 ± 0.0015	–	0.013 ± 0.001
$7.5x10^{-2}$	$7.5x10^{-2}$	1.8 ± 0.1	7.77 ± 0.17	9.6 ± 0.3	0.033 ± 0.004	0.0032 ± 0.0004	–	0.0052 ± 0.0003
0.30	0.30	9.7 ± 0.1	-	9.7 ± 0.1	0.021 ± 0.001	0.00064 ± 0.00003	–	0.00062 ± 0.0001

± are standard deviations based on three replicates.

Table 5.2 Results obtained by varying the amount of total chloride, C_{Cl}, in solutions containing a fixed concentration of total silver, C_{Ag}, $1x10^{-4}$ M, 0.3 M total ionic strength and pH 7 buffered. The solutions were equilibrated with the 1.4 g resin column for 40 minutes at a flow rate of 7 ml $min.^{-1}$. The eluent was 0.05 M EDTA. Silver chloride precipitate was dissolved from the membrane filter using the same eluent. The values of free silver concentration are plotted in Figure 5.4 and 5.7.

Total chloride, M	Free chloride, [Cl⁻], M	$C_{Ag,sol}$ µmol l^{-1}	$n_{AgCl(s)}/V$ µmol l^{-1}	C_{Ag} [mass balance] µmol l^{-1}	Values of [Ag⁺] obtained by the ion-exchange method, µmol l^{-1}		Values of [Ag⁺] obtained by the ISE method µmol l^{-1}	Predicted values of [Ag⁺] µmol l^{-1}
					Before correction	After correction		
$3.0x10^{-6}$	$2.81x10^{-6}$	95.4 ± 0.4	-	95.4 ± 0.4	102 ± 4.8	102 ± 4.8	102 ± 1.7	99.8 ±1.0
$3.0x10^{-5}$	$5.17x10^{-6}$	74.2 ± 0.1	24.2± 0.2	98.4 ± 0.3	74.8 ± 1.8	74.8 ± 1.8	74.3 ± 1.2	75.2 ±0.8
$7.5x10^{-5}$	$1.08x10^{-5}$	34.8 ± 0.3	64.6 ± 0.6	99.4 ± 0.9	35.1 ± 1.1	35.1 ± 1.1	35.8 ± 0.6	35.8 ±0.4
$3.0x10^{-4}$	$2.02x10^{-4}$	1.90 ± 0.1	95.1 ± 0.9	97.0 ± 1.0	2.17 ± 0.08	2.17 ± 0.08	1.94 ± 0.04	1.92 ±0.02
$7.5x10^{-4}$	$6.51x10^{-4}$	0.87 ± 0.04	96.5 ± 0.7	97.4 ± 0.7	0.87 ± 0.04	0.697 ± 0.032	0.656 ± 0.016	0.60 ±0.01
$3.0x10^{-3}$	$2.90x10^{-3}$	0.43 ± 0.03	96.9 ± 0.8	97.3 ± 0.8	0.28 ± 0.01	0.163 ± 0.006	–	0.13 ±0.002
$7.5x10^{-3}$	$7.40x10^{-3}$	0.40 ± 0.08	98.2 ± 0.1	98.6 ± 0.2	0.18 ± 0.01	0.067 ± 0.004	–	0.053 ±0.001
$3.0x10^{-2}$	$2.99x10^{-2}$	0.78 ± 0.09	94.3 ± 1.0	95.1 ± 1.1	0.049 ± 0.001	0.0090 ± 0.0002	–	0.013 ±0.001
$7.5x10^{-2}$	$7.49x10^{-2}$	2.00 ± 0.13	94.3 ± 0.2	96.3 ± 0.3	0.043 ± 0.001	0.0036 ± 0.0001	–	0.0052 ±0.0001
0.30	0.30	96.8 ± 0.6	-	96.8 ± 0.6	0.043 ± 0.032	0.0018 ± 0.0013	–	0.0013 ±0.0001

± are standard deviations based on three replicates.

Table 5.3 Comparison of the experimental (fitted) and the litrature (corrected to an ionic strength of 0.3) values of stability and solubility product constants.

Equilibrium	Parameters	Values in Table 2.1 corrected to an ionic strength of 0.3	Values obtained from experimental data (curve-fitting)
$[AgCl]/[Ag][Cl]$	$\log \beta_{1,Cl}$	2.88	2.83
$[AgCl_2]/[Ag][Cl]^2$	$\log \beta_{2,Cl}$	4.88	4.49
$[AgCl_3]/[Ag][Cl]^3$	$\log \beta_{3,Cl}$	5.0	5.37
$[AgCl_4]/[Ag][Cl]^4$	$\log \beta_{4,Cl}$	5.93	5.94
$[Ag][Cl]$	log Ksp	-9.47	-9.41

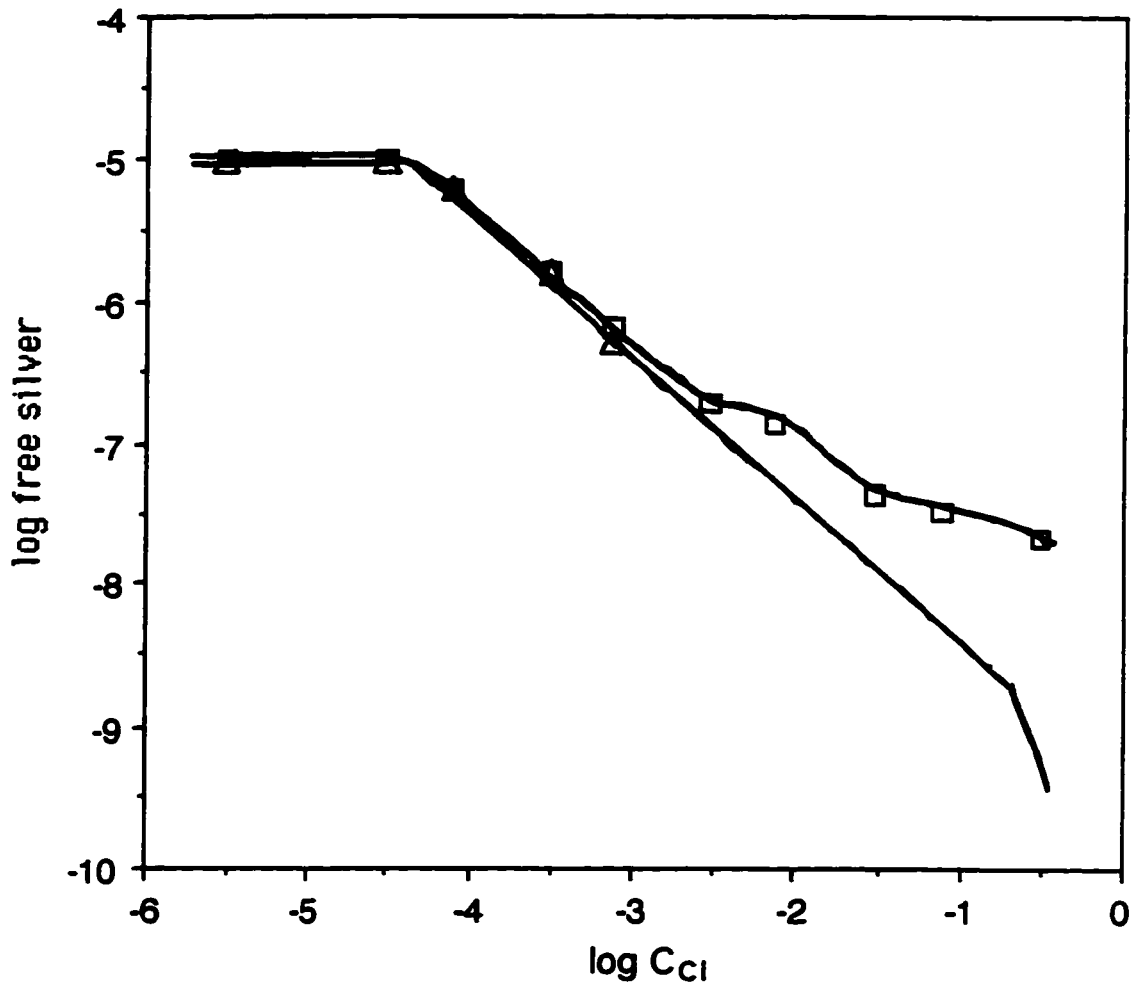

Figure 5.3 Variation of free silver ion concentration, [Ag^+], with total chloride concentration, C_{Cl}, in pH 7 buffered solutions containing fixed concentration of total silver, $C_{Ag} = 1x10^{-5}$ M and 0.3 M total ionic strength. The solutions were equilibrated with the 1.4 g resin column for 40 minutes at a flow rate of 7 ml $min.^{-1}$. As measured by: the column equilibration method (before correcting for sorption of AgCl) (□); the ion-selective electrode method (Δ); the bottom solid line shows the predicted values if only Ag^+ sorbs, and the top solid line shows the predicted values if both Ag^+ and AgCl(aq) sorb. The data are given in Table 5.1.

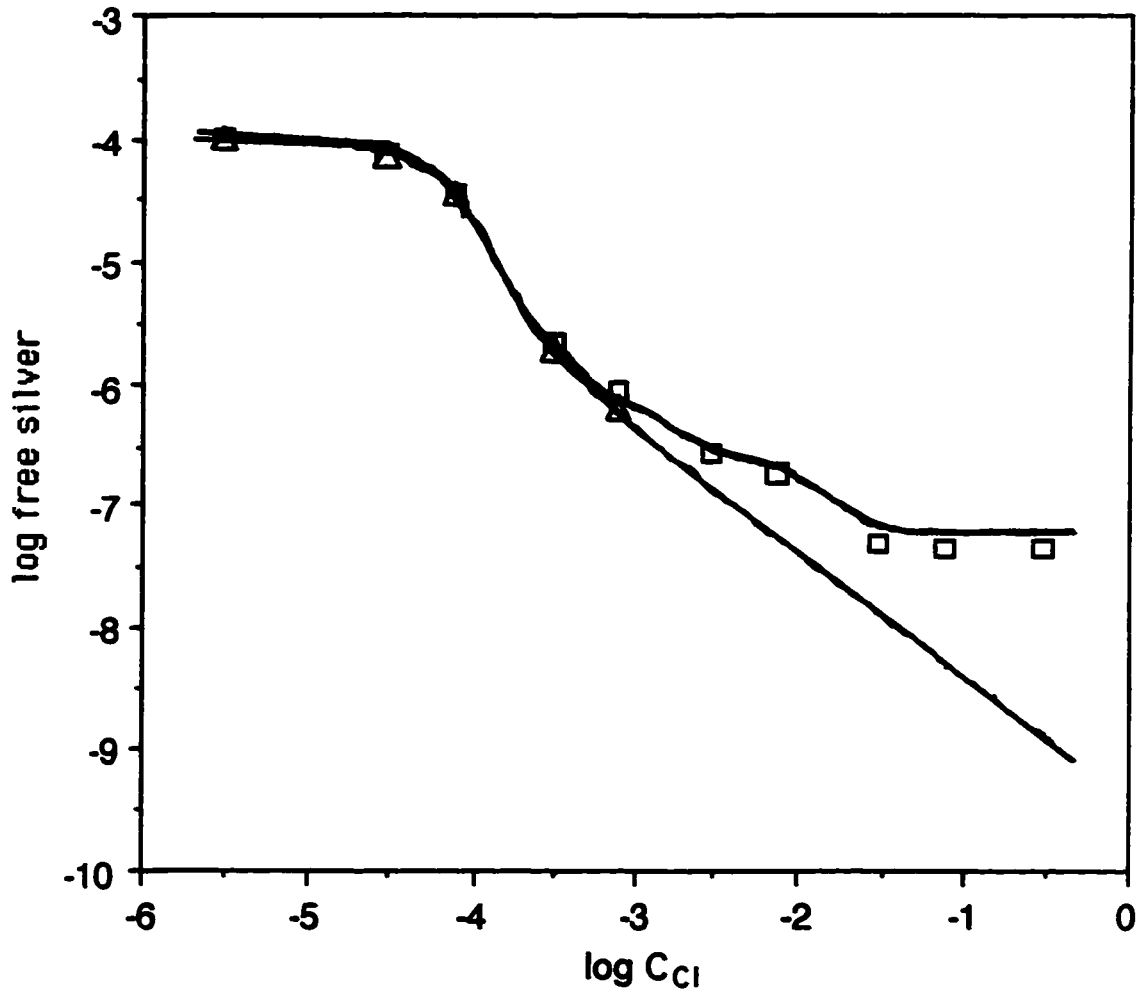

Figure 5.4 Variation of free silver ion concentration, $[Ag^+]$, with total chloride concentration, C_{Cl}, in pH 7 buffered solutions containing fixed concentration of total silver, $C_{Ag} = 1x10^{-4}$ M and 0.3 M total ionic strength. The solutions were equilibrated with the 1.4 g resin column for 40 minutes at a flow rate of 7 ml $min.^{-1}$. As measured by: the column equilibration method (before correcting for sorption of AgCl) (□); the ion-selective electrode method (Δ); the bottom solid line shows the predicted values if only Ag^+ sorbs, and the top solid line shows the predicted values if both Ag^+ and AgCl(aq) sorb. The data are given in Table 5.2.

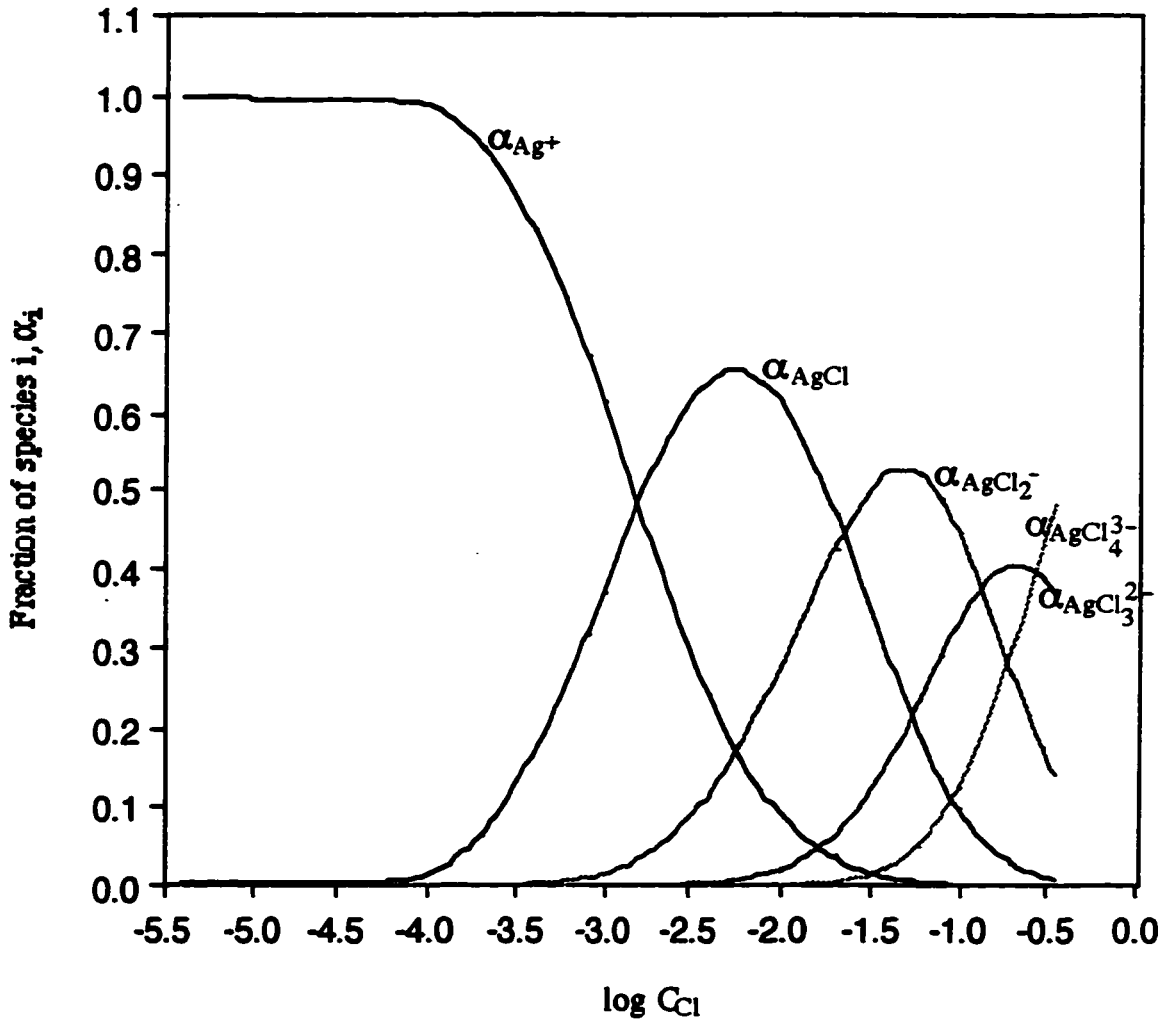

Figure 5.5 Silver species distribution as a function of log C_{Cl}.

calculation. Based on species distribution calculations, the results of which are illustrated in Figure 5.5, for total chloride concentration of $7.5x10^{-4}$ M , the predicted fraction of free silver in solution is about 65%. Clearly, when the fraction of free silver in solution is less than 65% (see Figure 5.5), the column equilibration method does not selectively measure free silver. High values for free silver ion concentration are obtained. The silver ion-selective electrode could not be used above total chloride concentration of $7.5x10^{-4}$ M because the concentration of Ag^+ in solution was less than the recommended limit ($1x10^{-6}$ M) for the use of the electrode [42].

The deviation observed for the values of free silver ion concentration obtained by the column equilibration method is due to sorption of other silver containing species. Species like $Ag(Cl)_2^-$, $Ag(Cl)_3^{2-}$, $Ag(Cl)_4^{3-}$ are not likely to be sorbed onto the cation exchanger due to co-ion exclusion. Also, filterable colloidal AgCl(s) species with particle size less than 0.45 μm, if present, are not likely to sorb onto the cation exchanger [58]. This is because when the fraction of Ag^+ is less than 65%, pAg is greater than 6.3. Since the point of zero charge (PZC) for colloidal silver chloride is pAg 4.6 [62-64], the particles are negatively charged, ($AgCl(s) \cdot Cl_X^{-X}$), and therefore they will be excluded from the cation exchanger particles. A possible explanation for the observed deviation could be sorption of the neutral silver chloride, AgCl(aq), species. If this is true, the concentration of sorbed silver in the eluate as quantified by the AAS is the concentration of total silver sorbed, C_{RAg}, (i.e. the concentration of silver sorbed as [RAg] and [R.AgCl].

The theoretical considerations and equations for quantitatively testing for sorption of the neutral metal-ligand species, AgCl(aq), together with metal ion, Ag^+, are given in section 2.2.4. Equation 2.2.17, can be re-written in the form shown below:

$$C_{RAg,cal} = (\lambda_{Ag+}\,\alpha_{Ag+} + \lambda_{AgCl}\,\alpha_{AgCl})\,C_{Ag,sol} \qquad \ldots\ldots\ 5.1$$

where $C_{RAg,cal}$ is the predicted concentration of total silver sorbed and all other symbols have their usual meanings (see Chapter 2).

The values of α_{Ag+}, α_{AgCl}, and $C_{Ag,sol}$ can be calculated for any chloride concentration by using the literature values of stability constants and the free chloride concentration, [Cl^-]. The value of λ_{Ag+} is the slope of the linear region of the ion-exchange calibration curve (e.g. Figure 4.21). In this case the value of 0.144 ± 0.001 lg^{-1} was used. The computer program A.5 and the spreadsheet in Table A.5 were used to estimate the value of the distribution coefficient, λ_{AgCl} of AgCl between the resin phase and the solution phase, as described in Appendix A.

The value of λ_{AgCl} which gives the best-fit to the experimental data was found to be 0.0642 ± 0.0220 lg^{-1}. The fraction of silver sorbed as free silver, f_{RAg}, is obtained by substituting the values of λ_{AgCl}, λ_{Ag+} and the corresponding values of α_{Ag+}, α_{AgCl} and $C_{Ag,sol}$ into equation 5.2 below, which is obtained by rearranging equation 5.1.

$$f_{RAg} = \frac{\lambda_{Ag+}\ \alpha_{Ag+}}{(\lambda_{Ag+}\ \alpha_{Ag+} + \lambda_{AgCl}\ \alpha_{AgCl})} \qquad \text{..... 5.2}$$

The amount of silver sorbed as free silver, [RAg], is calculated by multiplying f_{RAg} by the experimentally measured total silver sorbed, $C_{RAg,exp}$. The amount of silver sorbed as the neutral complex, [R.AgCl], is calculated by difference; i.e.

$$[R.AgCl] = C_{RAg,exp} - [RAg] \qquad \text{..... 5.3}$$

The top solid line in Figures 5.3 and 5.4 show the predicted values of [Ag^+] which would be obtained if both Ag^+ and AgCl(aq) sorb onto the resin.

The corrected value of free silver ion concentration is calculated by substituting [RAg] in place of $C_{RAg,exp}$. The values of free silver ion concentration obtained after correction for sorption of AgCl(aq) species in this way are given in column 7 of Tables 5.1 and 5.2. Figures 5.6 and 5.7 show the same results as Figures 5.3 and 5.4 after correction for

sorption of AgCl(s) species. The agreement of the column equilibration, (□), the ion-selective electrode, (Δ), and the theoretically predicted values (solid line) is good. This suggests that the cause of deviation from behavior predicted by equation 2.2.5 is indeed the sorption of AgCl(aq) together with Ag^+ by the exchanger. From these results it is evident that column equilibration method can be used to measure much lower concentrations of free silver ion than the ion-selective electrode.

5.3.1.3 Determination of free silver ion concentration under non-trace conditions

As discussed in section 2.2.3, when an ion-exchange resin bed is equilibrated with solutions containing high concentrations of Ag^+, the concentration of silver sorbed,[RAg], on the resin is not directly proportional to the concentration of free silver ion, [Ag^+], in solution; i.e. trace ion-exchange conditions are not met. In order to achieve trace ion-exchange conditions for solutions with high concentration of free silver ion, a high concentration of electrolyte ($NaNO_3$) in solution is required. The main disadvantage of this approach is that a high concentration of the electrolyte leads to perturbation of Ag-ligand equilibria. Another approach is to use a small resin column under non-trace conditions. This approach was used previously in the determination of ionic Ca^{2+} and Mg^{2+} with satisfactory results [79].

An experiment was conducted to measure free silver ion concentration under non-trace conditions. The small column recycle flow system (Figure 3.4) was used. All solutions were prepared as described in section 5.2.2.1. The sample solutions with total silver concentrations of $1x10^{-2}$ M, $1x10^{-3}$ M and $1x10^{-4}$ M were adjusted to various free silver ion concentrations by adding different amounts of chloride ligand as shown in column 3 of Table C.3. The solutions were buffered at pH 7. The total ionic strength of each solution was adjusted to 0.3 M by adding the appropriate amount of sodium nitrate. In all these

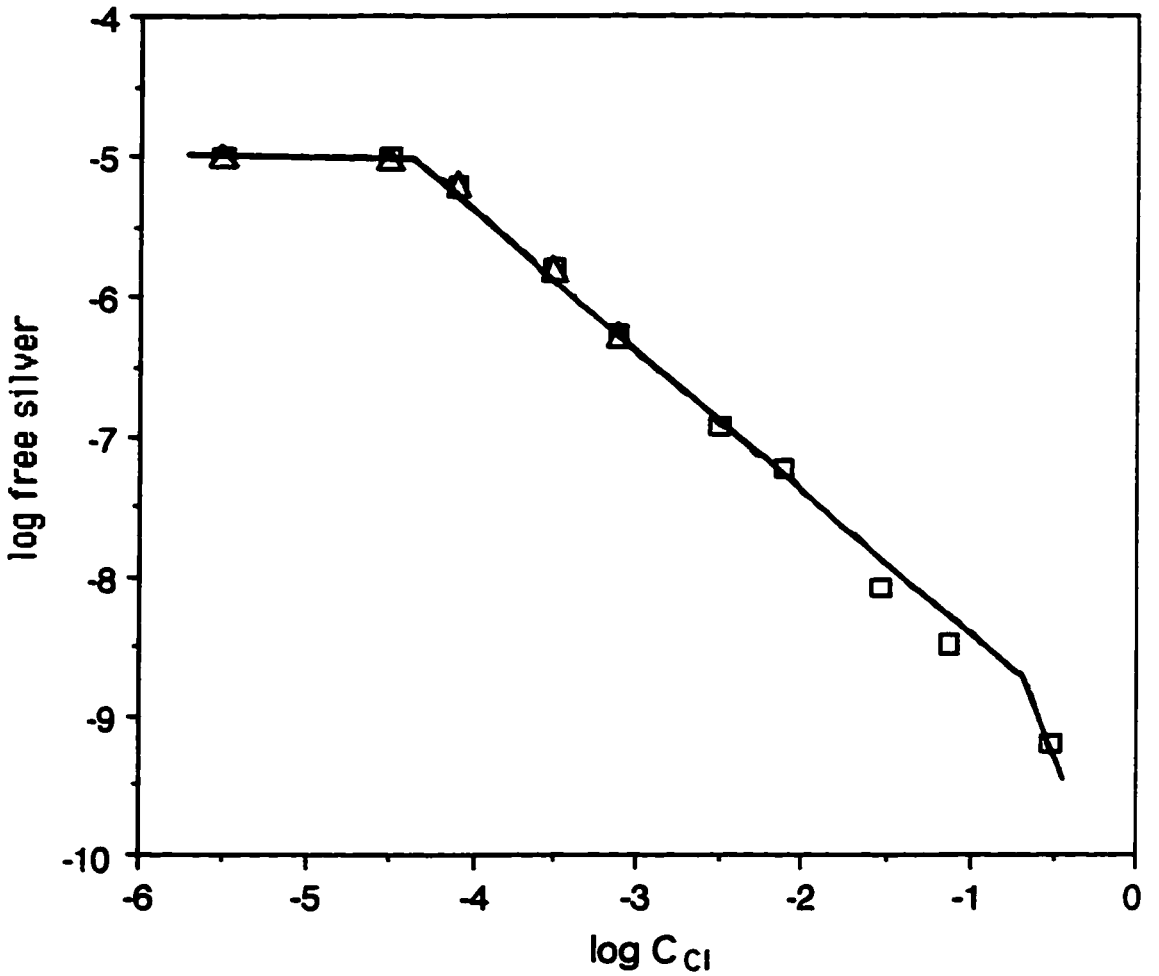

Figure 5.6 Variation of free silver ion concentration, [Ag^+] with total chloride concentration in pH 7 buffered solutions containing fixed concentration of total silver, $C_{Ag} = 1x10^{-5}$ M and 0.3 M total ionic strength as measured by: the column equilibration method (after correcting for sorption of AgCl), (□); the ion-selective electrode method (Δ) and; the predicted values (solid line). The data are given in Table 5.1.

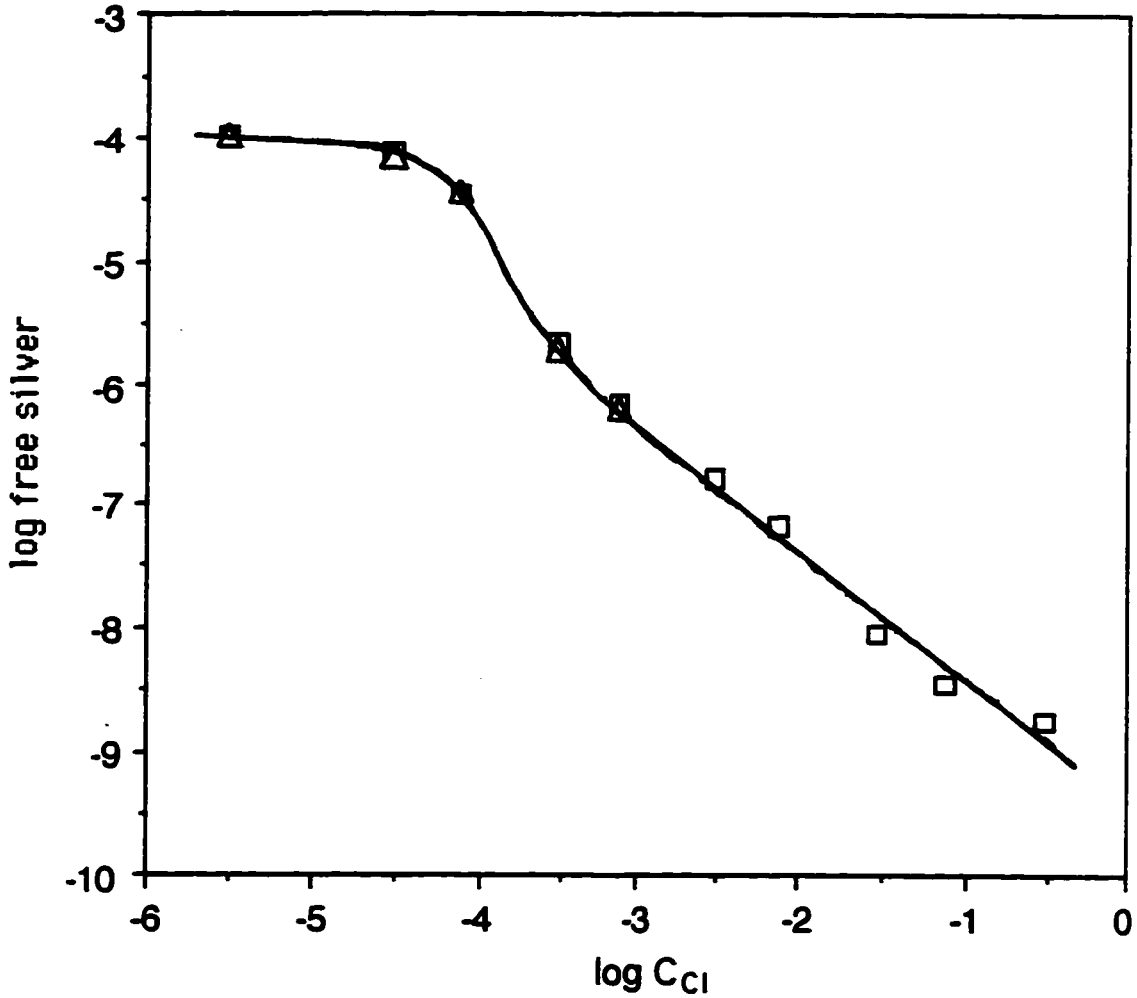

Figure 5.7 Variation of free silver ion concentration, [Ag^+] with total chloride concentration in pH 7 buffered solutions containing fixed concentration of total silver , C_{Ag} = $1x10^{-4}$ M and 0.3 M total ionic strength as measured by: column equilibration method (after correcting for sorption of AgCl) (□); the ion-selective electrode method (Δ) and; the predicted values (solid line). The data are given in Table 5.2.

solutions solid silver chloride, AgCl(s), was present. The solutions were filtered using an on-line filter (0.45 μm Nylon 66 membrane filter) as shown in Figure 3.4.

Using the procedure described in section 5.2.3, each sample and standard solution was loaded onto the resin column at a flow rate of 6 ml $min.^{-1}$ for a period of 5 minutes. The ion-exchange calibration curve, Figure 5.8, which was used to quantitate the values of free silver ion concentration, is convex. The curvature is a result of non-trace conditions at the high concentrations of Ag^+ used. For example, when the concentration of silver in solution is $1x10^{-3}$ M, the amount of silver sorbed onto the resin is about 73.3 μmol g^{-1}. This amount accounts for approximately 1.4% (see equation 4.2) of the total resin sites. With the aid of the computer software, Cricket graph version 1.3, the best-fit polynomial equation was obtained, from which the values of free silver ion concentration were interpolated. The values of free silver ion concentration measured by the column equilibration method and by the ion-selective electrode method, and by the theoretical equilibrium calculations using computer program A.4, are shown in Figure 5.9. The data are given in Table C.3.

Figure 5.9 reveals that the values of free silver ion concentration obtained by the column equilibration method (□) and the ion-selective electrode method (Δ) are both in good agreement with those obtained by the theoretical equilibrium calculations (●). Both techniques measure free silver ion concentration. Under these experimental conditions (especially the ionic strength) the sorption of AgCl(aq) is not significant because the fraction of AgCl(aq) in solution is relatively small (< 20%) compared to that of free silver ion. In section 5.3.1.2 (under similar conditions) it has been demonstrated that the sorption of AgCl(s) starts to be significant when the fraction of AgCl(aq) is about 30%.

From these results it can be concluded that free silver ion concentration can be measured with reasonable accuracy even when the column is operated under non-trace conditions provided that the curvature of the calibration curve (isotherm) is not severe.

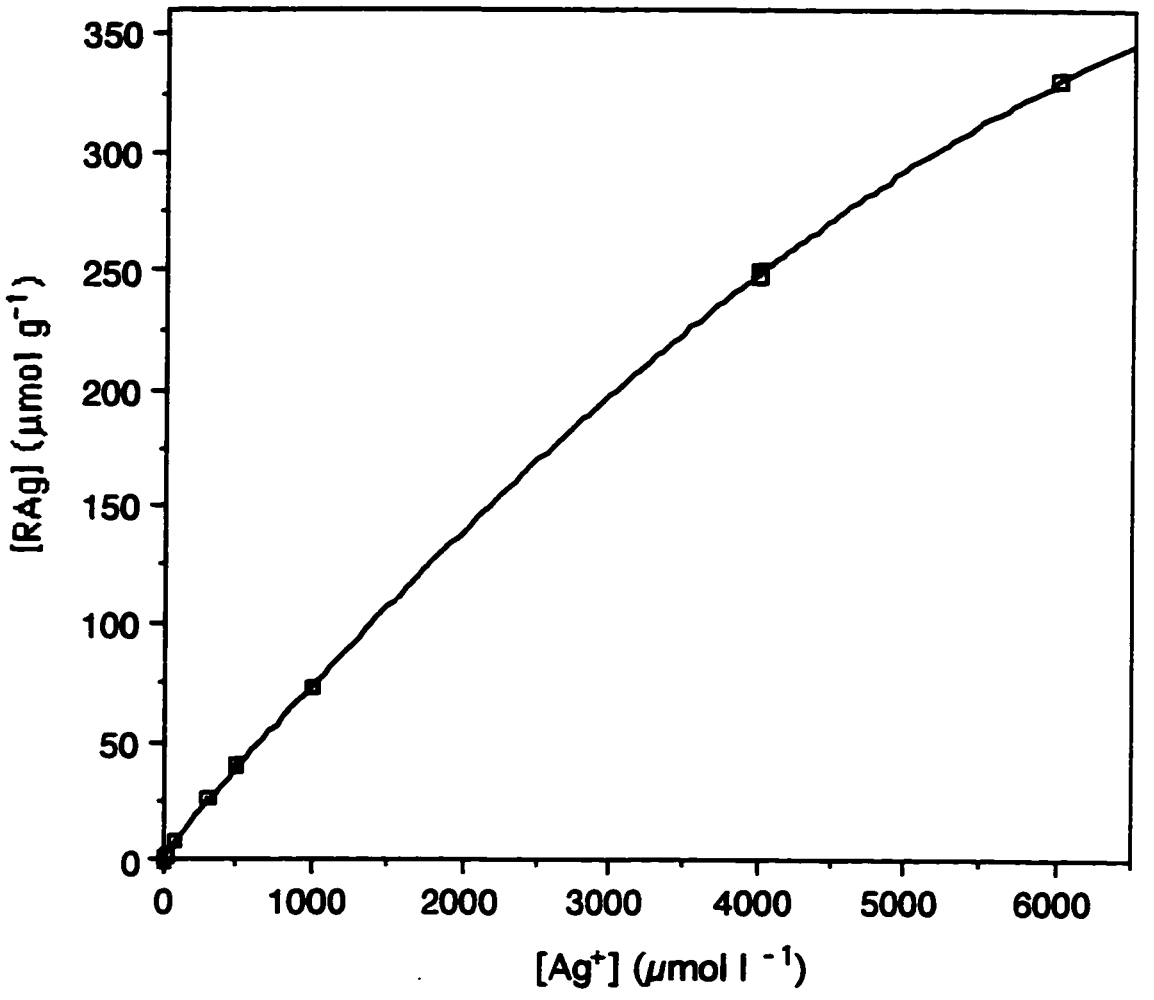

Figure 5.8 Ion-exchange calibration curve (sorption isotherm) for Ag^+ in 0.3 M total ionic strength and pH 7 buffered standard solutions. The silver standard solutions were loaded onto a 15 mg resin column (Figure 3.4) at a flow rate of 6 ml $min.^{-1}$. The eluent was 0.05 M EDTA at pH 10.

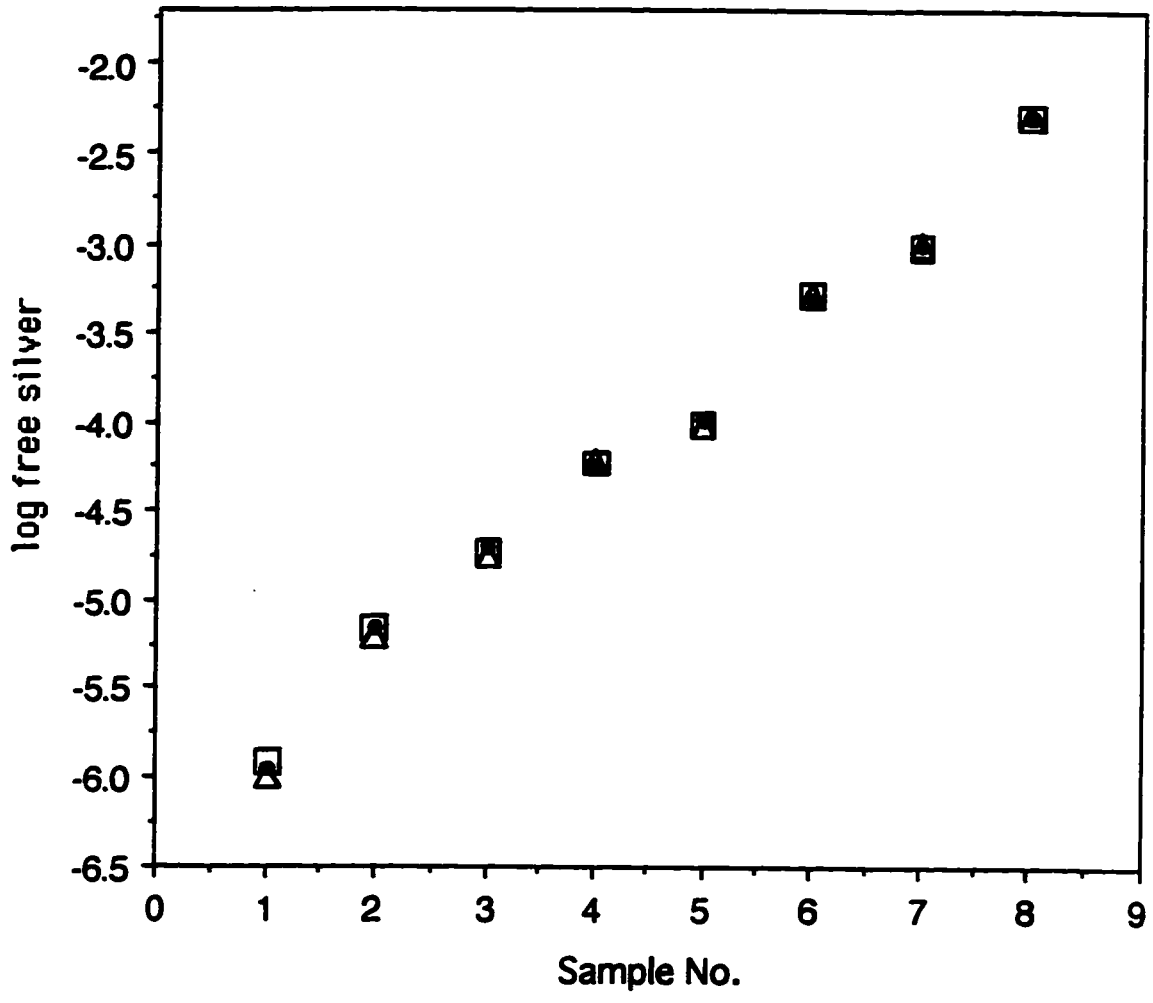

Figure 5.9 Comparison of values of free silver ion concentration, [Ag^+] in pH 7 buffered synthetic solutions of 0.3 M total ionic strength loaded onto a 15 mg resin column (Figure 3.4) at a flow rate of 6 ml $min.^{-1}$. As measured by: the column equilibration method (□); the ion-selective electrode method (Δ) and; the predicted values (●). The data are given in Table C.3.

5.3.1.4 Effect of ionic strength and aging of AgCl(s) on Ag^+ concentration

An experiment was carried out to determine free silver ion concentration at the three different ionic strengths of 0.3 M, 0.15 M and 0.05 M. The small column single pass flow system (Figure 3.3) was used. The sample and standard solutions of desired ionic strength were prepared as described in section 5.2.2.1. The ionic strength was adjusted by adding varying amounts of sodium nitrate in the silver standard and the sample solutions. The amount of $NaNO_3$ in each solution was in large excess. All sample solutions were saturated with AgCl(s) were filtered through a 0.45 μm membrane filter either immediately after preparation, after aging for an hour, or after aging for 15 hours. The filtrates were analyzed for free silver ion concentration by both the column equilibration and the ion-selective electrode methods.

Using the procedure described in section 5.2.3, each solution was passed through the resin bed at a flow rate of 7 ml $min.^{-1}$ for different equilibration (loading) times as shown in Table 5.4 below. The composition of the sample solutions and other parameters are also given in the Table 5.4. The results obtained are shown in Tables 5.5a through 5.5c. The times for which the solutions were left to age are shown in column 1, the values of total concentration of silver in the filtrate, $C_{Ag,sol}$, are shown in column 2; the concentration of silver chloride solid, AgCl(s), $n_{AgCl(s)}$ /V, is shown in column 3; and the mass balance obtained by adding the values in column 2 and 3 are shown in column 4. An average recovery of 98 ± 2% was obtained. Columns 5, 6 and 7 show the values of free silver ion concentration obtained by the column equilibration method, the ion-selective electrode method and the theoretical equilibrium calculations as calculated using the computer program A.4.

It can be seen by comparing the last columns among Tables 5.5a - c that as the ionic strength increases the predicted values of free silver ion concentration slightly increase.

Table 5.4 Composition of sample solutions and other parameters used in the determination of $[Ag^+]$ at different ionic strengths.

Total ionic strength, M	0.30	0.15	0.050
Total silver conc. (C_{Ag}), M	$1.0x10^{-4}$	$1.0x10^{-4}$	$1.0x10^{-4}$
Total choride conc. (C_{Cl}), M	$3.0x10^{-5}$	$3.0x10^{-5}$	$3.0x10^{-5}$
pH	7.0	7.0	7.0
Sample loading time, min.	2 - 15	8 - 12	10 - 15
Standard loading time, min.	5	8	10
Loading flow rate, ml $min.^{-1}$.	7.0	7.0	7.0

Table 5.5 Results obtained for the determination of free silver ion concentration in the presence of varying amounts of $NaNO_3$ (ionic strength) in solutions of fixed total silver ($1x10^{-4}$ M) and total chloride ($3x10^{-5}$ M) concentrations. The solutions were left to age for different period of time before filtering. The filtrates were loaded onto a 15 mg , Figure 3.3 at a flow rate of 7 ml $min.^{-1}$.

Table 5.5a Ionic strength = 0.05 M

Aging time	$C_{Ag,sol}$ $\mu mol\ l^{-1}$	$n_{AgCl(s)}/V$ $\mu mol\ l^{-1}$	C_{Ag} $\mu mol\ l^{-1}$	Values of $[Ag^+]$ obtained by the ion-exchange method in $\mu mol\ l^{-1}$	Values of $[Ag^+]$ obtained by the ISE method in $\mu mol\ l^{-1}$	Predicted values of $[Ag^+]$ in $\mu mol\ l^{-1}$
After mixing	73.8 ± 1.0	24.8 ± 0.2	98.6 ± 1.2	73.5 ± 1.4	73.1 ± 1.2	74.2 ± 0.8
After 1 hour	72.2 ± 4.9	26.2 ± 0.2	98.4 ± 5.1	71.9 ± 1.6	70.6 ± 1.1	74.2 ± 0.8
After 15 hours	73.4 ± 0.5	24.5 ± 0.1	97.9 ± 0.6	72.2 ± 1.6	72.2 ± 1.2	74.2 ± 0.8

± are standard deviations based on four replicates.

Table 5.5b Ionic strength = 0.15 M

Aging time	$C_{Ag,sol}$ μmol l^{-1}	$n_{AgCl(s)}/V$ μmol l^{-1}	C_{Ag} μmol l^{-1}	Values of $[Ag^+]$ obtained by the ion-exchange method in μmol l^{-1}	Values of $[Ag^+]$ obtained by the ISE method in μmol l^{-1}	Predicted values of $[Ag^+]$, in μmol l^{-1}
After mixing	74.3 ± 0.5	25.7 ± 0.2	100 ± 1	74.1 ± 1.5	74.4 ± 1.2	74.8 ± 0.8
After 1 hour	74.3 ± 0.1	23.7 ± 0.2	98.0 ± 0.3	73.4 ± 1.4	73.4 ± 1.2	74.8 ± 0.8
After 15 hours	74.8 ± 0.5	24.6 ± 0.9	99.4 ± 1.4	74.2 ± 1.4	73.0 ± 1.2	74.8 ± 0.8

± are standard deviations based on four replicates.

Table 5.5c I = 0.3 M

Aging time	$C_{Ag,sol}$ μmol l^{-1}	$n_{AgCl(s)}/V$ μmol l^{-1}	C_{Ag} μmol l^{-1}	Values of $[Ag^+]$ obtained by the ion-exchange method in μmol l^{-1}	Values of $[Ag^+]$ obtained by the ISE method in μmol l^{-1}	Predicted values of $[Ag^+]$, in μmol l^{-1}
After mixing	76.4 ± 3.0	24.5 ± 3.5	101 ± 7	76.8 ± 1.4	75.1 ± 1.2	75.2 ± 0.8
After 1 hour	66.5 ± 2.1	29.0 ± 1.4	95.5 ± 3.5	65.9 ± 1.1	65.4 ± 1.1	75.2 ± 0.8
After 15 hours	74.1 ± 2.5	23.0 ± 0.7	97.1 ± 3.2	72.4 ± 1.0	72.5 ± 1.2	75.2 ± 0.8

± are standard deviations based on four replicates.

This is due to the decrease in the activity coefficient with increase in ionic strength. Based on the theoretical calculations, the activity coefficient, γ_{Ag^+}, changes by only 10% when the ionic strength is changed from 0.05 - 0.3 M. Also, it is evident that, for any given aging time and ionic strength, the values of free silver ion concentration measured by both the column equilibration and the ion-selective electrode methods are in good agreement with one another. Both techniques measure free Ag^+ concentration. At 15 hours, the experimental values of $[Ag^+]$ are equal to the theoretical predicted values within the limits of experimental error. For the lower ionic strengths of 0.05 M and 0.15 M the experimental values of $[Ag^+]$ obtained for different aging times are not different from one another within the limits of the experimental error. However, for the highest ionic strength of 0.3 M the values of $[Ag^+]$ are different for different aging times. The difference is attributed to the behavior of colloidal silver chloride with time.

For the solution which was filtered just after preparation the value of $[Ag^+]$ is higher than the value at one hour. In spite the fact that the formation of silver chloride precipitate at high concentrations is rapid, at low concentrations of Ag^+ and Cl^- the rate of reaction is slow. Thus, in such a short time, equilibrium has not yet been reached, i.e. AgCl(s) is still precipitating, so that the level of free silver in solution is relatively higher.

For the solution which was filtered after aging for an hour the value of $[Ag^+]$ has decreased compared to the initial value. This is because after a period of one hour, precipitation is complete so that more AgCl(s) has precipitated. In solution Ag^+ is in excess compared to Cl^- ($Ag^+ : Cl^- \approx 15 : 1$), therefore some Ag^+ will be adsorbed on the AgCl(s) particles [80,81]. Upon filtration through a 0.45 μm membrane filter, especially with high concentration of dispersed particles and large sample load, clogging of the filter pores occurs [82-85]. The clogging leads to the formation of a gel-layer (induced coagulation). Thus the effective pore size of the filter is reduced. As a result of this, much smaller

particles with Ag^+ adsorbed on them are trapped on the membrane filter [83]. Overall relatively less free Ag^+ will remain in solution.

Finally, for the solution which was filtered after aging for 15 hours the level of Ag^+ has increased above the value at one hour. This is probably the result of slow spontaneous coagulation of the colloidal AgCl(s) particles. When the particles coagulate, the total surface area of the particles decreases and some Ag^+ which was adsorbed in between the particles is released into the solution. Thus, the concentration of Ag^+ in solution increases but that of the dispersed particles decreases. These changes are more evident at a higher ionic strength of 0.3 M than lower ionic strengths of 0.05 M and 0.15 M. This is because high concentration of electrolyte enhances the coagulation of colloidal particles. Also, at the high ionic strength of 0.3 M, the surface charge density is relatively higher than at lower ionic strengths of 0.05 M and 0.15 M. Thus upon coagulation a significant amount of Ag^+ is released into the solution.

From the values of $[Ag^+]$ obtained by the ion-selective electrode method and the amount of adsorbed AgCl(s) a possible size for the colloidal AgCl(s) primary particle can be estimated as follows:

Let us assume that the AgCl(s) particle is a sphere of radius r, therefore:

$$\frac{\text{Total volume of the precipitate}}{\text{Total surface area of the precipitate}} = \frac{\frac{4}{3} \times \pi (r_p)^3 \times n_p}{4 \pi (r_p)^2 \times n_p} = \frac{r}{3} \qquad \text{.....5.4}$$

Where n_p is the total number of the AgCl(s) particles.

From the concentration of the precipitate (column 3 in Table 5.5c), the formula weight of AgCl(s) and the density of AgCl(s) (5.56 g cm^{-3}) we can calculate the volume of the precipitate as follows:

Weight of AgCl(s) precipitate = 29×10^{-6} mol l^{-1} x 1 l x 143.32 g/ mole = 0.0042 g

$$\text{Total volume of the precipitate} = \frac{0.0042\ \text{g}}{5.56\ \text{g cm}^{-3}} = 7.55 \times 10^{-4}\ \text{cm}^3 \qquad \text{.....5.5}$$

Based on the values of $[Ag^+]$ at 1 hour and 15 hours, the amount of Ag^+ desorbed is:

$$(72.5 - 65.4) \times 10^{-6}\ \text{mol l}^{-1} \times 1\ \text{l} = (7.1 \pm 2.3) \times 10^{-6}\ \text{moles}$$

To calculate the total area of the precipitate on which 7.1×10^{-6} moles of Ag^+ was adsorbed, we need to know the value for the mono-layer coverage. The mono-layer coverage based on the crystal radius and the hydrated radius of Ag^+ are 3.33×10^{-9} and 8.46×10^{-10} moles cm^{-2}, respectively. Since, the surface charge on the particles is low near the point of zero charge, we can assume that Ag^+ occupies a small fraction of the mono-layer, e.g. if the surface concentration of Ag^+ hydrated is about 20% of the mono-layer value (5% for the non-hydrated ion), then:

$$\text{Total area of the precipitate} = \frac{7.1 \times 10^{-6}\ \text{moles}}{0.2 \times 8.46 \times 10^{-10}\ \text{moles cm}^{-2}} = 4.2 \times 10^4\ \text{cm}^2 \qquad \text{.....5.6}$$

Combining equations 5.5 with equation 5.6, we can calculate the radius of the AgCl(s) particle as follows:

$$r = 3 \times \frac{7.55 \times 10^{-4}\ \text{cm}^3}{4.2 \times 10^4\ \text{cm}^2} = 5.4 \times 10^{-8}\ \text{cm} = 0.54\ \text{nm}$$

The diameter of the AgCl(s) particle is therefore, 1.1 ± 0.2 nm.

Based on the radii of the hydrated (0.25 nm) [86] or non-hydrated (0.126 nm) [87] Ag^+ we can calculate the number of Ag^+ adsorbed on one AgCl(s) particle as four ions per particle. For example, using the Ag^+ hydrated radius we obtain:

$$\text{No. of } Ag^+(H_2O)_x \text{ per particle} = \frac{0.2 \times \text{surface area of the particle}}{\text{cross-sectional area of the hydrated } Ag^+} \qquad \text{.....5.7}$$

$$= \frac{0.2 \times 4 (r_p)^2}{(r_{Ag^+(H2O)})^2} = 4$$

From its radius (0.54 nm) and its density (5.56 g cm^{-3}) the mass of one average AgCl(s) colloidal particle is $3.88x10^{-21}$ g. Such a particle will contain 16 "molecules" of AgCl.

Thus from the above results the AgCl(s) particle with four Ag^+ adsorbed on it is as shown in Figure 5.10.

The colloidal state is comprised of particles having size between 1-100 nm. Thus, the value of 1.1 nm obtained for the diameter of the AgCl(s) particle falls within the range of the colloidal state, but the particles are very small. This could be a result of very dilute solutions used to form the particles. When very dilute solutions are used, the supersaturation is still sufficient for extensive nucleation to occur, but the rate of particle growth is low due to limited reagent, as described by Shaw [88]. Thus, a high degree of dispersion is obtained and very small particles are formed.

From these results we can conclude that the column equilibration technique, combined with prior filtration through a 0.45 μm pore size membrane filter, can be used to measure free silver ion concentration in solutions of various ionic strengths. In the presence of AgCl(s), the concentration of free silver ion in the solution depends not only on the activity coefficient of the Ag^+, but also on the kinetics of precipitation and colloidal formation.

5.3.2 Determination of free silver ion concentration, [Ag^+], in the presence of hydroxide ligand

The underlying idea for these studies is to determine the concentration of free silver ion in the presence of silver-hydroxo species. Therefore, the complexing ligand hydroxide will be used. By varying the buffered pH, sample solutions having various fixed concentrations of free silver ion can be obtained.

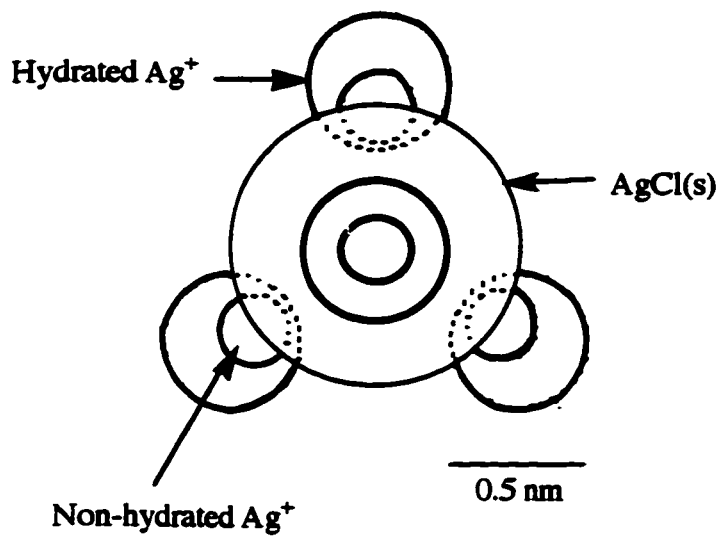

Figure 5.10 A pictorial model of AgCl(s) particle with $Ag^+ (H_2O)_x$ adsorbed on it, drawn to scale to show their relative dimensions. The colloidal AgCl(s) particle contains 16 "molecules" of AgCl and is assumed to be spherical for ease of calculations. The hydrated Ag^+ are arbitrarily assumed to be at the corners of a tetrahedron to minimize electrostatic repulsion among them.

5.3.2.1 Equilibrium sorption of Ag^+ in the presence of hydroxide ligand and $Ag_2O(s)$

In section 4.7 sorption isotherms of Ag^+ on Dowex 50W-X8 at pH 7 were measured. At this pH the concentration of Ag^+ in solution can be raised to about 0.43 M before $Ag_2O(s)$ starts to precipitate. However, if the pH of the solution is raised to pH 10, $Ag_2O(s)$ will start to precipitate when the concentration of free Ag^+ in solution is above 4.3×10^{-4} M. Silver oxide is also a colloidal precipitate. Its point of zero charge (PZC) is at about pH 10.4 [89]. An experiment was conducted to examine the sorption of Ag^+ in the presence of hydroxide ligand and $Ag_2O(s)$.

Sample solutions of varying concentration of Ag^+ but the same total ionic strength of 0.3 M were prepared as described in section 5.2.2.2. The pH of each solution was adjusted to pH 10. For sample solutions with Ag^+ concentration greater than 4.3×10^{-4} M, brownish-black precipitate of $Ag_2O(s)$ was observed. These solutions were filtered by using the 0.45 μm Nylon 66 membrane filter before being loaded onto the resin column. Using the procedure given in section 4.7.2, each sample solution was equilibrated with the 15 mg resin column (Figure 3.3) for 5 minutes at a flow rate of 7 ml $min.^{-1}$. The results obtained are shown in Figure 5.11 and the data are given in Table C.4.

Two regions are evident in Figure 5.11. The first region, which is shown in Figure 5.12 shows that as the concentration of Ag^+ in solution is increased, the concentration of silver sorbed,[RAg], also increases. This region represents the sorption isotherm of Ag^+ at pH 10. In this region there is no solid silver oxide, $Ag_2O(s)$, present. At pH 10, the fraction of Ag^+ which is free is almost 99% (see Figure 5.14 below). Thus, the presence of OH^- ligand can be ignored.

The second region shows that as the concentration of Ag^+ in solution is increased, the concentration of silver sorbed, [RAg], remains unchanged. This is evident as a plateau in Figure 5.11. The plateau is not due to saturation of the resin in the column but of the solutions which are passed through the resin. The concentration of Ag^+ in the saturated

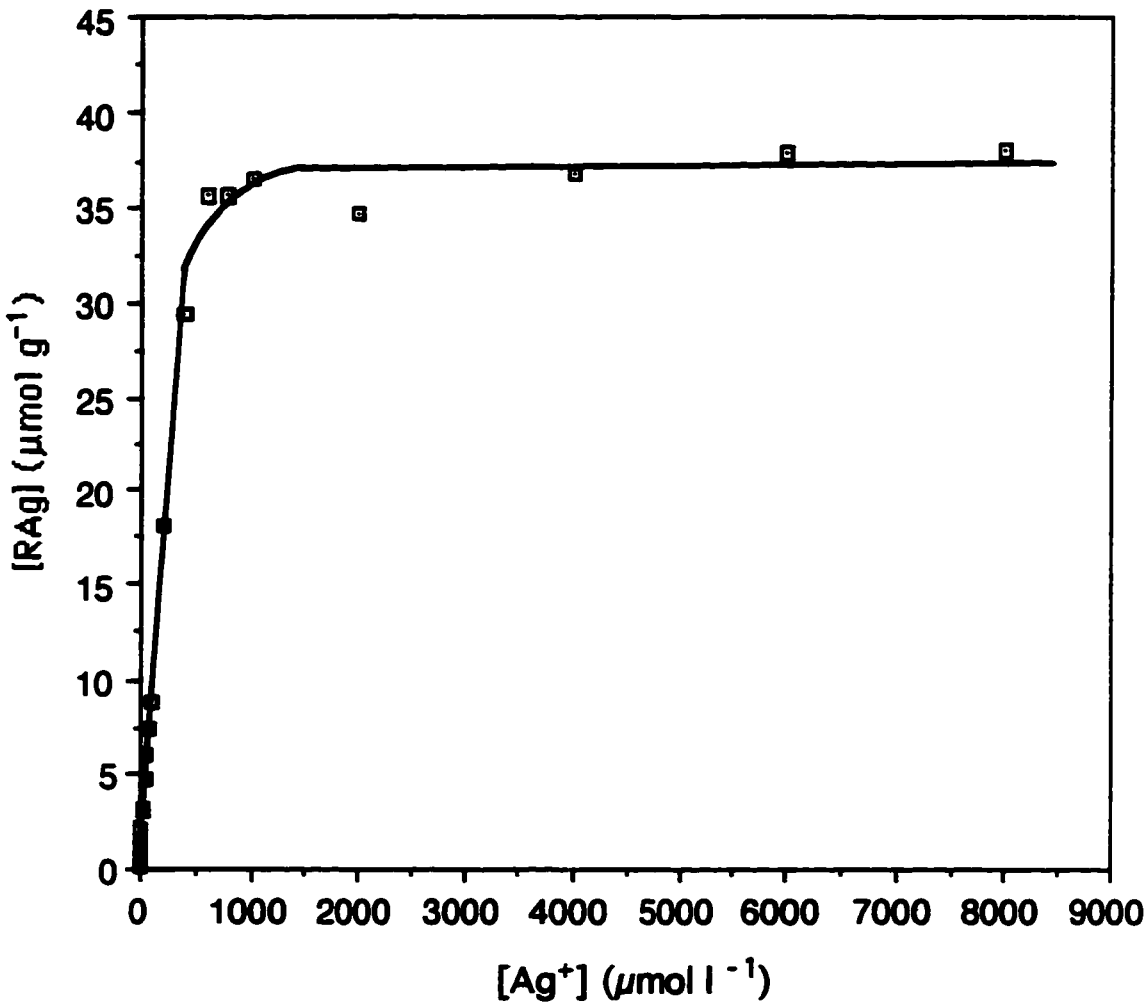

Figure 5.11 Equilibrium sorption of Ag^+ on Dowex 50W-X8 resin in the presence of hydroxide ligand and $Ag_2O(s)$. Solutions of differing concentrations of Ag^+ in 0.3 M $NaNO_3$ at pH 10 were loaded onto a 15 mg resin column for 5 minutes at a flow rate of 7 ml $min.^{-1}$. The eluent was 0.05 M EDTA at pH 10. The data are given in Table C.4.

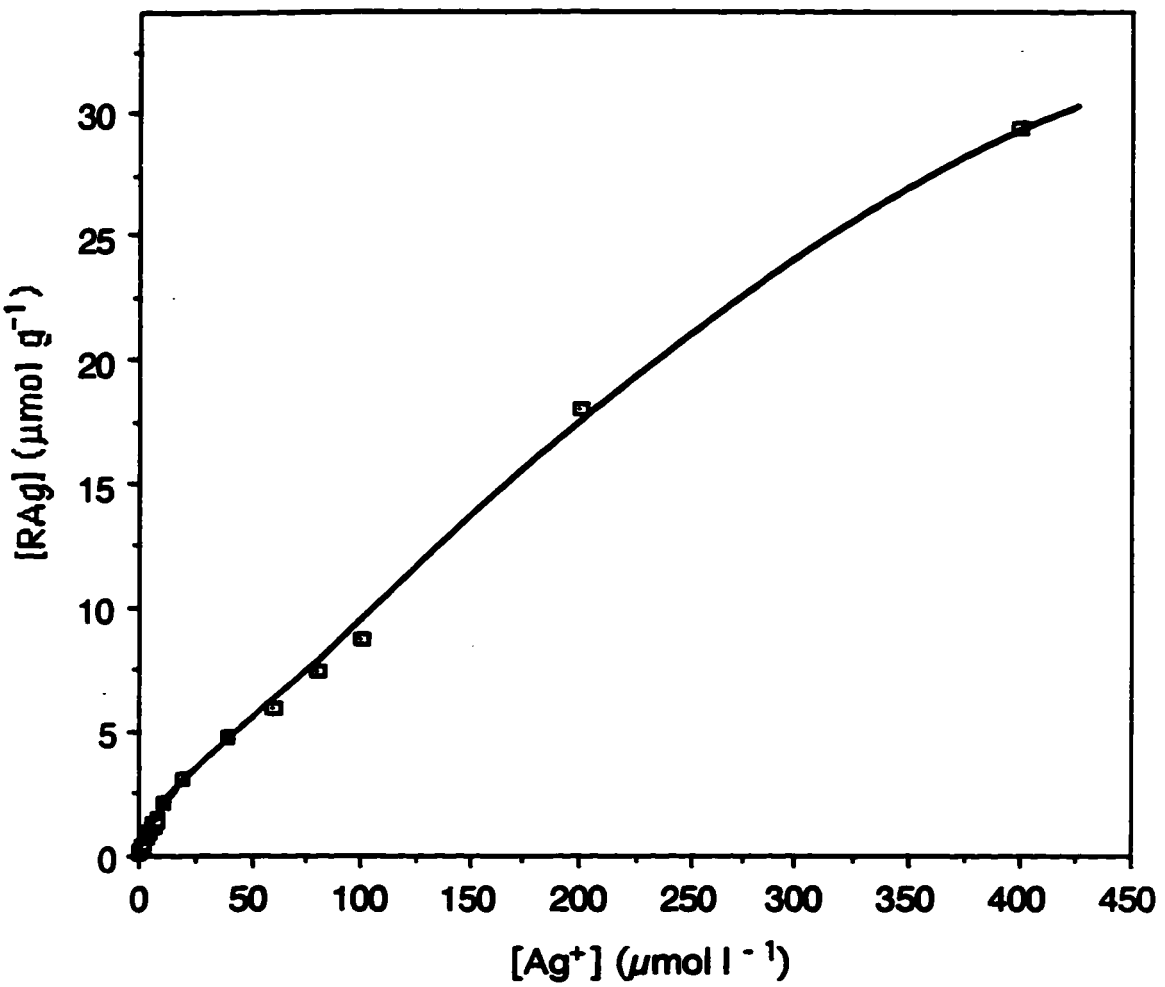

Figure 5.12 Low concentration region (the first region) of Figure 5.10 above.

solution is set by the solubility product constant, Ksp, of silver oxide. Its value at an ionic strength of 0.3 M is 4.27×10^{-8}. This value was estimated using equations given in section 2.12b. The literature value [53] is given in Table 2.1.

The concentration of sorbed silver, [RAg], obtained by loading the saturated solutions was used to estimate the concentration of Ag^+ in the saturated solutions by interpolating the value of $[Ag^+]$ from the ion-exchange calibration curve shown in Figure 5.13. The ion-selective electrode was also used to measure the concentration of free Ag^+ in the filtered saturated solutions. The values of $[Ag^+]$ measured by the ion-selective electrode and by the column equilibration methods and calculated using free ligand concentration, $[OH^-]$ and the solubility product constant are shown in Table 5.6, below.

It can be seen that the concentration of free silver ion in the saturated solutions is constant. Within the limits of experimental error, the average value of $[Ag^+]$ obtained by the column equilibration $(4.36 \pm 0.09) \times 10^{-4}$ M and the ion-selective electrode $(4.29 \pm 0.01) \times 10^{-4}$ M methods (± are pooled standard deviations) are both in good agreement with the predicted value $(4.27 \pm 0.06) \times 10^{-4}$ M. This means that both methods measure free silver ion concentration and that if present, colloidal silver oxide particles are neither sorbed nor filtered out by the cation exchanger.

5.3.2.2 Determination of free silver ion concentration at different pH

Hydroxide is a ligand for silver. According to species distribution calculations, the results of which are illustrated in Figure 5.14, up to pH 10, 99% of soluble silver species is free silver, Ag^+. However at pH greater than 10, the fraction of other silver-hydroxo soluble species is high enough to significantly reduce the fraction of Ag^+ in solution. An experiment was carried out to measure free silver ion concentration between pH 11 and 13.

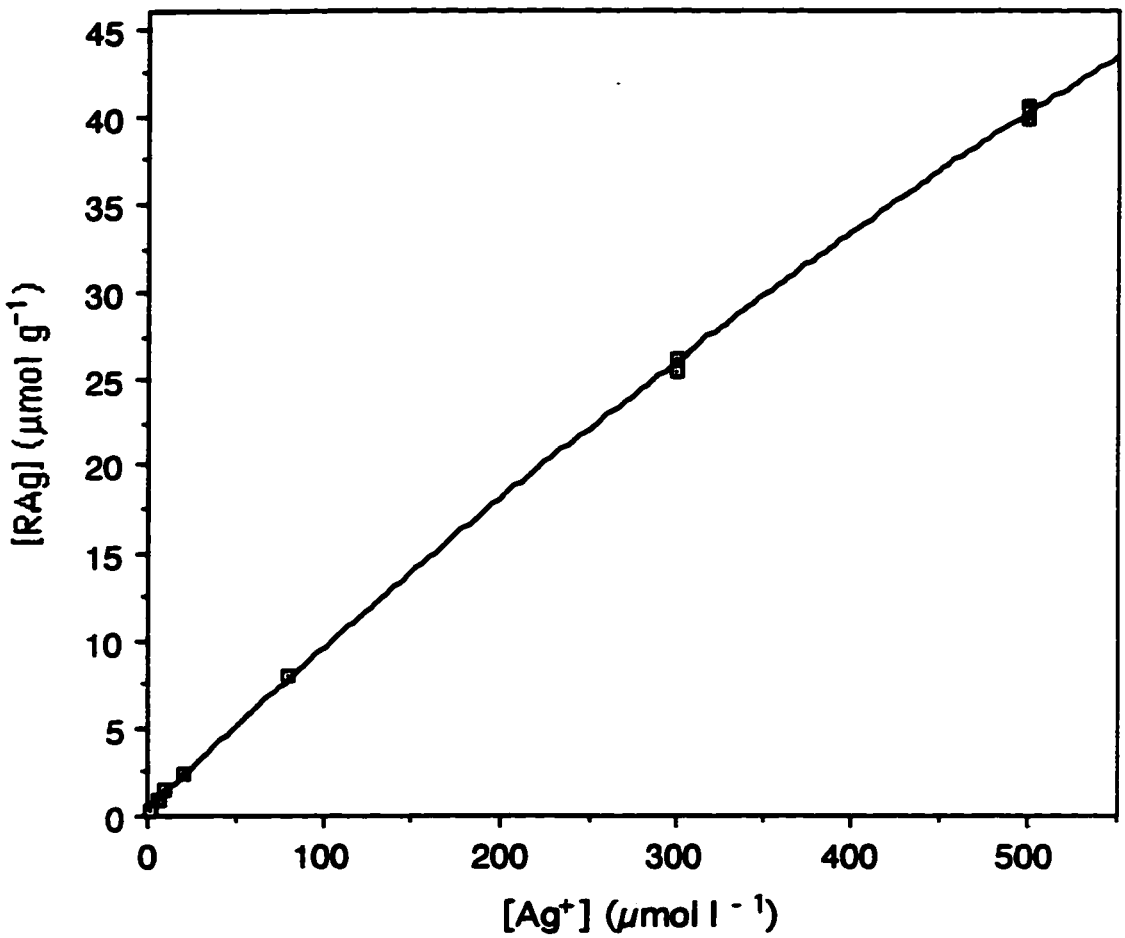

Figure 5.13 Ion-exchange calibration curve (sorption isotherm) for Ag^+ in 0.3 M total ionic strength and pH 7 buffered standard solutions.

Table 5.6 Values of $[Ag^+]$ for filtered saturated solutions of $Ag_2O(s)$. The solutions were loaded onto a 15 mg resin column for 5 minutes at a flow rate of 7 ml $min.^{-1}$. The eluent, 0.05 M EDTA (pH10) was passed at a flow rate of 2 ml $min.^{-1}$.

Total silver, C_{Ag} $\mu mol\ l^{-1}$	Values of $[Ag^+]$ obtained by the ion-exchange method in $\mu mol\ l^{-1}$	Values of $[Ag^+]$ obtained by the ISE method in $\mu mol\ l^{-1}$	Predicted values of $[Ag^+]$ in $\mu mol\ l^{-1}$
600.0	424 ± 10	440 ± 7	427 ± 6
800.0	423 ± 10	403 ± 7	427 ± 6
1000.0	438 ± 9	428 ± 7	427 ± 6
2000.0	411 ± 9	410 ± 7	427 ± 6
4000.0	442 ± 10	435 ± 7	427 ± 6
6000.0	455 ± 9	445 ± 8	427 ± 6
8000.0	458 ± 9	445 ± 8	427 ± 6

± are standard deviations based on three and five replicates for the ion-exchange and ion-selective methods, respectively.

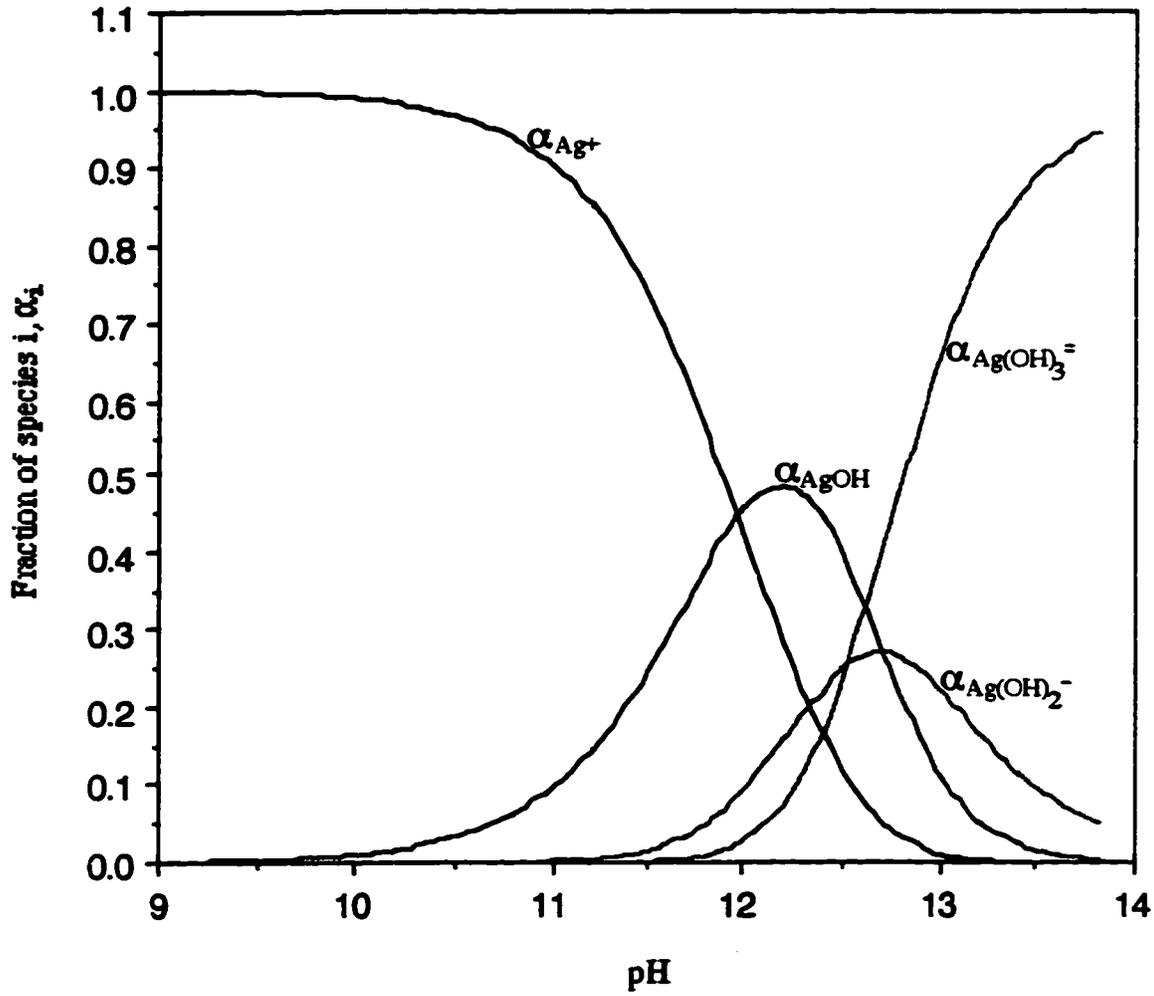

Figure 5.14 Silver species distribution as a function of pH.

The small column recycle flow system (Figure 3.4) was used. The pre-conditioning, standard, and sample solutions were prepared as described in section 5.2.2.2.

Six sample solutions were prepared in such a way that the fraction of free silver ion in each solution was different. The initial and final pH values (as described in section 5.2.2.2) of the solutions are shown in columns 3 and 4 of Table 5.7, respectively. The final pH values in column 4 were used to calculate the free hydroxide ion concentration which, in turn, was used to calculate the fractions of different species present in solution. The total concentration of silver, C_{Ag}, and concentration of $NaNO_3$ in each solution are shown in columns 2 and 5, respectively. Each sample and standard solution was equilibrated with the resin bed at a flow rate of 6 ml $min.^{-1}$ for 5 minutes. The results obtained by the column equilibration method, by the ion-selective electrode method, and the predicted values of free silver ion concentration are shown in Figure 5.15 and the data are given in Table C.5. The predicted values of $[Ag^+]$ were calculated by using the free ligand concentration and values of Ksp, $\beta_{1,OH}$, $\beta_{2,OH}$ and $\beta_{3,OH}$ from Table 2.1 corrected to an ionic strength of 0.3.

Figure 5.15 reveals that there is a good agreement between the predicted values of free silver ion concentration and the values obtained by using the ion-selective electrode method. Also, as expected, the concentration of Ag^+ decreases with increasing pH. The values of $[Ag^+]$ obtained by using the column equilibration method are very high compared to both the predicted and the ion-selective electrode values. This shows that the column equilibration method does not selectively measure the concentration of free silver ion . The predicted fractions of different silver-hydroxo species between pH 9 and 13.5 are shown in Figure 5.14 where it can be seen that the fraction of AgOH(aq), α_{AgOH}, passes through a maximum at about pH 12.3. This maximum is consistent with the maximum observed at about pH 12.5 in the values of free silver ion concentration obtained by the column equilibration method. This suggest that the deviation observed for the values of free silver

Table 5.7 Composition of sample solutions used for the determination of the concentration of free silver ion in solutions of different pH.

Sample No	C_{Ag+} mol l^{-1}	Initial pH	Final pH	$NaNO_3$ mol l^{-1}
1	$1.50x10^{-5}$	11.71	11.43	0.30
2	$2.50x10^{-5}$	12.12	11.89	0.29
3	$3.70x10^{-5}$	12.50	12.29	0.28
4	$5.20x10^{-5}$	12.68	12.49	0.26
5	$6.70x10^{-5}$	12.88	12.71	0.24
6	$1.00x10^{-4}$	13.08	12.97	0.20

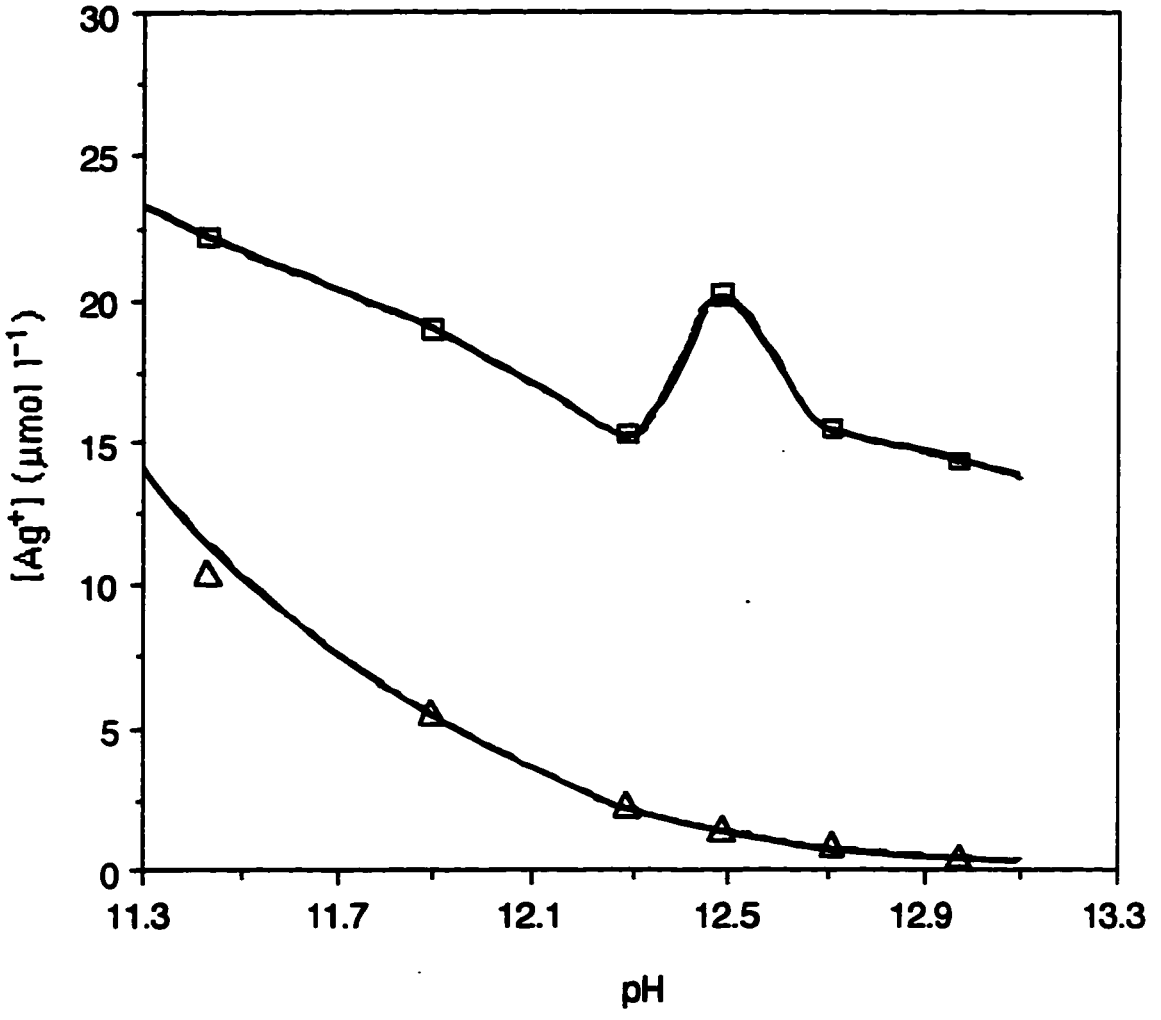

Figure 5.15 Variation of free silver ion concentration with pH in solutions of 0.3 M total ionic strength loaded onto a 15 mg resin column (Figure 3.4) at flow rate of 6 ml $min.^{-1}$. As measured by: the column equilibration method (before correction for sorption of AgOH) (□); the ion-selective electrode method (Δ) and; the bottom solid line shows the predicted values if only Ag^+ sorbs and, the top solid line shows the predicted values assuming that both Ag^+ and AgOH(aq) also sorb. The data are given in Table C.5.

ion concentration as obtained by the column equilibration method is due to sorption of the silver hydroxide neutral species, AgOH(aq).

As in the case of silver-chloride system, species like $Ag(OH)_2^-$ and $Ag(OH)_3^{2-}$ are not likely to sorb onto the cation exchanger [58]. Also, colloidal silver oxide species with particle size less than 0.45 μm, if present, are not likely to sorb onto the cation exchanger. This is because the pH of the solutions is greater than 11 while the point of zero charge (PZC) for colloidal silver oxide is pH 10.4 [89]. Thus, the particles are negatively charged, $(Ag_2O(s).OH^-_X)$, therefore they will be excluded from the cation exchanger particles [58].

The equation and the procedure for the estimation of the distribution coefficient, λ_{AgOH}, of AgOH(aq) between the resin phase and solution phase are similar to the one discussed in section 5.3.1.2. The values of α_{Ag+}, α_{AgOH}, and $C_{Ag,sol}$, as calculated using free ligand concentration, $[OH^-]$, stability and solubility product constants are shown in Table A.6 (Appendix A).

The ion-exchange calibration curve shown in Figure 5.16 was obtained by equilibrating the resin bed with silver standard solutions as described in section 5.2.3. The calibration curve is best described by the non-linear fit of the form:

$$[RAg] = 0.12451 + 0.13618[Ag^+] - 5.0022e\text{-}4[Ag^+]^2 \qquad R^2 = 0.999 \quad ..... \quad 5.3$$

The value of λ_{Ag+} was calculated for each data point in the calibration curve, Figure 5.16. These values with corresponding values of α_{Ag+}, α_{AgOH}, and $C_{Ag,sol}$, were substituted in equation 5.1 to obtain the corresponding values of λ_{AgOH}. The spreadsheet used to estimate the values of λ_{AgOH} (for each data point) which give the best-fit to the experimental data is shown in Table A.6. The average values of λ_{Ag+} and λ_{AgOH} are 0.142 ± 0.031 lg^{-1} and 0.415 ± 0.051 lg^{-1}, respectively . However, as it turned out, all of the sample solutions corresponding to the points in Figure 5.15 (after correction for sorption of AgCl(aq)) had

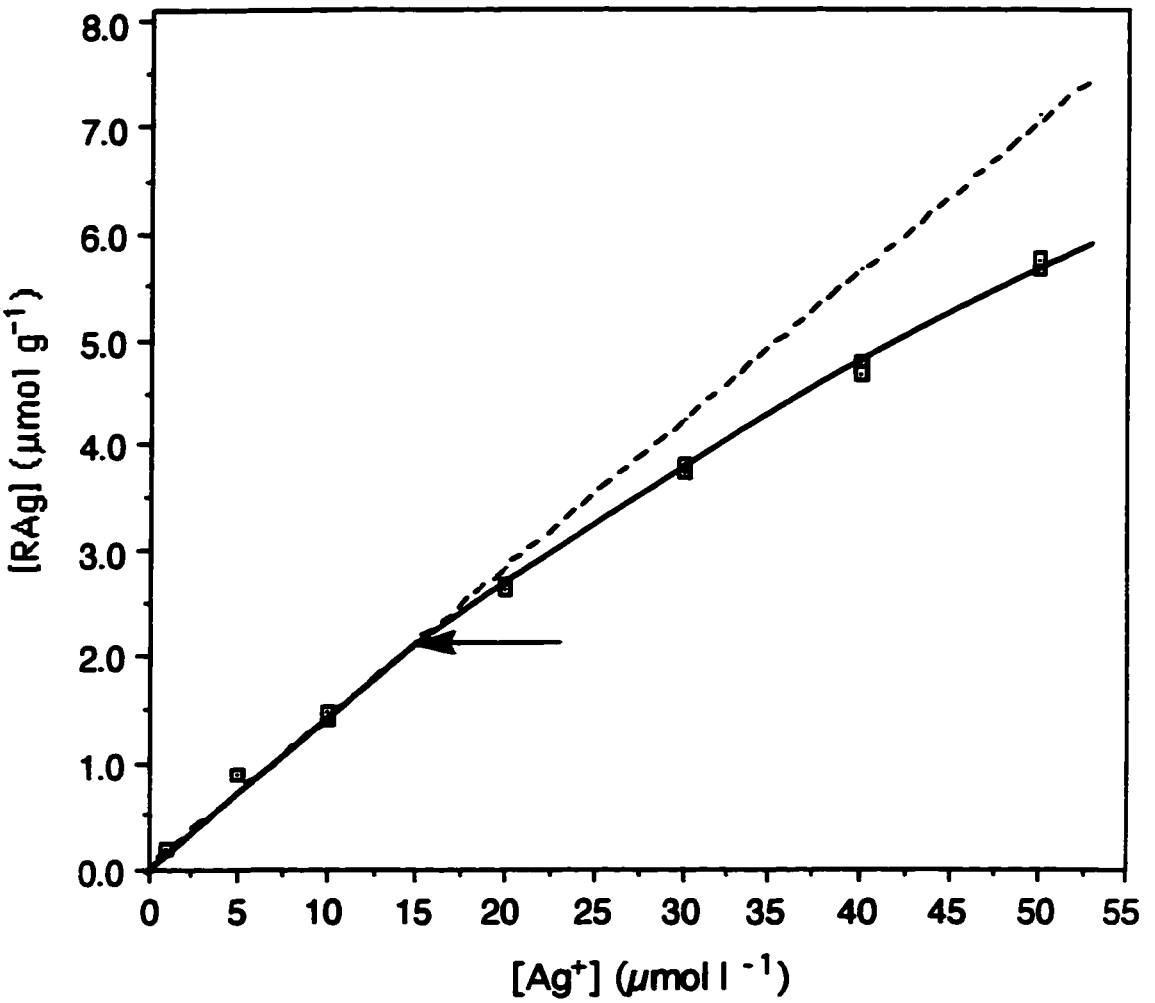

Figure 5.16 Ion-exchange calibration curve (sorption isotherm) for Ag^+ in 0.3 M total ionic strength and pH 7 buffered standard solutions. The silver standard solutions were loaded onto a 15 mg resin column (Figure 3.4) at a flow rate of 6 ml $min.^{-1}$. The eluent was 0.05 M EDTA at pH 10. The arrow indicates the highest [RAg] read from the curve after correction for sorption of AgCl(aq).

$[Ag^+] < 15\ \mu mol\ l^{-1}$, so that they were all in the linear region of the ion-exchange calibration curve (isotherm) in Figure 5.16.

Therefore it was possible to simplify the calculations by using the average value of the distribution coefficient, $\lambda_{Ag^+} = 0.142 \pm 0.031\ lg^{-1}$ (the slope of the dotted line in Figure 5.16) from this linear region to calculate the corrected values of $[Ag^+]$.

The fraction, f_{RAg}, and the concentration, [RAg], of silver sorbed as free silver and the concentration of silver sorbed as the neutral species,[R.AgOH], are calculated in the same way as described in section 5.3.1.2. The top solid line in Figure 5.15 shows the predicted values assuming that both Ag^+ and AgOH(aq) sorb onto the resin.

The values of free silver ion concentration obtained after correction for sorption of AgOH(aq) species are shown in Figure 5.17. The agreement of the column equilibration values (□) with the ion-selective electrode values (Δ) and the theoretically predicted values (solid line) is good. This suggest that the cause of deviation from behavior predicted by equation 2.2.5 was indeed the sorption of AgOH(aq) together with Ag^+ by the exchanger.

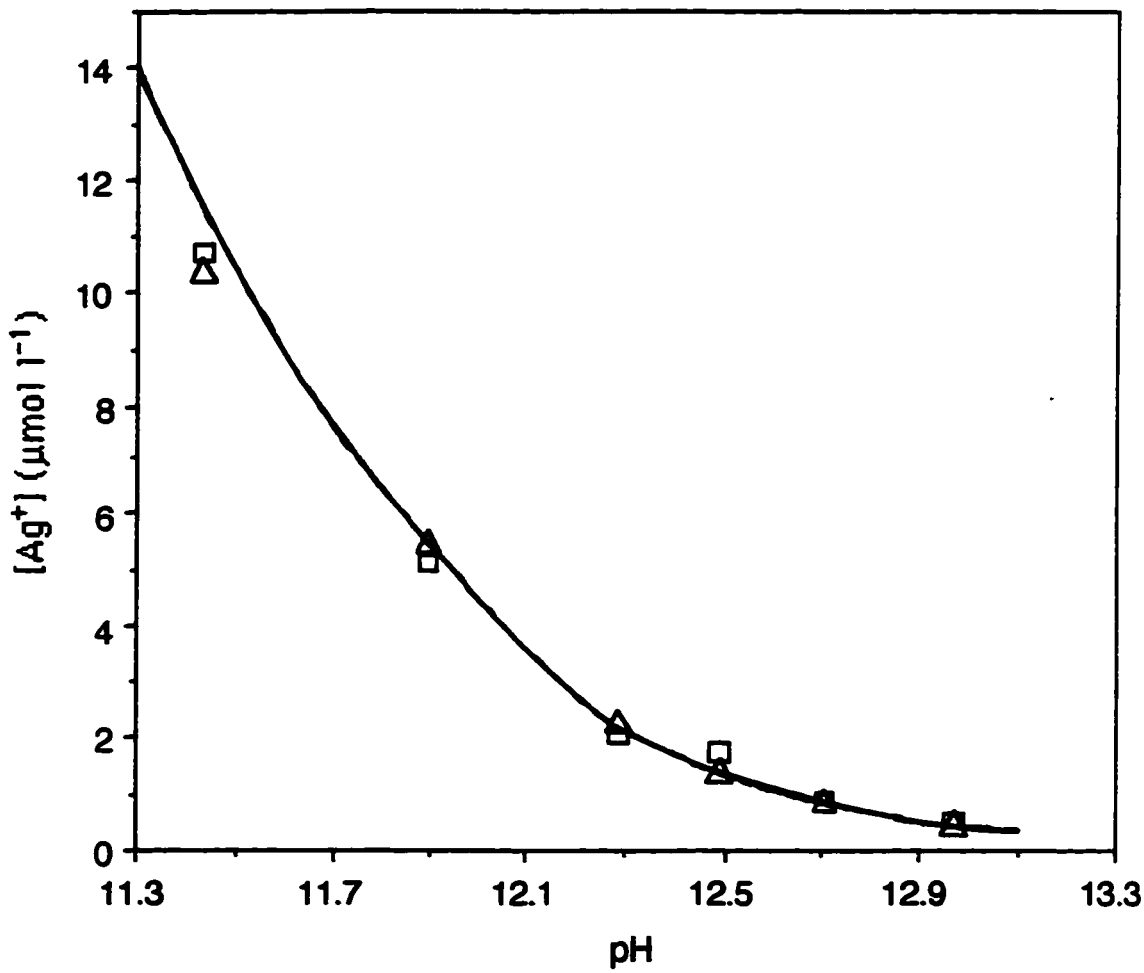

Figure 5.17 Values of free silver ion concentration shown in Figure 5.5 after correction for sorption of AgOH. As obtained by: the column equilibration method (after correction for sorption of AgOH). (□); ion-selective electrode method (Δ) and; the solid line shows the predicted values. The data are given in Table C.5.

5.4 Summary and conclusion

The ion-exchange column equilibration technique for the determination of free silver ion concentration in synthetic solutions was first characterized by measuring the breakthrough curves, elution curves, equilibration curves and sorption isotherms. It was found that the elution and equilibration of solution containing silver ions with Dowex 50W-X8 resin depends more on the amount of analyte supplied than on the rate at which the analyte is supplied (contact time), i.e. elution and equilibration are supply limited. The sorption isotherm was found to be linear up to 10.0 μmol l^{-1} Ag^+; in this region the distribution coefficient of Ag^+ between the resin phase and the solution phase is constant (see Figure 4.21).

The technique was characterized with respect to its selectivity for the free Ag^+ species in the presence of silver chloro and hydroxo species. It was found that the resin sorbs both the free Ag^+ and the neutral AgCl(aq) and AgOH(aq) species, but does not sorb negatively charged soluble silver species like $AgCl_2^{2-}$, $AgCl_3^{2-}$, $AgCl_4^{3-}$, $Ag(OH)_2^-$ and $Ag(OH)_3^{2-}$ and colloidal silver chloride and silver oxide at pAg and pH above their points of zero charge, (PZC). After filtration through a 0.45 μm pore size membrane filter and at pAg and pH just below their PZC, positively charged colloidal silver chloride and silver oxide seem to cause no significant interference, sections 5.3.11 and 5.3.2.1, respectively. The procedure for correction of the interference of the AgCl(aq) and AgOH(aq) species has been proposed and tested. After correction, good agreement has been obtained between the values of free silver ion concentration measured by the column equilibration method and the predicted values, down to nanomolar levels. The proposed procedure can be applied only if the appropriate equilibrium constants are known beforehand. With known equilibrium constants the value of free ligand concentration and therefore the fractions of the species, α_i can be estimated.

The ion-selective electrode method is generally selective for Ag^+ for the ligands studied. However, it is not applicable to Ag^+ concentrations below $1x10^{-6}$ M. Hence, the ion-exchange column equilibration method is three orders of magnitude more sensitive than the silver ion-selective electrode method. However, it requires longer analysis times than the ion-selective electrode method.

The column equilibration method can be modified to compensate for some of its limitations. For example, the analysis time can be decreased by reducing the amount of resin in the column. Thus, equilibration and elution time will be reduced. Since the construction of the resin column is relative simple, a variety of columns containing differing amounts and types of resin can be prepared beforehand, and interchanged as required to match sample solution properties or sample volumes.

The method can be modified to improve its selectivity for Ag^+ over the neutral soluble silver species by lowering the ionic strength of the solutions, thus increasing the selectivity by increasing the distribution coefficient of the Ag^+ species.

Bibliography

[1] Florence, T. M.; Morrison, G. M.; Stauber, J. L. Sci. Total Environ. 1992, 125, 1-13.

[2] Jasinki, R.; Trachtenberg, I.; Andrychuk, D. Anal. Chem. 1974, 46, 364-369.

[3] Gachter, R.; Davies, J. S.; Nares, A. Envir. Sci. and Tech. 1978, 12, 1416-1421.

[4] Allen, H. E.; Hall, R. H.; Brisbin, T. D. Envir. Sci. and Tech. 1980, 14, 441-443.

[5] Sunda, W. G.; Engel, D. W.; Thuotte, R. M. Envir. Sci. and Tech. 1978, 12 (4), 409-413.

[6] Zorkin, N. G.; Grill, E. V.; Lewis, A. G. Anal. Chem. Acta. 1986, 183, 163-177.

[7] Sunda, W.; Guillard, R. R. L. J. Mar. Res. 1976, 34, 511-529.

[8] Mowat, A. J. Water Pollut. Control Fed. 1976, 48 (5), 853-866.

[9] Modak, S. M.; Fox, C. L. Biochem. Pharmacol. 1973, 22, 2391-2404.

[10] Terhaar, C. J.; Ewell, W. S.; Dziuba, S. P.; White, W. W.; Murphy, P. J. Water Res. 1977, 11, 101-110.

[11] Stokes, P. M.; Hutchinson, T. C.; Krauter, K. Water Pollut. Res. Can. 1973, 8, 178-201.

[12] Davies, P. H.; Goettl, J. P.; Sinley, J. R. Water Res. 1978, 12, 113-117.

[13] Bard, C. C.; Murphy, J. J.; Stone, D. L.; Terhaar, C. J. J. Water Pollut. Control Fed. 1976, 48 (2), 389-394.

[14] Cooper, C. F.; Jolly, W. C. A review. Water Resources Res. 1970, 6 (1), 88-98.

[15] Hutchinson, T. C. Water Pollut. Res. Canada. 1972, 8, 68-90.

[16] Albright, L. J.; Wentworth, J. W.; Wilson, E. M. Water Res. 1972, 6, 1589-1596.

[17] Sokol, R. A.; Klein, D. A. J. Environ. Qual. 1975, 4, 211-214.

[18] Janes, N.; Playle, R. C. Environ. Toxico. Chem. 1995, 14, 1847-1858.

[19] Ahearn, D. G.; May, L. L.; Gabriel, M. M. J. Ind. Microbiology. 1995, 15, 372-376.

[20] Smith, I. C.; Carson, B. L. Trace metals in the environment Vol. 2 - Silver. Ann Arbor Sci. Inc. 1977.

[21] Miller, L. A.; Bruland, K. W. Environ. Sci. Technol. 1995, 29, 2616-2621.

[22] Boyle, R. W. Geol. Surv. Can.Bull. No 160. Dept. Energy and Mines Res. Canada 1968.

[23] Thompson, N. R. Comprehensive inorganic chemistry. Pergamon Press: Toronto, 1973.

[24] Klein, D. A. Effects on humans. In Environmental impacts of artificial ice nucleating agents. 1978, 169-175.

[25] Sollmann, T. A manual of pharmacology and its applications to therapeutics and toxicology. 8th ed.; Saunders Co: Philadelphia, 1957.

[26] Campbell, P. G. C.; Tessier, A. In Metal speciation and recovery: Current status of metal speciation studies (201-242); Patterson, J.W.; Passino, R. Lewis Pub. Inc: 1986.

[27] Hoffman, M. R.; Yost, E. C.; Eisenreich, S. J.; Maier, W. J. Envir. Sci. and Tech. 1981, 15, 665-661.

[28] Shijo, Y.; Shimizu, T.; Tsunoda, T. Analytical Sciences. 1989, 5, 65-68.

[29] Van Loon, J. C. Anal. Chem. 1979, 51, 1139-1150A.

[30] Florence, T. M.; Batley, G. E. Talanta. 1977, 24, 151-158.

[31] Cantwell, F. F.; Nielsen, J. S.; Hrudey, S. E. Anal. Chem. 1982, 54, 1498-1503.

[32] Laxen, D. P. H.; Harrison, R. M. Sci.Total Environ. 1981, 19, 59-82.

[33] Wilson, S. A.; Huth, T. C.; Arndt, R. E.; Skogerboe, R. K. Anal. Chem. 1980, 52, 1515-1518.

[34] Fulton, R. B.; Kratochvil, B. Anal. Chem. 1980, 52, 546-552.

[35] Stiff, M. J. Water Res. 1971, 5, 585-599.

[36] Kabasakalis, V. Analytical letters, 1994, 27(14), 2789-2796.

[37] Sweileh, J. A.; Lucy, K. D.; Kratochvil, B.; Cantwell, F.F. Anal. Chem. 1987,59, 586-592.

[38] Hewavitharana, A. K.; Kratochvil, B. Can. J. Chem. 1993, 71, 17-20.

[39] Treit, J.; Nielsen, J. S.; Kratochvil, B.; Cantwell, F. F. Anal Chem. 1983, 55, 1650-1653.

[40] Orion Research, Ion-selective electrode catalog and guide to ion analysis, Orion Research Incorporated, Boston, USA, 1992.

[41] Cole-Parmer® Instrument Company, Niles,USA, 1995-1996 catalog.

[42] Orion Research Incorporated, laboratory product group research, Boston, USA, 1992.

[43] Vesel'y, J.; Jensen, O. J.; Nicolaisen, B. Anal. Chem. Acta. 1972, 62, 1-13.

[44] Bertine, K. K.; Goldberg, E. D. Science. 1971, 173, 233- 235.

[45] Bolie, V. W. J. Chem. Edu. 1958, 35, 449-451.

[46] Forbes, G. S. J. Am. Chem. Soc. 1911, 33, 1937-1956.

[47] Forbes, G. S.; Cole, H. I.; J. Am. Chem. Soc. 1921, 43, 2492-2497.

[48] Jonte, J. H.; Martin, D. S. J. Am. Chem. Soc. 1952, 74, 2052-2054.

[49] Ramette, R. J. Chem. Edu. 1960, 37, 348-354.

[50] Fritz, J. J. J. Solution Chemistry. 1985, 14, 865-879.

[51] Meites, L. An introduction to chemical equilibrium and kinetics. Vol. 1 Pergamon press, 1981.

[52] Laitinen, H.; Harris, W. E. Chemical analysis, 2nd ed.; McGraw-Hill: Toronto, 1975.

[53] Smith, R. M.; Martell, A. E. Critical stability constants. vol. 1,2, Plenium Press: N.Y, 1975.

[54] Ringbom, A. Complexation in analytical chemistry. Interscience: NY, 1963.

[55] Johnston, H. L.; Cuta, F.; Garrett, A. B. J. Am. Chem. Soc. 1933, 55, 2311-2325.

[56] Incezedy, J. Analytical applications of complex equilibria. Wiley and Son Inc: 1976.

[57] Davies, C.W. Ion association. Butterworth: Toronto, 1962.

[58] Nakao, Y.; Kaeriyama, K. J. Colloid and Interface Science. 1989, 131, 186-191.

[59] Tischer, T. H. Silver compounds. In Kirk-Othmer Encyclopedia of chemical technology. Vol.18, 2nd ed. 1969, 295-309.

[60] Kolthoff, I. M.; Yutzy, H. C. J. Am. Chem. Soc. 1937, 59, 1215-1219.

[61] John, D. H. O.; Field, G. T. J. Photographic Chemistry. Reinhold Pub.Co. 1963.

[62] Bagchi, P.; Gray, B. V.; Birnbaum, S. S. J. Colloid and Interface Science. 1979, 69, 502-528.

[63] Hoyen (Jr), H. A.; Cole, R. M. J. Colloid and Interface Science. 1972, 41, 93-96.

[64] Honig, E. P.; Hengst, J. H. TH. J. Colloid and Interface Science. 1969, 29, 510-520.

[65] Bonner, O. D.; Rhett, V. J. Phys. Chem. 1953, 57, 254-256.

[66] Schubert, J. J. Phys. Colloid Chem. 1948, 52, 340-357.

[67] Bonner, O. D.; Smith, L. L. J. Phys. Chem. 1957, 61, 326-329.

[68] Bonner, O. D.; Livingston, L. J. Phys. Chem. 1956, 60, 530-532.

[69] Bonner, O. D.; Argersinger, W. J.; Davidson, A.W. J. Phys. Chem. 1952, 74, 1044-1047.

[70] Kunin, R.; Myers, R. J. J. Phys. Colloid Chem. 1947, 51, 1111-1130.

[71] Persaud, G.; Cantwell, F. F. Anal. Chem. 1992,64, 89-94.

[72] Persaud, G.; Cantwell, F. F. Can. J. Chem. 1992, 70, 926-930.

[73] Helfferich, F. Ion exchange. McGraw-Hill: New York, 1962.

[74] Blaedel, W. J.; Dinwiddie, D. E. Anal. Chem. 1974, 46, 873-877.

[75] Walton, H. F; Rieman 111, W. Ion-exchange in analytical chemistry, Vol 38 Pergamon Press NY, 1970.

[76] Abrams, I. M. Ind. Eng. Chem. 1956, 48, 1469-1472.

[77] Cantwell, F. F.; Pietrzyk, D. J. Anal. Chem. 1974, 46, 344-350.

[78] Stolzberg, R. J. Anal. Chem. 1981, 53, 1286-1291.

[79] Hewavitharana, A. K., Ph.D. Thesis, Department of Chemistry, University of Alberta, Edmonton, Alberta, Canada, 1991.

[80] Kolthoff, I. M.; Lauer, W. M; Sunde, C. J. J. Am. Chem. Soc. 1929, 51, 3273-3277.

[81] Kolthoff, I. M.; Lingane, J. J. J. Am. Chem. Soc. 1936, 58, 1528-1533.

[82] Igawa, M.; Yoshida, T.; Ohtake, C.; Hayashita, T. Bull. Chem. Soc. Jpn. 1987, 60, 3183-3188.

[83] Danielsson, L. G. Water Res. 1982,16, 179-182.

[84] de Mora, S. J.; Harrison, M. R. Water Res. 1983, 17, 723-733.

[85] Brevik, E. M.; Ramback, J. P. Talanta. 1985, 32, 907-913.

[86] Kielland, J. J. Am. Chem. Soc. 1937, 59, 1675-1678.

[87] Handbook of Chemistry and Physics, Weast 70th ed. 1989-90.

[88] Shaw, D. J. Introduction to colloid and surface chemistry 4th ed. Butterworth-Heinemann Ltd. 1992.

[89] Chan, L.; Porter, M. D. J. Colloid and Interface Science. 1991, 145, 283-286.

APPENDIX A

COMPUTER PROGRAMS

The computer software, Excel, version 5.0 was used to write simple computer programs. The programs were used for the calculations of species distribution and free chloride concentration using stability and solubility product constants shown in column 4, Table 5.3. For the hydroxide ligand the values of $\beta_{1,OH}$, $\beta_{2,OH}$, $\beta_{3,OH}$ from Table 2.1 corrected to an ionic strength of 0.3 were used. The corrected values are shown in column A of Table A.4. Also, the programs were used for the estimation of the distribution coefficients of AgCl(aq), λ_{AgCl}, and AgOH(aq), λ_{AgOH}, and estimation of Ksp, $\beta_{1,Cl}$, $\beta_{2,Cl}$, $\beta_{3,Cl}$, and $\beta_{4,Cl}$ for the Ag-Cl system. These programs are shown as computer programs A.1, A.2, A.3, A.4 and A.5. A **bold** alphabetical letter and a number are used to describe a given cell. For example: in the spreadsheet, Table A.1, the cell which contains the value for the coefficient A* ($\beta_{4,cl}$) is described as **$B$2**. The **$** sign means that the value is a constant. The values of $[Cl^-]$ obtained are shown in column **I** (Table A.1), they are described as **Ix**, where x means that in column **I** more than one entry for $[Cl^-]$ is shown.

COMPUTER PROGRAM A.1

ESTIMATION OF THE CONCENTRATION OF FREE CHLORIDE, [Cl^-], IN THE ABSENCE OF SOLID AgCl(s) AND Ag_2O(s) AND WITH CHLORIDE NOT IN LARGE EXCESS

The computer program A.1 is used to estimate the free chloride concentration (i.e the value of [Cl^-] that satisfies equation 2.1.18, Chapter 2; see below) by using known values of conditional stability constants, β', total chloride concentration, C_{Cl}, total silver concentration, C_{Ag} and, fraction of free silver when OH^- is the only ligand present, α_{AgOH}. The value of [Cl^-] is obtained by first assuming that all the chloride is free; i.e. $C_{Cl} = [Cl^-]$.

For each entry, the square of the difference (SQD) between the calculated value (a number very close to zero) and ZERO is calculated. The squares of the difference are summed up to give the sum of the squares of the difference (SSQD). The computer was programmed to minimize the SSQD, (cell L15, Table A.1) by adjusting the value of [Cl^-], under certain specified conditions until equation 2.1.18 is satisfied within the desired accuracy. The calculated values of [Cl^-] and other parameters which are used in the calculations are shown in Table A.1.

Recall, equation 2.1.18, Chapter 2:

$$A^* [Cl^-]^5 + B^* [Cl^-]^4 + C^* [Cl^-]^3 + D^* [Cl^-]^2 + E^* [Cl^-] - F^* = 0$$

$$A^* = \beta'_{4,Cl} = \$B\$2$$

$$B^* = 4C_{Ag,sol}\beta'_{4,Cl} - C_{Cl}\beta'_{4,Cl} + \beta'_{3,Cl} \quad = 4 * \$A\$10 * \$B\$2 - Hx * \$B\$2 + \$A\$3 = Cx$$

$C^* = 3C_{Ag,sol}\beta'_{3,Cl} - C_{Cl}\beta'_{3,Cl} + \beta'_{2,Cl}$ = 3 * $A$10 * $A$3 - Hx * $A$3 + $A$5 = Dx

$D^* = 2C_{Ag,sol}\beta'_{2,Cl} - C_{Cl}\beta'_{2,Cl} + \beta'_{1,Cl}$ = 2 * $A$10 * $A$5 - Hx * $A$5 + $A$7 = Ex

$E^* = C_{Ag,sol}\beta'_{1,Cl} - C_{Cl}\beta'_{1,Cl} + 1/\alpha_{Ag+,OH}$ = $A$10 * $A$7 - Hx * $A$7 + (1/ $A$23) = Fx

$F^* = C_{Cl} /\alpha_{Ag+,OH}$ = Hx/$A$23 = Gx

$\alpha_{Ag+,OH}$ = 1 /(1+ $A$13 * $A$20 + $A$15 * ($A$20)^2 + $A$17 * ($A$20)^3) = $A$23

$[Cl^-]$ = Ix (varied until Jx is close to Zero)

Calculated value, Z_{Cal} = $B$2 * (Ix) ^5 + Cx * (Ix)^4 + Dx * (Ix)^3 + Ex * (Ix)^2
+ Fx * (Ix) - Gx = Jx

Theoretical value, Z_{The} = 0 = Kx

Square of the difference (SQD) $(Z_{Cal} - Z_{The})^2$ = (Jx - Kx)^2 = Lx

Sum of the squares of the difference (SSQD) = $\sum$ (Jx - Kx)^2 = L15

Table A.1 The spreadsheet used to estimate the value of the concentration of free chloride, $[Cl^-]$, using computer program A.1.

	A	B	C	D	E	F	G
1		$A^*(\beta'_{4,Cl})$	B*	C*	D*	E*	F*
2	$\beta'_{3,Cl}$	863009	233036	30971	678.5	1.0048	3.0E-06
3	233004	863009	233013	30965	677.7	0.9865	3.0E-05
4	$\beta'_{3,Cl}$	863009	-25867	-38930	-8611.0	-202.4	0.30
5	30965						
6	$\beta'_{1,Cl}$						
7	678						
8							
9	$C_{Ag,sol}$		H	I	J	K	L
10	1.0E-05						
11			C_{Cl}	$[Cl^-]$	Zc_{al}	Z_{The}	$(Z_{cal} - Z_{The})^2$ (SQD)
12	$\beta'_{1,OH}$		3.0E-06	2.98E-06	-3.4E-21	0.0	1.15E-41
13	107		3.0E-05	2.98E-05	-4.4E-20	0.0	1.94E-39
14	$\beta'_{2,OH}$		0.30	3.00E-01	-2.0E-12	0.0	3.91E-24
15	2139						SSQD
16	$\beta'_{3,OH}$						3.91E-24
17	63095						
18							
19	$[OH^-]$						
20	1.0E-07						
21							
22	$\alpha_{Ag+,OH}$						
23	0.99999						

COMPUTER PROGRAM A.2

ESTIMATION OF THE CONCENTRATION OF FREE CHLORIDE, [Cl⁻], IN THE PRESENCE OF SOLID AgCl(s) AND THE ABSENCE OF SOLID Ag_2O(s)

The computer program A.2 is used to estimate the free chloride concentration (i.e. the value of [Cl⁻] that satisfies equation 2.1.29, Chapter 2; see below) in the presence of solid AgCl(s) and the absence of solid Ag_2O(s).

The procedure and parameters which are used are similar with those described for the computer program A.1 except that, the solubility product constant, (Ksp) for silver chloride is also used in the calculations. The calculated values of [Cl⁻] and other parameters which are used in the calculations are shown in Table A.2.

Recall, equation 2.1.29, Chapter 2:

$$A'[Cl^-]^4 + B'[Cl^-]^3 + C'[Cl^-]^2 - D'[Cl^-] - E' = 0$$

$A' = 3\beta_{4,Cl} Ksp$ = 3 * $G$21 * $H$15 = $H$23

$B' = 2\beta_{3,Cl} Ksp$ = 2 * $G$19 * $H$15 = $H$21

$C' = (1 + \beta_{2,Cl} Ksp)$ = (1 + $G$17 * $H$15) = $H$19

$D' = (C_{Cl} - C_{Ag})$ = (Ax - $H$17) = Bx

$E' = Ksp/\alpha_{Ag+,OH}$ = $H$15 / $I$24

$\alpha_{Ag+,OH}$ = 1 / (1 + $I$15 * $I$21 + $I$17 * ($I$21)^2 + $I$19 * ($I$21)^3) = $I$24

[Cl⁻] = Cx (varied until Dx is close to Zero)

Calculated value, Z_{Cal} = **$H$23 * (Cx)^4 + $H$21* (Cx)^3 + $H$19 * (Cx)^2 - (Bx) * Cx - ($H$15 / $I$24) = Dx**

Theoretical value, Z_{The} = 0 = **Ex**

Square of the difference (SQD) $(Z_{Cal} - Z_{The})^2$ = **(Dx - Ex)^2 = Fx**

Sum of the squares of the difference (SSQD) = $\sum$ **(Dx - Ex)^2 = F9**

Table A.2 The spreadsheet used to estimate the value of the concentration of free chloride, [Cl^-], using computer program A.2.

	A	B	C	D	E	F
	C_{Cl}	D'	[Cl^-]	Z_{cal}	Z_{The}	$(Z_{cal} - Z_{The})^2$ (SQD)
1	7.5E-05	6.50E-05	7.051E-05	-2.6E-21	0.0	6.5847E-42
2	3.0E-04	2.90E-04	2.913E-04	-2.4E-21	0.0	5.7313E-42
3	7.5E-04	7.40E-04	7.405E-04	-2.3E-21	0.0	5.1151E-42
4	3.0E-03	2.99E-03	2.990E-03	-6.9E-21	0.0	4.7891E-41
5	7.5E-03	7.49E-03	7.490E-03	-2.0E-20	0.0	4.1914E-40
6	3.0E-02	3.00E-02	2.999E-02	-1.7E-19	0.0	2.8747E-38
7	7.5E-02	7.50E-02	7.499E-02	-4.0E-18	0.0	1.5715E-35
8						SSQD
9						1.5745E-35
10						
11						
12	G	H	I			
13						
14	$\beta'_{1,Cl}$	Ksp	$\beta'_{1,OH}$			
15	678.0	3.89E-10	107			
16	$\beta'_{2,Cl}$	C_{Ag}	$\beta'_{2,OH}$			
17	30965	1.00E-05	2139			
18	$\beta'_{3,Cl}$	C'	$\beta'_{3,OH}$			
19	233004	1.000	63095			
20	$\beta'_{4,Cl}$	B'	[OH^-]			
21	863009	0.00018	1.0E-07			
22		A'				
23		0.001	$\alpha_{Ag^+,OH}$			
24			0.999989			

COMPUTER PROGRAM A.3

This computer program is used to estimate the values of Ksp and β's for the Ag-Cl system by using the values of total silver in solution in the presence of AgCl(s) obtained experimentally, $C_{Ag,sol}$. These values are given in column 3 in Table 5.1.
Equation 2.1.8 is written in terms of Ksp as shown below:

$$C_{Ag,sol(theory)} = \frac{Ksp}{[Cl^-]} + \beta_{1,Cl}Ksp + \beta_{2,Cl}\,Ksp[Cl^-] + \beta_{3,Cl}\,Ksp[Cl^-]^2 + \beta_{4,Cl}Ksp[Cl^-]^3 \quad \text{..... A.1}$$

A four stage process was used to obtain final values for Ksp, $\beta_{1,Cl}$, $\beta_{2,Cl}$, $\beta_{3,Cl}$ and $\beta_{4,Cl}$:

Stage 1: At low total chloride concentrations, C_{Cl}, ($7.5x10^{-5}$ - $7.5x10^{-3}$ M) the fraction of higher complexes are very small, therefore, terms with $\beta_{2,Cl}$, $\beta_{3,Cl}$ and $\beta_{4,Cl}$ can be neglected and equation A.1 reduces to

$$C_{Ag,sol(theory)} = \frac{Ksp}{[Cl^-]} + \beta_{1,Cl}Ksp \quad \text{..... A.2}$$

this equation is used in the first stage iteration procedure to calculate the values of Ksp and $\beta_{1,Cl}$.

Initial estimates of the conditional stability and solubility product constants corresponding to a solution of 0.3 M total ionic strength and pH 7 were first calculated starting with the literature values given in Table 2.1. These constants were used to make a first estimate of the concentration of free chloride, $[Cl^-]$, using equation 2.1.29 and computer program A.2. Then, the value of $[Cl^-]$ obtained for each total chloride concentration, C_{Cl}, and the values of Ksp and $\beta_{1,Cl}$ are substituted into equation A.2. The theoretical total concentration of silver in solution, $C_{Ag,sol(theory)}$, is calculated for each total

chloride concentration. For each total C_{Cl} the square of the difference (SQD) between the experimental $C_{Ag,sol}$ and $C_{Ag,sol(theory)}$ is calculated. The squares of the difference are summed up to give the sum of the square of the difference (SSQD). The computer was programmed to minimize the SSQD (cell G7, Table A.3a) by changing the values of Ksp and $\beta_{1,Cl}$ under the condition that the values of Ksp and $\beta_{1,Cl}$ are greater than zero. The new values of Ksp and $\beta_{1,Cl}$ obtained at the end of this first iteration are substituted back in into equation 2.1.29 and new values of $[Cl^-]$ are calculated. The new values of $[Cl^-]$, Ksp and $\beta_{1,Cl}$ are substituted back into equation A.2 to obtain newer values of Ksp and $\beta_{1,Cl}$ which were used to calculate a newer $[Cl^-]$. This iterative process was repeated over and over until the values of Ksp, $\beta_{1,Cl}$ and $[Cl^-]$ which give a best-fit to the experimental data in the range $C_{Cl} = 7.5x10^{-5}$ - $7.5\ x10^{-3}$ M were obtained. The results of the multiple iterations are shown in Table A.3a

Stage 2: At high total chloride concentrations, C_{Cl}, ($3x10^{-2}$ - $7.5x10^{-2}$ M) the fractions of higher complexes are significant. Therefore equation A.1 was used to calculate the values of $\beta_{2,Cl}$, $\beta_{3,Cl}$ and $\beta_{4,Cl}$. The value of $[Cl^-]$ for each C_{Cl} was first estimated using the just determined values of Ksp and $\beta_{1,Cl}$ from Table A.3a along with the initial estimate of the conditional stability constants for $\beta_{2,Cl}$, $\beta_{3,Cl}$ and $\beta_{4,Cl}$ from Table 5.3. The same type of multiple iteration procedure as described above was used to obtain the values of $\beta_{2,Cl}$, $\beta_{3,Cl}$ and $\beta_{4,Cl}$, except that in this case equation A.1 was used and only $\beta_{2,Cl}$, $\beta_{3,Cl}$ and $\beta_{4,Cl}$ were allowed to change (Ksp and $\beta_{1,Cl}$ were kept constant). The resulting values of $\beta_{2,Cl}$, $\beta_{3,Cl}$ and $\beta_{4,Cl}$ are shows in Table A.3b.

Stage 3: All values of β's and the Ksp were allowed to change simultaneously in a multiple iteration procedure. Initial values of Ksp, $\beta_{1,Cl}$, $\beta_{2,Cl}$, $\beta_{3,Cl}$ and $\beta_{4,Cl}$ were taken from Table A.3b. The results are shown in Table A.3c.

Stage 4: The final values of the Ksp and $\beta_{1,Cl}$, $\beta_{2,Cl}$, $\beta_{3,Cl}$ and $\beta_{4,Cl}$ were obtained by averaging the values in Tables A.3b and A.3c. The average values are shown in Table A.3d. The logarithm of these values are compared with the logarithm of conditional stability and solubility product constants (corrected for ionic strength of o.3 M) in columns 4 and 3 of Table 5.3.

Equation A.2: Table A.3a

$C_{Ag,sol(theory)}$ = $C$1/Bx + $D$1*$C$1

$(C_{Ag,sol} - C_{Ag,sol(theory)})^2$ = (Ex - Fx)^2 = Gx

∑(Ex - Fx)^2 = G1+ G2 + G3 + G4 + G5 = G7

Equation A.1: Tables A.3b and A.3c

$C_{Ag,sol(theory)}$ = $C$1/Bx + $D$1*$C$1 + $E$1*$C$1*Bx + $F$1*$C$1*(Bx)^2 + $G$1*$C$1*(Bx)^3

$(C_{Ag,sol} - C_{Ag,sol(theory)})^2$ = (Hx - Ix)^2 = Jx

∑(Hx - Ix)^2 = J9+ J10 = J12

Table A.3a The spreadsheet used to estimate the value of Ksp and $\beta_{1,Cl}$ (Stage 1)

	A	B	C	D	E	F	G
	C_{Cl}, M	[Cl⁻], M	Ksp x10^6	$\beta_{1,Cl}$	$C_{Ag,sol}$	$C_{Ag,sol(theory)}$	$(C_{Ag,sol} - C_{Ag,sol(theory)})^2$
					x10^6 M	x10^6 M	(SQD)
1	7.5E-05	7.05E-05	3.88E-04	755	5.80	5.79	5.64E-05
2	3.0E-04	2.91E-04	3.88E-04	755	1.60	1.62	5.70E-04
3	7.5E-04	7.41E-04	3.88E-04	755	0.80	0.82	2.71E-04
4	3.0E-03	2.99E-03	3.88E-04	755	0.40	0.42	5.05E-04
5	7.5E-03	7.49E-03	3.88E-04	755	0.33	0.34	2.12E-04
6							SSQD
7							1.61E-03

Table A.3b The spreadsheet used to estimate the value of $\beta_{2,Cl}$, $\beta_{3,Cl}$, and $\beta_{4,Cl}$ (Ksp and $\beta_{1,Cl}$ kept constant) (Stage 2)

	A	B	C	D	E	F	G
	C_{Cl}, M	[Cl], M	Ksp x10^6	$\beta_{1,Cl}$	$\beta_{2,Cl}$	$\beta_{3,Cl}$	$\beta_{4,Cl}$
1	3.0E-03	3.00E-02	3.88E-04	755	30956	235037	867190
2	7.5E-02	7.50E-02	3.88E-04	755	30956	235037	867190
3							
4					H	I	J
5							
6					$C_{Ag,sol}$	$C_{Ag,sol(theory)}$	$(C_{Ag,sol} - C_{Ag,sol(theory)})^2$
7					x10^6 M	x10^6 M	(SQD)
8							
9					0.70	0.76	3.22E-03
10					1.80	1.85	2.75E-03
11							SSQD
12							5.97E-03

Table A.3c The spreadsheet used to estimate the value of Ksp, $\beta_{1,Cl}$, $\beta_{2,Cl}$, $\beta_{3,Cl}$, and $\beta_{4,Cl}$

(Stage 3)

	A	B	C	D	E	F	G
	C_{Cl}, M	[Cl], M	Ksp x10^6	$\beta_{1,Cl}$	$\beta_{2,Cl}$	$\beta_{3,Cl}$	$\beta_{4,Cl}$
1	3.0E-03	3.00E-02	3.89E-04	602	30974	230971	858828
2	7.5E-02	7.50E-02	3.89E-04	602	30974	230971	858828
3							
4					H	I	J
5							
6					$C_{Ag,sol}$	$C_{Ag,sol(theory)}$	$(C_{Ag,sol} - C_{Ag,sol(theory)})^2$
7					x10^6 M	x10^6 M	(SQD)
8							
9					0.70	0.70	1.67E-06
10					1.80	1.79	9.49E-05
11							SSQD
12							9.65E-05

Table A.3d The spreadsheet shows the average values of Ksp, $\beta_{1,Cl}$, $\beta_{2,Cl}$, $\beta_{3,Cl}$, and $\beta_{4,Cl}$

(Stage 4)

	A	B	C	D	E	F	G
	C_{Ag}, M	[Cl], M	Ksp x10^{6}	$\beta_{1,Cl}$	$\beta_{2,Cl}$	$\beta_{3,Cl}$	$\beta_{4,Cl}$
1	7.5E-05	7.05E-05	3.89E-04	678	30965	233004	863009
2	3.0E-04	2.91E-04	3.89E-04	678	30965	233004	863009
3	7.5E-04	7.41E-04	3.89E-04	678	30965	233004	863009
4	3.0E-03	2.99E-03	3.89E-04	678	30965	233004	863009
5	7.5E-03	7.49E-03	3.89E-04	678	30965	233004	863009
6	3.0E-03	3.00E-02	3.89E-04	678	30965	233004	863009
7	7.5E-02	7.50E-02	3.89E-04	678	30965	233004	863009
8							
9					H	I	J
10							
11					$C_{Ag,sol}$	$C_{Ag,sol(theory)}$	$(C_{Ag,sol} - C_{Ag,sol(theory)})^2$
12					x10^{6} M	x10^{6} M	(SQD)
13							
14					5.8	5.77	6.3345E-04
15					1.6	1.60	6.4097E-06
16					0.8	0.79	1.3556E-04
17					0.4	0.39	4.1604E-05
18					0.33	0.32	2.1111E-04
19					0.70	0.73	7.7770E-04
20					1.80	1.82	4.6909E-04
21							SSQD
22							2.2749E-03

COMPUTER PROGRAM A.4

CALCULATION OF SPECIES DISTRIBUTION

The computer program A.4 is used to calculate the fraction of free silver in solution, α_{Ag+} and the fractions of other metal-ligand species by using equations 2.1.19 and 2.1.20a through 2.1.20g, Chapter 2. The concentrations of various species are also calculated. Values of $[Cl^-]$ obtained using the computer programs A.1 and A.2 are entered in column C. Other parameters which are used in the calculations are shown in column A of Table A.4. Equation 2.1.8 (see Chapter 2) is used to calculate $C_{Ag,sol}$ and the concentration of silver chloride precipitate, $n_{AgCl(s)}/V$; (AgCl(s) is dissolved in EDTA at pH 10 and it's concentration is determined by AAS) is calculated by difference; i.e.

$$n_{AgCl(s)}/V = C_{Ag} - C_{Ag,sol} \qquad \text{..... A.3}$$

Sample calculations are shown in Table A.4.

$$\alpha_{Ag+} = 1 / (1 + \$A\$1 * (Cx) + \$A\$3 * (Cx)\text{^}2 + \$A\$5 * (Cx)\text{^}3 + \$A\$7 * (Cx)\text{^}4 + \$A\$15 * (\$A\$22) + \$A\$17 * (\$A\$22)\text{^}2 + \$A\$19 * (\$A\$22)\text{^}3) = Dx$$

$$\alpha_{AgCl} = \beta'_{1,Cl} [Cl^-] \alpha_{Ag+} = \$A\$1 * (Cx) * Dx = Ex$$

$$\alpha_{AgCl2} = \beta'_{2,Cl} [Cl^-]^2 \alpha_{Ag+} = \$A\$3 * (Cx)\text{^}2 * Dx = Fx$$

$$\alpha_{AgCl3} = \beta'_{3,Cl} [Cl^-]^3 \alpha_{Ag+} = \$A\$5 * (Cx)\text{^}3 * Dx = Gx$$

$$\alpha_{AgCl4} = \beta'_{4,Cl} [Cl^-]^4 \alpha_{Ag+} = \$A\$7 * (Cx)\text{^}4 * Dx = Hx$$

$$\alpha_{AgOH} = \beta'_{1,OH} [OH^-] \alpha_{Ag+} = \$A\$15 * (\$A\$22) * Dx = Ix$$

$\alpha_{Ag(OH)2}$ = $\beta'_{2,OH}[OH^-]^2\,\alpha_{Ag+}$ = $A$17 * ($A$22)^2 * Dx = Jx

$\alpha_{Ag(OH)3}$ = $\beta'_{3,OH}[OH^-]^3\,\alpha_{Ag+}$ = $A$19 * ($A $22)^3 * Dx = Kx

$[Ag^+]$ = Ksp/$[Cl^-]$ = $A$9 / Cx = Lx (Only if solid AgCl(s) is present)

$[Ag^+]$ = $\alpha_{Ag+}\,C_{Ag,sol}$ = Dx * Qx = Lx (Only if solid AgCl(s) is absent)

[AgCl] = $\alpha_{AgCl}\,C_{Ag,sol}$ = Ex * Qx = Mx

$[AgCl_2^-]$ = $\alpha_{AgCl2}\,C_{Ag,sol}$ = Fx * Qx = Nx

$[AgCl_3^{2-}]$ = $\alpha_{AgCl3}\,C_{Ag,sol}$ = Gx * Qx = Ox

$[AgCl_4^{3-}]$ = $\alpha_{AgCl4}\,C_{Ag,sol}$ = Hx * Qx = Px

[AgOH] = $\alpha_{AgOH}\,C_{Ag,sol}$ = Ix * Qx = Sx

$[Ag(OH)_2^-]$ = $\alpha_{Ag(OH)2}\,C_{Ag,sol}$ = Jx * Qx = Tx

$[Ag(OH)_3^{2-}]$ = $\alpha_{Ag(OH)3}\,C_{Ag,sol}$ = Kx * Qx = Ux

$C_{Ag,sol}$ = Lx + Mx + Nx + Ox + Px + Sx + Tx + Ux = Qx

$C_{AgCl(s)}$ = $A$12 - Qx = Rx

Table A.4 The spreadsheet used to calculate the species distribution of Ag-Cl system using computer program A.4.

	A		B	C	D	E	F
	$\beta'_{1,Cl}$		C_{Cl}, M	[Cl]	α_{Ag+}	α_{AgCl}	α_{AgCl2}
1	678		3.00E-06	2.98E-06	0.998	0.0020	2.74E-07
2	$\beta'_{2,Cl}$		3.00E-05	2.98E-05	0.980	0.0198	2.70E-05
3	30965		7.50E-05	7.05E-05	0.954	0.0456	1.47E-04
4	$\beta'_{3,Cl}$		3.00E-04	2.91E-04	0.833	0.165	2.19E-03
5	233004		7.50E-04	7.41E-04	0.658	0.330	0.0112
6	$\beta'_{4,Cl}$		3.00E-03	2.99E-03	0.302	0.612	0.0836
7	863009		7.50E-03	7.49E-03	0.126	0.642	0.219
8	Ksp		3.00E-02	3.00E-02	0.018	0.362	0.496
9	3.89E-10		7.50E-02	7.50E-02	0.003	0.145	0.495
10			0.3	3.00E-01	0.00006	0.013	0.171
11	C_{Ag},(M)						
12	1.00E-05						
13			G	H	I	J	K
14	$\beta'_{1,OH}$						
15	107		α_{AgCl3}	α_{AgCl4}	α_{AgOH}	$\alpha_{Ag(OH)2}$	$\alpha_{Ag(OH)3}$
16	$\beta'_{2,OH}$		6.15E-12	6.79E-17	1.07E-05	2.13E-11	6.30E-17
17	2139		6.04E-09	6.67E-13	1.05E-05	2.10E-11	6.18E-17
18	$\beta'_{3,OH}$		7.79E-08	2.04E-11	1.02E-05	2.04E-11	6.02E-17
19	63095		4.80E-06	5.18E-09	8.92E-06	1.78E-11	5.26E-17
20			6.23E-05	1.71E-07	7.04E-06	1.41E-11	4.15E-17
21	[OH^-]		1.88E-03	2.08E-05	3.23E-06	6.46E-12	1.91E-17
22	1.0E-07		0.01237	0.00034	1.35E-06	2.70E-12	7.97E-18
23			0.11189	0.01243	1.91E-07	3.81E-13	1.12E-18
24			0.27952	0.07763	3.04E-08	6.09E-14	1.80E-19
25			0.38661	0.42954	6.58E-10	1.31E-15	3.88E-21

Table A.4 continues

Table A.4 continues

	L	M	N	O	P
26	$[Ag^+]$,M	[AgCl],M	$[AgCl_2]$,M	$[AgCl_3]$,M	$[AgCl_4]$,M
27	9.98E-06	2.02E-08	2.74E-12	6.15E-17	6.79E-22
28	9.80E-06	1.98E-07	2.70E-10	6.04E-14	6.67E-18
29	5.51E-06	2.63E-07	8.48E-10	4.50E-13	1.18E-16
30	1.33E-06	2.63E-07	3.51E-09	7.68E-12	8.29E-15
31	5.25E-07	2.63E-07	8.91E-09	4.97E-11	1.36E-13
32	1.30E-07	2.63E-07	3.60E-08	8.10E-10	8.97E-12
33	5.19E-08	2.63E-07	9.01E-08	5.08E-09	1.41E-10
34	1.30E-08	2.63E-07	3.61E-07	8.14E-08	9.05E-09
35	5.18E-09	2.63E-07	9.02E-07	5.09E-07	1.41E-07
36	6.15E-10	1.25E-07	1.71E-06	3.87E-06	4.30E-06
37					
38					
39	Q	R	S	T	U
40					
41	$C_{Ag,sol}$,M	$C_{AgCl(s)}$,M	[AgOH]	[Ag(OH)2]	[Ag(OH)3]
42	1.00E-05	0	1.07E-10	2.13E-16	6.30E-22
43	1.00E-05	0	1.05E-10	2.10E-16	6.18E-22
44	5.78E-06	4.22E-06	1.02E-10	2.04E-16	6.02E-22
45	1.60E-06	8.40E-06	8.92E-11	1.78E-16	5.26E-22
46	7.97E-07	9.20E-06	7.04E-11	1.41E-16	4.15E-22
47	4.30E-07	9.57E-06	3.23E-11	6.46E-17	1.91E-22
48	4.11E-07	9.59E-06	1.35E-11	2.70E-17	7.97E-23
49	7.28E-07	9.27E-06	1.91E-12	3.81E-18	1.12E-23
50	1.82E-06	8.18E-06	3.04E-13	6.09E-19	1.80E-24
51	1.00E-05	0	6.58E-15	1.31E-20	3.88E-26

COMPUTER PROGRAM A.5

This computer program is used to estimate the distribution coefficient, λ_{AgCl} of AgCl(aq) between the solution phase and the resin phase using equation 5.1, Chapter 5. For each value of total silver sorbed obtained experimentally, $C_{RAg,exp}$, corresponding values of α_{Ag+}, α_{AgCl} and $C_{Ag,sol}$ were calculated by using the computer program A.4. The values obtained are shown in Table A.5. For λ_{Ag+}, the value of 0.144 lg^{-1} was used.

The values of the above parameters are substituted into equation 5.1. For the value of λ_{AgCl}, any number is initially substituted into equation 5.1 and the calculated value of total silver sorbed, $C_{RAg,cal}$ is then computed. For each entry, the square of the difference (SQD) between $C_{RAg,exp}$ and $C_{RAg,cal}$ is calculated. The squares of the difference are summed up to give the sum of the square of the difference (SSQD). The computer was programmed to minimize the SSQD, (cell I8, Table A.5) by changing the value of λ_{AgCl}, under certain specified conditions. Finally, the value of λ_{AgCl} which gives a best-fit to the experimental data was obtained.

Recall equation 5.1, Chapter 5:

$$C_{RAg} = (\lambda_{Ag+}\,\alpha_{Ag+} + \lambda_{AgCl}\,\alpha_{AgCl})\,C_{Ag,sol}$$

$C_{RAg,cal}$ = ($D$1 * Cx + $F$1 * Ex) * Bx = Hx

$(C_{RAg,exp} - C_{RAg,cal})^2$ = (Gx - Hx)^2

$\sum$(Gx - Hx)^2 = I1 + I2 + I3 + I4 + I5 + I6 = I8

Table A.5 The spreadsheet used to estimate the value of the distribution coefficient, λ_{AgCl} of AgCl(aq) between the resin phase and the solution phase using computer program A.5.

	A	B	C	D	E	F	G	H	I
	C_{Cl}, M	$C_{Ag,sol}$, μmol l^{-1}	α_{Ag+}	λ_{Ag+}, lg^{-1}	α_{AgCl}	λ_{AgCl}, lg^{-1}	$C_{RAg,exp}$, μmol l^{-1}	$C_{RAg,cal}$, μmol l^{-1}	$(C_{RAg,exp} - C_{RAg,cal})^2$ (SQD) (μmol l^{-1})^2
1	$7.5x10^{-4}$	0.80	0.66	0.144	0.33	0.0642	0.094	0.093	$5.18x10^{-9}$
2	$3.0x10^{-3}$	0.43	0.30	0.144	0.61	0.0642	0.034	0.036	$9.74x10^{-6}$
3	$7.5x10^{-3}$	0.41	0.13	0.144	0.64	0.0642	0.027	0.025	$1.15x10^{-6}$
4	$3.0x10^{-2}$	0.73	0.018	0.144	0.36	0.0642	0.018	0.019	$6.91x10^{-5}$
5	$7.5x10^{-2}$	1.82	0.0028	0.144	0.15	0.0642	0.016	0.018	$6.74x10^{-5}$
6	0.3	10.0	0.000061	0.144	0.013	0.0642	0.009	0.008	$3.47x10^{-8}$
7									SSQD
8									$1.47x10^{-3}$

Table A.6 The spreadsheet used to estimate the value of the distribution coefficient, λ_{AgOH} of AgOH(aq) between the resin phase and the solution phase using computer program A.5.

	A	B	C	D	E	F	G	H	I
	pH	$C_{Ag,sol}$, μmol l^{-1}	α_{Ag+}	λ_{Ag+}, lg^{-1}	α_{AgOH}	λ_{AgOH}, lg^{-1}	$C_{RAg,exp}$, μmol l^{-1}	$C_{RAg,cal}$, μmol l^{-1}	$(C_{RAg,exp} - C_{RAg,cal})^2$ (SQD) (μmol l^{-1})^2
1	11.40	15.0	0.766	0.114	0.221	0.43	2.74	2.74	$4.24x10^{-17}$
2	11.89	10.9	0.503	0.119	0.418	0.38	2.39	2.39	$4.51x10^{-13}$
3	12.29	9.56	0.229	0.125	0.478	0.37	1.98	1.98	$6.96x10^{-19}$
4	12.49	11.4	0.122	0.132	0.403	0.51	2.52	2.52	$2.88x10^{-12}$
5	12.71	17.2	0.048	0.175	0.266	0.41	2.00	2.00	$1.68x10^{-12}$
6	13.00	37.0	0.012	0.187	0.123	0.39	1.88	1.88	$8.37x10^{-13}$
7									SSQD
8									$5.85x10^{-12}$

APPENDIX B

TABLES FOR CHAPTER FOUR

In this appendix data which were presented in some of the figures in Chapter 4 are tabulated. The corresponding figure in which the data were plotted is indicated in the tables.

Table B.1 Ag^+ breakthrough data on Dowex 50W-X8 resin for 1.85 μmol l^{-1} and 46.35 μmol l^{-1} Ag^+ in 0.2 M $NaNO_3$ and pH 7 buffer (HEPES). The solutions were loaded onto a 1.4 g column at a flow rate 7 ml $min.^{-1}$. The data are plotted in Figure 4.1.

Time (min.)	Ce/Ci C_{Ag+} = 1.85 μmol l^{-1}	Ce/Ci C_{Ag+} = 46.35 μmol l^{-1}
20	0.020 ± 0.001	0.335 ± 0.086
40	0.650 ± 0.047	0.931 ± 0.015
60	0.930 ± 0.001	0.998 ± 0.005
80	0.970 ± 0.047	1.000 ± 0.003
90	1.000 ± 0.001	0.995 ± 0.012
100	1.000 ± 0.001	1.000 ± 0.004
120	1.000 ± 0.001	1.000 ± 0.001

± are standard deviations based on two replicates.

Table B.2 Ag^+ breakthrough data on Dowex 50W-X8 resin for 1.85 μmol l^{-1} and 46.35 μmol l^{-1} Ag^+ in 0.3 M $NaNO_3$ and pH 7 buffer (HEPES). The solutions were loaded onto a 1.4 g column at a flow rate 7ml $min.^{-1}$. The data are plotted in Figure 4.2.

Time (min.)	Ce/Ci C_{Ag+} = 1.85 μmol l^{-1}	Ce/Ci C_{Ag+} = 46.35 μmol l^{-1}
20	0.40 ± 0.04	0.60 ± 0.01
40	1.00 ± 0.04	1.00 ± 0.02
50	1.00 ± 0.04	1.00 ± 0.01
60	1.00 ± 0.04	1.00 ± 0.01
70	1.00 ± 0.04	1.00 ± 0.01
80	1.00 ± 0.04	-
90	1.00 ± 0.05	1.00 ± 0.01

± are standard deviations based on two replicates.

Table B.3 Ag^+ breakthrough data on Dowex 50W-X8 resin for $1x10^{-4}$ M Ag^+ in 0.3 M $NaNO_3$ and pH 7 buffer. The solution was loaded onto a 15 mg resin column (Figure 3.3) at a flow rate 7ml $min.^{-1}$. The data are plotted in Figure 4.5.

Time (min.)	Ce/Ci
0.73	0.66 ± 0.07
1.50	1.00 ± 0.02
2.20	1.00 ± 0.02
2.93	1.00 ± 0.01
3.58	1.00 ± 0.01
4.33	1.00 ± 0.01
5.00	1.00 ± 0.01
10.00	1.00 ± 0.01
15.00	1.00 ± 0.01

± are standard deviations based on two replicates.

Table B.4 Pre-conditioning data for 10.0 μmol l^{-1} Ag^+ in 0.3 M $NaNO_3$ and pH 7 buffer.

The resin was pre-conditioned for different lengths of time. The Ag^+ containing solution was loaded onto a 1.4 g column for 40 minutes at a flow rate 7ml $min.^{-1}$. The eluent was 0.04 M EDTA at pH 10. The data are plotted in Figure 4.6

Pre-conditioning time (min.)	μmols of Ag^+ eluted
0	1.04 ± 0.01
2	1.03 ± 0.01
4	1.03 ± 0.01
6	1.03 ± 0.01
10	1.03 ± 0.01
15	1.04 ± 0.01

± are standard deviations based on two replicates.

Table B.5 Elution data for Ag^+ on Dowex 50W-X8 resin for 92.7 μmol l^{-1} Ag^+ in 0.3 M $NaNO_3$ and pH 7 buffer. The solution was loaded onto a 1.4 g column for 40 minutes at a flow rate 7ml $min.^{-1}$. Different concentrations of ammonium buffer were added in the eluent (0.05 M EDTA at pH 10). The eluent was passed at a flow rate of 2 ml $min.^{-1}$. The data are plotted in Figure 4.7.

Volume (ml.)	Time (min.)	NH_4^+/NH_3 0 M μmols of Ag+ eluted	NH_4^+/NH_3 0.02 M μmols of Ag+ eluted	NH_4^+/NH_3 0.05 M μmols of Ag+ eluted
0	0	0.000 ± 0.000	0.000 ± 0.000	0.000 ± 0.000
10	5	7.770 ± 0.211	7.130 ± 0.044	3.630 ± 0.140
20	10	0.185 ± 0.042	0.639 ± 0.032	1.880 ± 0.260
30	15	0.046 ± 0.035	0.204 ± 0.006	1.220 ± 0.140
40	20	0.026 ± 0.023	0.081 ± 0.012	0.682 ± 0.093
50	25	0.019 ± 0.007	0.037 ± 0.011	0.341 ± 0.057
60	30	0.015 ± 0.006	0.020 ± 0.005	0.171 ± 0.037
70	35	0.014 ± 0.006	0.012 ± 0.006	0.088 ± 0.016
80	40	0.013 ± 0.005	0.007 ± 0.002	0.050 ± 0.010
90	45	0.012 ± 0.006	0.004 ± 0.002	0.029 ± 0.006
100	50	0.010 ± 0.004	0.003 ± 0.002	0.017 ± 0.006
110	55	0.010 ± 0.005	0.001 ± 0.002	0.011 ± 0.003
120	60	0.009 ± 0.004	0.000 ± 0.000	0.008 ± 0.003
130	65	0.007 ± 0.004	0.000 ± 0.000	0.006 ± 0.003

± are standard deviations based on two replicates.

Table B.6 Elution data for Ag^+ on Dowex 50W-X8 resin for 92.7 μmol l^{-1} Ag^+ in 0.3 M $NaNO_3$ and pH 7 buffer. The solution was loaded onto a 1.4 g column for 40 minutes at a flow rate 7ml $min.^{-1}$. The eluent 0.04 M EDTA at pH 10 was passed at a flow rate of 1 ml $min.^{-1}$. The data are plotted in Figures 4.8 and 4.9.

Time (min.)	Volume (ml.)	μmols of Ag^+ eluted
0	0	0.000 ± 0.000
10	10	8.500 ± 0.240
20	20	0.103 ± 0.066
30	30	0.039 ± 0.017
40	40	0.015 ± 0.006
50	50	0.006 ± 0.004
60	60	0.002 ± 0.002
70	70	0.000 ± 0.001
80	80	0.000 ± 0.000
90	90	0.000 ± 0.000
100	100	0.000 ± 0.000
110	110	0.000 ± 0.000
120	120	0.000 ± 0.000

± are standard deviations based on two replicates.

Table B.7 Elution data for Ag^+ on Dowex 50W-X8 resin for 92.7 μmol l^{-1} Ag^+ in 0.3 M $NaNO_3$ and pH 7 buffer. The solution was loaded onto a 1.4 g column for 40 minutes at a flow rate 7ml $min.^{-1}$. The eluent 0.04 M EDTA at pH 10 was passed at a flow rate of 2 ml $min.^{-1}$. The data are plotted in Figures 4.8 and 4.9.

Time (min.)	Volume (ml.)	μmols of Ag^+ eluted
0	0	0.000 ± 0.000
5	10	7.780 ± 0.110
10	20	0.208 ± 0.005
15	30	0.084 ± 0.004
20	40	0.040 ± 0.002
25	50	0.023 ± 0.004
30	60	0.014 ± 0.003
35	70	0.009 ± 0.003
40	80	0.006 ± 0.003
45	90	0.004 ± 0.003
50	100	0.003 ± 0.002
55	110	0.000 ± 0.003
60	120	0.000 ± 0.000
65	130	0.000 ± 0.000
70	140	0.000 ± 0.000

± are standard deviations based on two replicates.

Table B.8 Elution data for Ag^+ on Dowex 50W-X8 resin for 92.7 μmol l^{-1} Ag^+ in 0.3 M $NaNO_3$ and pH 7 buffer. The solution was loaded onto a 1.4 g column for 40 minutes at a flow rate 7ml $min.^{-1}$. The eluent 0.04 M EDTA at pH 10 was passed at a flow rate of 10 ml $min.^{-1}$. The data are plotted in Figures 4.8 and 4.9.

Time (min.)	Volume (ml.)	μmols of Ag^+ eluted
0	0	0.000 ± 0.000
1	10	5.710 ± 0.530
2	20	1.072 ± 0.280
3	30	0.561 ± 0.162
4	40	0.348 ± 0.095
5	50	0.221 ± 0.057
6	60	0.148 ± 0.037
7	70	0.101 ± 0.024
8	80	0.069 ± 0.016
9	90	0.047 ± 0.010
10	100	0.031 ± 0.006
11	110	0.023 ± 0.004
12	120	0.015 ± 0.003

± are standard deviations based on two replicates.

Table B.9 Elution data for Ag^+ on Dowex 50W-X8 resin for 0.005, 0.01 and 0.1μmol l^{-1} Ag^+ in 0.3 M $NaNO_3$ and pH 7 buffer. The solutions were loaded onto a 1.4 g column (Figure 3.2) for 40 minutes at a flow rate 7ml $min.^{-1}$. The eluent 0.05 M EDTA at pH 10 was passed at a flow rate of 2 ml $min.^{-1}$. Each fraction represents 5 ml of eluent collected in a 5 ml volumetric flask. The data are plotted in Figure 4.10.

C_{Ag^+} (μmol l^{-1})	5 ml portions	AAS signal
0.005	1	0.006 ± 0.001
0.005	2	0.000 ± 0.000
0.005	3	0.000 ± 0.000
0.005	4	0.000 ± 0.000
0.01	1	0.011 ± 0.003
0.01	2	0.002 ± 0.0004
0.01	3	0.000 ± 0.000
0.01	4	0.000 ± 0.000
0.1	1	0.025 ± 0.003
0.1	2	0.004 ± 0.001
0.1	3	0.000 ± 0.000
0.1	4	0.000 ± 0.000

± are standard deviations based on two replicates.

Table B.10 Elution data for Ag^+ on Dowex 50W-X8 resin for 92.7 μmol l^{-1} Ag^+ in 0.3 M $NaNO_3$ and pH 7 buffer. The solution was loaded onto a 1.4 g column for 40 minutes at a flow rate 7 ml $min.^{-1}$. Different concentrations of eluent (EDTA) at pH 10 were used for elution. In each case the eluent was passed at a flow rate of 2 ml $min.^{-1}$. The data are plotted in Figure 4.11.

Volume (ml)	Time (min.)	0.02 MEDTA μmols of Ag^+ eluted	0.04 MEDTA μmols of Ag^+ eluted	0.08 MEDTA μmols of Ag^+ eluted
0	0	0.000 ± 0.000	0.000 ± 0.000	0.000 ± 0.000
10	5	6.360 ± 0.002	7.820 ± 0.124	7.930 ± 0.010
20	10	0.991 ± 0.024	0.208 ± 0.037	0.166 ± 0.034
30	15	0.428 ± 0.009	0.082 ± 0.031	0.052 ± 0.032
40	20	0.195 ± 0.004	0.038 ± 0.021	0.023 ± 0.021
50	25	0.101 ± 0.002	0.020 ± 0.011	0.011 ± 0.011
60	30	0.058 ± 0.002	0.013 ± 0.006	0.007 ± 0.007
70	35	0.029 ± 0.001	0.007 ± 0.004	0.003 ± 0.004
80	40	0.020 ± 0.002	0.004 ± 0.003	0.002 ± 0.003
90	45	0.010 ± 0.002	0.003 ± 0.001	0.000 ± 0.001
100	50	0.005 ± 0.002	0.000 ± 0.002	0.000 ± 0.000
110	55	0.002 ± 0.002	0.000 ± 0.000	0.000 ± 0.000
120	60	0.000 ± 0.000	0.000 ± 0.000	0.000 ± 0.000
130	65	0.000 ± 0.000	0.000 ± 0.000	0.000 ± 0.000
140	70	0.000 ± 0.000	0.000 ± 0.000	0.000 ± 0.000

± are standard deviations based on two replicates.

Table B.11 Elution data for Ag^+ on Dowex 50W-X8 resin for 1.0, 10 and 100 μmol l^{-1} Ag^+ in 0.3 M $NaNO_3$ and pH 7 buffer. The solutions were loaded onto a 15 mg column (Figure 3.3) for 5 minutes at a flow rate 7ml $min.^{-1}$. The eluent 0.05 M EDTA at pH 10 was passed at a flow rate of 2 ml $min.^{-1}$. Each fraction represents 5 ml of eluent collected in a 5 ml volumetric flask. The data are plotted in Figure 4.12.

C_{Ag^+} (μmol l^{-1})	5 ml portions	AAS signal
1.0	1	0.005 ± 0.0003
1.0	2	0.000 ± 0.000
1.0	3	0.000 ± 0.000
1.0	4	0.000 ± 0.000
10.0	1	0.030 ± 0.001
10.0	2	0.000 ± 0.000
10.0	3	0.000 ± 0.000
10.0	4	0.000 ± 0.000
100.0	1	0.230 ± 0.004
100.0	2	0.001 ± 0.0001
100.0	3	0.000 ± 0.000
100.0	4	0.000 ± 0.000

± are standard deviations based on two replicates.

Table B.12 Ag^+ loading curve data on Dowex 50W-X8 resin for 9.27 μmol l^{-1} Ag^+ in 0.3 M $NaNO_3$ and pH 7 buffer. The solution was loaded onto a 1.4 g column for different lengths of time and different flow rates. The eluent 0.05 M EDTA at pH 10 was passed at a flow rate of 2 ml $min.^{-1}$. The data are plotted in Figure 4.13.

Loading time (min.)	μmols of Ag^+ sorbed		
	Flow rate 2 ml min^{-1}	Flow rate 7 ml min^{-1}	Flow rate 10 ml min^{-1}
0	0.000 ± 0.000	0.000 ± 0.000	0.000 ± 0.000
10	0.132 ± 0.007	0.451 ± 0.002	0.541 ± 0.007
20	0.269 ± 0.014	0.659 ± 0.004	0.677 ± 0.004
30	0.390 ± 0.030	0.696 ± 0.006	0.699 ± 0.018
40	0.486 ± 0.002	0.694 ± 0.015	0.695 ± 0.001
50	0.589 ± 0.031	0.696 ± 0.013	0.696 ± 0.006
60	0.642 ± 0.010	0.696 ± 0.013	0.699 ± 0.016
100	0.699 ± 0.015	-	-
150	0.703 ± 0.007	-	-

± are standard deviations based on two replicates.

Table B.13 Ag^+ loading curve data on Dowex 50W-X8 resin. The solution composition and experimental conditions are the same as in Table B.12. The data are plotted in Figure 4.14.

Flow rate 2 ml min^{-1}		Flow rate 7 ml min^{-1}		Flow rate 10 ml min^{-1}	
Volume (ml.)	µmols of Ag^+ sorbed	Volume (ml.)	µmols of Ag^+ sorbed	Volume (ml.)	µmols of Ag^+ sorbed
0	0.000 ± 0.000	0	0.000 ± 0.000	0	0.000 ± 0.000
20	0.132 ± 0.007	20	0.134 ± 0.002	20	0.146 ± 0.005
40	0.269 ± 0.014	40	0.275 ± 0.004	40	0.266 ± 0.006
60	0.390 ± 0.030	60	0.396 ± 0.004	60	0.396 ± 0.006
80	0.486 ± 0.002	80	0.481 ± 0.002	80	0.473 ± 0.008
100	0.589 ± 0.031	210	0.696 ± 0.006	100	0.541 ± 0.001
200	0.699 ± 0.015	280	0.694 ± 0.015	200	0.677 ± 0.004
300	0.703 ± 0.007	350	0.696 ± 0.013	300	0.699 ± 0.018
-	-	420	0.696 ± 0.013	400	0.695 ± 0.000
-	-	-	-	500	0.696 ± 0.006
-	-	-	-	600	0.699 ± 0.016

± are standard deviations based on two replicates.

Table B.14 Ag^+ loading curve data on Dowex 50W-X8 resin for 1.0 μmol l^{-1} Ag^+ in solutions of different ionic strength (X M $NaNO_3$) and pH 7 buffer. The solutions were loaded onto a 15 mg column for different lengths of time and at a fixed flow rates of 7 ml $min.^{-1}$. The eluent 0.05 M EDTA at pH10 was passed at a flow rate of 2 ml $min.^{-1}$. The data are plotted in Figure 4.15a through 4.15e.

Loading Time	μmol g^{-1} of silver sorbed				
(min.)	I = 0.001 M	I = 0.01 M	I = 0.05 M	I = 0.15 M	I = 0.3 M
0.5	-	-	-	-	0.18 ± 0.01
1	0.43 ± 0.01	0.45 ± 0.06	0.43 ± 0.01	0.31 ± 0.06	0.18 ± 0.01
2	0.80 ± 0.02	0.82 ± 0.01	0.61 ± 0.01	0.40 ± 0.06	0.18 ± 0.01
3	-	-	-	-	0.19 ± 0.04
4	1.67 ± 0.06	1.56 ± 0.01	0.74 ± 0.06	0.40 ± 0.01	0.19 ± 0.04
5	-	-	-	-	0.19 ± 0.04
6	2.47 ± 0.01	2.13 ± 0.01	0.69 ± 0.01	0.40 ± 0.01	-
8	3.18 ± 0.18	2.46 ± 0.01	0.69 ± 0.01	0.40 ± 0.01	-
10	3.97 ± 0.01	2.67 ± 0.01	0.69 ± 0.01	0.40 ± 0.01	0.19 ± 0.04
12	4.63 ± 0.01	2.71 ± 0.01	0.69 ± 0.01	0.40 ± 0.01	
15	5.52 ± 0.06	2.67 ± 0.06	0.65 ± 0.06	0.40 ± 0.06	
20	8.85 ± 0.01	-	-	-	-
25	10.13 ± 0.78	-	-	-	-
30	12.19 ± 0.06	-	-	-	-
35	13.65 ± 0.06	-	-	-	-
40	14.97 ± 0.13	-	-	-	-
50	17.34 ± 0.25	-	-	-	-

± are standard deviations based on two replicates.

Table B.15 Data showing the values of distribution coefficient of Ag^+ between the resin phase and solution phase at different ionic strengths. The values were calculated by using the data from Table B.14. These data are plotted in Figure 4.16

Ionic strength (M)	λ_{Ag+} (lg^{-1})
0.01	2.68 ± 0.11
0.05	0.69 ± 0.03
0.15	0.40 ± 0.02
0.3	0.19 ± 0.01

Table B.16 Ag^+ loading curve data on Dowex 50W-X8 resin for 0.1μmol l^{-1}, 1.0 μmol l^{-1} and 10.0 μmol l^{-1} Ag^+ in 0.3 M $NaNO_3$ and pH 7 buffer. The solutions were loaded onto a 1.4 g column for different lengths of time and at a fixed flow rate of 7 ml min.$^{-1}$. The eluent 0.05 M EDTA at pH 10 was passed at a flow rate of 2 ml min.$^{-1}$. The data are plotted in Figure 4.17.

Loading Time (min.)	C_{Ag} = 0.1 μmol l^{-1}	C_{Ag} = 1.0 μmol l^{-1}	C_{Ag} = 10.0 μmol l^{-1}
	μmol g^{-1} of Ag^+ sorbed	μmol g^{-1} of Ag^+ sorbed	μmol g^{-1} of Ag^+ sorbed
0	0.000 ± 0.000	0.000 ± 0.000	0.000 ± 0.000
10	0.006 ± 0.001	0.060 ± 0.001	0.576 ± 0.006
20	0.010 ± 0.001	0.111 ± 0.004	1.043 ± 0.021
30	0.014 ± 0.001	0.151 ± 0.003	1.343 ± 0.021
40	0.014 ± 0.003	0.166 ± 0.003	1.457 ± 0.035
50	0.014 ± 0.003	0.170 ± 0.006	1.457 ± 0.007
60	0.014 ± 0.001	0.172 ± 0.003	1.457 ± 0.014

± are standard deviations based on two replicates.

Table B.17 Ag^+ loading curve data on Dowex 50W-X8 resin for 1.0 μmol l^{-1}, 10.0μmol l^{-1} and 100 μmol l^{-1} Ag^+ in 0.3 M $NaNO_3$ and pH 7 buffer. The solutions were loaded onto a 15 mg column for different lengths of time and at a fixed flow rate of 7 ml $min.^{-1}$. The eluent 0.05 M EDTA at pH10 was passed at a flow rate of 2 ml $min.^{-1}$. The data are plotted in Figure 4.18.

Loading time (min)	C_{Ag+} = 1.0 μmol l^{-1}	C_{Ag+} = 10.0 μmol l^{-1}	C_{Ag+} = 100.0 μmol l^{-1}
	μmol g^{-1} of Ag^+ sorbed	μmol g^{-1} of Ag^+ sorbed	μmol g^{-1} of Ag^+ sorbed
0.0	0.00 ± 0.00	0.00 ± 0.00	0.00 ± 0.00
0.5	0.26 ± 0.02	1.05 ± 0.02	8.05 ± 0.06
1.0	0.26 ± 0.02	1.22 ± 0.02	8.82 ± 0.06
2.0	0.26 ± 0.02	1.32 ± 0.02	9.03 ± 0.02
3.0	0.29 ± 0.04	1.32 ± 0.02	8.91 ± 0.06
4.0	0.29 ± 0.04	1.32 ± 0.02	8.99 ± 0.06
5.0	0.29 ± 0.04	1.32 ± 0.02	8.95 ± 0.02
10.0	0.32 ± 0.02	1.32 ± 0.02	9.03 ± 0.02

± are standard deviations based on two replicates.

Table B.18 Ag^+ sorption isotherm data on Dowex 50W-X8 resin. The solutions contain different concentrations of Ag^+ in 0.3 M $NaNO_3$ and pH 7 buffer. The solution were loaded onto a 1.4 g column (Figure 3.2) for 40 minutes at a flow rate 7 ml $min.^{-1}$. The eluent 0.05 M EDTA at pH 10 was passed at a flow rate of 2 ml $min.^{-1}$. The data are plotted in Figures 4.19 and 4.21

$[Ag^+]$, μmol l^{-1}	$[RAg^+]$, μmol g^{-1}	% of resin sites occupied by Ag^+
0.005	0.002 ± 0.001	0.000039
0.008	0.005 ± 0.001	0.000098
0.01	0.006 ± 0.002	0.00012
0.015	0.007 ± 0.002	0.00014
0.05	0.011 ± 0.001	0.00022
0.1	0.019 ± 0.001	0.00037
0.5	0.078 ± 0.004	0.0015
1.0	0.140 ± 0.002	0.0027
1.5	0.208 ± 0.001	0.0041
2.0	0.279 ± 0.003	0.0055
4.0	0.590 ± 0.008	0.012
5.0	0.724 ± 0.004	0.014
10.0	1.39 ± 0.03	0.027
15.0	1.89 ± 0.04	0.037
20.0	2.29 ± 0.01	0.045
35.0	3.88 ± 0.32	0.076
50.0	5.23 ± 0.01	0.1
75.0	7.51 ± 0.02	0.15
100.0	9.73 ± 0.04	0.19
125.0	11.5 ± 0.1	0.23
150.0	13.5 ± 0.1	0.26

± are standard deviations based on two replicates.

Table B.19 Ag^+ sorption isotherm data on Dowex 50W-X8 resin. The solutions contain different concentrations of Ag^+ in 0.3 M $NaNO_3$ and pH 7 buffer. The solutions were loaded onto a 15 mg column (Figure 3.3) for 5 minutes at a flow rate 7 ml $min.^{-1}$. The eluent 0.05 M EDTA at pH 10 was passed at a flow rate of 2 ml $min.^{-1}$. The data are plotted in Figures 4.20.

$[Ag^+]$, μmol l^{-1}	[RAg], μmol g^{-1}	% of resin sites occupied by Ag^+
0.1	0.07 ± 0.01	0.0014
0.2	0.14 ± 0.02	0.0027
0.5	0.21 ± 0.02	0.0041
0.8	0.28 ± 0.01	0.0055
1.0	0.33 ± 0.01	0.0065
2.0	0.55 ± 0.01	0.011
3.5	0.87 ± 0.01	0.017
5.0	1.15 ± 0.01	0.023
8.0	1.41 ± 0.01	0.028
8.5	1.46 ± 0.01	0.029
10.0	1.64 ± 0.01	0.032
20.0	2.61 ± 0.01	0.051
35.0	4.07 ± 0.06	0.080
50.0	5.16 ± 0.08	0.10
65.0	6.54 ± 0.06	0.13
80.0	7.20 ± 0.49	0.14
100.0	9.00 ± 0.05	0.18
200.0	16.8 ± 0.1	0.33
350.0	29.1 ± 0.1	0.57
500.0	38.2 ± 0.6	0.75
650.0	49.2 ± 0.6	0.97
800.0	57.5 ± 0.6	1.13
1000.0	69.4 ± 1.5	1.36

± are standard deviations based on two replicates.

APPENDIX C

TABLES FOR CHAPTER FIVE

In this appendix data which were presented in some of the figures in Chapter 5 are tabulated. The corresponding figure in which the data were plotted is indicated in the tables.

Table C.1 Ag^+ loading curve data on Dowex 50W-X8 resin for $1x10^{-4}$ M total silver and $3x10^{-5}$ M total chloride in 0.3 M $NaNO_3$ and pH 7 buffer. The solutions were left to age for different lengths of time before being loaded onto a 1.4 g resin column for different lengths of time at a flow rate of 7 ml $min.^{-1}$. The eluent 0.05 M EDTA at pH10 was passed at a flow rate of 2 ml $min.^{-1}$. The data are plotted in Figure 5.1.

Loading time (min.)	μmol g^{-1} of Ag^+ sorbed (After mixing)	μmol g^{-1} of Ag^+ sorbed (After 1 hour)	μmol g^{-1} of Ag^+ sorbed (After 15 hours)
20	6.46 ± 0.16	6.29 ± 0.29	7.14 ± 0.2
30	7.57 ± 0.15	7.50 ± 0.10	8.57 ± 0.1
40	8.07 ± 0.09	7.57 ± 0.21	8.57 ± 0.3
60	8.14 ± 0.13	7.57 ± 0.09	8.57 ± 0.2
120	8.00 ± 0.05	7.50 ± 0.21	8.57 ± 0.2
180	8.00 ± 0.06	7.64 ± 0.17	8.57 ± 0.1
240	8.29 ± 0.09	7.71 ± 0.15	8.57 ± 0.2

± are standard deviations based on three replicates.

Table C.2 Ag^+ loading curve data on Dowex 50W-X8 resin for $1x10^{-4}$ M total silver and $3x10^{-5}$ M total chloride in 0.3 M $NaNO_3$ and pH 7 buffer. The solutions were left to age for different lengths of time before being loaded onto a 15 mg resin column for different lengths of time at a flow rate of 7 ml $min.^{-1}$. The eluent 0.05 M EDTA at pH10 was passed at a flow rate of 2 ml $min.^{-1}$. The data are plotted in Figure 5.2.

Loading Time (min.)	µmol g^{-1} of Ag^+ sorbed (After mixing)	µmol g^{-1} of Ag^+ sorbed (After 1 hours)	µmol g^{-1} of Ag^+ sorbed (After 15 hours)
0.5	6.40 ± 0.10	5.90 ± 0.10	6.50 ± 0.10
1.0	6.70 ± 0.10	6.30 ± 0.10	7.10 ± 0.10
2.0	6.90 ± 0.10	6.40 ± 0.10	7.40 ± 0.10
3.0	6.90 ± 0.10	6.40 ± 0.10	7.30 ± 0.10
4.0	6.80 ± 0.10	6.30 ± 0.10	7.30 ± 0.10
5.0	6.90 ± 0.10	6.30 ± 0.10	7.30 ± 0.10
7.5	6.90 ± 0.10	6.30 ± 0.10	7.30 ± 0.10
10.0	6.90 ± 0.10	6.20 ± 0.10	7.20 ± 0.10
12.5	7.00 ± 0.10	6.20 ± 0.10	7.20 ± 0.10
15.0	7.00 ± 0.10	6.20 ± 0.10	7.20 ± 0.10

± are standard deviations based on three replicates.

Table C.3 Results obtained for the determination of free silver ion concentration in the presence of varying amounts of total silver and total chloride concentration. (0.3 M total ionic strength and pH 7 buffer). The solutions were loaded onto a 15 mg column, Figure 3.4 at a flow rate of 6 ml min.$^{-1}$. The data are plotted in Figure 5.9

Sample No.	C_{Ag}, M	C_{Cl}, M	$[Cl^-]$, M	Values of $[Ag^+]$ obtained by the ion-exchange method in μmol l^{-1}	Values of $[Ag^+]$ obtained by the ISE method in μmol l^{-1}	Predicted values of $[Ag^+]$, in μmol l^{-1}
1	$1x10^{-4}$	$4.5x10^{-4}$	$3.5x10^{-4}$	1.2 ± 0.2	1.00 ± 0.02	1.11 ± 0.03
2	$1x10^{-4}$	$1.5x10^{-4}$	$5.7x10^{-5}$	6.8 ± 0.7	6.21 ± 0.12	6.84 ± 0.14
3	$1x10^{-4}$	$1.0x10^{-4}$	$2.0x10^{-5}$	18.6 ± 0.8	17.8 ± 0.3	19.7 ± 0.2
4	$1x10^{-3}$	$9.5x10^{-4}$	$6.8x10^{-6}$	58.1± 2.5	59.5 ± 0.9	56.8 ± 1.1
5	$1x10^{-3}$	$9.0x10^{-4}$	$3.8x10^{-6}$	101 ± 4	95.9 ± 1.6	104 ± 2
6	$1x10^{-3}$	$5.0x10^{-4}$	$7.8x10^{-7}$	495 ± 18	507 ± 9	501 ± 7
7	$1x10^{-2}$	$9.0x10^{-3}$	$3.9x10^{-7}$	949 ± 34	993 ± 17	1000 ± 12
8	$1x10^{-2}$	$5.0x10^{-3}$	$7.8x10^{-8}$	4927 ± 100	5000 ± 49	5000 ± 49

± are standard deviations based on three replicates.

Table C.4 Ag^+ equilibrium sorption data for solutions contain different concentration of total silver, C_{Ag} in 0.3 M $NaNO_3$ at pH 10. The solutions were loaded onto a 15 mg column (Figure 3.3) for 5 minutes at flow rate 7ml $min.^{-1}$. The eluent 0.05 M EDTA at pH 10 was passed at a flow rate of 2 ml $min.^{-1}$. The data are plotted in Figures 5.11 and 5.12.

Silver in solution $[Ag^+]$, $\mu mol\ l^{-1}$	Silver sorbed [RAg], $\mu mol\ g^{-1}$
0.2	0.16 ± 0.01
0.4	0.21 ± 0.01
0.8	0.32 ± 0.01
1.0	0.43 ± 0.01
2.0	0.79 ± 0.01
4.0	1.03 ± 0.01
6.0	1.21 ± 0.01
8.0	1.43 ± 0.10
10.0	2.09 ± 0.10
20.0	3.09 ± 0.10
40.0	4.75 ± 0.10
60.0	6.01 ± 0.10
80.0	7.37 ± 0.10
100.0	8.79 ± 0.10
200.0	18.1 ± 0.5
400.0	29.4 ± 0.5
600.0	35.7 ± 0.7
800.0	35.6 ± 0.5
1000.0	36.6 ± 0.4
2000.0	34.8 ± 1.1
4000.0	36.9 ± 0.2
6000.0	37.8 ± 0.2
8000.0	38.0 ± 0.1

± are standard deviations based on three replicates.

Table C.5 Results obtained for the determination of free silver ion concentration in solutions of different pH and 0.3 M total ionic strength. The solutions were loaded onto 15 mg column, Figure 3.4 at a flow rate of 6 ml min.$^{-1}$. The data are plotted in Figures 5.15 and 5.17

pH	Values of [Ag^+] obtained by the ion-exchange method in μmol l^{-1} (before correction)	Values of [Ag^+] obtained by the ion-exchange method in μmol l^{-1} (After correction)	Values of [Ag^+] obtained by the ISE method in μmol l^{-1}	Predicted values of [Ag^+] in μmol l^{-1}
12.97	14.4 ± 0.4	0.43 ± 0.01	0.490 ± 0.012	0.38 ± 0.01
12.71	15.5 ± 0.2	0.80 ± 0.01	0.878 ± 0.020	0.69 ± 0.02
12.49	20.2 ± 0.6	1.64 ± 0.05	1.45 ± 0.032	1.15 ± 0.03
12.29	15.3 ± 0.9	1.95 ± 0.12	2.30 ± 0.05	1.83 ± 0.04
11.89	19.0 ± 0.4	5.06 ± 0.11	5.53 ± 0.11	4.59 ± 0.10
11.43	22.2 ± 0.8	11.5 ± 0.41	10.4 ± 0.19	13.2 ± 0.30

± are standard deviations based on three replicates.

APPENDIX D

DERIVATION OF AN EXPRESSION FOR THE FRACTION OF FREE SILVER IN THE PRESENCE OF EDTA AS THE ONLY COMPLEXING LIGAND.

EDTA, (Y^{4-}) forms two complexes with Ag^{+}. The formation expressions for these two complexes as given in [52] are as follows:

$$Ag^{+} + Y^{4-} \rightleftharpoons AgY^{3-}$$

$$K_1 = \frac{[AgY^{3-}]}{[Ag^{+}][Y^{4-}]} \qquad \text{..... D.1}$$

$$AgY^{3-} + H^{+} \rightleftharpoons AgHY^{2-}$$

$$K_2 = \frac{[AgHY^{2-}]}{[AgY^{3-}][H^{+}]} \qquad \text{..... D.2}$$

We want equatio D.2 to be in the form: silver + EDTA = silver-EDTA complex. Hence an equation of the form is also needed:

$$H^{+} + Y^{4-} \rightleftharpoons HY^{3-}$$

$$K_H = \frac{[HY^{3-}]}{[H^{+}][Y^{4-}]} \qquad \text{..... D.3}$$

From equation D.2 we can write:

$$[AgY^{3-}] = \frac{[AgHY^{2-}]}{K_2[H^{+}]} \qquad \text{..... D.4}$$

Also from equation D.3 we can write:

$$[Y^{4-}] = \frac{[HY^{3-}]}{K_H [H^+]} \quad \text{..... D.5}$$

Substituting equation D.4 and D.5 into equation D.1 above we obtain:

$$K_1 = \frac{K_H \ [AgHY^{2-}]}{K_2 \ [Ag^+] \ [HY^{3-}]} \quad \text{..... D.6}$$

Re-arranging equation D.6 we get:

$$K_x = \frac{K_1 K_2}{K_H} = \frac{[AgHY^{2-}]}{[Ag^+] \ [HY^{3-}]} \quad \text{..... D.7}$$

Where Kx is the equilibrium constant for the reaction:

$$Ag^+ + HY^{3-} \longleftrightarrow AgHY^{2-}$$

The conditional stability constants for Metal-EDTA complexes are given by:

$$K_1' = K_1 \alpha_{Y4-} = \frac{[AgY^{3-}]}{[Ag^+][Y']} \quad \text{..... D.8}$$

$$K_x' = \frac{[AgHY^{2-}]}{[Ag^+][Y']} \quad \text{..... D.9}$$

$$K_{Na+}' = K_{Na+} \alpha_{Y4-} = \frac{[NaY^{3-}]}{[Na^+][Y']} \quad \text{..... D.10}$$

Where $[Y^{4-}] = \alpha_{Y4-} [Y']$ and $[HY^{3-}] = \alpha_{HY3-} [Y']$

$[Y']$ is the total concentration of EDTA in solution that has not reacted with silver. It is given by the following equation:

$$[Y^{'}] = [Y^{4-}] + [HY^{3-}] + [NaY^{3-}] + [H_2Y^{2-}] + [H_3Y^{-}] + [H_4Y] +$$

$$[H_5Y^{+}] + [H_6Y^{2+}] \qquad \text{..... D.11}$$

The fraction of free silver in solution, in the presence of EDTA as the only complexing ligand is given by the following equation:

$$\alpha_{Ag+,EDTA} = \frac{[Ag^{+}]}{C_{Ag}} = \frac{[Ag^{+}]}{[Ag^{+}] + [AgY^{3-}] + [AgHY^{2-}]} \qquad \text{..... D.12}$$

Writing $[AgY^{3-}]$ and $[AgHY^{2-}]$ in terms of K, $[Ag^{+}]$ and $[Y^{'}]$ from equation D.8 and D.9 we obtain:

$$\alpha_{Ag+,EDTA} = \frac{1}{1 + (K_1' + K_x')[Y']} \qquad \text{..... D.13}$$

Let us define:

$$\beta'_{Ag,EDTA} = (K_1' + K_x')$$

We can re-write equation D.13 as follows:

$$\alpha_{Ag+,EDTA} = \frac{1}{1 + \beta'_{Ag,EDTA}[Y']} \qquad \text{..... D.14}$$

Equation D.14 is used in section 2.2.5.